AD
A066045

Austin Research Associates, Inc., TX.
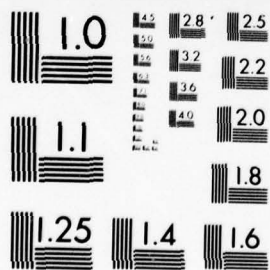
1901 Rutland Drive - Austin, Texas 78758 - Phone (512) 837-6623

6/

INTERACTIONS OF RELATIVISTIC CHARGED PARTICLE BEAMS.

LEVEL

by

10/

W. E./Drummond,
J. R./Thompson,
H. V./Wong,
G. I./Bourianoff
B. N./Moore
M. L. Sloan

9/

Final Scientific Report, 1 Jul 76 - 30 Sep 78,

for AFOSR Contract F49620-76-C-0002

15/

16/ 2301 17/ A7

Air Force Office of Scientific Research
Bolling Air Force Base, D.C.

12/ 286p.

11/ November 1978

403 703

79 03 16 025

REPORT DOCUMENTATION PAGE		READ INSTRUCTIONS BEFORE COMPLETING FORM
1. REPORT NUMBER	2. GOVT ACCESSION NO.	3. RECIPIENT'S CATALOG NUMBER
4. TITLE *(and Subtitle)* Interactions of Relativistic Charged Particle Beams		5. TYPE OF REPORT & PERIOD COVERED Final Scientific Report 7-1-76 to 9-30-78
		6. PERFORMING ORG. REPORT NUMBER 1-ARA-78-U-78 (ARA-331)
7. AUTHOR(s) W. E. Drummond, et al.		8. CONTRACT OR GRANT NUMBER(s) F49620-76-C-0002
9. PERFORMING ORGANIZATION NAME AND ADDRESS Austin Research Associates 1901 Rutland Drive Austin, Texas 78758		10. PROGRAM ELEMENT, PROJECT, TASK AREA & WORK UNIT NUMBERS 2301/A7 61102F 612300
11. CONTROLLING OFFICE NAME AND ADDRESS Air Force Office of Scientific Research ATTN: Captain Gullickson/NP, Building 410 Bolling Air Force Base, D.C. 20332		12. REPORT DATE November 1978
		13. NUMBER OF PAGES 284
14. MONITORING AGENCY NAME & ADDRESS*(if different from Controlling Office)*		15. SECURITY CLASS. *(of this report)* UNCLASSIFIED
		15a. DECLASSIFICATION/DOWNGRADING SCHEDULE

16. DISTRIBUTION STATEMENT *(of this Report)*

Approved for Public Release; Distribution Unlimited

17. DISTRIBUTION STATEMENT *(of the abstract entered in Block 20, if different from Report)*

18. SUPPLEMENTARY NOTES

19. KEY WORDS *(Continue on reverse side if necessary and identify by block number)*

Nonneutral Relativistic Electron Beam
Collective Ion Acceleration
Limiting Currents
Auto-Resonant Acceleration
Electron Cyclotron Wave

Beam-Plasma Heating
Unneutralized Beam Equilibrium
Linearized Beam Eigenmodes

20. ABSTRACT *(Continue on reverse side if necessary and identify by block number)*

During the performance period on this contract, from 1 July 1976 through 30 September 1978, we made substantial progress in our research on the interactions of high energy beams of charged particles. We investigated in considerable detail the interactions which may occur between a relativistic electron beam and a less dense species of ions, which is highly relevant to schemes for collective ion acceleration. We found that the lack of charge neutrality importantly influences this interaction. A number of mechanisms by which wave growth may be nonlinearly saturated were identified. We found that for cyclotron wave

DD _{1 JAN 73} FORM 1473   EDITION OF 1 NOV 65 IS OBSOLETE

20.(Abstract--Continued)

interactions, transverse effects tend to be dominant, and it appears that such ion-electron interactions are (i) probably unsuitable as a wave growth/ion loading mechanism, but (ii) unlikely to disrupt the process of collective acceleration. A stability analysis of a two-dimensional sheet beam of electrons was completed. We have also determined accurately the limiting currents for magnetized injection of an unneutralized relativistic electron beam into a cylindrical drift tube. The previously cited interpolation formula was found to underestimate the true limiting current by over 20% in some cases, and the corresponding expression for the axial electron energy sometimes overestimates the ture limiting energy by more than an order of magnitude. The influence of a spatial variation in γ on the structure of the relativistic electron beam cyclotron mode was examined, and found to increase the peakedness of the radial electric fields near the beam edge when $\gamma(r)$ increases. The influence of this radial variation in γ on the longitudinal plasma mode was also examined in the strong magnetic field limit. Previous results, that the plasma wave phase velocity could only be made small (for ion loading, prior to collective acceleration) by increasing the beam current nearly to the limiting current, were extended from the pencil beam regime to arbitrary values of beam and waveguide radii and arbitrary density profiles. The plasma wave eigenfunctions were found to have increased peakedness near the beam axis as the limiting current conditions are approached. An iterative calculation was performed of the slowly precessing fluid beam equilibrium which is achieved by a θ-symmetric, steady state, initially solid electron beam injected into a cylindrical waveguide along a finite magnetic guide field. This calculation incorporates the space charge slowing associated with the waveguide injection, as well as the acquisition of precessional motion and associated diamagnetism, centrifugal and Coriolis forces. A generalization of the limiting current formula was obtained to incorporate the finite axial magnetic field effects--reducing B_z increases I_L. Several small parameters were isolated during the equilibrium calculation, which may be used to quantify the validity of the common assumptions of (i) infinite magnetic fields, or (ii) ultrarelativistic electron beams. An examination of linearized collective beam waves was completed for the important case in which the parameter characterizing centrifugal and Coriolis forces, and plasma-cyclotron mode coupling, was retained in the analysis. The resulting fourth-order radial eigenvalue problem was solved in terms of Bessel functions, and the mode coupling effects on the dispersion relation were examined. This general theoretical framework allows the inclusion of longitudinal beam compression effects upon cyclotron waves, and the inclusion of transverse gyroeffects upon plasma waves. An analysis was completed of the effect of a finite thermal spread in the axial beam velocity on the electron cyclotron wave. A fairly nonrestrictive sufficient condition was obtained such that the cyclotron modes may propagate undamped by kinetic effects. Finally, we reviewed some previous work on relativistic electron beam-plasma heating, wherein we found that very high density plasmas may be heated with reasonably efficiency by high quality, ultrarelativistic electron beams via the primary beam-plasma streaming interaction.

TABLE OF CONTENTS

gamma ≠ on

next page

S E C T I O N   I

INTRODUCTION AND SUMMARY OF RESULTS
OF RESEARCH ACCOMPLISHED

This research program concerns very high energy,
high power beams of charged particles and the interac-
tions which they may have with one another, with other
species of charged particles, or with surrounding
waveguide-diode structures via external or self-consistent
electromagnetic fields. The potential of such beams for
rapidly transporting energy may prove to have a number of
important applications for the Air Force. One ultimate
possibility is the creation of advanced new charged
particle weapons for the Air Force. A more immediate goal,
which has received significant attention in recent years,
is the possibility of generating ion beam pulses at
relativistic (i.e., GeV) ion energy by utilizing the
powerful collective electromagnetic fields which may be
sustained by relativistic electron beams. This research

program is aimed at supporting, among other things, the development of such collective ion accelerators.

The research problems of central importance to this objective focus generally on obtaining a good understanding of the stable behavior of unneutralized or partially neutralized electron and ion beams, the interaction of such electron beams with ions, and the interaction of such beams with background plasmas. The study of these beam interactions is naturally prerequisite to achieving the beam control required by the various schemes for ion acceleration. The interactions are predominately collisionless, within an environment without gross charge neutrality, and occur via powerful electromagnetic fields which are frequently influenced appreciably by the presence of both passive external waveguide structures and active charge or current sources (e.g., guide magnetic field coils).

We initiated our investigation of these problems of relativistic electron and ion beam interactions under our previous AFOSR Contract F44620-72-C-0071, which

terminated on June 30, 1976. A technical description of this initial research is given in reference 1. Work in this area then continued under AFOSR Contract No. F49620-76-C-0002, which began on July 1, 1976 and terminated on September 30, 1978. This research is summarized in this final report. Some additional research is also included for completeness, which was not accomplished under this contract, as is noted in the remainder of this section. We believe that substantial progress was achieved in this research on the interactions of high energy, charged particle beams, as described more fully below.

A problem of considerable relevance to schemes for collective ion acceleration concerns the interactions which may occur between a relativistic electron beam and

---

1. W. E. Drummond, J. R. Thompson, et al., "Turbulent Heating of Plasmas by High Energy Particle Beams," Final Scientific Report for AFOSR Contract No. F44620-72-C-0071, August 1976. I-ARA-76-U-80.

a less dense species of ions. The motivation for con-

sidering this problem is severalfold. Of primary impor-

tance to ion acceleration schemes is the fact that such

interactions between the subject ions and the background

electron beam will occur during the process of accelera-

tion, when the interactions have no desired purpose, but

must be assessed to determine how disruptive they are

on the electron beam and on the process of acceleration.

On the other hand, interaction between the electron beam

and the subject ions is also of interest as a possible

mechanism for both wave growth and ion loading into the

wave, provided that the growth saturates via ion

trapping. This possibility has been considered by

Indykul, et al. (reference 2), whose analysis was

supported by a one-dimensional, single wave computer

calculation of the nonlinear ion dynamics. Finally,

---

2. V. P. Indykul, I. P. Panchenko, V. D. Shapiro, and
V. I. Shevchenko, JETP Letters 20, 65 (1974).

such electron-ion interactions stimulate the growth of
unstable eigenmodes on the electron beam, which may
eventually achieve large amplitudes before nonlinear
effects cause saturation of the growth. Consequently,
the electron-ion interaction problem is a handy vehicle
for the study of large wave, nonlinear effects, which
in turn are crucial to the determination of the maximum
accelerating electric field amplitudes which may be
sustained by the electron beam.

Reference 1 contains a discussion and references
to our early work on this problem, including both work
sponsored under AFOSR Contract F44620-72-C-0071 and also
work sponsored under Contract F29601-75-C-0029 on the
Auto-Resonant acceleration scheme. One finds that the
ions may interact with either of two "negative energy"
electron modes: longitudinal electron plasma oscillations
or electron cyclotron interactions. The former inter-
actions, in general, are much better understood from the
vast amount of prior research conducted across the country
on beam-plasma interaction via plasma waves. We have

concentrated our research on the latter cyclotron
interactions, which will tend to be the faster growing
when the electron beam is sufficiently energetic and
intense that $(\Omega_e/\gamma_e\omega_{pe})^{1/3} < 1$. [Here $\Omega_e = eB_z/\gamma_e mc$ is
the relativistic cyclotron frequency, $\omega_{pe} = (4\pi N_e e^2/\gamma_e m)^{1/2}$
is the relativistic plasma frequency, and $(\gamma_e-1)mc^2$ is the
electron kinetic energy per particle.]

The work on these ion-electron cyclotron inter-
actions which we did prior to the July 1, 1976 beginning
of this contract was primarily concerned with the linear
theory of the interactions in waveguide geometry. One
important change from the usual charge-neutral linear
theory is that the ion response is strongly influenced by
the radial ion bouncing which occurs in the self electric
field of the electron beam, at frequency $\omega_{B\perp} = (2\gamma_e m/M)^{1/2}\omega_{pe}$.
In fact, when the ion density is low enough that the
growth rate of the interaction falls below $\omega_{B\perp}$, then this
bouncing will be crucial to the interaction, and the wave
phase velocity will be proportional to $\omega_{B\perp}$ and independent
of the ion density.

Research on the nonlinear phase of these ion-electron cyclotron interactions was begun under Contract F29601-75-C-0046 on the Auto-Resonant Accelerator experiment, and was continued in the early months of this AFOSR Contract F49620-76-C-0002. An internal ARA report on these nonlinear effects was compiled in September, 1976 and is included as Appendix A, herein, in its entirety, for the benefit of the reader. However, it should be noted that the material in Sections III, V, and a portion of VII of Appendix A was sponsored under Contract F29601-75-C-0046, and has been previously published in reference 3. The rest of Appendix A describes the AFOSR-sponsored nonlinear work. This material in Appendix A was also presented in Paper 2T3 of the 18th Annual Meeting of the Division of Plasma Physics of the American Physical Society in November, 1976.

---

3. W. E. Drummond, et. al. "Conceptual Design of an Auto-Resonant Accelerator Experiment," Final Report for Contract F29601-75-C-0046, May 1976. I-ARA-76-U-44.

The chief results of this research on the nonlinear phase of ion-electron cyclotron interactions were the identification of a number of mechanisms by which the wave growth could be saturated. Some were electron effects, such as a nonlinear shift in the frequency of the cyclotron wave, and some were ion effects, such as an evolution of the ion trajectories in perpendicular $(x_\perp, v_\perp)$ phase space to a point where the ions ceased to gain energy. As shown in Eq. (75) of Appendix A, the negative energy cyclotron mode can only grow so long as the ions also gain energy. As summarized in Eq. (78), the nonlinear effects are important for short wavelength modes at lower wave amplitudes than for long wavelength modes, and hence the longer wavelength (e.g., small $k_\perp$) modes should achieve the largest amplitudes if their growth is otherwise allowed. One of the most important results of this analysis (which is also confirmed by the two-dimensional computer simulations which were performed) is that for a wide range of parameters, nonlinear effects associated with the transverse electron or ion dynamics in the cyclotron wave enter to saturate the wave amplitude before it becomes large enough

8

for longitudinal ion trapping. Hence, the intuition
gained from the study of plasma wave interactions does
not extend to cyclotron wave interactions, where trans-
verse effects tend to dominate. The neglect of such
transverse effects in the Indykul analysis (reference 2)
therefore appears to be a serious deficiency. Our own
calculations support the general conclusion that ion-
electron cyclotron interactions tend to saturate at
wave amplitudes too low for longitudinal ion trapping,
and before there is catastrophic disruption of the
electron beam. Therefore, it appears that such inter-
actions are (i) probably unsuitable as a wave growth/ion
loading mechanism, but (ii) unlikely to disrupt the
acceleration process itself. We believe that this
research on the interactions between a sparse ion species
and the cyclotron modes of an electron beam, which was
sponsored about 50% under these AFOSR Contracts F44620-
72-C-0071 and F49620-76-C-0002, represents a significant
research contribution in this field.

A second problem attacked under this AFOSR contract was a stability analysis of a two-dimensional sheet beam of electrons, in a magnetic field in a conducting waveguide. This calculation is included as Appendix B herein. It is common practice in the theoretical analysis of problems concerning unneutralized electron beams within waveguides, to employ both cylindrical and cartesian (slab) geometry. For certain analyses, the trigonometric eigenfunctions which apply for slab geometry afford a measure of convenience compared to cylindrical Bessel eigenfunctions, and yet there is usually little difference in the underlying physical interactions. Nevertheless, there is a constant need for vigilance and comparison, to insure that the slab analyses overlook no important effects which might be rooted in cylindrical geometry. To this end, the slab geometry stability calculation is important, and it may be compared with the previous calculation we have published for cylindrical geometry (reference 4).

---

4. H. V. Wong, M. L. Sloan, J. R. Thompson, and A. T. Drobot, Physics of Fluids 16, 902 (1973).

Naturally, it is crucial to understand the conditions
under which the electron beam itself will be stable,
before addressing more complex questions of beam
interaction.

For this analysis, we also imposed a restriction
to two dimensional perturbations, assuming that one
coordinate is ignorable for both equilibrium and pertur-
bed quantities. Although this limits the generality of
our result, such a restriction is appropriate to two-
dimensional slab geometry computer codes which have been
frequently employed to examine relativistic electron beam
phenomena.

The approach of the calculation is to compute the
second order quantity $\int d^3x \ \underline{J}_1 \cdot \underline{E}_1$, which drives the
electromagnetic field energy in time according to Maxwell's
equations. Under our assumptions, it is possible to
employ the linearized Vlasov equation to express this
quantity as a total time derivative, thereby obtaining an
energy constant of the motion. This in turn leads to an
energy principle for the stability of a common class of
slab equilibria. One finds that $N_e b/\gamma_e B_z$ must be bounded

11

above to insure stability, where N_e is the beam density

and b is the half-width of the conducting waveguide.

This scaling agrees with the previous cylindrical

result.

Another task we have undertaken for this AFOSR

contract is to determine accurately the limiting currents

for magnetized injection of an unneutralized relativistic

electron beam into a cylindrical drift tube. This

problem has been extant for years, but so far only the

nonrelativistic solution (reference 5) and an approxi-

mate interpolation formula (reference 6) for the rela-

tivistic solution have been published. Our work is

included as Appendix C herein, in the form of an article

appearing in the November, 1978 issue of The Physics

of Fluids. A portion of this work was also supported

---

5. L. P. Smith and P. L. Hartman, Journal of Applied
Physics 11, 220 (1940).

6. L. S. Bogdankevich and A. A. Rukhadze, Soviet Physics
Uspekhi, 14, 163 (1971).

under Contract DASG60-76-C-0045 by the Ballistic Missile Defense Advanced Technology Center.

This problem is to calculate the steady state, propagating beam equilibrium for a laminar, unneutralized, cylindrical relativistic electron beam, which is initially solid and monoenergetic at the anode plane. The beam, of radius a and initial kinetic energy $(\gamma_o - 1)mc^2$ is injected along a very strong axial magnetic guide field into a coaxial drift tube of radius $b \geq a$, and length $L \gg b$. The tube end-effects and beam-front transients are neglected. As the beam electrons propagate into the drift tube, the central electrons are axially slowed by space charge effects more than the edge electrons, so that the beam density $n(r)$ becomes peaked on axis while the relativistic factor $\gamma(r)$ becomes hollowed on axis. For given values of γ_o and b/a, the injected current is a peaked function of $\gamma_c = \gamma(r = 0)$, as illustrated in Fig. 1

13

of Appendix C. It is desired to know the value of the peak, or limiting current I_L which may be injected into the drift tube, as well as the corresponding factor γ_{cL} of the center electrons, as a function of the parameters γ_0 and b/a.

Previously published relativistic analyses have essentially ignored the radial dependence of the axial density compression which occurs, and have considered only the special cases of needle beams ($\ln b/a >> 1$) or ultrarelativistic beams ($\gamma_0 >> 1$). The interpolation formula (from reference 6) which is widely cited is

$$I_L = \frac{mc^3}{e} \frac{(\gamma_0^{2/3}-1)^{3/2}}{1+2 \ln b/a}$$

and the corresponding value of γ_c is $\gamma_{cL} = \gamma_0^{1/3}$. The more exact analysis which we have performed indicates that this interpolation formula underestimates the true limiting current by over 20 percent in some cases. Furthermore, the corresponding expression for the axial electron energy overestimates the true "limiting energy" by more than an order of magnitude in some cases. For

14

example, in the limit of a fat (i.e., $3 + 2 \ln b/a < < \gamma_0^{2/3}$), ultrarelativistic electron beam, we find

$$\gamma_{cL} \sim \sqrt{\frac{1}{2}\left(\ln \gamma_0 + 1 + 2 \ln \frac{b}{a}\right)} < < \gamma_0^{1/3}.$$

Since this limiting current problem is of such broad relevance to various electron beam applications, we feel that our theoretical analysis under this AFOSR contract, supplemented by numerical calculations and ultrarelativistic theory under contract DASG60-76-C-0045, will be considered an important contribution to this field of research. For example, schemes have recently been proposed by Miller, et. al. at AFWL, Kirtland AFB, New Mexico for the collective acceleration of ions which rely on the controlled motion of a virtual cathode (where $\gamma_c = 1$ and some center electrons are reflected) created in an intense relativistic electron beam. Since virtual cathode formation occurs due to excess space charge slowing soon after $I > I_L$, and since the incremental distance to formation of the virtual cathode is dependent on γ_{cL}, it is desired to know both I_L and γ_{cL} accurately in designing the motion of the virtual cathode. We believe that our calculations fill this need, and we have in fact been

informed by Miller that good agreement has been observed between our predictions for the limiting current threshold and relativistic particle simulations of virtual cathode formation. Our work on this problem appears to complement similar work at AFWL which has been based on a different approach, and has focused more on the case of hollow electron beams.

A fourth problem which we have pursued under this AFOSR contract is the radial structure of linear beam eigenmodes in waveguide geometry. We have begun with a theoretical examination of the influence which a radial dependence in the relativistic factor $\gamma(r)$ has on the structure of the relativistic electron beam cyclotron mode, and this calculation is included as Appendix D herein. Such a radial dependence in $\gamma(r)$ may be created by the above mentioned space charge slowing which occurs non-uniformly when a beam is injected into a waveguide. Knowledge of the radial eigenmode structure is important to almost any application which would exploit the cyclotron waves, including particularly the ion acceleration and microwave generation schemes based on these waves.

It is found in Appendix D that a variational principle can be formulated which allows an accurate determination of the eigenvalues of $k_\perp a$, where 'a' is the radius of a beam bounded by a conducting wall. These eigenvalues are found to increase significantly as $\gamma(r)$ varies from being uniform (as at the anode) to having the asymptotic radial dependence approached far down the waveguide. For instance, the value of $k_\perp a$ for the lowest (no nodes) cylindrically symmetric eigenmode increases from 2.95 to 5.77. Accompanying this increase in $k_\perp a$ is an evolution in the field profiles toward more peakedness at the beam edge. This is particularly true of the radial electric fields and the perturbed perpendicular electron velocities. However, the axial electric fields of the wave do not have a significantly altered radial structure due to the $\gamma(r)$ dependence.

One reason that this calculation is important, is that the larger the eigenvalue $k_\perp a$, the closer is the cyclotron motion of the electrons to resonance with the oscillating fields of the corresponding eigenmode. Hence, the $\gamma(r)$ dependence may significantly alter the threshold

17

for the onset of nonlinearities, and may impose somewhat more stringent restrictions on the beam "temperature" threshold at which Landau damping effects become important. In addition, of course, for many applications the eigenmode structure is relevant in and of itself.

Appendices E and F contain material describing research on relativistic electron beam-plasma heating, which was conducted under our previous AFOSR Contract F44620-72-C-0071 and was reviewed under this present AFOSR Contract F49620-76-C-0002. The material in Appendix E is some previously unpublished lecture notes summarizing some of our conclusions on relativistic electron beam-plasma heating. These notes were compiled for a July 1974 presentation by Dr. Drummond at the Fourth National School on Plasma Physics, Novosibirsk, which was mentioned in reference 1. Appendix F is comprised of three letters in which this beam-plasma heating research is reviewed and in which our conclusions are compared in some respects to those of Thode, et al. (as described in several references listed in the third letter of Appendix F). The primary result is that we

seem to be in agreement that very high density plasmas may be heated with reasonable efficiency by high quality (low angular scatter), high-γ (ultrarelativistic) electron beams, via the primary beam-plasma longitudinal streaming interaction.

In Appendix G we reexamine the problem of the self-consistent equilibria which exist for an unneutralized, relativistic electron beam injected into a cylindrical wave-guide along an external magnetic guide field. One objective of this equilibrium analysis is to determine the self-consistent radial profiles of all equilibrium quantities, including the electromagnetic fields and the number density and flow velocity of the electron beam. These equilibrium properties are in turn needed to determine the linearized eigenmodes (or waves) which may be supported upon the electron beam.

In order to self-consistently compute the various equilibrium quantities, assumptions about the nature of the beam equilibria are required, since many different equilibria are possible in general. It is most accurate to make these assumptions about the conditions of creation of the beam at

19

the cathode, with conservation equations then utilized to complete determination of the equilibrium quantities in the downstream region of the waveguide where the beam energy is to be extracted for the application of interest. In this way the problem of mating the beam to the waveguide is addressed, and the accessibility of the equilibrium is included in the calculation--which would not be the case if ad hoc assumptions were instead made about the downstream equilibrium.

The use of equations for the conservation of particle number, particle energy, and particle canonical angular momentum--which will be valid for all steady state, θ-symmetric electron beams--allows the downstream equilibrium to be linked to the known cathode conditions while avoiding the chore of computing the actual beam trajectories all the way downstream from the cathode. However, even with the aid of such conservation equations, the complete set of equations which determine the beam equilibrium is highly nonlinear in general and mathematically tractable only to numerical computer solution. Fortunately, there exist a number of small

20

parameters which are exploited in Appendix G to obtain an iterative analytical solution for the equilibrium, and these parameters remain small throughout the parameter space anticipated for many electron beam applications. These same small parameters also permit the simplification of the linear theory of waves supported by the electron beam equilibrium. These parameters, and the underlying physical phenomena which they reflect are itemized below.

$$(1) \quad \varepsilon_1 \simeq \left[\frac{I_e(kA)}{5\, B_z(kG)\, a(cm)\, \gamma \beta_z} \right]^2 \quad \text{--Axial Diamagnetism, Relativistic Beam Frame Precession}$$

Because of the electromagnetic self-fields produced by the space charge and current of the unneutralized electron beam, an axial magnetic guide field must be present for equilibrium and the beam must precess in this field with an angular velocity $\beta_\theta(r)c$ to create a $\beta_\theta B_z$ pinch force. However, this θ-precession causes a diamagnetic reduction in the strength of the B_z field witin the electron beam, and the relative magnitude of this reduction is characterized by

21

ε_1. Also, in the beam frame of reference, $\beta_{\theta B}(a) \simeq \varepsilon_1^{1/2}$, so that $\varepsilon_1^{1/2}$ characterizes effects of relativistic precession in the beam frame.

$$(2) \quad \beta_\theta(a) \simeq \frac{\varepsilon_1^{1/2}}{\gamma} \text{ -- } \beta_\theta \times \underline{\tilde{B}} \text{ Forces, } \beta_\theta \tilde{n} \text{ Current Density Sources, } \frac{\beta_\theta}{r} \frac{\partial}{\partial \theta} \text{ Convective Derivative Terms}$$

Because the beam equilibrium contains a zero order θ-velocity, the linearized equations which describe the waves supported by the equilibrium will have a number of complicating terms traceable to this velocity. These terms reflect such physical phenomena as perturbed $\hat{\theta}$ skin currents on the beam, and they can permit resonances at the laboratory frame frequencies of interest which involve $\hat{\theta}$ fluting modes (i.e., $\ell \neq 0$).

$$(3) \quad \varepsilon_2 \simeq \left[\frac{I_e(kA)}{0.7 \ B_z^2(kG) a^2(cm) \gamma \beta_z} \right] \text{ --Centrifugal and Coriolis Forces}$$

Because of the precession of the electron beam, there are outward radial centrifugal forces $\gamma m \beta_\theta^2/r$ which must be

22

contained to achieve an equilibrium, and in the linearized
equations of motion, there are both centrifugal and Coriolis
forces which influence the nature of the waves. Further-
more $\varepsilon_2 \simeq 2\omega_{pe}^2/\gamma^2\Omega_e^2$, where ω_{pe} is the relativistic plasma
frequency and Ω_e is the relativistic cyclotron frequency.
Consequently, $(\varepsilon_2/2)^{1/2}$ characterizes the ratio of the
longitudinal plasma frequency ω_{pe}/γ to the cyclotron
frequency, and hence characterizes the degree of coupling
which exists between these linear eigenmodes.

$$(4) \quad \gamma^{-2} -- \tilde{\beta}_z, \ 1 - \beta_z \quad \text{Longitudinal Beam Compression}$$

When this parameter is small, the beam is ultrarelativistic
in the laboratory frame of reference, and the difference
between the beam velocity $\beta_z c$ and the speed of light c
may be neglected. If β_ϕ is also small, there can be no
longitudinal compression of the beam within linear theory.

$$(5) \quad \frac{\Delta\gamma}{\gamma} \simeq \frac{2\varepsilon_1}{\varepsilon_2} \simeq \frac{I_e(kA)}{17} \frac{1}{\gamma\beta_z}; \quad \frac{\Delta\beta_z}{\beta_z} \simeq \frac{\Delta\gamma}{\gamma^3\beta_z^2} \quad -- \text{Space Charge Limitations}$$

23

These parameters characterize the relative magnitude of
the radial variation in γ and β_z of the beam, which
arises when the central electrons are preferentially
slowed by the space charge forces which oppose the propa-
gation of the beam into a conducting waveguide. If these
parameters are too large, it is even possible for a virtual
cathode to be established in the waveguide, from which
electrons may be axially reflected.

In Appendix G, analytical expressions for the beam
equilibrium quantities are derived through an iterative
process in which the parameters of (1), (2), (3), and (5)
are treated as small but finite. Expressions are obtained
which describe many of the features discussed above. One
interesting result is a generalization of the pencil beam
limiting current formula to the case in which the magnetic
guide field is not infinite:

$$I_L \simeq \frac{mc^3}{e} \frac{(\gamma_o^{2/3} - 1)^{3/2}}{1 + 2 \ln \frac{b}{a} - \frac{1}{4} \varepsilon_1 (\gamma = \gamma_o^{1/3})} \quad .$$

24

This result suggests that the limiting current should increase somewhat as the magnetic field is decreased, which agrees with reported observations from numerical simulations of this problem. However, so long as the parameter ϵ_1 is small, this effect should be weak, and consequently the infinite magnetic field limiting current results of Appendix C should retain their validity so long as $\epsilon_1 \ll 1$.

The phenomena represented by the above five parameters can also significantly effect the linear waves supported by an unneutralized electron beam. Two limits which have often been invoked in prior calculations are the infinite magnetic limit (for studying plasma waves) and the ultrarelativistic limit (for studying cyclotron waves). In the infinite magnetic field limit, the parameters ϵ_1, β_θ, and ϵ_2 are neglected, and the perturbed velocities $\tilde{\beta}_\theta$, $\tilde{\beta}_r$ also tend to zero. Hence the perturbed electron motion is strictly axial in this case, and plasma modes are allowed.

By comparison, in the ultrarelativistic limit, the parameters γ, B_z, and I_e are tended to infinity in

25

such a way that the ratio of any two of these quantities remains finite. In this way, the relativistic cyclotron and plasma frequencies (Ω_e and ω_{pe}) remain finite, but longitudinal mass terms and precessional terms tend to zero. In this limit the parameters ε_1, β_θ, ε_2, and γ^{-2} all are neglected, and the perturbed velocity $\tilde{\beta}_z$ also tends to zero. Hence the perturbed electron motion is strictly transverse in this case, and cyclotron modes are allowed.

In either the ultrarelativistic or the infinite magnetic field limits, there is no coupling between the cyclotron and plasma modes. Also, in neither of these limits are the $\Delta\gamma$ space charge effects intrinsically small, and the radial dependence which they entail greatly complicates the mathematical eigenvalue problem within linear theory. Consequently, we have examined these space charge effects in separate calculations. In Appendix D the space charge effects on the electron cyclotron wave are considered within the ultrarelativistic limit, while in Appendix I the space charge effects on the longitudinal

26

plasma wave are considered within the infinite magnetic field limit.

In Appendix H, the linear theory of collective waves supported by an unneutralized relativistic electron beam is examined in the limit that the parameters ε_1, β_θ, $\Delta\gamma/\gamma$, and $\Delta\beta_z/\beta_z$ are negligible, but the parameters ε_2 and γ^{-2} remain finite. This allows the linear theory to be solved in terms of relatively simple eigenfunctions (i.e., Bessel functions), while retaining the effects of longitudinal compression, centrifugal and Coriolis forces, which are significant for many applications. In this way, the dispersion relation for plasma and cyclotron waves may be derived which retains the coupling effect between these waves. Either the ultrarelativistic or the infinite magnetic limits may still be taken if desired, but at a later stage in the calculation. For both plasma waves and cyclotron waves, the coupling to the other mode is characterized by the ε_2 parameter. For example, the dispersion relation for the negative energy cyclotron wave, subject to certain orderings discussed in Appendix H, may be approximately given by

27

$$\omega - k_z \beta_z c \simeq - \left[\frac{k^4 c^4 \left(\Omega_e^2 - \frac{2\omega_{pe}^2}{\gamma^2} \right)}{(k^2 c^2 + \omega_{pe}^2)^2} + \frac{\omega_{pe}^2}{\gamma^2} \frac{k_\perp^2}{k^2} \right]^{1/2}$$

where $k^2 = k_\perp^2 + k_z^2$. Here the $2\omega_{pe}^2/\gamma^2$ correction term reflects the centrifugal and Coriolis forces, while the $\omega_{pe}^2 k_\perp^2/\gamma^2 k^2$ correction reflects the longitudinal beam compression. These longitudinal plasma wave corrections are in opposite directions, and upon expanding the square root, their net size relative to the cyclotron frequency is seen to be about $\frac{1}{4} \epsilon_2$.

In Appendix I, the $\Delta\gamma$ space charge effects on the longitudinal plasma wave are considered in the infinite magnetic field limit. Previous calculations[7] in the pencil beam limit $\gamma_o^{2/3} << 1 + 2 \, \ell n \, b/a$ had suggested that the normalized plasma wave phase velocity $\beta_\phi \equiv \omega/k_z c$ could only be made small (as desired for ion loading in a Converging Guide Accelerator) by increasing the electron current extremely close to the limiting current which can be

_____

7. R. J. Briggs, Phys. Fluids <u>19</u>, 1257 (1976).

28

propagated without virtual cathode formation. In this Appendix I, we found through both analytical and numerical calculations, that this unfortunate result appears to also hold for more realistic nonpencil beam geometries where the radial variation in the equilibrium quantities γ, β_z, N_e is significant. The plasma wave eigenfunctions were also examined, and found to be somewhat more peaked near the beam axis when the limiting current conditions were approached.

Finally, in Appendix J we have examined the effect of a finite thermal spread in the axial beam velocity on the dispersion relation for the electron cyclotron beam mode in the ultrarelativistic limit. The calculation is performed in slab geometry, and the equilibrium distribution function is taken to be a δ-function in energy with a spread in transverse momentum. This approximates the thermal spread acquired by a relativistic electron beam upon passage through an anode foil. The result which was found is that if the transverse velocity scatter $\overline{v}$ is low enough so that

$$\overline{v}^2 < \frac{2 \; \Omega_e \; \omega_{pe}^2}{k^2 \; k_z c} \simeq \frac{2 \; \omega_{pe}^2}{k^2} \quad ,$$

and if finite Larmor radius effects can be neglected

$$\overline{v}^2 < \frac{\Omega_e^2}{k_\perp^2} \quad ,$$

then the electron cyclotron beam modes will propagate undamped by kinetic effects.

We believe that the results produced under this contract have been substantial, and have relevance to a moderately broad spectrum of problems of interest to the Air Force. We believe that this research has helped to raise the level of understanding of beam interactions to a point that will soon permit the practical and efficient realization of a number of applications, such as collective ion acceleration and microwave generation.

SECTION II

LIST OF PUBLICATIONS AND PRESENTED PAPERS

Some of the research accomplished under this contract was included in the following talks and papers:

1. "Nonlinear Effects on the Cyclotron Mode of a Relativistic Electron Beam,"--Poster Paper 2T3 presented by H. V. Wong, G. I. Bourianoff, and J. R. Thompson at the 18th Annual Meeting of the Division of Plasma Physics of the American Physical Society, San Francisco, California, November 1976.

2. "Ion-Electron Beam Interactions and Nonlinear Effects"--an invited seminar presented by J. R. Thompson at The University of Texas at Austin, Texas, February 28, 1977.

3. "Limiting Currents of An Unneutralized Magnetized Electron Beam in a Cylindrical Drift Tube," J. R. Thompson and M. L. Sloan, Phys. Fluids $\underline{21}$, 2032 (1978). This material was also presented as Poster Paper 5A8 by J. R. Thompson and M. L. Sloan at the 19th Annual Meeting of the Division of Plasma Physics of the American Physical Society, Atlanta, Georgia, November 1977. In addition it was published in the Proceedings of the 2nd International Topical Conference on High Power Electron and Ion Beam Research and Technology, Cornell University, Vol. II, 729 (1977).

4. "A High Current Collective Ion Accelerator,"--Invited Paper R10.5 presented by J. R. Thompson at the Fifth Conference on the Application of Small Accelerators, Denton, Texas, November 1978.

SECTION III

TECHNICAL APPENDICES

A. <u>Nonlinear Effects in Auto-Resonant Acceleration</u>

(This appendix was an internal ARA report, compiled in
September 1976. It is included in its entirety, for the
benefit of the reader; however, the material in Sections
III, V, and a portion of VII of this appendix was sponsored
under Contract F29601-75-C-0046, and has been previously
published. The rest of this appendix describes the
AFOSR-sponsored nonlinear work. This material was also
presented in Paper 2T3 of the 18th Annual Meeting of the
Division of Plasma Physics of the American Physical Society
in November 1976.)

B. <u>Stability of Slab Electron Beam Equilibria</u>

C. <u>Limiting Currents of An Unneutralized Magnetized Electron</u>
<u>Beam In a Cylindrical Drift Tube</u>

(This appendix is the journal publication: J. R. Thompson

and M. L. Sloan, Phys. Fluids 21, 2032 (1978). The material

was also published in Proceedings of the 2nd International

Topical Conference on High Power Electron and Ion Beam

Research and Technology, Cornell University, Vol. II, 729

(1977). The work was partly supported under Contract

DASG60-76-C-0045.)

D. Influence of Spatial Variation in γ on The

Relativistic Electron Beam Cyclotron Mode

E. Relativistic E-Beam Plasma Heating

(This material consists of previously unpublished lecture

notes compiled for a July 1974 presentation at the Fourth

National School on Plasma Physics, Novosibirsk, U.S.S.R.

The work was sponsored under our previous AFOSR Contract

F44620-72-C-0071, and is included here since it was

reviewed under this present contract and is referenced in

the following Appendix F.)

F. Letter Summary of Beam-Plasma Heating Research and

Comparison of Results with those of Thode, et al.

(This material consists of three letters: Brendan B.
Godfrey to James R. Thompson, James R. Thompson to
Richard L. Gullickson, and James R. Thompson to Brendan
B. Godfrey. It contains a review and comparison,
accomplished under this contract, of prior beam-heating
research.)

G. Self Consistent Equilibria of Unneutralized Relativistic
Electron Beams

H. Linear Theory of Collective Waves Supported by an
Unneutralized Relativistic Electron Beam

I. Linear Theory of Plasma Waves Supported by a Radially
Varying Electron Beam in a Magnetized Waveguide

J. The Effects of Finite Thermal Spread on the Electron
Cyclotron Beam Modes

APPENDIX A

NONLINEAR EFFECTS IN AUTO-RESONANT ACCELERATION

by

W. E. Drummond
J. R. Thompson
H. V. Wong
G. I. Bourianoff

(Appendix A Contains 74 Pages)

35

TABLE OF CONTENTS

NONLINEAR EFFECTS IN AUTO-RESONANT ACCELERATION

by

W. E. Drummond
J. R. Thompson
H. V. Wong
G. I. Bourianoff

Austin Research Associates, Inc.

I. INTRODUCTION

In recent years, a number of collective ion accelera-
tion methods have been proposed. In 1973, a passively con-
trolled method (known as Auto-Resonant acceleration) of
collectively accelerating ions within the potential troughs of
a negative energy mode of the electron beam was suggested,[1,2]
which appears to afford the possibility of producing up to
kiloamperes of ion current, at relativistic ion energy, with
pulse durations which might be an appreciable fraction of
the electron beam pulse duration. Among the attractive
features of this concept are the following:

(i) the collective feature allows fairly large

accelerating electric fields of order MV/cm,

permitting reasonably short accelerators;
in addition the collective fields of the
electron beam permit substantial ion currents
in the range of 0.1 - 1 percent of the electron
current to be produced without unacceptable
performance degradation;

(ii)   the use of a travelling body wave of the
electron beam, rather than a localized
potential depression, permits the acceleration
of a quasi-continuous train of ions throughout
a major portion of the electron beam pulse
duration; in addition, the ion energy per
particle can be raised to a level bounded
theoretically only by the ion-to-electron mass
ratio times the electron energy per particle;

(iii)   the passive method of controlling the accelera-
tion of the wave (and ions) avoids technological
switching difficulties; and

(iv)   the negative energy feature of the wave permits
the electron beam to automatically supply power
both for accelerating the ions and for sustaining

-2-

the electric potential of the travelling

wave as it accelerates the ions.

Although one or another of these features are common to

various other schemes of ion acceleration, in combination

they seem to be unique to Auto-Resonant acceleration.

The negative energy electron beam mode which was

selected for Auto-Resonant acceleration was the lower (slower)

electron cyclotron eigenmode. This mode was selected because

it alone seemed to possess the desired characteristics of a

phase velocity which could be varied from a value much less

than c (the speed of light) to near the beam velocity, as

well as a simple method of passively controlling the phase

velocity: flaring the guide magnetic field to spatially

reduce its strength.

Although the central features of this accelerator

concept are embodied in a single "accelerator section"

wherein the magnetic field strength is reduced to accelerate

the cyclotron wave, a number of other sections or components

will be necessary to complete a practical accelerator system.

These components may be conceptually itemized as follows:

(1) High-voltage power supply

(2) Electron-beam diode

(3) Beam-compression/tailoring section (optional)

(4) Cyclotron wave-growth section

(5) Ion loading section

(6) Ion-wave accelerator section

(7) Accelerator termination

Since these components are intrinsically interrelated, a program of theoretical support for the construction of such a system must encompass each of these areas. We describe herein the results of only a small portion of such theoretical research, concerning nonlinearities in the cyclotron wave amplitude, which may affect the central components (4), (5), and (6).

Naturally much of the early calculations of the Auto-Resonant Accelerator have been based upon linear analysis of the electron cyclotron mode, which is valid when the mode amplitude is sufficiently small. For example, the detailed investigation of various means of growing the cyclotron eigenmode has been conducted within linearized theory, as

-4-

has the analysis of ion loading and acceleration. However, it is of interest to determine the mode amplitude level at which nonlinear effects first become important for a number of reasons:

(1) the successful functioning of the accelerator for nonlinear wave amplitudes has not yet been theoretically established (or disproven);

(2) nonlinear effects may well cause saturation of the linear growth mechanisms, establishing an upper bound to the achievable mode amplitude;

(3) theoretical knowledge of such nonlinear saturation amplitudes and mechanisms is needed for comparison with computational and experimental investigations; and

(4) knowledge of the magnitude and parameter scaling of nonlinear mode amplitudes is a valuable design tool, since this information bears heavily on the required length of both the growth and acceleration sections of the accelerator.

Therefore we have examined situations where the amplitude of the electron cyclotron mode increases, such as

-5-

for an electron-ion instability or an electron-waveguide
instability, to determine the amplitude level at which
nonlinearities become important. The latter case may
include either a resistive liner interaction, where the
resistance allows the negative energy cyclotron mode to
grow in amplitude, or else an interaction between beam
modes and modes supported by some form of surrounding slow
wave structure. Such interactions are relevant as possible
growth mechanisms for the cyclotron mode prior to ion load-
ing and wave acceleration.

On the other hand, interaction between the electron
beam and the subject ions is also of interest as possible
mechanism for both wave growth and ion loading, provided
that the growth saturates via ion trapping. This possibility
has been considered by Indykul, et al.,[3] whose analysis was
supported by a one-dimensional, single wave computer calcula-
tion of the nonlinear ion dynamics. In addition, electron-ion
interaction will also occur during the process of accelera-
tion, when it has no desired purpose, but must be assessed to
determine how disruptive the interaction is on the electron
beam and on the acceleration process. This electron-ion

-6-

interaction problem has been selected as the vehicle of our detailed nonlinear calculations, although some of the results are also relevant when the cyclotron mode is excited in a different fashion.

The influence of nonlinear effects may be broadly characterized in two different ways, and our results have been divided into the resulting four categories as shown on the chart below:

	Electron Effects	Ion Effects
Violation of primary conditions for linearity	Section III	Section IV
Growth saturation without violating primary linearity conditions	Section V	Section VI

The first division separates nonlinearities which influence the electron-wave dynamics from those which influence the ion-wave dynamics. For example, the Indykul calculation

-7-

would encompass only ion nonlinearities since the electrons were "legislated" to obey linear theory; likewise, an electron-waveguide instability can manifest only electron nonlinearities.

The second division separates those cases where it is possible to construct a nonlinear theory which retains its validity to the point of growth saturation, so that the saturation amplitudes are known precisely, from cases for which linear approximations breakdown before a saturation mechanism appears. In this latter circumstance, experience frequently suggests a correlation between wave-growth saturation and the breakdown of linear approximations, which can often be substantiated by computer simulations or by experiment.

Before describing our analytical results, we first describe briefly our approximations and the linear theory of the electron cyclotron wave.

II. APPROXIMATIONS AND LINEAR THEORY

Below are definitions of the symbols and notation which has been used:

(x,y,z) = coordinates of slab geometry

$\hat{z}$ = unit vector in the axial direction

$\hat{x}$ = unit vector in the radial direction, normal to the beam and waveguide boundaries

$\hat{y}$ = unit vector in the transverse, ignorable direction

b = radius (half-width) of the conducting waveguide

c = speed of light

B_{oz} = external magnetic guide field

E_{ox} = DC self electric field of the electron beam

B_{oy} = DC self magnetic field of the electron beam

Φ_o = DC self electric potential of the electron beam

$(\tilde{E}_x, \tilde{E}_y, \tilde{E}_z)[\text{or}(E_x, E_y, E_z)]$ = perturbed components of the wave electric field

$(\tilde{B}_x, \tilde{B}_y, \tilde{B}_z)[\text{or}(B_x, B_y, B_z)]$ = perturbed components of the wave magnetic field

-9-

$\tilde{A}^{\pm}$ (or $A^{\pm}$) = certain linear combinations of $\tilde{E}_x$, $\tilde{E}_y$, $\tilde{B}_x$, $\tilde{B}_y$

$\tilde{\Phi}$ (or Φ) = perturbed electric potential function

k_z (or k_o) = axial component of the wave vector

κ^+ (or $k_\perp$) = radial component of the wave vector

k^2 = $k_\perp^2 + k_o^2$

ω (or ω_o) = frequency of the electron cyclotron wave

$-e, m$ = electron charge, mass

n_o = mean electron number density

a = electron beam radius

$u_o = \beta_o c$ = DC electron axial flow velocity

γ_o = $(1 - \beta_o^2)^{-1/2}$ = DC electron γ-factor

$v_{oy}(x)$ = mean transverse electron drift for radial equilibrium

ω_p = $(4\pi n_o e^2 / \gamma_o m)^{1/2}$ = relativistic electron plasma frequency

Ω = $(e B_{oz} / \gamma_o mc)$ = relativistic electron cyclotron frequency

$\delta\omega$ = $\Omega \omega_p^2 / k^2 c^2$ = width of cyclotron resonance

$\tilde{n}$ = perturbed electron density

$\tilde{x}$ = perturbed radial electron coordinate

$\tilde{\beta}_x c$ = perturbed radial electron velocity

$\tilde{\beta}_z c$ = perturbed axial electron velocity

$\tilde{\gamma}$ = perturbed electron γ-factor

-10-

e, M = ion charge, mass

$N_i(\underline{x}, t)$ = total ion number density

$\bar{n}_{oi}$ = mean ion number density

a_i = radius of ion distribution

x_{oi} = radial coordinate of equilibrium ion motion

v_{ox} = radial velocity of equilibrium ion motion

ω_B = $(4\pi n_o e^2/M)^{1/2}$ = radial bounce frequency of an ion the self electric field E_{ox} of the electrons

ω_{Bz}, ω_{Bx} = $k_z, k_\perp [e\tilde{\Phi}(0)/M]^{1/2}$ = axial, radial bounce frequency of ion in the wave electric field

ω_{pi} = $(4\pi \bar{n}_{oi} e^2/M)^{1/2}$ = ion plasma frequency

Ω_i = $(e B_{oz}/Mc)$ = ion cyclotron frequency

$\tilde{n}_i$ (or n_i) = perturbed ion density

$\tilde{x}_i$ = perturbed radial ion coordinate

$\tilde{v}_x$ = perturbed radial ion velocity

$\tilde{v}_z$ = perturbed axial ion velocity

$\tilde{J}$ (or J)   = perturbed total current density

$\tilde{\rho}$ (or ρ)   = perturbed total charge density

Γ = linear growth rate of electron cyclotron wave

$\Delta\omega$ = nonlinear frequency shift of the electron cyclotron wave

Perturbed quantities with a tilde (e.g., $\tilde{E}_x$) are representations in the usual configuration space, while those without

-11-

the tilde (e.g., E_x) are representations of the Fourier coefficients for the basis functions $\exp(-i\omega t + ik_z z)$. Also, the quantities ω, k_z, κ^+ are the frequency/wavenumber components for a general wave, while ω_0, k_0, $k_\perp$ are the particular values existing for a pure electron cyclotron mode.

As a basis for the nonlinear calculations to be described later, we first consider a slab model equilibrium in which a cold relativistic electron beam of uniform density n_0 propagates with uniform velocity $u_0 \to c$ along a uniform guide field B_{oz} in the z-direction, and interacts with a sparse group of ions whose axial velocity is zero. For ready reference, a number of the approximations or restrictions which underlie this calculation are listed below.

$$\frac{\partial}{\partial z} = \frac{\partial}{\partial t} = 0 \quad \text{for equilibrium} \tag{1}$$

$$\frac{\partial}{\partial y} = 0 \quad \text{for both equilibrium and waves} \tag{2}$$

$$\tilde{E}_z(x) = \tilde{E}_z(-x) \tag{3}$$

$$\omega_o^2 < k_o^2 c^2 \simeq \Omega^2 \tag{4}$$

$$k_o^2 a^2 + \frac{\omega_p^2 a^2}{2c^2} \simeq \frac{\Omega^2 a^2}{c^2} + \frac{\omega_p^2 a^2}{2c^2} \lesssim \mathcal{O}(1) < k_\perp^2 a^2 \tag{5}$$

$$\frac{b-a}{a} < 1 \tag{6}$$

$$\frac{\partial n_o}{\partial x} = \frac{\partial \gamma_o}{\partial x} = 0 \tag{7}$$

$$\gamma_o > 1, \quad \beta_o \simeq 1, \quad \tilde{\beta}_z < 1 \tag{8}$$

$$\frac{\omega_p^2 a}{\gamma_o \Omega c} < 1 \tag{9}$$

$$\frac{\omega_p^2}{\gamma_o^2 \Omega^2} < 1 \tag{10}$$

$$\frac{\bar{n}_{oi}}{n_o} < \gamma_o^{-2} \tag{11}$$

$$\frac{\Gamma}{\omega_B} \sim \left[\frac{(\bar{n}_{oi}/n_o)}{8(\gamma_o m/M)^{1/2} (\Omega/\omega_p)} \right]^{1/2} < 1 \qquad (12)$$

$$\frac{2\omega_B}{\Omega} = 2(\gamma_o m/M)^{1/2} (\omega_p/\Omega) < 1 \qquad (13)$$

$$\frac{\Omega_i}{\omega_B} = (\gamma_o m/M)(\Omega/\omega_p) < 1 \qquad (14)$$

$$\frac{\Gamma}{\delta\omega} \sim \left[\frac{(\bar{n}_{oi}/n_o)}{8(M/\gamma_o m)^{1/2} (\Omega^3 \omega_p/k^4 c^4)} \right]^{1/2} < 1 \qquad (15)$$

$$\frac{\Gamma(\text{axial ion response})}{\Gamma} \sim \left[\frac{0.08(\gamma_o m/M)^{1/2}(\Omega^5 a^4/\omega_p c^4)}{(\bar{n}_{oi}/n_o)} \right]^{1/6} < 1 \qquad (16)$$

(It is desired that these inequalities be well satisfied.)

-14-

Both the electron beam and the ions are assumed to be infinite in the z- and y-directions, but are bounded by conducting plates at $x = \pm b \simeq \pm a$; Eq. (6) avoids the need for a multiple region calculation.

The electron beam dynamics is described by the cold fluid equations:

$$\frac{\partial n}{\partial t} + \nabla \cdot (n\underline{v}) = 0$$

$$\frac{d}{dt} m(\gamma \underline{v}) = -e\underline{E} - \frac{e}{c}(\underline{v} \times \underline{B}) \tag{17}$$

with closure obtained through the usual Maxwell equations.

The velocities and electromagnetic fields of the beam equilibrium are

$$\underline{v}_o = \left(0, \ v_{oy} = \frac{4\pi n_o e c x}{B_{oz} \gamma_o^2} \to 0, \ u_o\right)$$

$$\underline{E}_o = \left(E_{ox} = -4\pi n_o e x, \ 0, \ 0\right) \tag{18}$$

$$\underline{B}_o = \left(0, \ B_{oy} = -\frac{4\pi n_o e u_o x}{c}, \ B_{oz}\right)$$

-15-

The electrons are assumed ultrarelativistic, according to Eqs. (8) - (10), which allow neglect of the transverse drift velocity v_{oy} as well as the diamagnetic corrections to the guide magnetic field. The electron equilibrium is assumed uniform, as indicated in Eq. (7).

If we subject this equilibrium to small amplitude perturbations, electron beam-cyclotron modes propagate along the beam. These cyclotron modes will be largely decoupled from the longitudinal plasma modes due to the high-γ assumptions, and they are the subject of this linear analysis. Let us define the new variables

$$\tilde{A}^{\pm} = \tilde{E}_x \pm i\,\tilde{E}_y \pm i\,\frac{u_o}{c}\,(\tilde{B}_x \pm i\,\tilde{B}_y)$$

From Maxwell's equations, we obtain the following equation for $\tilde{A}^{\pm}$.

$$\left(\nabla^2 - \frac{1}{c^2}\frac{\partial^2}{\partial t^2}\right)\tilde{A}^{\pm} = 4\pi\left(\frac{\partial}{\partial x} \pm i\,\frac{\partial}{\partial y}\right)\left(\tilde{\rho} - \frac{u_o}{c^2}\tilde{J}_z\right)$$

$$+ \frac{4\pi}{c^2}\left(\frac{\partial}{\partial t} + u_o\,\frac{\partial}{\partial z}\right)\left(\tilde{J}_x \pm i\,\tilde{J}_y\right) \tag{19}$$

-16-

where the boundary conditions on $\tilde{A}^{\pm}$ at $x = \pm a$ are:

$$\tilde{A}^+ = \tilde{A}^-$$

$$\frac{\partial \tilde{A}^+}{\partial x} + \frac{\partial \tilde{A}^-}{\partial x} = 8\pi \left(\tilde{\rho} - \frac{u_o}{c^2} \tilde{J}_z \right) \tag{20}$$

If we restrict the analysis to perturbation with no variations in $y (\partial/\partial y = 0)$, and consider perturbations of the form $\exp(-i\omega t + i k_z z)$, then from Eq. (17) and Eq. (19), we obtain:

$$\left(\frac{\partial^2}{\partial x^2} + \kappa^{\pm 2} \right) A_o^{\pm} = 0 \tag{21}$$

where

$$\kappa^{\pm 2} \equiv - k_z^2 + \frac{\omega^2}{c^2} - \frac{\omega_p^2 (\omega - k_z u_o)}{c^2 (\omega - k_z u_o \pm \Omega)} \tag{22}$$

Assumption (8) allows neglect of the perturbations in the axial electron velocity because of the large longitudinal mass. Likewise, the electron high-γ_o assumptions imply that $\tilde{\rho}_e - (u_o/c^2) \tilde{J}_{ze} \to 0$ and may be neglected.

-17-

Solving Eq. (21) subject to assumptions (4), (5),
and the boundary conditions (20), yields the dispersion
relation for the electron beam cyclotron mode ($\omega = \omega_o$,
$k_z = k_o$, $\kappa^+ = k_\perp$) symmetric in E_z:

$$\omega_o = k_o u_o - \frac{\Omega\, k^2\, c^2}{(k^2\, c^2 + \omega_p^2)}$$

$$k^2 = k_o^2 + k_\perp^2 \tag{23}$$

$$\tan k_\perp a = - k_\perp a$$

Here assumption (4) for nonrelativistic wave speed tends to
be justified for these interactions with ions, and permits
simplification of the cyclotron eigenfunctions by decoupling
the light modes. Assumption (5) implies strong decoupling
of the positive and negative energy cyclotron modes, which
also simplifies the cyclotron eigenfunctions.

For the lowest modes, $\kappa^+ a = k_\perp a \approx 2$, 4.9, 8, ...
The eigenfunctions are

$$A_o^+(x) = A_o \sin \kappa^+ x$$

$$A_o^-(x) = A_o \frac{\sin \kappa^+ a}{\sin \kappa^- a} \sin \kappa^- x \qquad (24)$$

$$\approx A_o \frac{x}{a} \sin \kappa^+ a \quad .$$

Letting $A_o = |A_o| e^{i\varphi}$, it may be shown that the perturbed electric potential function is

$$\tilde{\Phi}(\underline{x},t) \simeq - \left(\frac{k_\perp c^2 |A_o|}{\Omega^2} \right) \cos k_\perp x \cos (k_o z - \omega_o t + \varphi) \qquad (25)$$

so that

$$\left| \frac{e\tilde{\Phi}(0)}{\gamma_o mc^2} \right| = \left| \frac{k_\perp e A_o}{\gamma_o m \Omega^2} \right| \qquad (26)$$

and the corresponding perturbed electric fields are

$$\tilde{E}_z = - \frac{\partial}{\partial z} \tilde{\Phi} , \qquad \tilde{E}_x = - \frac{\partial}{\partial x} \tilde{\Phi} \qquad (27)$$

As indicated by assumption (3) we are considering only those waves symmetric in $\tilde{E}_z(x)$. Qualitatively similar results may easily be derived for the antisymmetric waves.

-19-

If a small fraction of ions with mean density $\bar{n}_{oi}$ is introduced into the electron beam, electron-ion streaming instabilities occur due to coupling of electron beam-cyclotron modes to the ion motion. Assumption (11) insures that the equilibrium is not appreciably affected by the ions, and we obtain for $A^{\pm}$:

$$\left(\frac{\partial^2}{\partial x^2} + \kappa^{\pm 2} \right) A^{\pm} \approx 4\pi e \frac{\partial}{\partial x} n_i(x) \tag{28}$$

where $n_i(x)$ is the perturbed ion density.

Equation (28) may be solved by first order perturbation expansion about the cyclotron mode. Let

$$A^{\pm}(x) = A_o^{\pm} + A_1^{\pm} + \ldots$$

$$\omega = \omega_o + \omega_1$$

$$k_z = k_o + k_1$$

where

$$A_1^{\pm} < A_o^{\pm}, \quad \omega_1 < \omega_o, \quad k_1 < k_o,$$

and $A_o^{\pm}$ is given by Eq. (24).

The most stringent condition for the convergence of this perturbation expansion is obtained from the perturbation

of the quantity κ^{+2}, defined in Eq. (22). This convergence condition eventually leads to Eq. (15) that the growth rate Γ be less than $\delta\omega \equiv \Omega \omega_p^2 / k^2 c^2$.

By subtracting Eq. (21) from Eq. (28), and forming a Rayleigh-Ritz integral to avoid solving for the first order eigenfunctions $A_1^{\pm}$, we obtain

$$
\int_{-a}^{+a} dx \, A_o^{+*}(x) \left[\omega_1 \frac{\partial}{\partial \omega_o} \kappa^{+2} + k_1 \frac{\partial}{\partial k_o} \kappa^{+2} \right] A_o^{+}(x)
$$

$$
\approx 4\pi e \int_{-a}^{+a} dx \left[A_o^{+*}(x) + A_o^{-*}(x) \right] \frac{\partial}{\partial x} n_i(x)
$$

(29)

To complete the dispersion relation, we need the perturbed ion density $n_i(x)$.

Since the ions will be non-relativistic in the laboratory frame of the calculation, the dominant forces on the ions are those due to the electric fields, and in the limit of Eq. (5), $\kappa^{+2} \equiv k_\perp^2 > k_z^2$, and the E_x-component is the largest. Thus, we obtain for the ion dynamics:

-21-

$$\frac{dx}{dt} = v_x$$

(30)

$$\frac{dv_x}{dt} = - \omega_B^2 x + \frac{e}{M} \tilde{E}_x (x,z,t)$$

where the term $- \omega_B^2 x$ is the radial restoring force due to the self-electric field E_{ox} of the electron beam, and the perturbed electric field is $\tilde{E}_x$ of Eq. (27).

For sufficiently high ion density and for low magnetic field strength, the growth rate of these ion-electron cyclotron interactions can exceed the perpendicular bounce frequency ω_B and these equilibrium oscillations may be ignored. However, for electron beam and magnetic field parameters typical of state of the art experimental facilities, this may require ion loading corresponding to kiloamperes of output ion current. Hence, we shall not discuss this regime herein, but will address the more likely regime of lower ion density, where the growth rate is below ω_B as in Eq. (12), and the perpendicular ion oscillations are very important. However, it will also generally be true that $2 \omega_B < \Omega$ as in Eq. (13), so that the cyclotron wave phase velocity is non-relativistic

-22-

and the wave number k_o is not much perturbed from the value $\Omega/\beta_o c$. In addition, $\Omega_i < \omega_B$ as in Eq. (14), so that the ion coupling to the guide field is truly negligible.

From the linearized Vlasov equation for the ions, we determine the perturbed ion density, assuming it to be dominated by the transverse ion dynamics. After substitution in the right hand side of Eq. (29), we obtain the dispersion relation

$$a(1 + \alpha s^2 k_\perp a) \; \frac{k^4 c^2}{\omega_p^2 \Omega} \left[-\omega_1 + k_1 u_o \right]$$

$$= - \frac{4\pi^2 e^2 k_\perp^2}{M \, k_o^2} \int_0^a d\alpha \; \frac{\partial g_o}{\partial \alpha} \; \frac{\ell \, J_\ell^2(k_\perp \alpha)}{\omega_1} \quad (31)$$

where

$$\alpha^2 = x^2 + \frac{v_x^2}{\omega_B^2} \; ,$$

and the equilibrium ion distribution function is $F_o = g_o(\alpha) \, \delta(v_y) \, \delta(v_z)$. To satisfy the condition for resonant interaction between the ion modes and the cyclotron mode, one selects $\omega_o = \ell\omega_B$, where ℓ is an even integer, and

-23-

$k_o u_o \approx [(k^2c^2)/(k^2c^2 + \omega_p^2)] \Omega + \ell\omega_B$ from the zero order

dispersion relation (23).

An equilibrium ion distribution for which all ions

have the same energy and the same radial turning points is

given by

$$g_o(\alpha) = \frac{2 \bar{n}_{oi} a_i}{\pi \, \omega_B} \, \delta(\alpha^2 - a_i^2) \tag{32}$$

where $\bar{n}_{oi}$ is the average ion density, and $a_i \leq a$ is the

amplitude of the equilibrium ion trajectory. The equilibrium

ion density function will be peaked near the turning points

$x = \pm a_i$.

From Eq. (31),

$$\omega_1 - k_1 u_o \approx - \frac{2 \ell \omega_{pi}^2 \omega_p^2 J_\ell(k_\perp a_i) J'_\ell(k_\perp a_i)}{\omega_1 \omega_B \Omega k_\perp a (1 + \cos^2 k_\perp a)}$$

$$\equiv - \frac{\Lambda_o^2}{\omega_1} J_\ell(k_\perp a_i) J'_\ell(k_\perp a_i)$$

where

$$\Lambda_o^2 = \frac{2 \ell \omega_{pi}^2 \omega_p^2}{\omega_B \Omega k_\perp a (1 + \cos^2 k_\perp a)}$$

-24-

For maximum growth, $k_1 = 0$, and

$$\Gamma \equiv \operatorname{Im} \omega_1 = \Lambda_o \left[J_\ell(k_\perp a_i) \; J'_\ell(k_\perp a_i) \right]^{1/2} \tag{33}$$

An alternate choice for the equilibrium ion distribution, for which the ion density is parabolic in x, peaked about the beam center, is

$$g_o(\alpha) = \frac{2 \, \bar{n}_{oi}}{\pi \, \omega_B a_i} \; \Theta(a_i - \alpha) \tag{34}$$

where Θ is the unit step function. For this distribution, the maximum growth rate is given by

$$\Gamma = \Lambda_o \left[\frac{J_\ell^2(k_\perp a_i)}{k_\perp a_i} \right]^{1/2} \tag{35}$$

which is fairly close to the prior result.

The assumption that the interaction of the ions is dominated by the transverse ion response rather than the axial response is quantified in Eq. (16) for the case $a_i \simeq a$--which insures that the axial response yield a smaller growth rate. This inequality bounds the magnetic field strength from above and the ion density from below, contrary

-25-

to most of the other restrictions, and tends to require
smaller magnetic fields than Eq. (14).

Conditions (5) and (13) will also insure that
$\Omega \, \omega_B a_i^2 < 4c^2$ so that the influence of $v_{ox} B_{oy}$ forces
on the axial ion motion will not affect the interaction
appreciably.

In addition to the ion-electron cyclotron inter-
actions which we are considering, there may be longitudinal
ion-electron plasma interactions and transverse Weibel-like
interactions which can occur for $k_z \to 0$. However,
assumption (10) that the longitudinal electron plasma
frequency be below the electron cyclotron frequency, assures
that the plasma and cyclotron modes are well decoupled, and
also that the plasma oscillations occur in the "magnetized"
regime. Consequently the large transverse $k_\perp$-component
indicated in Eq. (5) is sufficient for electromagnetic
effects to stabilize the fastest longitudinal plasma
oscillations for which $k_z \beta_o c \simeq \omega_p/\gamma_o$. There will remain
much slower, longer wavelength plasma oscillations with
$k_z \beta_o c \simeq \omega_{pi}$, but the growth rate of these modes will be

-26-

below the cyclotron mode growth rate under the given assumptions.

For magnetic field strengths large enough to obey Eq. (13) well, the transverse Weibel interactions also appear to be stabilized by the ω_B-oscillations of the ions. Only for smaller magnetic fields would these interactions be unstable with significant growth rates.

Therefore, for the equilibrium conditions and assumptions which have been set forth herein, the fastest ion-electron interaction occurs between modes of transverse ion oscillation in the beam electric field and electron cyclotron modes. To determine the wave amplitude at which nonlinearities become significant, we shall focus on the electron cyclotron dynamics and the ion ω_B-oscillations.

III. BREAKDOWN OF LINEAR ELECTRON BEHAVIOR

In this section, a brief survey is presented of a number of nonlinear electron effects, in which one or another of the primary conditions for linearity is violated. Rough estimates are given of the magnitude and scaling of the mode amplitude level at which these effects become important. Many of the effects may be seen to be related to one another. Although care has been taken to preserve the numerical coefficients, which are presented here for the case of slab geometry, the very nature of these formulae is merely to indicate the level at which linear approximations lose their validity, and this occurs gradually rather than sharply as a function of amplitude. The correlation between the breakdown of linear approximations and wave growth saturation must remain inferential, pending the accumulation of additional theoretical or computational evidence.

In addition to the cyclotron eigenmode structure, which was presented in Eqs. (24) through (27), one may derive from linear theory the expression for the perturbed radial coordinate of an electron:

$$\tilde{x}(x) = \frac{k^2 c^2}{\omega_p^2} \frac{e \, \tilde{\Phi}(0)}{\gamma_o \, mc^2} \frac{\sin k_\perp x}{k_\perp} \tag{36}$$

which is the magnitude of the perturbation amplitude--with

the z, t phase information supressed. Likewise $\tilde{\Phi}(0)$ is

the magnitude of the perturbed electric potential amplitude

at the beam axis $x = 0$. This expression characterizes the

electron particle dynamics in the wave, and shows that

electrons near the beam edge are the most strongly perturbed

for the broadest perpendicular eigenmode (for which $k_\perp \simeq 2/a$).

The various conditions wherein nonlinear effects

become significant are listed below for ready comparison

with one another; a discussion of the different nonlinear

effects follows.

$$\frac{\tilde{n}}{n_o} \simeq \frac{k^2 c^2}{\omega_p^2} \frac{e \, \tilde{\Phi}(0)}{\gamma_o \, mc^2} \geqslant 1 \tag{37}$$

$$k_\perp \tilde{x}_{max} \simeq \frac{k_\perp c \tilde{\beta}_x}{\Omega} \simeq \left| \frac{\partial \tilde{x}}{\partial x} \right|_o \simeq \frac{\tilde{n}}{n_o} \geqslant 1 \tag{38}$$

$$\frac{\tilde{E}_x(0)}{E_{ox}(0)} \simeq k_\perp a \frac{\tilde{E}_{x\,max}}{E_{ox}(a)} \simeq \frac{(k_\perp a)^2}{2} \frac{\tilde{\Phi}(0)}{\Phi_o(a)} \simeq \frac{k_\perp^2}{k^2} \frac{\tilde{n}}{n_o} \geqslant 1 \tag{39}$$

$$\tilde{\beta}_x \simeq \frac{k_z}{k_\perp} \left| \frac{\partial \tilde{x}}{\partial x} \right|_0 \gtrsim 1 \tag{40}$$

$$\frac{\tilde{\gamma}}{\gamma_0} \simeq \tilde{\beta}_x \frac{E_{0x}(a)}{B_{0z}} \left[1 + \left(\frac{k_\perp a}{k^2 a^2} \right)^2 \right]^{1/2}$$

$$\simeq \left(\frac{\omega_p^2 a^2}{k_\perp a \, c^2} \right) \left[1 + \left(\frac{k_\perp a}{k^2 a^2} \right)^2 \right]^{1/2} \frac{\tilde{n}}{n_0} \gtrsim 1 \tag{41}$$

$$\frac{\delta_\gamma |\omega - k_z c \beta_z + \Omega|}{\delta\omega} \simeq \frac{k^2 c^2}{\omega_p^2} \frac{\tilde{\gamma}}{\gamma_0} \simeq \left[\left(\frac{k^2 a^2}{k_\perp a} \right)^2 + 1 \right]^{1/2} \frac{\tilde{n}}{n_0} \gtrsim 1 \tag{42}$$

$$\frac{\delta_\beta |\omega - k_z c \beta_z + \Omega|}{\delta\omega} \simeq \frac{\left[\left(\dfrac{\gamma_0 \, \omega_p^2 a^2}{k_\perp a \, c^2} \right)^2 + 1 \right]^{1/2}}{\gamma_0^2} \left(\frac{\tilde{n}}{n_0} \right)$$

$$+ \frac{k_z^2}{k^2} \frac{c^2}{2 \, \omega_p^2 \, a^2} \left(\frac{k^2 a^2}{k_\perp a} \frac{\tilde{n}}{n_0} \right)^2 \gtrsim 1 \tag{43}$$

Condition (37) prescribes the wave amplitude level at which the electron density fluctuations due to the wave

become comparable with the mean electron density. These density fluctuations will be strongest on axis for this equilibrium where n_0 and γ_0 are uniform in x, and at this wave amplitude the electron density will vary from near zero to around twice the ambient density.

Condition (37) also indicates that these density nonlinearities will be come important at an amplitude level smaller by ω_p^2/k^2c^2 from that for which longitudinal trapping of the electrons by the wave potential would occur.

Condition (38) indicates three other nonlinear effects which enter at the same wave amplitude level. The first of these is the condition that the radial displacement of an electron by the wave be as large as the scale length $k_\perp^{-1}$ characterizing the perpendicular eigenmode structure. This is judged to be more accurate than the criterion for displacements as large as the beam radius, which requires higher wave amplitudes. Equation (36) indicates that the displacements will be largest at about 0.8 times the beam radius. One physical consequence of radial displacements as large as $k_\perp^{-1} \simeq a/2$ is that wall collisions might occur unless a sufficiently wide vacuum gap was available. The

-31-

second condition in Eq. (38) is that finite electron

gyroradius effects become important because of the perpen-

dicular kinetic energy excited by the wave. The third

condition is that the radial motion of the electrons

becomes nonlaminar by virtue of radial "crossings" of

electron trajectories. This may be easily seen to occur

when $|\partial \tilde{x}/\partial x|$ exceeds 1, which occurs first for particles

on axis. These last two conditions in Eq. (38) are

symptomatic of the breakdown of the fluid nature of the

wave due to nonlinear turbulence.

Condition (39) prescribes when the perpendicular

wave electric field exceeds the self radial field of the

beam, which tends to occur first on axis. This requires

a wave amplitude larger than that for density nonlinearity

by only $k^2/k_\perp^2$. Condition (39) also reveals the connection

between these various criteria of nonlinearity and the

measurable ratios such as $\tilde{E}_{x\,max}/E_{ox}(a)$ which are con-

veniently extracted from computer simulations as a diagnostic.

One physical consequence of the nonlinearity suggested by

Eq. (39) is the possibility of electron field emission at

the conductor walls. The self-field E_{ox} is typically much

larger than the threshold amplitude required for field emission, but is in the wrong direction. One might think that if the wave fields became larger than the self-field and had the opposite radial sense, then field emission might result. However, this is a deception of the linear theory which is breaking down, since Poisson's equation shows that even for nonlinear waves, the electrostatic portion of the electric field must always point toward a region of net negative charge. Hence, the only possibility of field emission is due to the inductive or electro-magnetic portion of the electric field, which is small for nonrelativistic phase velocity, or else to the presence of the ions whose density might locally exceed the nonlinearly reduced electron density. Although this criterion for field emission is not quantified herein, we anticipate that the required ion density will be a significant fraction of the electron density, since the electron wave fields are geometrically reduced below their peak value at the walls, and the peak value does not exceed the self-field until $(\tilde{n}/n_o) \gtrsim k^2 a^2 / k_\perp a$ according to Eq. (39).

Condition (40) for the radial electron oscillations in the wave to become relativistic will be stronger than condition (38) only if k_z exceeds $k_\perp$. It is possible that this might be modestly true in the growth section and at the beginning of the accelerator section, but toward the end of the accelerator section k_z will be below $k_\perp$ and $\tilde{\beta}_x \ll 1$.

The significance of the $\tilde{\beta}_x \gtrsim 1$ nonlinearity is that it implies a significant fluctuation $\tilde{\gamma}$ in the electron γ-factor as shown in condition (41). This occurs because the electrons are perturbed by the wave to move with or against the radial self-field of the beam. At the beginning of the accelerator where $\tilde{\beta}_x$ is largest, $E_{ox}(a)/B_{oz}$ is smallest and may be somewhat less than 1. The net product of these terms yields an expression, also shown in Eq. (41), which indicates that $\tilde{\gamma}/\gamma_o$ is generally somewhat less than $\tilde{n}/n_o$.

However, condition (42) indicates that the variation $\tilde{\gamma}/\gamma_o$ is magnified by $k^2 c^2/\omega_p^2$ to produce a variation in the fluid electron cyclotron resonance $|\omega - k_z c\beta_z + \Omega|$ which may be comparable to its ambient value (i.e., $\delta\omega$). This

-34-

nonlinear spreading of the cyclotron resonance occurs due

to the γ-dependence of Ω; it is sometimes called "resonance

broadening." It is also symptomatic of the breakdown of

fluid theory and the conversion of the cyclotron mode to

a kinetic regime due to nonlinear turbulence. Condition

(42) indicates that this nonlinear resonance broadening

effect is felt at wave amplitudes somewhat below those for

density nonlinearity, and hence is the most sensitive

nonlinear effect yet discussed. Experience would suggest

that this resonance broadening would reduce the wave growth

rate when the wave amplitude reaches the level given by

Eq. (42).

Condition (43) gives the corresponding resonance

broadening which occurs due to changes in the axial electron

velocity. The first terms of Eq. (43), which are linear in

the wave amplitude $\tilde{n}/n_o$, are relatively unimportant as

usual for $\gamma_o \gg 1$. However, the last term of Eq. (43),

which is quadratic in the wave amplitude, may be seen to be

more (or less) important than the $\tilde{\gamma}/\gamma$ resonance broaden-

ing, depending on whether $k_z^2 c^2 / 2k^2 \omega_p^2 a^2$ is greater (or

less) than 1. This quadratic term in the wave amplitudes

reflects the perturbation in $\tilde{\beta}_z$ due to linear perturbations in $\tilde{\beta}_\perp$, according to

$$\tilde{\beta}_z \simeq -\frac{1}{2}\tilde{\beta}_\perp^2 + \text{linear terms}$$
$$+ \text{other quadratic terms} \qquad (44)$$

which follows immediately from a perturbation expansion of $\gamma(\beta)$.

The square brackets in conditions (41) through (43) are hybrid representations in which the dominant first term reflects the influence of transverse electromagnetic fields on the electrons, such as $\tilde{\beta}_x E_{ox}$, while the smaller second term shows the influence of the perturbed axial electric field $\tilde{E}_z$.

The mode amplitude at which these nonlinear effects appear is reduced for higher values of k^2, and consequently the higher-k modes should saturate in growth at lower amplitudes than the lower-k modes. Hence, when exciting or growing the cyclotron wave, care should be taken (as in designing computer simulations) that the lowest k mode is not discriminated against by any frequency or wavenumber selection which may be imposed.

Although this list of electron nonlinearities includes a variety of effects, it is by no means complete. As just one further example, the possibility of a nonlinear three-wave decay of the electron cyclotron wave was examined and found to be disallowed by the coupling selection rules.

IV. BREAKDOWN OF LINEAR ION BEHAVIOR

As in the previous section, we here present estimates of the perturbation amplitude level at which certain primary conditions of ion linearity cease to be valid. As before, these estimates are rough, and the inference of wave growth saturation at these wave amplitude levels will again be tentative pending additional theoretical or computational evidence.

The radial ion motion is described by Eq. (30); the zero order ion motion is seen to be simple harmonic oscillation at frequency ω_B, with uniform amplitude $x_{oi} = a_i$ for the distribution of Eq. (32). Any ion distribution symmetric in x will be carried by the zero order particle motion into an equivalent state during one-half bounce period, or π/ω_B. If this time also equals an integral number of wave periods, then the perturbed wave quantities will have also returned to their initial state. Consequently $\ell\omega_B$ are the resonant frequencies of the linear ion-electron cyclotron interaction, where $\ell = 2, 4, 6, \ldots$.

Equation (30) may also be solved for the perturbed ion motion, and the result for the simplest $\ell = 2$ interaction is

$$\frac{\tilde{v}_x}{\omega_B} = \tilde{x}_{i\,max} = \frac{k_\perp^2 c^2}{4\,\Gamma\,\omega_B}\ \frac{e\,\tilde{\Phi}(0)}{Mc^2}\ a_i \quad . \tag{45}$$

The axial ion motion is described by $dv_z/dt \simeq (e/M)\,\tilde{E}_z(x, z, t)$ since conditions (5) and (13) render the $v_{ox}\,B_{oy}$ forces unimportant. This equation may be solved to yield the perturbed axial ion motion

$$\frac{\tilde{v}_z}{c} = \frac{2\,k_o c}{\omega_o}\ \frac{e\,\tilde{\Phi}(0)}{Mc^2} \simeq \frac{\Omega}{\omega_B}\ \frac{e\,\tilde{\Phi}(0)}{Mc^2} \quad . \tag{46}$$

Based upon an examination of the ion dynamics, the following conditions for primary ion nonlinearity may be derived.

$$\frac{\omega_{Bx}^2}{\omega_B^2} = \frac{\tilde{E}_x(0)}{E_{ox}(o)} = \frac{k_\perp^2\,\tilde{\Phi}(0)}{4\pi\,e\,n_o} = \frac{k_\perp^2}{k^2}\ \frac{\tilde{n}}{n_o} \geqslant 1 \tag{47}$$

-39-

$$k_\perp \tilde{x}_{i\,max} = \frac{k_\perp \tilde{v}_x}{\omega_B} = \frac{k_\perp a_i}{4} \frac{\omega_{Bx}^2}{\Gamma\,\omega_B} \geqslant 1 \qquad (48)$$

$$\frac{\omega_{Bz}^2}{\omega_B^2} = \frac{k_z^2}{k^2}\,\frac{\tilde{n}}{n_o} \geqslant 1 \qquad (49)$$

$$\frac{k_o \tilde{v}_z}{\Gamma} = \frac{\omega_{Bz}^2}{\Gamma\,\omega_B} \geqslant 1 \qquad (50)$$

where according to Eqs. (33) or (35), the magnitude of the $\ell = 2$, $a_i = a$ growth rate is about

$$\Gamma \simeq \frac{\omega_{pi}\,\omega_p}{\sqrt{3}\,\Omega\,\omega_B} \qquad (51)$$

The first two conditions (47) and (48) relate to the transverse ion dynamics, while the latter conditions (49) and (50) relate to the axial dynamics. In addition, conditions (48) and (50) are sensitive to the ion density through Γ, while conditions (47) and (49) are not.

-40-

Condition (47) prescribes the wave amplitude level at which the radial ion bouncing near the axis is influenced by the wave fields as much as by the DC self-field of the electron beam. Quantitatively this condition is exactly the same as condition (39). Since the ion-electron interaction is strongly affected by the resonance with DC ion bouncing, one suspects that this wave amplitude would completely alter the coherence of the interaction.

Condition (48) is that the radial displacement of an ion be as large as the scale length $k_\perp^{-1}$ of the perpendicular eigenmode. At this amplitude level, which may be fairly low when Γ is small, one would expect the growth rate to decline as it might when the ions had a transverse "temperature."

Condition (49) is that some ions be longitudinally trapped by the wave. This is the growth saturation mechanism appealed to in the one-dimensional calculation of Indykul, et al.[3] However, it may be seen here to require fairly large wave amplitudes, particularly when k_z is small. This is because at low ion density, the frequency and phase velocity of the unstable wave cease to depend on

$\bar{n}_{oi}$ through ω_{pi} and are instead determined by the frequency ω_B of radial bouncing. Hence the wave speed does not approach closer and closer to the ion speed as $\bar{n}_{oi}$ is reduced. Condition (49) will occur before or after condition (47) according to the ratio $k_z/k_\perp$.

Condition (50) prescribes the wave amplitude level at which the perturbed axial velocity of the ions broadens the resonance at $\omega \approx 2\omega_B$ by an amount comparable to its ambient value (i.e., Γ). This effect will be felt at a wave amplitude lower than that required for longitudinal ion trapping by Γ/ω_B. However, it will not occur before condition (48) so long as the usual ordering $k_z < k_\perp$ is obeyed.

Compared to some of the electron nonlinearities, these ion conditions are not quite as sensitive to high k-values, but two of the ion conditions are sensitive to low ion density and hence can occur in some cases well before the electron nonlinearities.

V. GROWTH SATURATION VIA NONLINEAR
ELECTRON FREQUENCY SHIFT

In this section, we discuss the effects of
nonlinearities in the electron response which produce a
nonlinear shift in the wave frequency of the electron
beam-cyclotron mode. We expect nonlinear frequency shifts
will influence the time evolution of the beam cyclotron
mode since growth is determined by resonant coupling to the
bounce motion of the ions.

It is assumed throughout that a fluid description
of the electron beam is adequate. In evaluating the non-
linear frequency shift, the procedure is to calculate the
nonlinear generation of the zeroth and second harmonic
components of the fundamental mode. The nonlinear inter-
action of the fundamental with these harmonics then leads
to corrections to the linear dispersion relation.

The details of this calculation will not be presented
here. The result obtained for the frequency shift $\Delta\omega$ is

$$\Delta\omega \approx -\frac{\Omega}{8} \frac{k^2 c^2}{\omega_p^2} \left|\frac{e\, k_\perp A_o}{m\, \gamma_o\, \Omega^2}\right|^2 \left[4.15 + 3.33 \frac{k_o^2 c^2}{\omega_p^2}\right]$$

$$\equiv -\Delta\, |A_o|^2 \tag{52}$$

where the fundamental is taken to be the lowest beam

cyclotron mode with $k_\perp a \approx 2$. In deriving Eq. (52), which is

insensitive to the method of exciting the electron cyclotron

mode, we have assumed the primary linearity condition

$$\left|\frac{e\, \tilde{\Phi}(0)}{\gamma_o\, mc^2}\right| = \left|\frac{e\, k_\perp A_o}{m\, \gamma_o\, \Omega^2}\right| < \frac{\omega_p^2}{k^2 c^2} \tag{53}$$

as well as the frequency ordering

$$|\Delta\omega| < \delta\omega = \Omega\, \omega_p^2 / k^2 c^2 \quad . \tag{54}$$

Condition (53) is just the reverse of the nonlinear condition

(37), while condition (54) is a time-ordering criterion

invoked to allow calculation of the "slow" shift in the

wave frequency.

If we denote the complex mode amplitude A_o by

$A_o \equiv a\, e^{i\varphi}$, and insert this nonlinear electron frequency

-44-

shift into the equations describing the growth of the
ion-electron cyclotron instability, then we obtain the
following equation for the time evolution of the mode
amplitude

$$\frac{d}{dt} a\, e^{i\varphi} = \Gamma^2 \int^{t} a\, e^{i\varphi}\, dt' + i\, \Delta\, a^3\, e^{i\varphi} \tag{55}$$

where Γ is the linear growth rate of Eqs. (33) or (35),
and Δ is the frequency shift coefficient of Eq. (52).

Decomposing this equation into its real and
imaginary parts, we obtain:

$$\frac{d^2 a}{dt^2} - \left(\frac{d\varphi}{dt}\right)^2 a = \Gamma^2 a - \Delta\, a^3\, \frac{d\varphi}{dt} \tag{56}$$

$$2\, \frac{d\varphi}{dt}\, \frac{da}{dt} + a\, \frac{d^2\varphi}{dt^2} = 3\, \Delta\, a^2\, \frac{da}{dt} \tag{57}$$

The first integral of Eq. (57) is

$$a^2\, \frac{d\varphi}{dt} - \frac{3}{4}\, \Delta\, a^4 = C \equiv \text{constant} \tag{58}$$

-45-

Asserting the initial condition $d\varphi/dt = 0$ when $\alpha = 0$, we obtain $C = 0$. Finally, substituting $d\varphi/dt$ from Eq. (58) into Eq. (56) yields

$$\frac{d^2\alpha}{dt^2} = \Gamma^2 \, \alpha - \frac{3}{16} \, \Delta^2 \, \alpha^5 \equiv - \frac{dV_1}{d\alpha} \, (\alpha) \qquad (59)$$

Eq. (59) is the equation of motion of a "particle" in a "potential well" $V_1(\alpha)$, illustrated in Figure 1 below. It describes the time evolution of α from given initial conditions $\alpha(0)$ and $d\alpha/dt(0)$.
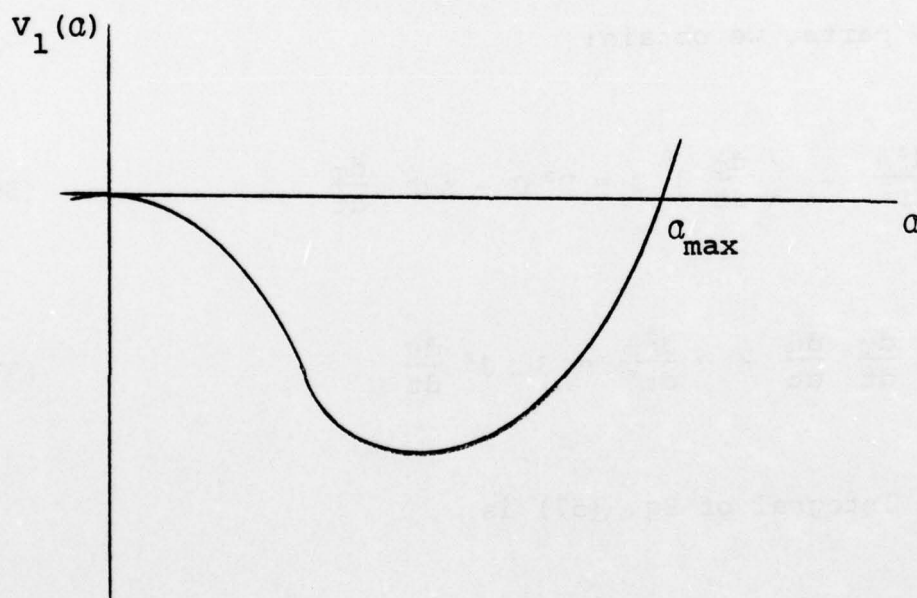

Figure 1. "Potential Well" $V_1(\alpha)$

-46-

For small $\alpha [$i.e., $\alpha < (\Gamma/\Delta)^{1/2}]$, α contains a component growing exponentially with the linear growth rate Γ. However, when $\Delta^2 \alpha^4/16 \simeq \Gamma^2$, $d\alpha/dt = 0$, and growth ceases. Thereafter the amplitude decreases and then may continue to oscillate in time, depending upon the precise choice of initial conditions. The maximum amplitude attained is given by

$$\frac{e \, \tilde{\Phi}_{max}(x=0)}{\gamma_o \, mc^2} = \frac{e \, k_\perp \, \alpha_{max}}{m \, \gamma_o \, \Omega^2} = \left[\frac{32}{\left(4.15 + 3.32 \, \dfrac{\Omega^2}{\omega_p^2}\right)} \, \frac{\omega_p^2}{k^2 c^2} \, \frac{\Gamma}{\Omega} \right]^{1/2}$$

(60)

which corresponds to

$$\left| \frac{\tilde{E}_{x\,max}}{E_{ox}(a)} \right| = \frac{k_\perp^2 \, \alpha_{max}}{k_o^2 \, 4\pi \, n_o \, ea} = \left[\frac{32}{\left(4.15 + 3.32 \, \dfrac{\Omega^2}{\omega_p^2}\right)} \right]^{1/2} \frac{c}{a\omega_p} \left[\frac{\Gamma}{\Omega} \right]^{1/2}$$

$$\approx \frac{1.9 \, \dfrac{c}{a\Omega} \left(\dfrac{\bar{n}_{oi}}{n_o} \right)^{1/4} \left(\dfrac{\gamma_o m}{M} \right)^{1/8} \left(\dfrac{\Omega}{\omega_p} \right)^{1/4}}{\left[\dfrac{\Omega^2}{\omega_p^2} + 1.25 \right]^{1/2}} \quad , \quad (61)$$

-47-

where the growth rate has been inserted for the interaction
with $a_i = a \simeq 2/k_\perp$ and $\ell = 2 = \omega_o/\omega_B$. It may be observed
that this maximum wave amplitude is lower than the lowest
amplitude for electron resonance broadening [given in Eqs.
(42) and (43)] by about (2 to 6) $\sqrt{\Gamma/\delta\omega}$, which tends to be
small due to assumptions (15) and (54).

VI. GROWTH SATURATION VIA PHASE MIXING OF NONLINEAR ION TRAJECTORIES

In this section, we discuss the effects of nonlinearities in the ion response on the time evolution of the unstable electron beam-cyclotron mode.

We again treat the ions as a small perturbation and evaluate the nonlinear trajectories of the ions in the wave-fields of the electron beam-cyclotron mode. Substituting

$$\tilde{E}_x(x, z, t) = - \frac{k_\perp^2}{k_o^2} \, a \, \sin k_\perp x \, \cos (k_z z + \varphi - \omega_o t)$$

in Eq. (30), and defining the new variables α, ξ, τ,

$$x = \alpha \, \sin (\omega_B t + \xi)$$

$$v_x = \alpha \, \omega_B \, \cos (\omega_B t + \xi)$$

$$\tau = \frac{\ell}{\omega_B} \, \frac{k_\perp^3 \, e}{M \, k_o^2} \int_o^t a \, dt'$$

(62)

we obtain from Eq. (30)

-49-

$$\frac{dp}{d\tau} = \frac{\partial H}{\partial q}$$

(63)

$$\frac{dq}{d\tau} = -\frac{\partial H}{\partial p}$$

where

$$H = J_\ell \left(\sqrt{2p} \right) \cos (q + \varphi)$$

$$p = \frac{(k_\perp \alpha)^2}{2}$$

$$q = k_o z + \ell \xi$$

$\omega_o = \ell \omega_B$, and ℓ is even.

In Eq. (63), we have neglected terms which are oscillatory
in t. These equations describe the slow variation of α
and ξ due to the resonant interaction of the ions with the
oscillatory electric field.

Assuming that φ is independent of τ [see Eq. (67)],
H is a constant of the motion. Since p and q must vary
such that $J_\ell (\sqrt{2p})$ and $\cos (q + \varphi)$ never pass through zero,
the variations of p and q are bounded.

-50-

Figure 2 shows a sketch of the ion trajectories in the polar coordinate phase space $(\sqrt{2p}, q)$ due to resonant coupling to modes with frequency $\omega_o = 2\omega_B$. The points given by $J_2'(k_\perp \alpha_s) = 0$, $\sin(q_s + \varphi) = 0$, (i.e. $k_\perp \alpha_s \approx$ 3, 6.7, . . . ; $q_s + \varphi = 0, \pi$) are stable stationary points. The dashed circles have radii $k_\perp x_a$ given by $J_2(k_\perp x_a) = 0$, i.e., $k_\perp x_a \approx 5.1, 8.4, \ldots$. The ion trajectories indicated by the solid lines, are restricted to regions bounded by the dashed circles. The initial equilibrium ion distribution of Eq. (32) would be a circle of radius $\sqrt{2p} = k_\perp a_i$, while that of Eq. (34) would be the interior of the same circle. The conducting boundary is a circle of radius $\sqrt{2p} = k_\perp a$.

If all the ions initially have energy such that $k_\perp x_i < k_\perp a$, 5.1:

     (a) The ion trajectories eventually intersect the wall due to interaction with the lowest beam cyclotron mode $k_\perp a = 2$;

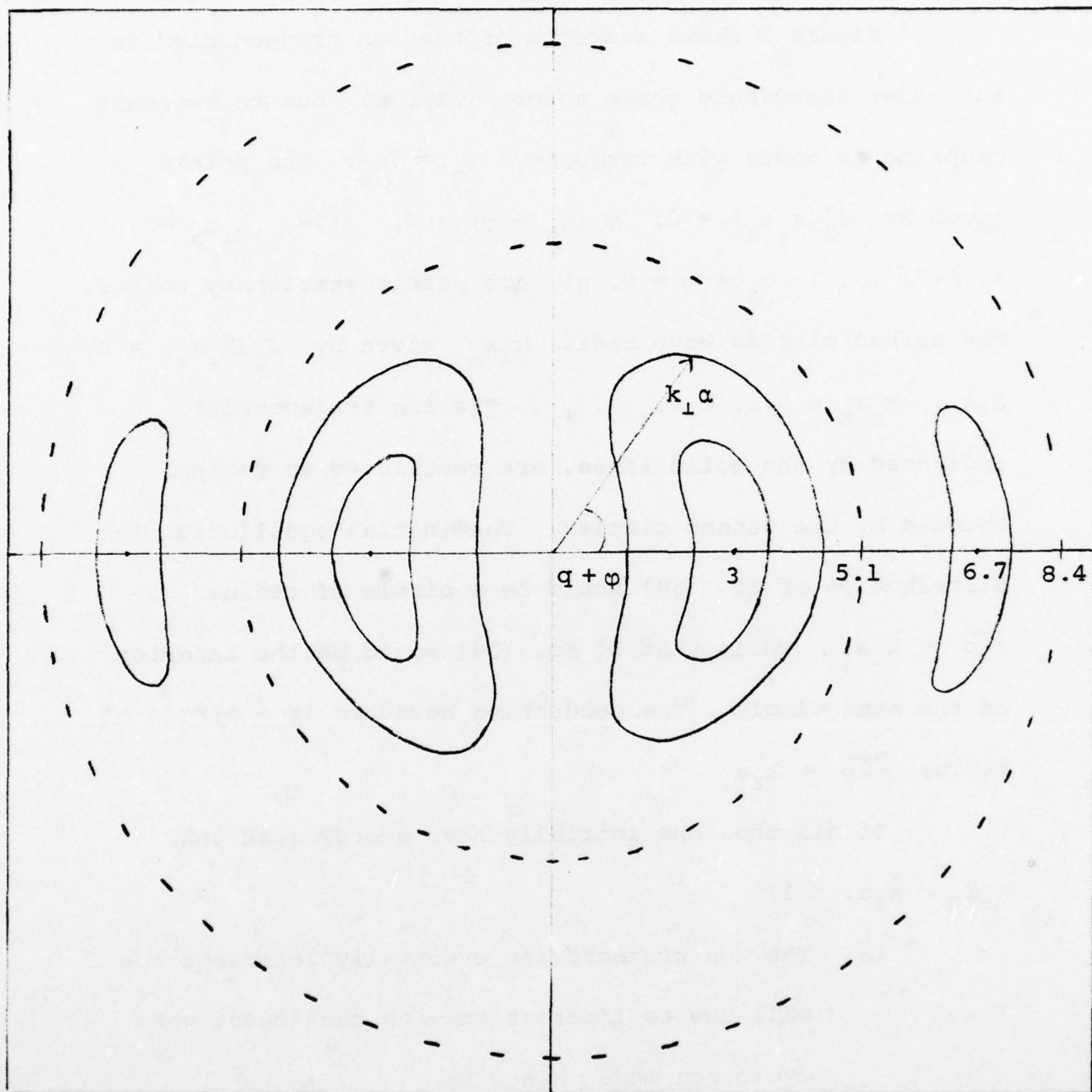   (b) A small fraction of the ion trajectories intersects the wall when $k_\perp a = 4.9$;

Figure 2. Ion Trajectories in the Polar Coordinate Phase Space
$[\sqrt{2p} = k_{\perp}\alpha, \quad q+\varphi]$

(c) The ion trajectories do not intersect the wall

when $k_\perp a = 8$, or for higher $k_\perp$ modes.

From Eq. (63), we obtain for p:

$$\frac{dp}{d\tau} = \pm \left[J_\ell^2(\sqrt{2p}) - Q^2 \right]^{1/2} \tag{64}$$

where $Q \equiv$ constant. This equation can be solved by
quadrature with the initial conditions

$$p = p_o \equiv \frac{(k_\perp \alpha_o)^2}{2}, \quad q = q_o \equiv k_o z + \ell \xi_o$$

at "time" $\tau = 0$.

Since $g_o = g_o[\alpha_o(x, v_x)]$ is the initial ion distri-
bution of the ions, the ion density at time t is given by

$$N_i(x, z, t) = \int_{-\infty}^{+\infty} dv_x \, g_o\left[v_{ox}(x, z, v_x, t), x_o(x, z, v_x, t) \right] \tag{65}$$

where (x_o, v_{ox}) is the point in phase space at time t = 0
which arrives at (x, v_x) at time t.

The contribution of the perturbed ion density to the right hand side of Eq. (29) is given by

$$I \equiv \mathop{\mathcal{L}t}\limits_{L \to \infty} \; 4\pi e \; \alpha \int\limits_{-a}^{+a} dx \; \sin k_\perp x \int\limits_{-\frac{L}{2}}^{\frac{L}{2}} \frac{dz}{L} \int\limits_{0}^{T} \frac{dt}{T}$$

$$\left\{ e^{i\omega_o t - i k_o z - i\varphi} \; \frac{\partial}{\partial x} \; N_i(x,z,t) \right\}$$

(66)

$$= - \; 4\pi e \; k_\perp \omega_B \; \alpha \int\limits_{0}^{a} d\alpha_o \; \alpha_o \; g_o(\alpha_o) \int\limits_{0}^{2\pi} dq_o$$

$$\left\{ J_\ell(\sqrt{2p}) \left[\cos \, (q + \varphi) - i \, \sin \, (q + \varphi) \right] \right\}$$

where

$$p = p(p_o, \, q_o, \, \tau), \quad q = q(p_o, \, q_o, \, \tau)$$

are the solutions of Eq. (63). $\int\limits_{0}^{T} dt/T$ is a time averaging operator, where $1/\Gamma > T > 1/\omega_o$.

Equating the real and imaginary parts of Eq. (29), using Eq. (66), we obtain

$$\alpha \; \frac{d\varphi}{d\tau} = 0$$

(67)

$$\frac{d^2\tau}{dt^2} = \Lambda_o^2 \, G(\tau) \equiv - \frac{dV_2}{d\tau}(\tau) \tag{68}$$

where

$$G(\tau) = - \frac{k_\perp \, \omega_B}{2 \, \bar{n}_{oi}} \int_0^a d\alpha_o \, \alpha_o \, g_o(\alpha_o) \int_0^{2\pi} dq_o \, J_\ell(k_\perp \alpha) \, \sin(q + \varphi) \tag{69}$$

Equation (68) is the equation of motion of a "particle" moving in a "potential well" $V_2(\tau)$, and it describes the time evolution of a, which is proportional to $d\tau/dt$. For small values of $\tau < 1$,

$$J_\ell(k_\perp \alpha) \, \sin(q + \varphi) \approx J_\ell(k_\perp \alpha_o) \, \sin(q_o + \varphi)$$

$$- \tau \, \frac{J_\ell(k_\perp \alpha_o) \, J'_\ell(k_\perp \alpha_o)}{k_\perp \, \alpha_o} \tag{70}$$

and it follows from Eqs. (68) through (70) that the amplitude a grows exponentially with the linear growth rate.

-55-

It is apparent from Eq. (63) that nonlinear modifications to the exponential linear growth of the instability occur when $\delta q > \pi/2$, that is

$$\left| \frac{e \, \tilde{\Phi}(0)}{\gamma_0 \, mc^2} \right| = \frac{e \, k_\perp \, a}{m \, \gamma_0 \, \Omega^2} > 2\pi \, \frac{\Gamma}{\ell \omega_B} \, \frac{\omega_p^2}{k_\perp^2 \, c^2} \tag{71}$$

or

$$\left| \frac{\tilde{E}_{x \, max}}{E_{ox}(a)} \right| > \frac{2\pi}{k_\perp a} \, \frac{\Gamma}{\ell \omega_B} \tag{72a}$$

$$\sim 0.1 \left(\frac{\bar{n}_{oi}}{n_0} \right)^{1/2} \left(\frac{M}{m \, \gamma_0} \right)^{1/4} \left(\frac{\omega_p}{\Omega} \right)^{1/2} \, , \tag{72b}$$

for $k_\perp a = k_\perp a_i = 2 = \ell$. These conditions (71) and (72) will occur for wave amplitudes smaller than those given in the primary electron nonlinearity conditions (37) through (39) by the factor $\Gamma/\ell \omega_B < 1$. However, the wave amplitudes of (71) and (72) are only higher by a numerical factor of about $\pi/2$ from the nonlinear ion condition (48), since this condition addresses the same physical effects.

A detailed description of the nonlinear time evolution of α requires the evaluation of $V_2(\tau)$, which is analytically arduous. However, a representation of the nonlinear time evolution of α which has immediate physical significance and can be related to the nonlinear ion trajectories of Figure 2, can be obtained as follows.

We begin by verifying that the linear dispersion relation for unstable growth, as well as the generalization to include the effects of nonlinear ion dynamics, is consistent with energy conservation:

$$\frac{1}{2} \; \frac{\partial}{\partial t} \int \frac{d^3 r}{V} \left(E^2 + B^2 \right) + 4\pi \int \frac{d^3 r}{V} \; \underline{J} \cdot \underline{E} = 0 \qquad (73)$$

The electron contribution is

$$4\pi \int \frac{d^3 r}{V} \; \underline{J}_e \cdot \underline{E} = - \frac{\omega_o \, k^4 \, c^4}{2 \; \Omega^3 \; \omega_p^2} \; (1 + \omega^2 \, k_\perp a) \; \alpha \; \frac{\partial \alpha}{\partial t}$$

$$- \frac{k_\perp^4 \, c^4}{2 \; \Omega^4} \; (1 + \omega^2 \, k_\perp a) \; \alpha \; \frac{\partial \alpha}{\partial t}$$

-57-

The ion contribution is:

$$4\pi \int \frac{d^3 r}{V} \underline{J}_i \cdot \underline{E} = 4\pi \int \frac{d^3 r}{V} \int d^3 v \; e \, E_x \, v_x \, f_i(\underline{x}, \underline{v}, t)$$

$$= 4\pi \frac{d}{dt} \int \frac{d^3 r}{V} \int d^3 v \; \frac{M v_x^2}{2} f_i(\underline{x}, \underline{v}, t)$$

$$= -2\pi \, \alpha \, \frac{e \, \ell \omega_B^2 c^2}{k_\perp a \, \Omega^2} \int_0^{2\pi} dq_0 \int_0^{\frac{a}{|\sin q_0|}} dp_0$$

$$\left\{ g_0(\alpha_0) \; J_\ell(\sqrt{2p}) \sin(q + \varphi) \right\}$$

where $\omega_0 = \ell \omega_B$, and ℓ is an even integer.

The field contribution is

$$\frac{1}{2} \frac{\partial}{\partial t} \int \frac{d^3 r}{V} (E^2 + B^2) = \frac{k_\perp^4 c^4}{2 \, \Omega^4} (1 + \varpi^2 k_\perp a) \; \alpha \frac{\partial \alpha}{\partial t}$$

V is the volume of integration in the above expressions.

Thus from Eq. (73)

$$\frac{d\alpha^2}{dt} = \frac{8\pi \; \Omega^3 \; \omega_p^2}{\ell\omega_B k_\perp^4 c^4 (1 + \cos^2 k_\perp a)} \; \lim_{L\to\infty} \frac{d}{dt} \int_{-\frac{L}{2}}^{\frac{L}{2}} \frac{dz}{L} \int_{-a}^{+a} \frac{dx}{a} \int_{-\infty}^{+\infty} dv_x$$

$$\left\{ \frac{M v_x^2}{2} \, g_i(x,z,v_x,t) \right\}$$
(74a)

$$= -\frac{\alpha \, 8\pi \, e \, \Omega \, \omega_p^2 \, \omega_B}{k_\perp^3 c^2 a (1 + \cos^2 k_\perp a)} \int_0^a d\alpha_0 \, \alpha_0 \, g_0(\alpha_0) \int_0^{2\pi} dq_0$$

$$\left\{ J_\ell(k_\perp \alpha) \, \sin(q + \varphi) \right\}$$
(74b)

which is identical to Eq. (68).

Eq. (74) can be integrated in time, using the version (74a), to yield

$$\left|\frac{\tilde{E}_{x\,max}}{E_{ox}(a)}\right|^2 = \left(\frac{k_\perp^2 \, \alpha(t)}{k_0^2 \, 4\pi \, n_0 e a}\right)^2$$

$$= \frac{\bar{n}_{oi}}{n_0} \; \frac{\omega_p^2}{\ell\omega_B \, \Omega} \; \Delta\mathcal{E}_i$$
(75)

where $\alpha(0) \simeq 0$, and

-59-

$$\Delta \mathcal{E}_i = \frac{1}{\bar{n}_{oi}\omega_B^2 a^2 (1 + \cos^2 k_\perp a)} \int_{-\frac{L}{2}}^{+\frac{L}{2}} \frac{dz}{L} \int_{-a}^{+a} \frac{dx}{a} \int_{-\infty}^{+\infty} dv_x$$

$$v_x^2 \left\{ \left[g_i(x,z,v_x t) - g_o(x,v_x) \right] \right\}$$

(76)

Consequently, the increase in the wave amplitude is directly related to the transverse energy gained by the ions in the interaction.

We expect the "coarse gained" ion distribution function will evolve to a state where it is flattened (i.e., made uniform by phase mixing) in the region of phase space $(k_\perp \alpha, q)$ traversed by the ions. For example, in the case where the ion trajectories do not intersect the wall, and with reference to Figure 2, if the initial ion distribution is that of Eq. (34), where

$$g_o(x, v_x) = g_o(\alpha_o) = \frac{2 \bar{n}_{oi}}{\pi \omega_B a_i} \Theta(a_i - \alpha),$$

with $k_\perp a_i < 5.1$, $\omega_o = 2\omega_B$, $k_\perp x_a = 5.1$, $k_\perp a = 8$, then the predicted final state distribution would be

-60-

$$g_i(t \to \infty) \to \frac{2 \, \bar{n}_{oi} \, a_i}{\pi \, \omega_B \, x_a^2} \, \Theta(x_a - \alpha) \quad .$$

Thus

$$\Delta \mathcal{E}_i \approx \frac{1}{2} \, \frac{a_i}{a^3} \, \frac{(x_a^2 - a_i^2)}{(1 + \cos^2 k_\perp a)}$$

and substitution in Eq. (75) yields an estimate of the

final wave amplitude

$$\left| \frac{\tilde{E}_x(x = 0, \, t \to \infty)}{E_{ox}(0)} \right| \simeq k_\perp a \, \left| \frac{\tilde{E}_{x \, max}(t \to \infty)}{E_{ox}(a)} \right|$$

$$\simeq \frac{\Gamma}{2 \, \omega_B} \left[\frac{k_\perp^2 \, a_i \, \sqrt{x_a^2 - a_i^2}}{2} \right] \tag{77}$$

where Γ is the linear growth rate of Eq. (35). This differs

from the prior estimate of Eq. (72a) only by $1/2\pi$ times the

square bracket term, which may vary from 0 to 1.03 depending

on the size of a_i/x_a. Here the final state amplitude

approaches zero as $a_i \to x_a$ simply because it is not possible

-61-

for the ions to increase their net energy by much if they
are initially filled approximately to the boundary of
allowed phase space trajectories. As remarked earlier,
the RHS of Eq. (77) contains the small factor $\Gamma/2\omega_B$ which
may produce a result below the various other conditions of
nonlinearity. If not, then such other nonlinearities might
prevent the approach to this phase-mixed final state. In
addition, it must be recognized that this "final" state may
also be unstable, since perturbations of the outermost ions
may place them on new trajectories outside the "boundary
at x_a.

VII. RESULTS OF TWO-DIMENSIONAL SLAB COMPUTER CALCULATIONS

During the past year or so, we have been running and
improving large computer simulation codes, which are fully
electromagnetic and fully relativistic, and operate in a
two-dimensional slab configuration space. We have applied
these codes to the problems of ion-electron streaming
interactions and resistive growth interactions in an external
magnetic field, and have observed the growth of the electron
beam cyclotron mode. For these runs in which an instability
is computed from the initial noise levels, periodic boundary
conditions are applied in the axial dimension and conducting
boundary conditions are applied in the radial dimension.
The gross charge is non-neutral, since even for the cases
of ion-electron interaction, the ion density is much below
that of the relativistic electron beam. For a number of
reasons described below, we have not yet been able to put
the previously described theory of nonlinearities to a
good test, and so we do not claim that this theory is
substantiated by the computer results. Nevertheless, we

wish to describe some of the significant general features of the computer runs, in which behavior characteristic of the transverse dynamical effects which we have analyzed is in fact manifested.

In order to achieve a good simulation test of the nonlinear theory, it is necessary to design a run in which most of the essential conditions (1) to (16) are obeyed, together with a number of practical constraints for completing a numerically stable and accurate simulation within an affordable period of time. Although we have accumulated about a half dozen large and lengthy (i.e. many thousand time steps with many thousand particles) simulation runs during the past year, most of these failed to satisfy some of the important conditions (1) to (16). This was partly because the initial computer runs were designed before the desired theoretical constraints were known. In addition, the instability domain has proved to be rich with variations, so that in several runs in which certain inequalities were only weakly obeyed, several competing effects are believed to have been present--complicating the interpretation of results. For example when γ_0 is not too large (i.e.,

$\gamma_o \sim 3$), then some longitudinal plasma mode effects will be coupled into the electron cyclotron mode behavior.

It has been necessary to devote significant attention during the simulation effort to curing certain purely numerical instabilities that are unique to relativistic, electromagnetic codes. Central among these is the numerical Cherenkov instability, in which the finite differencing of Maxwell's equations allows light modes with wavelengths on the order of the cell size to have phase velocities below c, so that they may interact unstably with electron beam modes. These may be cured by filtering out the shortest wavelength modes, and arranging for the wavelengths of physical interest to be many cell lengths.

The simulation runs which have been completed, although violating some of the theoretical constraints, have shown the following common behavior. When the electrons and ions are released in approximate conditions of equilibrium, modes at the predicted axial wavenumber $k_z \sim \Omega/c$, and with low transverse wavenumber components, grow from noise for a few e-folds at a rate generally faster than the

-65-

theoretical estimate of the linear growth rate. However, this initial growth phase terminates with the mode amplitude well within the bounds of linear theory [e.g., $\tilde{\Phi}/\Phi_o \sim$ few $\times 10^{-3}$], and is usually followed by a phase of growth at a rate from 1 to 0.2 times the estimate of the linear growth rate, with the growth rate declining in time in several cases. In some runs the wave growth saturated, with the amplitude in one case ranging up to $\tilde{\Phi}/\Phi_o \sim 7\%$, while in other cases the run was terminated with $\tilde{\Phi}/\Phi_o$ a few percent but still slowly growing. For the runs which showed amplitude saturation, rough theoretical estimates suggested that nonlinearities such as electron cyclotron resonance broadening should have been felt at amplitudes about a factor of two below the observed saturation. For the runs which did not saturate, rough theoretical estimates indicate that nonlinearities should not have been felt for an additional 1 to 2 e-foldings.

Rather than attach any significance to the degree of quantitative agreement between these runs and the only partly relevant theoretical estimates of growth rates and

saturation amplitudes, we would emphasize the following

qualitative results:

(1) The desired electron cyclotron mode was excited
    to significant amplitudes, and the expected
    transverse electron dynamics were visible in
    the phase space diagnostics--as shown in Figure
    3 (where y is the axial coordinate).

(2) The radial ion bouncing in the electric fields
    of the beam and wave clearly dominated the ion
    dynamics, and no significant axial motion of
    the ions was detectable. In no case were the
    ions "trapped" longitudinally by the wave.

(3) In those cases where the wave approached the
    "nonlinear" amplitude level, symptoms of the
    breakdown of the electron fluid nature were
    evident--such as trajectory crossings and other
    significant phase space distortions. However,
    in no case were the distortions so severe that
    the electrons were "ripped apart," or reflected
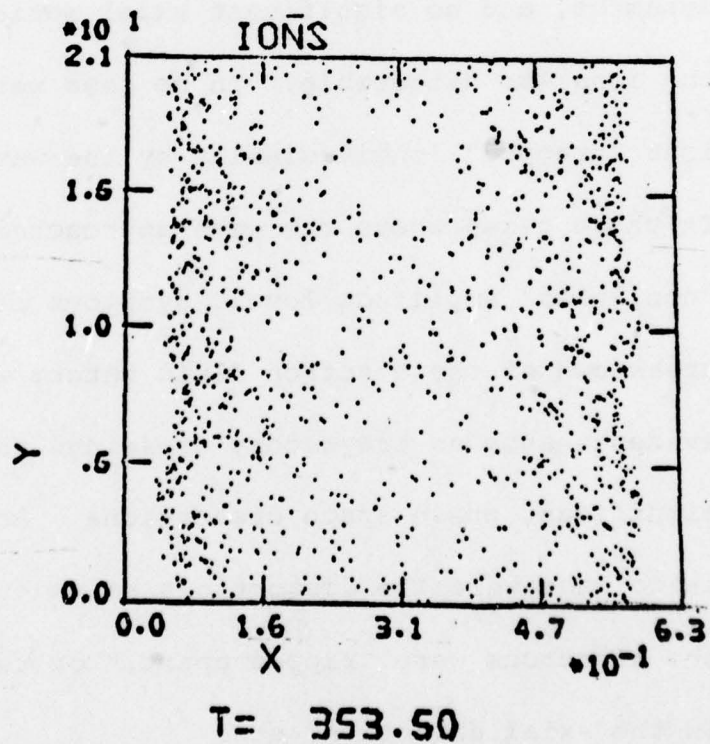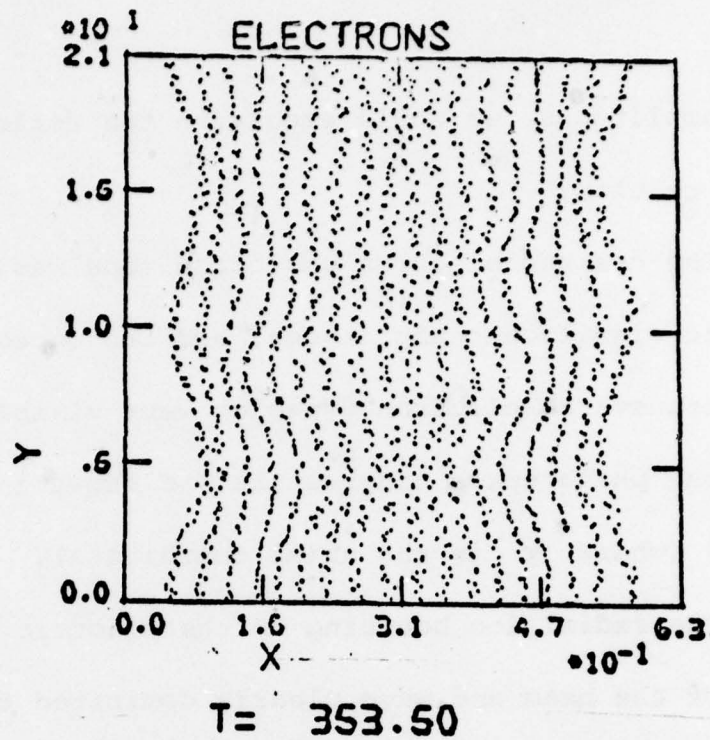   in the axial direction, etc.

Figure 3. Configuration Space of Electrons and
Ions at Late Time

We are presently involved in constructing runs in which a very quiet equilibrium state is established, with a number of diagnostics added to verify all of the linear wave characteristics. Then we will proceed to a run in which this nonlinear theory may be tested.

VIII. CONCLUSIONS

We have calculated herein certain nonlinear effects which appear when the amplitude of the cyclotron eigenmode of a relativistic electron beam is increased sufficiently. We have used as the vehicle of this calculation, the streaming interaction which arises between relativistic electrons and a sparse group of ions which are axially at rest in the reference frame of the calculation. Both electron and ion nonlinear effects were isolated, and the electron nonlinearities are generally relevant for other situations without ions, where the cyclotron wave is excited via some other beam-waveguide type of interaction.

These calculations were completed subject to a number of parameter restrictions, including those of conditions (1) to (16), which are generally appropriate to an Auto-Resonant ion acceleration device. Under these restrictions, the negative energy cyclotron wave is well decoupled from the longitudinal plasma modes, light modes, and the positive energy cyclotron mode, and the interaction of the

ions with the cyclotron mode is faster than any other
ion-electron interactions. The ion density was assumed
small enough that the ion coupling to the cyclotron wave
could be calculated via perturbation theory, and small
enough that the growth rate of the interaction was below
both the perpendicular ion bounce frequency ω_B, and
the width of the electron cyclotron resonance

$$\delta\omega = \Omega \; \omega_p^2/k^2c^2.$$

The estimates of nonlinear effects were evaluated
in detail for the specific case where a single unstable
eigenmode dominated the wave spectrum, with the axial
wave electric field symmetric in the transverse coordinate
x, with the lowest perpendicular wave number $k_\perp \simeq 2/a > k_z$,
and with the lowest resonant wave frequency $\omega_o = 2\omega_B < k_zc$.

A hybrid expression which summarizes the chief
results of the various calculations of the wave amplitude
required for strong nonlinearity is

$$\frac{\tilde{\Phi}_{max}(x=0)}{\Phi_o(x=a)} \geq \frac{1}{k^2a^2} \left\{ \frac{\left[D_1, \; D_2\,(\Gamma/\delta\omega)^{1/2} \right]_{lesser}}{\left[k^2a^2 + D_4\,\dfrac{\Omega^2}{\omega_p^2} \right]^{1/2}}, D_3\,\frac{\Gamma}{\omega_B} \right\}_{lesser}$$

(78)

-71-

where $[e \Phi_o(a)/\gamma_o mc^2] \simeq \omega_p^2 a^2/2c^2$ in slab geometry.
The coefficients D_1, D_2, D_3, D_4 are of order unity and
will generally vary somewhat for different eigenmode
characteristics $k_\perp$, ℓ, etc. The D_1 term represents
the primary electron nonlinearities, of which the most
sensitive is cyclotron resonance broadening. The D_2
term represents the nonlinear electron frequency shift
effect, which is important when $\Gamma/\delta\omega$ is very small.
The D_3 term represents the ion nonlinearities due to
transverse phase space trajectories or to axial resonance
broadening (depending on whether $k_\perp$ or k_z dominates
the k^{-2} coefficient), and these ion effects are
important when Γ/ω_B is very small.

The nonlinear effects become important for short
wavelength, high-k modes at lower wave amplitudes than
are needed for the low-k modes. Hence if the low-k modes
are not discriminated against in the parameter selection,
one may expect them to grow to the largest amplitudes
before nonlinear growth saturation occurs.

Both the theoretical analysis and the two-
dimensional computer simulations indicate that these

-72-

ion-electron cyclotron interactions saturate at wave amplitudes too low for longitudinal ion trapping, and generally before there is catastrophic disruption of the electron beam. Therefore for Auto-Resonant ion acceleration, it appears that ion-electron cyclotron interactions are (i) probably unsuitable as a wave growth/ion loading mechanism, but (ii) unlikely to disrupt the acceleration process itself.

REFERENCES

1. M. L. Sloan and W. E. Drummond, Phys. Rev. Letters 31,
    1234 (1973).

2. M. L. Sloan and W. E. Drummond, "The Autoresonant
    Accelerator Concept," Proc. IX International Con-
    ference on High Energy Accelerators (Springfield,
    Virginia: National Technical Info. Serv., U.S.
    Dept. of Commerce, 1974), p. 283ff.

3. V. P. Indykul, I. P. Panchenko, V. D. Shapiro, and
    V. I. Shevchenko, "Theory of Resonance Ion Accelera-
    tion by a Strong-Current Relativistic Beam," JETP
    Lett., Vol. 20, No. 3, Aug. 5, 1974, pp. 65-67.

APPENDIX B

STABILITY OF SLAB ELECTRON BEAM EQUILIBRIA

(Appendix B Contains 9 Pages)

A P P E N D I X   B

STABILITY OF SLAB ELECTRON

BEAM EQUILIBRIA

In this report, the stability of a certain class
of slab electron beam equilibria is discussed. These
equilibria would describe relativistic electron sheet
beams propagated between parallel conducting plates along
a uniform guide field. Such equilibria have been
utilized in some numerical simulations to investigate a
variety of electron beam phenomena. A sufficient condition
is determined for stability of the slab equilibria to two-
dimensional perturbations which vary across the slab and
along the direction of propagation. The restriction to
two-dimensional perturbations is a significant limitation
in the analysis, but this limitation is relevant for the
problem of constructing stable equilibria for two-
dimensional computer simulation, for which the third
coordinate is ignorable.

Equilibrium

It is convenient to move to a frame of reference moving with the electron beam. The electron slab equilibrium is assumed to be uniform in z and y, extending from $z = -\infty$ to $z = +\infty$, $y = -\infty$ to $y = +\infty$, and is bounded in x by conducting plates at $x = \pm b$. The electrons gyrate around an externally imposed magnetic guide field in the z-direction.

There are three constants of the electron motion:

$$H_o = \frac{1}{2} mv^2 - e\Phi_o(x)$$

$$P_{oy} = mv_y - \frac{e}{c} A_{oy}(x)$$

$$P_{oz} = mv_z$$

where the motion in the beam frame is considered to be nonrelativistic. $\underline{v}$ is the electron velocity, Φ_o is the scalar potential, A_{oy} is the y-component of the vector potential.

The distribution function $f_o(x, \underline{v})$ for the slab equilibria can be expressed in terms of the constants of the electron motion.

The stability analysis will be restricted to distribution functions of the form

$$f_o(x, \underline{v}) = F_o\left(H_o + \frac{\alpha}{2m} P_{oy}^2\right) \tag{1}$$

where α is a parameter which characterizes the magnitude of the mean electron velocity in the y-direction. The equilibrium charge and current densities are

$$N_o(x) = \quad d^3v \, F_o$$

$$J_{ox} = -e \int d^3v \, v_x \, F_o = 0$$

$$J_{oy} = -e \int d^3v \, v_y \, F_o$$

$$= -N_o(x) \frac{\alpha}{(1 + \alpha)} \frac{e^2}{mc} A_{oy}$$

$$\equiv -N_o e \langle v_y \rangle$$

$$J_{oz} = 0$$

3

Φ_o and A_{oy} satisfy the equations

$$\frac{\partial^2 \Phi_o}{\partial x^2} = 4\pi e\, N_o \tag{2}$$

$$\frac{\partial^2 A_{oy}}{\partial^2 x} = \frac{4\pi\, N_o\, e^2}{mc^2}\; \frac{\alpha}{(1+\alpha)}\; A_{oy} \qquad . \tag{3}$$

The equilibrium electric and magnetic fields, $\underline{E}_o$ and $\underline{B}_o$, are given by

$$\underline{E}_o = \left(-\frac{\partial \Phi_o}{\partial x}\, ,\; 0,\; 0 \right)$$

$$\underline{B}_o = \left(0,\; 0,\; \frac{\partial A_{oy}}{\partial x} \right) \qquad .$$

Stability

The equilibrium is subjected to time dependent perturbations which vary only in x and z:

$$\underline{E} = \underline{E}_o(x) + \underline{E}_1(x,\, z,\, t)$$

4

$$\underline{B} = \underline{B}_o(x) + \underline{B}_1(x, z, t)$$

$$f = f_o(x, \underline{v}) + f_1(x, z, \underline{v}, t) \quad .$$

In terms of the perturbed scalar potential $\Phi(x, z, t)$ and vector potential $\underline{A}_1(x, z, t)$:

$$\underline{E}_1 = -\nabla \Phi_1 - \frac{1}{c} \frac{\partial \underline{A}_1}{\partial t}$$

$$\underline{B}_1 = \nabla \times \underline{A}_1$$

where

$$\nabla \cdot \underline{A}_1 + \frac{1}{c} \frac{\partial \Phi_1}{\partial t} = 0 \quad .$$

The perturbed distribution function f_1 is determined by the linearized Vlasov equation:

$$\frac{df_1}{dt} = \frac{e}{m}\left(\underline{E}_1 + \frac{\underline{v} \times \underline{B}_1}{c}\right) \cdot \frac{\partial F_o}{\partial \underline{v}}$$

$$= -\alpha \frac{e}{mc} P_{oy} \frac{\partial F_o}{\partial W} \frac{dA_{1y}}{dt} + e \underline{E}_1 \cdot \underline{v} \frac{\partial F_o}{\partial W} \tag{4}$$

5

where   d/dt   is the time derivative following the

equilibrium trajectory and

$$W = H_o + \frac{\alpha}{2m} P_{oy}{}^2$$

$$= \frac{1}{2} m \left(v_x{}^2 + v_z{}^2 + s^2 \right) - e\Phi_o$$

$$+ \frac{1}{2} \frac{\alpha}{(1 + \alpha)} \frac{e^2}{mc^2} A_{oy}{}^2$$

$$s = (1 + \alpha)^{1/2} \left(v_y - \frac{\alpha}{1 + \alpha} \frac{e}{mc} A_{oy} \right) \quad .$$

Thus,

$$\int d^3r \ \underline{J}_1 \cdot \underline{E}_1 = -e \int d^3r \ \int d^3v \ \underline{E}_1 \cdot \underline{v} f_1$$

$$= \frac{\partial}{\partial t} \int d^3r \ d^3v \left\{ \frac{\left(f_1 + \alpha \frac{e}{mc} P_{oy} A_{1y} \frac{\partial F_o}{\partial W} \right)^2}{2(-\partial F_o/\partial W)} \right.$$

$$\left. - \frac{\alpha e}{2mc^2} v_y P_{oy} A_{1y}{}^2 \frac{\partial F_o}{\partial W} \right\} \quad . \quad (5)$$

6

Since $\int d^3r \, \underline{J}_1 \cdot \underline{E}_1$ has now been expressed as a total time derivative, it is possible to obtain from Maxwells equations the following energy constant K:

$$K = \int d^3r \left(\frac{E_1^{\,2}}{8\pi} + \frac{B_1^{\,2}}{8\pi} \right)$$

$$+ \int d^3r \, d^3v \; \frac{\left\{ f_1 + \frac{\alpha e}{c} A_{1y} \frac{\partial F_o}{\partial W} \frac{s}{(1+\alpha)^{1/2}} \right\}^2}{2(-\partial F_o/\partial W)}$$

$$- \int d^3r \, d^3v \; \frac{\alpha}{(1+\alpha)} \frac{e^2}{2c^2} A_{1y}^{\,2} \, s^2 \, \frac{\partial F_o}{\partial W}$$

$$- \int d^3r \; \frac{\alpha}{(1+\alpha)} \frac{e}{4\pi mc} A_{oy} A_{1y} \, \nabla \cdot \underline{E}_1 \quad .$$

This constant K may in turn be bounded below by the quantity

$$C \equiv \int d^3r \; d^3v \; \frac{\left(f_1 + \frac{\alpha e}{c} A_{1y} \frac{\partial F_o}{\partial W} \frac{s}{(1 + \alpha)^{1/2}} \right)^2}{2(-\partial F_o/\partial W)}$$

$$+ \int d^3v \left[\frac{E_1^{\;2}}{8\pi} + \frac{B_1^{\;2}}{8\pi} + \frac{N_o \; \alpha}{(1 + \alpha)} \frac{e^2}{2c^2} A_{1y}^{\;2} \right]$$

$$- \frac{1}{2} \int d^3r \; \frac{\alpha}{(1 + \alpha)} \; \frac{e}{4\pi mc^2} \left\{ \left| A_{oy} \right| \left(\left| E_{1x} \right|^2 \right. \right.$$

$$+ \left| E_{1z} \right|^2 + \left| B_{1x} \right|^2 + \left| B_{1z} \right|^2 \right)$$

$$+ \left| B_{oz} \right| b \left(\left| E_{1x} \right|^2 + \frac{\left| A_{1y} \right|^2}{b^2} \right) \bigg\} \; . \tag{6}$$

Finally, if

$$\frac{\partial F_o}{\partial W} < 0 \tag{7}$$

and

$$1 > \left\{ \left| \frac{\langle v_y \rangle}{c} \right| + \left| \frac{b}{c} \frac{d}{dx} \langle v_y \rangle \right| \right\}_{max} \tag{8}$$

8

then

$$K \geq C > 0 \qquad ,$$

and all the perturbed quantities must remain infinitessimal
in order for K to stay constant at its initially infini-
tessimal value.

Equations (7) and (8) are, therefore, the
sufficient conditions for stability to two-dimensional
perturbations of slab equilibria described by $F_o(W)$ and
bounded by parallel conducting plates.

Examination of the equilibrium expressions for
$\langle v_y \rangle$ reveals that the RHS of Eq. (8) contains a term
proportional to $N_{oL} b / \gamma_o B_{oz}$, which must, therefore, not
be too large if this equilibrium condition is to be
guaranteed. (Here N_{oL} is the beam density as seen in
the lab frame of reference.)

APPENDIX C

LIMITING CURRENTS OF AN UNNEUTRALIZED

MAGNETIZED ELECTRON BEAM IN A

CYLINDRICAL DRIFT TUBE

(Appendix C contains 6 Pages)

37

Limiting currents of an unneutralized magnetized electron beam in a cylindrical drift tube

J. R. Thompson and M. L. Sloan

Austin Research Associates, Austin, Texas 78758

Results of an investigation of the steady state injection of a uniform unneutralized, magnetized, relativistic electron beam into a cylindrical drift tube are presented. The space-charge-limited current and the asymptotic kinetic energy of electrons on axis is determined both numerically and analytically as a function of the input kinetic energy $(\gamma_0 - 1) mc^2$ and of the ratio of beam—to—wall radii. A previously cited "interpolation formula" is obtained in the pencil beam limit, but more accurate limiting current expressions are developed for other cases (such as the fat beam limit) where the interpolation formula is as much as 20% in error. The corresponding axial electron energy is also found to be significantly smaller than the previously cited value of $(\gamma_0^{1/3} - 1) mc^2$ except in the strong pencil beam limit.

I. INTRODUCTION

Significant advances of recent years in high voltage, pulsed power technology have stimulated the exploitation of high current electron accelerators for varied applications. For many such cases, the determination of space-charge-limited currents is of high interest and has been repeatedly discussed in the literature [cf. Ref. 1 and the bibliography given there]. We consider herein a small but relevant subclass of the general limiting current problem.

Specifically, we restrict our attention to the following:

(i) A cold, cylindrically symmetric, unneutralized electron beam of radius a propagating in steady-state interior to an evacuated waveguide of radius b along an axial magnetic guide field which is sufficiently large to render the equilibrium precessional velocity and radial excursions of the beam negligible.

(ii) The beam is injected through an anode which is grounded to the cylindrical drift tube. At the anode plane, the electron number density n_0, the axial velocity $\beta_0 c$, and the particle energy $(\gamma_0 - 1) mc^2$ are assumed independent of radius r.

(iii) The ratio of the length to radius of the drift tube is very large, so that end effects are negligible.

Here we consider only those limitations on beam current which derive from the conditions for propagation in a steady-state equilibrium subject to the preceding assumptions. We do not, for example, consider limitations derived from stability considerations, although we note that previous work[2] has indicated that such an electron beam in a cylindrical waveguide is absolutely stable for a sufficiently large magnetic guide field.

The exact numerical solution of this limiting current problem was obtained long ago[3] for nonrelativistic $(\beta_0 \ll 1)$ beams, but relativistic solutions have only been published for the special cases of pencil beams $(\ln b/a \gg 1)$ or ultra-relativistic beams $(\gamma_0 \gg 1)$ for which the radial variations in the downstream quantities γ, β, n are unimportant. A generalization [see Eq. (17a)] of the pencil beam result has been presented[4] as an "interpolation formula" for the limiting current and has been wide-

ly employed in related calculations in the literature. Although this formula indicates the correct zero-order parameter scaling of the limiting current, it is found to be quantitatively in error by over 20% in some cases. Furthermore, the expression for the axial electron energy [see Eq. (17b)] which is commonly associated with this interpolation formula is grossly incorrect (i.e., by more than an order of magnitude) in some cases.

We describe relativistically correct analytical approximations to the limiting current problem for arbitrary values of b/a and compare the results to exact numerical solutions. The parameter range of validity of these approximations is delineated.

II. GOVERNING EQUATIONS AND NATURE OF NUMERICAL SOLUTIONS

Adopting the usual cylindrical coordinates r, θ, z, we consider the anode injection plane to be located at $z = 0$. The injected beam current density is then given by

$$\mathbf{J}(r, 0) = \begin{cases} -n_0 e \beta_0 c \hat{z} , & r \le a , \\ 0 , & r > a , \end{cases} \tag{1}$$

where e is the magnitude of the electron charge.

Since the injection anode plane is grounded to the conducting waveguide, the potential function $\phi(r, z)$ attains the boundary values

$$\phi(r, 0) = \phi(b, z) = 0 ; \tag{2}$$

we note that $\phi(r, z) \le 0$.

The large magnetic guide field approximation implies that the radius of each electron is fixed. For steady-state flow, the space charge in the drift tube will create fields to reduce the energy of each beam electron, such that

$$\gamma \equiv \gamma(r, z) = \gamma_0 + \frac{e}{mc^2} \phi(r, z) \tag{3}$$

with a corresponding beam charge density

$$\rho(r, z) = -n_0 e \beta_0 \gamma / (\gamma^2 - 1)^{1/2} , \tag{4}$$

where $\gamma_0 = (1 - \beta_0^2)^{-1/2}$.

2032

1

Far downstream of the injection plane ($z \gg b$), the variation in ϕ is purely radial and is described by the radial Poisson equation, which, from Eq. (3), may be expressed in terms of $\gamma(r)$:

$$\frac{1}{r}\frac{d}{dr} r \frac{d\gamma}{dr} = \begin{cases} \dfrac{4\nu}{a^2}\dfrac{\gamma}{(\gamma^2-1)^{1/2}}, & r \le a, \quad (5a) \\[2mm] 0, & r > a, \quad (5b) \end{cases}$$

with boundary conditions that $\gamma(0)$ be regular and $\gamma(b) = \gamma_0$. The parameter ν is defined

$$\nu \equiv \frac{\pi n_0 e^2 a^2 \beta_0}{mc^2} = \frac{I_e}{mc^3/e} = \frac{I_e}{17\,kA} \tag{6}$$

which differs by a factor of β from the usual Budker parameter, so that ν is constant in r, z and proportional only to the current.

By integrating Eq. (5b) through the vacuum region, and applying the boundary condition $\gamma(b) = \gamma_0$, one may contend only with the single beam-region Eq. (5a) subject to the mixed boundary condition

$$\left(\gamma + \ln\left(\frac{b}{a}\right) r \frac{d\gamma}{dr}\right)_{r=a} = \gamma_0. \tag{7}$$

For given values of γ_0 and b/a, it is desired to determine the largest value of ν (and hence I_e) for which a solution to Eq. (5a) exists, subject to the boundary condition, Eq. (7). This largest value is called ν_l and the corresponding electron current is called the limiting current.

The increase in the right-hand side of Eq. (5a), which occurs as γ is reduced, reflects the axial density compression due to electron slowing. Equation (5a) (with boundary conditions) requires that $\gamma(r)$ be monotonically
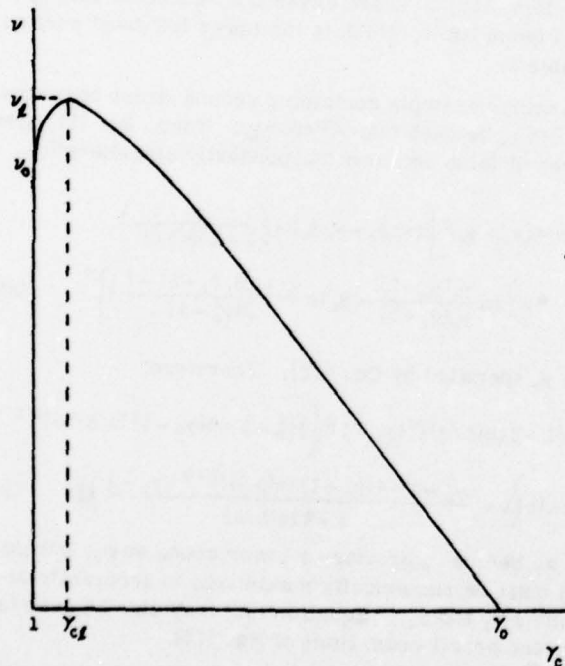

FIG. 1. Dimensionless current ν as a function of the relativistic factor γ_c of center electrons with γ_0, b/a fixed.

TABLE I. Numerical solutions for ν_l / γ_{cl}.

	$\gamma_0 = 2$	$\gamma_0 = 5$	$\gamma_0 = 7$	$\gamma_0 = 100$
$\dfrac{b}{a} = 1$	$\dfrac{0.553}{1.12}$	$\dfrac{3.12}{1.26}$	$\dfrac{4.98}{1.31}$	$\dfrac{97.06}{1.68}$
$\dfrac{b}{a} = 2$	$\dfrac{0.221}{1.14}$	$\dfrac{1.27}{1.31}$	$\dfrac{2.05}{1.37}$	$\dfrac{40.61}{1.74}$
$\dfrac{b}{a} = 5$	$\dfrac{0.118}{1.18}$	$\dfrac{0.695}{1.41}$	$\dfrac{1.12}{1.48}$	$\dfrac{22.90}{1.89}$
$\dfrac{b}{a} = 20$	$\dfrac{0.069}{1.21}$	$\dfrac{0.407}{1.50}$	$\dfrac{0.659}{1.61}$	$\dfrac{13.75}{2.14}$

increasing, indicating that the electrons on axis are slowed the most below their injection velocity. The previous relativistic treatments of this limiting current problem have essentially ignored the radial dependence of this axial density compression, approximating the right-hand side of Eq. (5a) as a constant.

In principle, if one specifies a value for the γ of the electrons at the center of the beam, $\gamma_c \equiv \gamma(0)$, then Eq. (5a) determines $\gamma(r)$ throughout the beam as a function of γ_c, ν, a. Applying the boundary condition, Eq. (7), then allows one to solve for ν as a function of γ_c, γ_0, b/a. The resulting dependence of ν on γ_c for fixed values of γ_0, b/a is illustrated in Fig. 1. The maximum value of ν is the desired ν_l, and the corresponding value of γ_c is γ_{cl}. The value of ν at $\gamma_c = 1$ is denoted ν_0. One may show from Eqs. (5a) and (7) that $\gamma_{cl} > 1$ and $\nu_l > \nu_0$. Thus, Fig. 1 is qualitatively correct for all cases.

It is of interest in some applications to know γ_{cl} as well as ν_l, with a fair degree of accuracy. For example, schemes have recently been proposed[5] for collective acceleration of ions which rely on the controlled motion of a virtual cathode, created in an intense relativistic electron beam by approaching the limiting current conditions. If the motion of the virtual cathode is to be well controlled, the limiting current conditions must be known precisely.

It should also be noted that both the accessibility and the stability of steady-state injection is questionable for the branch of Fig. 1, where $1 < \gamma_c < \gamma_{cl}$. However, the branch $\gamma_{cl} < \gamma_c < \gamma_0$ may be traversed by slowly increasing the diode current from zero while holding the voltage constant.

A set of scaled equations based upon Eqs. (5a) and (7), which allow very efficient numerical determination of the limiting current parameters, is presented in the Appendix. A representative spectrum of the numerical solutions obtained via these equations is listed in Table I. The monotonic dependence of ν_l and γ_{cl} on separate variations of γ_0 or b/a may be observed.

III. APPROXIMATE ANALYTICAL SOLUTIONS

In this section we describe several theoretical approaches to the limiting current problem, which yield approximate solutions that are useful in different regions of parameter space.

2

A. Iteration of integral equation

Equations (5) and (7) may be combined into a single integral equation, which may be written in iterative form as

$$\gamma^{(N)}(x) = \gamma_0 - 4\nu \ln\left(\frac{b}{a}\right) \int_0^1 \frac{dy\,y}{\beta^{(N-1)}(y)} - 4\nu \int_x^1 \frac{dw}{w} \int_0^w \frac{dy\,y}{\beta^{(N-1)}(y)} , \tag{8}$$

where $x = r/a$, $\beta = (1 - \gamma^{-2})^{1/2}$, and the superscripts in parentheses indicate the order of the iteration. If $\gamma^{(0)}(x)$ is chosen to be constant, the iteration may be readily carried out to second order, yielding the following equations:

$$\gamma^{(0)}(x) = \gamma_k , \tag{9}$$

$$\gamma^{(1)}(x) = \gamma_c + (\gamma_e - \gamma_c)x^2 , \tag{10}$$

$$\frac{1}{\nu}\left[\gamma_0 - \gamma^{(2)}(x)\right](\gamma_e - \gamma_c) = 2(\gamma_e \beta_e - \gamma_c \beta_c)\ln\frac{b}{a}$$

$$+ \left[\gamma_e \beta_e - \gamma^{(1)}(x)\beta^{(1)}(x)\right] + \gamma_c \ln\frac{\gamma_e(\beta_e + 1)}{\gamma^{(1)}(x)\left[\beta^{(1)}(x) + 1\right]}$$

$$- \gamma_c \beta_c \ln\frac{\gamma_c \gamma_e(\beta_c \beta_e + 1) - 1}{\gamma_c \gamma^{(1)}(x)\left[\beta_c \beta^{(1)}(x) + 1\right] - 1} , \tag{11}$$

where

$$\gamma_e = \frac{\gamma_0 + 2\gamma_c \ln(b/a)}{1 + 2\ln(b/a)} , \tag{12}$$

and

$$\nu = \beta_k(\gamma_e - \gamma_c) . \tag{13}$$

Here and in the following text, the γ's and β's with like subscripts or superscripts are related in an obvious manner.

There remains the freedom to specify the constant γ_k. For example, if one selects $\gamma_k = \gamma_0$, then Eqs. (12) and (13) yield

$$\nu = \frac{\beta_0(\gamma_0 - \gamma_c)}{1 + 2\ln(b/a)} \tag{14}$$

and hence

$$\nu_1 = \nu_0 = \frac{\beta_0(\gamma_0 - 1)}{1 + 2\ln(b/a)} , \tag{15a}$$

$$\gamma_{c1} = 1 \tag{15b}$$

which is a previously published result.[6]

Another possibility is to select $\gamma_k = \gamma_c$ to obtain

$$\nu = \frac{\beta_c(\gamma_0 - \gamma_c)}{1 + 2\ln(b/a)} \tag{16}$$

and hence

$$\nu_1 = \frac{(\gamma_0^{2/3} - 1)^{3/2}}{1 + 2\ln(b/a)} , \tag{17a}$$

$$\gamma_{c1} = \gamma_0^{1/3} , \tag{17b}$$

$$\nu_0 = 0 . \tag{17c}$$

Equation (17a) is the previously mentioned and widely cited interpolation formula.[4] The corresponding value of γ_{c1} in Eq. (17b) has also been previously published.[7]

The results of Eqs. (14)–(17) are essentially first-order iterations, since no use was made of the second order Eq. (11). Consequently, they can be expected to have only limited accuracy. The two examples may be expected to bracket the correct solutions, since they represent the two extreme choices for γ_k, and indeed this is found to be the case.

An example which contains second-order accuracy is to let γ_k be such that $\gamma^{(2)}(1) = \gamma_e$. From Eqs. (11) and (12), one obtains

$$\nu = \frac{(\gamma_e - \gamma_c)^2}{(\gamma_e \beta_e - \gamma_c \beta_c)} = \left(\frac{\gamma_0 - \gamma_c}{1 + 2\ln(b/a)}\right)^2$$

$$\times \left\{\left[\left(\gamma_c + \frac{\gamma_0 - \gamma_c}{1 + 2\ln(b/a)}\right)^2 - 1\right]^{1/2} - (\gamma_c^2 - 1)^{1/2}\right\}^{-1} \tag{18}$$

and hence

$$\nu_0 = \frac{(\gamma_0 - 1)^{3/2}}{[1 + 2\ln(b/a)][\gamma_0 + 1 + 4\ln(b/a)]^{1/2}} . \tag{19}$$

Although Eq. (18) is sufficiently complex so that it does not yield closed form algebraic solutions for ν_1 and γ_{c1}, it is still fairly useful since it may be numericall maximized in minutes on the presently available scientific hand calculators. Also, Eq. (19) provides a lower bound on ν_1.

Equation (18) may further be used to determine the bounds of validity of Eq. (16). If one assumes the usual pencil beam limit $\gamma_e - \gamma_c \ll \gamma_c$ (i.e., the fractional variation in γ across the beam is small), Eq. (18) reduces to Eq. (16). This pencil beam ansatz specifically requires the ordering $\gamma_0^{2/3} \ll 1 + 2\ln b/a$ for validity. Therefore, Eqs. (16)–(17) are essentially accurate only in the pencil beam limit, which is the lower left-hand portion of Table I.

Another example containing second-order accuracy is to let γ_k be such that $\gamma^{(2)}(0) = \gamma_c$. Then, Eq. (11) gives the result (also obtained independently elsewhere)[8]:

$$\nu = (\gamma_e - \gamma_c)^2\left[(\gamma_e \beta_e - \gamma_c \beta_c) + \left(\frac{\gamma_c}{1 + 2\ln(b/a)}\right)\right.$$

$$\times \left.\left(\ln\frac{\gamma_e(\beta_e + 1)}{\gamma_c(\beta_c + 1)} - \beta_c \ln\frac{\gamma_c \gamma_e(\beta_c \beta_e + 1) - 1}{2(\gamma_c^2 - 1)}\right)\right]^{-1} \tag{20}$$

with γ_e specified by Eq. (12). Therefore,

$$\nu_0 = [1 + 2\ln(b/a)]^{-1}(\gamma_0 - 1)^2\left[[\gamma_0^2 - 1 + 4(\gamma_0 - 1)\ln(b/a)]^{1/2}\right.$$

$$+ \left.\ln\left(1 + \frac{[\gamma_0^2 - 1 + 4(\gamma_0 - 1)\ln(b/a)]^{1/2} + \gamma_0 - 1}{1 + 2\ln(b/a)}\right)\right]^{-1} \tag{21}$$

and as before ν_0 provides a lower bound on ν_1, but Eq. (20) must be numerically maximized to accurately determine ν_1 and γ_{c1}. Equation (20) may also be seen to have the pencil beam limit of Eq. (16).

If Eq. (20) is expanded in the limit $\gamma_e \gg \gamma_c \gg 1$, so that the variation in γ across the beam is large, one obtains

3

$$\nu \simeq \left[1 + 2\ln\left(\frac{b}{a}\right)\right]^{-1}\left[\gamma_0 - \gamma_c - \frac{1}{2\gamma_c}\left(\ln\frac{\gamma_e}{\gamma_c} + 2\ln\left(\frac{b}{a}\right)\right)\right] + \cdots \quad (22)$$

and

$$2\gamma_{cl}^2 \simeq \ln(\gamma_{el}/\gamma_{cl}) + 1 + 2\ln(b/a) + \cdots \quad . \quad (23)$$

The expansion ansatz specifically requires that $1 + 2\ln(b/a) \ll \gamma_0^{2/3}$ (hereafter, denoted the fat beam limit) which is the upper right-hand portion of Table I.

In summary, Eqs. (18) and (20) are accurate second-order representations of fairly wide validity; both equations have the correct pencil beam limit, and Eq. (20) also has the correct fat beam limit.

B. Variational principle

A variation principle which generates the differential Eq. (5a) and the boundary condition (7) is

$$I\left[\gamma(x)\right] = \int_0^1 dx\, x\left[\frac{1}{2}\left(\frac{d\gamma}{dx}\right)^2 + 4\nu(\gamma^2 - 1)^{1/2}\right]$$
$$- \frac{\gamma(x)\left[2\gamma_0 - \gamma(x)\right]}{2\ln(b/a)}\Bigg|_{x=1} , \quad (24)$$

where I is a functional of $\gamma(x)$, which is to be extremized with respect to possible trial functions $\gamma(x)$. One expects that fairly high accuracy may be achieved on the limiting current with only a modestly accurate guess at the trial function $\gamma(x)$.

A trial function of modest accuracy is that of Eq. (10), which contains the two free parameters γ_c and γ_e. These two parameters are then chosen to render the variational principle, Eq. (24), stationary. Carrying out this procedure and using the fact that $\nu_1(\gamma_c, \gamma_0, b/a)$ is itself an extremum at $\gamma_c = \gamma_{cl}$, one obtains the following parametric solution for the limiting current parameters.

$$\nu_1 = (\gamma_{el} - \gamma_{cl})^3\bigg[\gamma_{el}(\gamma_{el}\beta_{el} - \gamma_{cl}\beta_{cl})$$
$$- \gamma_{cl}\beta_{cl}(\gamma_{el} - \gamma_{cl}) - \ln\frac{\gamma_{el}(\beta_{el}+1)}{\gamma_{cl}(\beta_{cl}+1)}\bigg]^{-1} , \quad (25)$$

$$Q \equiv \frac{2\nu_1(\gamma_{el}\beta_{el} - \gamma_{cl}\beta_{cl})}{(\gamma_{el} - \gamma_{cl})^2} , \quad (26a)$$

$$\left[\ln\left(\frac{b}{a}\right)\right]^{-1} = (3 - Q)^2\left(3 - \frac{2\nu_1}{\beta_{cl}(\gamma_{el}-\gamma_{cl})}\right)^{-1} - 3 + 2Q$$
$$- \frac{2\nu_1}{\beta_{el}(\gamma_{el}-\gamma_{cl})} , \quad (26b)$$

$$\gamma_0 = \gamma_{el} + Q(\gamma_{el} - \gamma_{cl})\ln(b/a) . \quad (27)$$

These equations may be solved by first specifying trial values for γ_{cl} and γ_{el}, subject only to $\gamma_{el} > \gamma_{cl} > 1$, and then solving Eqs. (25)–(27) sequentially for the corresponding values of ν_1, b/a, γ_0. Trial values of γ_{cl} and γ_{el} which result in $b < a$ must be rejected. One may again be forced to make several calculations on a hand calculator to generate the desired values of γ_0 and b/a. The resulting solutions are found to be quite accurate except in the fat beam regime.

C. Ultrarelativistic perturbation expansion

If we restrict our attention to the case of a sufficiently highly relativistic beam where $\gamma_0 \gg 1$ and $2\gamma_{cl}^2 \gg 1$, so that we may use the expansion

$$1/\beta = \gamma(\gamma^2 - 1)^{-1/2} = 1 + 1/2\gamma^2 + \cdots , \quad (28)$$

Eq. (5a) may be solved iteratively to yield

$$\gamma(r) = \gamma_c + \frac{\nu r^2}{a^2} + \frac{1}{2\gamma_c}\ln\left(1 + \frac{\nu r^2}{\gamma_c a^2}\right) + \cdots . \quad (29)$$

Then, the boundary condition, Eq. (7), gives

$$\gamma_0 = \gamma_c + \nu\left[1 + 2\ln(b/a)\right]$$
$$+ \frac{1}{2\gamma_c}\left[\ln\left(1 + \frac{\nu}{\gamma_c}\right) + \frac{2\nu}{\nu + \gamma_c}\ln\left(\frac{b}{a}\right)\right] + \cdots . \quad (30)$$

The peak value of ν (i.e., ν_1) may be found by differentiating Eq. (30) with respect to γ_c and setting $\partial\nu/\partial\gamma_c = 0$, to obtain

$$2\gamma_{cl}^2 = \ln\left(1 + \frac{\nu_1}{\gamma_{cl}}\right) + \frac{\nu_1}{\nu_1 + \gamma_{cl}}\left[1 + 2\ln\left(\frac{b}{a}\right)\right]$$
$$+ \frac{2\nu_1\gamma_{cl}}{(\nu_1 + \gamma_{cl})^2}\ln\left(\frac{b}{a}\right) + \cdots . \quad (31)$$

Equations (30) and (31) may now be solved simultaneously to determine the limiting current parameters ν_1 and γ_{cl}.

1. Pencil beam case

For this limit, we assume the ordering

$$2\ln(b/a) \gg \gamma_0^{2/3} \gg 1 \quad (32)$$

and make the ansatz $\nu_1 \ll \gamma_{cl}$. We then obtain

$$\gamma_{cl} = \gamma_0^{1/3} - \frac{1}{2}\gamma_0^{-1/3} - \frac{\gamma_0}{4\ln(b/a)} + \cdots \quad (33)$$

$$\nu_1 = \frac{\gamma_0 - \frac{3}{2}\gamma_{cl} + \cdots}{2\ln(b/a)} = \frac{\gamma_0 - \frac{3}{2}\gamma_0^{1/3} + \cdots}{2\ln(b/a)} \quad (34)$$

which agrees with the pencil beam results of Eq. (17), when the latter are expanded under the pencil beam ordering of Eq. (32). This ordering is also sufficient to validate the ansatz $\nu_1 \ll \gamma_{cl}$. As we noted previously, the pencil beam regime is the lower left-hand portion of Table I; however, Eqs. (33) and (34) also require $\gamma_0^{2/3} \gg 1$ for validity, implying a shift toward the lower center of Table I.

2. Fat beam case

For this limit we assume the ordering

$$3 + 2\ln(b/a) \ll \gamma_0^{2/3} \quad (35)$$

and make the ansatz $\nu_1 \gg \gamma_{cl}$. Then, Eq. (31) becomes

$$2\gamma_{cl}^2 = \ln(\nu_1/\gamma_{cl}) + 1 + 2\ln(b/a) + \cdots \quad (36)$$

while Eq. (30) implies

$$\nu_1 = \frac{\gamma_0 - 2\gamma_{cl} + 1/(2\gamma_{cl}) + \cdots}{1 + 2\ln(b/a)} . \quad (37)$$

To obtain γ_{cl}, Eq. (37) may be inserted in Eq. (36), which may then be solved iteratively. Carrying the iteration to second order for improved accuracy, one obtains

J. R. Thompson and M. L. Sloan

$$\gamma_{cl} = \frac{1}{\sqrt{2}} \left\{ \ln\left[\sqrt{2}\, \gamma_0 \left\{ \ln\left(\frac{\gamma_0 - \frac{3}{2}}{1 + 2\ln(b/a)} \right) + 1 - 2\ln\left(\frac{b}{a}\right) \right\}^{-1/2} \right. \right.$$

$$\left. - 2 + \left\{ \ln\left(\frac{\gamma_0 - \frac{3}{2}}{1 + 2\ln(b/a)} \right) + 1 + 2\ln\left(\frac{b}{a}\right) \right\}^{-1} \right]$$

$$\left. + 1 + 2\ln(b/a) - \ln[1 + 2\ln(b/a)] \right\}^{1/2} . \qquad (38)$$

Once γ_{cl} has been computed from Eq. (38), then ν_l may be determined from Eq. (37). One finds that the ordering of Eq. (35) is sufficient to validate the ansatz $\nu_l \gg \gamma_{cl}$. It may also be seen that Eqs. (22) and (23) agree with Eqs. (36) and (37) for the fat beam limit.

When $\gamma_0 \gg 1$, the value of γ_{cl} given by Eq. (38) for the fat beam limit may be seen to be considerably less than the value given by Eqs. (17b) or (33) for the pencil beam limit. Consequently, it would be grossly inaccurate to assume that these pencil beam equations for γ_{cl} have a general validity as has been ascribed to the interpolation formula for ν_l, Eq. (17a).

D. Accuracy of the analytical approximations

Exact numerical solutions which have been obtained and which are illustrated in Table I may be used to gauge the accuracy of the various analytical approximations. Comparisons for several test cases are illustrated in Table II.

It may be seen that the second-order iteration solutions of Eqs. (18) and (20) bracket the numerical results much more tightly than do the first order iteration solutions of Eqs. (15) and (17). In particular, the "interpolation formula" Eq. (17a) is observed to significant underestimate the limiting current, while the corresponding Eq. (17b) grossly overestimates γ_{cl}.

The results of the variational calculation are seen to be the most accurate overall, except in the ultra-rela-

tivistic fat beam limit illustrated in the last column. There, the expansion formulae of Eqs. (37) and (38) are best, with the second-order iteration Eq. (20) also being fairly accurate. The ultra-relativistic pencil beam expansions are accurate only for very large values of b/a, as assumed in Eq. (32), and so they have been omitted from Table II.

APPENDIX: EQUATIONS FOR A NUMERICAL INVESTIGATION OF LIMITING CURRENT

A simple computational procedure may be used to investigate Eq. (5a) and directly determine the value of ν_l, γ_{cl}. More precisely, in this computational procedure we choose γ_{cl}, b/a and determine ν_l, γ_0 therefrom. Using the change of variables $y = (\nu r^2/a^2)$, Eq. (5a) may be written

$$\frac{\partial}{\partial y} y \frac{\partial \gamma}{\partial y} = \frac{\gamma}{(\gamma^2 - 1)^{1/2}} . \qquad (A1)$$

By requiring that γ be regular at the origin and attain the value $\gamma(0) = \gamma_c$, Eq. (A1) may be integrated numerically to generate a single parameter family of solutions $\gamma(y, \gamma_c)$. Using the boundary condition Eq. (7) and evaluating y at $r = a$ (i.e., $y = \nu$), we obtain

$$\gamma_0 = \left(\gamma + 2\ln\left(\frac{b}{a}\right) y \frac{\partial \gamma}{\partial y} \right) \Bigg|_{y = \nu} . \qquad (A2)$$

Thus, given b/a and γ_c, the direct integration of Eq. (A1) with the subsidiary condition, Eqs. (A2), yields the general solution $\gamma_0(b/a, \gamma_c, \nu)$.

TABLE II. Test of accuracy of analytical approximations.

	$\gamma_0 = 5$, $b/a = 2$			$\gamma_0 = 7$, $b/a = 4.985$			$\gamma_0 = 100$, $b/a = 1$	
	ν_l	γ_{cl}	γ_{el}	ν_l	γ_{cl}	γ_{el}	ν_l	γ_{cl}
Numerical computer results	1.273	1.313	⋯	1.125	1.480	⋯	97.06	1.676
Interpolation formula, Eqs. (17) (1st-order iteration)	1.12	1.71	3.09	1.03	1.91	3.12	93.12	4.64
Equations (15) (1st-order iteration)	1.64	1.00	2.68	1.41	1.00	2.42	99.00	1.00
Equation (18) (2nd-order iteration)	1.31	1.27	2.83	1.13	1.47	2.78	98.28	1.15
Equation (20) (2nd-order iteration)	1.26	1.38	2.90	1.12	1.53	2.83	96.96	1.82
Equations (25)–(27) (variational principle)	1.28	1.31	2.90	1.13	1.49	2.83	97.82	1.33
Equations (37)–(38) (ultra-relativistic fat beam)	1.35	1.11	⋯	1.09	1.39	⋯	97.13	1.59

2036   Phys. Fluids, Vol. 21, No. 11, November 1978   J. R. Thompson and M. L. Sloan   2036

5

In order to determine the limiting current ν_l, we must determine the value of γ_c such that $\partial\nu/\partial\gamma_c = 0$. However, since $\gamma_0 = \gamma_0(b/a, \gamma_c, \nu)$ we may write

$$0 = \frac{\partial\gamma_0}{\partial\gamma_c} + \frac{\partial\gamma_0}{\partial\nu}\frac{\partial\nu}{\partial\gamma_c}\bigg|_{\tau_0} . \tag{A3}$$

Therefore, the condition of limiting current, $\partial\nu/\partial\gamma_c = 0$, corresponds to a determination of the parameters b/a, γ_c, ν such that $\partial\gamma_0/\partial\gamma_c = 0$. From Eq. (A2) a straightforward differentiation yields

$$\frac{\partial\gamma_0}{\partial\gamma_c} = \left(T + 2\ln\left(\frac{b}{a}\right)y\,\frac{\partial T}{\partial y}\right)\bigg|_{y=\nu} \tag{A4}$$

where

$$T \equiv \partial\gamma(y,\gamma_c)/\partial\gamma_c = T(y,\gamma_c) .$$

The equation governing T may be obtained similarly from Eq. (A1) by differentiation with respect to γ_c:

$$\frac{\partial}{\partial y}\left(y\,\frac{\partial T}{\partial y}\right) = -\frac{T}{(\gamma^2 - 1)^{3/2}} , \tag{A5}$$

where $T(y=0)=1$ and T is regular at the origin.

Equations (A1) and (A5) may now be simultaneously integrated outward in y until a value $y = y_l$ is reached such that $(\partial\gamma_0/\partial\gamma_c)$, as given by Eq. (A4), vanishes. The limiting current ν_l is then given by $\nu_l = y_l$, with γ_0 determined from Eq. (A2). The initially specified quantity γ_c, of course, corresponds to γ_{cl} for this value $y = y_l = \nu_l$. It may be demonstrated that such a point $y_l > 0$ always exists for each choice of $\gamma_{cl} > 1$.

[1] L. S. Bogdankevich and A. A. Rukhadze, Usp. Fiz. Nauk 103, 609 (1971) [Sov. Phys.-Usp. 14, 163 (1971)].

[2] H. V. Wong, M. L. Sloan, J. R. Thompson, and A. T. Drobot, Phys. Fluids 16, 902 (1973).

[3] L. P. Smith and P. L. Hartman, J. Appl. Phys. 11, 220 (1940).

[4] L. S. Bogdankevich and A. A. Rukhadze, Usp. Fiz. Nauk 103, 617 (1971) [Sov. Phys.-Usp. 14, 167 (1971)].

[5] R. B. Miller, R. J. Faehl, T. C. Genoni, and W. A. Proctor, IEEE Trans. Nucl. Sci. NS-24, 1648 (1977).

[6] C. L. Olson and J. W. Poukey, Phys. Rev. A 9, 2631 (1974).

[7] R. J. Briggs, Phys. Fluids 19, 1257 (1976).

[8] W. A. Proctor and T. C. Genoni (private communication).

2037   Phys. Fluids, Vol. 21, No. 11, November 1978   J. R. Thompson and M. L. Sloan   2037

6

APPENDIX D

INFLUENCE OF SPATIAL VARIATION IN γ ON THE
RELATIVISTIC ELECTRON BEAM CYCLOTRON MODE

(Appendix D Contains 24 Pages)

APPENDIX D

INFLUENCE OF SPATIAL VARIATION IN γ

ON THE RELATIVISTIC ELECTRON

BEAM CYCLOTRON MODE

I. Introduction

In a cold relativistic electron beam moving with velocity $u \to c$ in a vacuum along a uniform guide field B_{oz} in the z-direction, electron beam cyclotron modes can propagate with frequency

$$\omega = k_z u - \frac{\Omega}{\left(1 + \dfrac{\omega_p^{\;2}}{k^2 c^2}\right)}$$

where

$$\Omega = \frac{eB_{oz}}{m_e \gamma c} \qquad ,$$

$$\omega_p^{\;2} = \frac{4\pi \, N_o e^2}{m_e \gamma}$$

$$\gamma = \left(1 - \frac{u^2}{c^2} \right)^{-1/2} \quad ,$$

$$k^2 = k_z{}^2 + k_\perp{}^2 \quad ,$$

and the beam density N_o together with γ are assumed constant.

In cylindrical geometry, there exists (for a given value of k_z and mode number m) an infinite denumerable set of modes having different values of $k_\perp$. For the cylindrically symmetric $m = 0$ mode, the lowest value of $k_\perp$ is $k_\perp a \approx 2.95$, where a is the beam radius and the beam is bounded by conducting walls.

The perpendicular electron velocity perturbation $v_\perp$ is proportional to $\left[1/\gamma \left(\omega - k_z u + \Omega \right) \right]$ and remains finite across the beam. If γ varies in magnitude from the inside to the outside of the beam:

$$\gamma = \gamma_o \left[1 + \frac{\alpha \omega_{po}{}^2}{4c^2} \left(r^2 - a^2 \right) \right]$$

2

spatial variations are introduced in $\left[1/\gamma\left(\omega - k_z u + \Omega\right)\right]$ which may not be negligibly small. In particular, for the case when the parameter $\alpha \sim 1$, the spatial variations are significant and must be included in the analysis of the electron cyclotron beam dispersion relation.

In this report, the propagation of electron beam cyclotron modes in the presence of spatial variations in γ is investigated. The eigenvalues are calculated using a variational approach. This obviates the necessity to obtain exact solutions of the eigenvalue equations. It is established that in comparison with constant γ, the corresponding eigenvalues $(k_\perp a)$ increase as the parameter α increases. The larger the eigenvalue $(k_\perp a)$ the closer is the cyclotron motion of the electron to resonance with the oscillating fields of the corresponding eigenmode. In addition, the perpendicular perturbed currents and electric fields become more sharply peaked on the surface of the beam.

II. Electron Beam Cyclotron Mode

The electron beam dynamics is described by the cold fluid equations:

$$\frac{\partial n}{\partial t} + \nabla \cdot n\underline{v} = 0$$

$$\frac{d}{dt} m\gamma\underline{v} = - e\underline{E} - \frac{e}{c}(\underline{v} \times \underline{B})$$

and closure is obtained through Maxwell's equations:

$$\nabla \times \underline{E} = - \frac{1}{c} \frac{\partial \underline{B}}{\partial t}$$

$$\nabla \times \underline{B} = \frac{1}{c} \frac{\partial \underline{E}}{\partial t} + \frac{4\pi}{c} \underline{J}$$

$$\nabla \cdot \underline{E} = 4\pi\rho$$

$$\nabla \cdot \underline{B} = 0$$

where

$$\rho = - en$$

$$\underline{J} = - en\underline{v}$$

$$\gamma = \left(1 - \frac{v^2}{c^2}\right)^{-1/2} \quad .$$

The velocities and electromagnetic fields of the beam equilibrium are:

$$\underline{v}_o = \left(0, \quad v_{o\theta} = \frac{2\pi N_o er}{B_{oz}\gamma^2} \to 0, \quad u_o\right)$$

$$\underline{E}_o = \left(E_{or} = -2\pi N_o er, \quad 0, \quad 0\right)$$

$$\underline{B}_o = \left(0, \quad B_{o\theta} = - \frac{2\pi N_o eur}{c}, \quad B_{oz}\right)$$

$$\gamma = \gamma_o\left\{1 + \alpha\frac{\omega_{po}^2}{4c^2}(r^2 - a^2)\right\} \gg 1 \quad .$$

5

The magnitude of the parameter α is a measure of the spatial variation in γ.

Let the perturbations be of the form $\exp[-i\omega t + ik_z z + im\theta]$. The following differential equations describe the electron beam cyclotron modes:

$$\frac{1}{\xi} \frac{\partial}{\partial \xi} \xi \frac{\partial A^+}{\partial \xi} - \frac{(m + 1)^2}{\xi^2} A^+ - q^2 a^2 A^+$$

$$+ \frac{4}{\alpha(Q - \xi^2)} A^+ = 0 \qquad (1)$$

$$\frac{1}{\xi} \frac{\partial}{\partial \xi} \xi \frac{\partial A^-}{\partial \xi} - \frac{(m - 1)^2}{\xi^2} A^- - p^2 a^2 A^- = 0 \qquad (2)$$

where

$$\xi = r/a$$

$$q^2 = k_z^2 - \frac{\omega^2}{c^2}$$

6

$$p^2 = q^2 + \frac{\omega_{po}^2}{2c^2}$$

$$Q = \frac{1}{\alpha} \left(\frac{2c}{\omega_{po} a} \right) \left[\frac{\Omega_o}{k_z u - \omega} - 1 \right] + 1$$

$$A^{\pm} = E_r \pm iE_\theta \pm i \frac{u}{c} \left(B_r \pm iB_\theta \right) \qquad .$$

It has been assumed that $\gamma > \omega_{po}/\Omega_o$ in order to neglect v_z-perturbations and that

$$\frac{\Omega_o}{k_z u - \omega} \sim 1 > \frac{\alpha}{4} \frac{\omega_{po}^2 a^2}{c^2} \qquad .$$

The boundary conditions on the conducting wall at $\xi = 1$ are

$$A^+ = A^- \tag{3}$$

$$\frac{1}{\xi} \frac{\partial}{\partial \xi} \xi \left(A^+ + A^- \right) = 0 \tag{4}$$

7

Equations (1) and (2) are solved for A^+, A^-, and after substitution in Eqs. (3) and (4), the eigenvalue equation for Q is obtained. In the low phase velocity limit $k_z^2 > \omega^2/c^2$, the frequency ω is given by

$$\omega = k_z u - \frac{\Omega_o}{\left(1 + \dfrac{\omega_{po}^2}{k^2 c^2}\right)} \tag{5}$$

where

$$k^2 = \frac{4}{\alpha(Q - 1)a^2} \quad . \tag{6}$$

The smaller the magnitude of $\omega_{po}^2/k^2 c^2$, the closer is the cyclotron motion of the electrons to strong coupling or resonance with the mode. In fact, it may be seen from Eqs. (1) and (6) that the radial location of the resonance is

$$\xi^2 = \frac{r^2}{a^2} = Q = 1 + \frac{4}{\alpha k^2 a^2} \tag{7}$$

which is just outside the beam edge.

8

The perturbed electron velocity and electro-magnetic fields are:

$$v^{\pm} = v_r \pm iv_\theta$$

$$= - \frac{ie}{m_e \gamma} \frac{A^{\pm}}{(\omega - k_z u \pm \Omega)}$$

$$E_z = \frac{i}{2\left(k_z - \frac{\omega u}{c^2}\right)a} \left[\frac{1}{\xi} \frac{\partial}{\partial \xi} \xi(A^+ + A^-) + \frac{m}{\xi}(A^+ - A^-)\right]$$

$$E_r = - \frac{i}{\left(k_z u - \omega\right)} \left[\frac{u}{a} \frac{\partial E_z}{\partial \xi} - \frac{i\omega}{2}(A^+ + A^-)\right]$$

$$E_\theta = \frac{1}{\left(k_z u - \omega\right)} \left[\frac{mu}{a} \frac{E_z}{\xi} + \frac{i\omega}{2}(A^+ - A^-)\right]$$

$$B_z = \frac{c}{2\left(k_z u - \omega\right)a} \left[\frac{1}{\xi} \frac{\partial}{\partial \xi} \xi(A^+ - A^-) + \frac{m}{\xi}(A^+ + A^-)\right]$$

9

$$B_r = -\frac{1}{(k_z u - \omega)} \left[\frac{mc}{a} \frac{E_z}{\xi} + \frac{ik_z c}{z} (A^+ - A^-) \right]$$

$$B_\theta = -\frac{1}{(k_z u - \omega)} \left[\frac{ic}{a} \frac{\partial E_z}{\partial \xi} + \frac{k_z c}{2} (A^+ + A^-) \right]$$

III. Eigenvalues

The solutions of Eqs. (1) and (2) for $\alpha = 0$ have been derived in previous reports. They are restated here for completeness and easy reference.

When $\alpha = 0$,

$$A^+ = a_o J_{m+1}(\kappa a \xi)$$

$$A^- = b_o I_{m-1}(p\xi)$$

where

$$\kappa^2 = -k_z^2 + \lim_{\alpha \to o} \frac{4}{\alpha Q a^2} \qquad .$$

10

J_{m+1} and I_{m-1} are Bessel and modified Bessel functions, respectively.

The eigenvalue equation for κa, obtained after substituting these solutions in Eqs. (3) and (4), is

$$2 + \kappa a \frac{K_{m+1}'(\kappa a)}{J_{m+1}(\kappa a)} + pa \frac{I_{m-1}'(pa)}{I_{m-1}(pa)} = 0 \qquad (8)$$

where

$$J_{m+1}'(\kappa a) = \frac{d}{d\kappa a} J_{m+1}(\kappa a) \quad .$$

Equation (5) determines the frequency with values of k given by

$$k^2 = \left(k_z^2 + \kappa^2 \right) \qquad .$$

If $pa < 1$, $m = 0$, Eq. (8) reduces

$$\kappa a \frac{J_o(\kappa a)}{J_1(\kappa a)} \approx -2$$

11

so that

$$\kappa a = 2.95, \ 5.84 \ \ldots \qquad\qquad .$$

If $\ pa < 1, \ \ m = -1, $ Eq. (8) reduces to

$$\kappa a = \frac{J_1(\kappa a)}{J_o(\kappa a)} \approx 4$$

so that

$$\kappa a = 1.91, \ 4.60, \ \ldots \qquad\qquad .$$

There exists an infinite denumerable set of eigen-values for each value of $\ m$.

When $\ \alpha \neq 0,\ $ the solutions of Eq. (1) are not expressible in terms of simple functions. However, a variational approach may be adopted to estimate the eigen-values, and exact solutions of Eq. (1) need not be known.

Let Eq. (1) be multiplied by $\ \xi A^{+*}(\xi)\ $ and integrated from $\ \xi = 0\ $ to $\ \xi = 1.\ $ After imposing the boundary conditions at $\ \xi = 1,\ $ namely, Eqs. (3) and (4), it may be verified that

$$- \left| b_o \right|^2 I_{m-1}(pa) \left[2I_{m-1}(pa) + pa \ I_{m-1}'(pa) \right] = \Lambda(A^{+*}, A^+)$$

$$(9)$$

where

$$\Lambda(A^{+*}, A^{+}) \equiv \int_0^1 \xi \left| \frac{\partial A^+}{\partial \xi} \right|^2 d\xi + \int_0^1 \frac{(m+1)^2}{\xi} |A^+|^2 d\xi$$

$$+ q^2 a^2 \int_0^1 \xi |A^+|^2 d\xi - \frac{4}{\alpha} \int_0^1 \frac{\xi |A^+|^2}{(Q - \xi^2)} d\xi \quad (10)$$

and the solution $A^- = b_o I_{m-1}(pa\xi)$ of Eq. (2) has been utilized.

The first variation of the functional Λ with respect to A^+ is stationary, that is, $\delta\Lambda = 0$, if A^+ is a solution of Eq. (1)

Thus by selecting a trial function A^+ which satisfies the boundary conditions and for which $\delta\Lambda = 0$, an approximate dispersion relation can be obtained from Eq. (9).

Consider the following trial function which is suitable for estimating the eigenvalues of the lowest eigenmode:

$$A^+ = \xi^{|m+1|} \left(g_o + g_2 \xi^2 + g_4 \xi^4 \right) \quad .$$

From Eqs. (3) and (4),

13

$$g_2 = b_o \left[-2g + \frac{1}{2} \left\{ (6 + |m + 1|) \, I_{m-1}(pa) \right. \right.$$

$$\left. \left. + pa I_{m-1}'(pa) \right\} \right]$$

$$g_4 = b_o \left[g - \frac{1}{2} \left\{ (4 + |m + 1|) \, I_{m-1}(pa) + pa I_{m-1}'(pa) \right\} \right]$$

where

$$g \equiv g_o/b_o$$

A^+ is, therefore, a trial function with one
parameter g. Substituting for A^+ in $\Lambda(A^{+*}, A^+)$,

$$\Lambda = |b_o|^2 \, \Lambda_o(m, \alpha, qa, pa, Q, g) \quad .$$

The parameter $g = \hat{g}$ is chosen such that

$$\frac{\partial \Lambda_o(\hat{g})}{\partial \hat{g}} = 0 \quad . \tag{11}$$

14

The eigenvalue equation for Q is then given by

$$\Lambda_o(m, \alpha, qa, pa, Q, \hat{g})$$

$$+ I_{m-1}(pa) \left[2I_{m-1}(pa) + pa\, I_{m-1}'(pa) \right] = 0 \quad . \quad (12)$$

Equation (12) is solved numerically to determine Q and hence the eigenvalue ka. Some representative solutions for the cylindrically symmetric $m = 0$ eigenmode with eigenfunction A^+ having no nodes are tabulated in Figures 1, 2, and 3.

Figures 1 and 2 display the increase in magnitude of the eigenvalue ka for given values of $\omega_{po}^2 a^2/c^2$ and $k_z a$ as the parameter α increases.

Figure 3 displays the increase in magnitude of the eigenvalue ka for given values of $\omega_{po}^2 a^2/c^2$ and α as $k_z a$ increases. It may be seen that $k_\perp a = \sqrt{k^2 a^2 - k_z^2 a^2}$ increases strongly with increasing $k_z a$ for $\alpha = 1$.

The accuracy of the variational calculation may be judged by comparison with analytic solutions of Eq. (1)

15

α	0.0	0.1	0.3	0.5	0.7	1.0
ka	2.95	3.13	3.53	4.01	4.61	5.77

Figure 1. Eigenvalue $ka(\alpha)$ for $m = 0$,

$$\omega_{po}{}^2 a^2 / c^2 = 0.06, \quad k_z a = 0.1$$

α	0.0	0.1	0.3	0.5	0.7	1.0
ka	3.07	3.27	3.73	4.31	5.03	6.48

Figure 2. Eigenvalue $ka(\alpha)$ for $m = 0$,

$$\omega_{po}{}^2 a^2 / c^2 = 1.0, \quad k_z a = 0.707$$

k_za	0.0	0.707	1.871	2.916
ka	5.82	6.48	10.98	24.43

Figure 3. Eigenvalue $ka(k_za)$ for $m = 0$, $\omega_{po}^2 a^2/c^2 = 1.0$, $\alpha = 1.0$

and (2). Thus for $m = 0$, $\omega_{po}^2 a^2/c^2 \ll 1$, $\omega^2 a^2/c^2 \ll k_z^2 a^2 \ll 1$, and $\alpha = 0.5$, the solution of Eq. (1) is

$$A^+ = a_o \xi (Q - \xi^2)$$

and the corresponding eigenvalue is $ka = 4$. The variational solution for $m = 0$, $\omega_{po}^2 a^2/c^2 = 0.06$, $k_z^2 a^2 = 0.01$, and $\alpha = 0.5$ is $ka = 4.01$. The eigenvalues obtained from the variational approach are indeed acceptable.

The trial function A^+ which minimize $\Lambda(A^{+*}, A^+)$ are plotted as functions of ξ in Figure 4. $A^+(\xi)$ is normalized so that $A^+(\xi = 1) = 1$. The associated fields $E_z(\xi)$ and $E_r(\xi)$, computed from the trial function $A^+(\xi)$, are plotted in Figures 5 and 6. The profiles of $A^+(\xi)$ and $E_z(\xi)$ are not appreciably altered with changes in the value of α. However, $E_r(\xi)$ becomes

18

m = 0

$k_z a = 0.1$, $\quad \dfrac{\omega_p^2 a^2}{c^2} = 0.06$

$A^+(\xi)$ normalized so that $A^+(1) = 1$

$\alpha = 0.1$

$\alpha = 0.5$

$\alpha = 1.0$

$A^+(\xi)$

1.5

1.0

0.5

0.5

1.0

Eigenfunction: $A^+(\xi)$

Figure 4

19
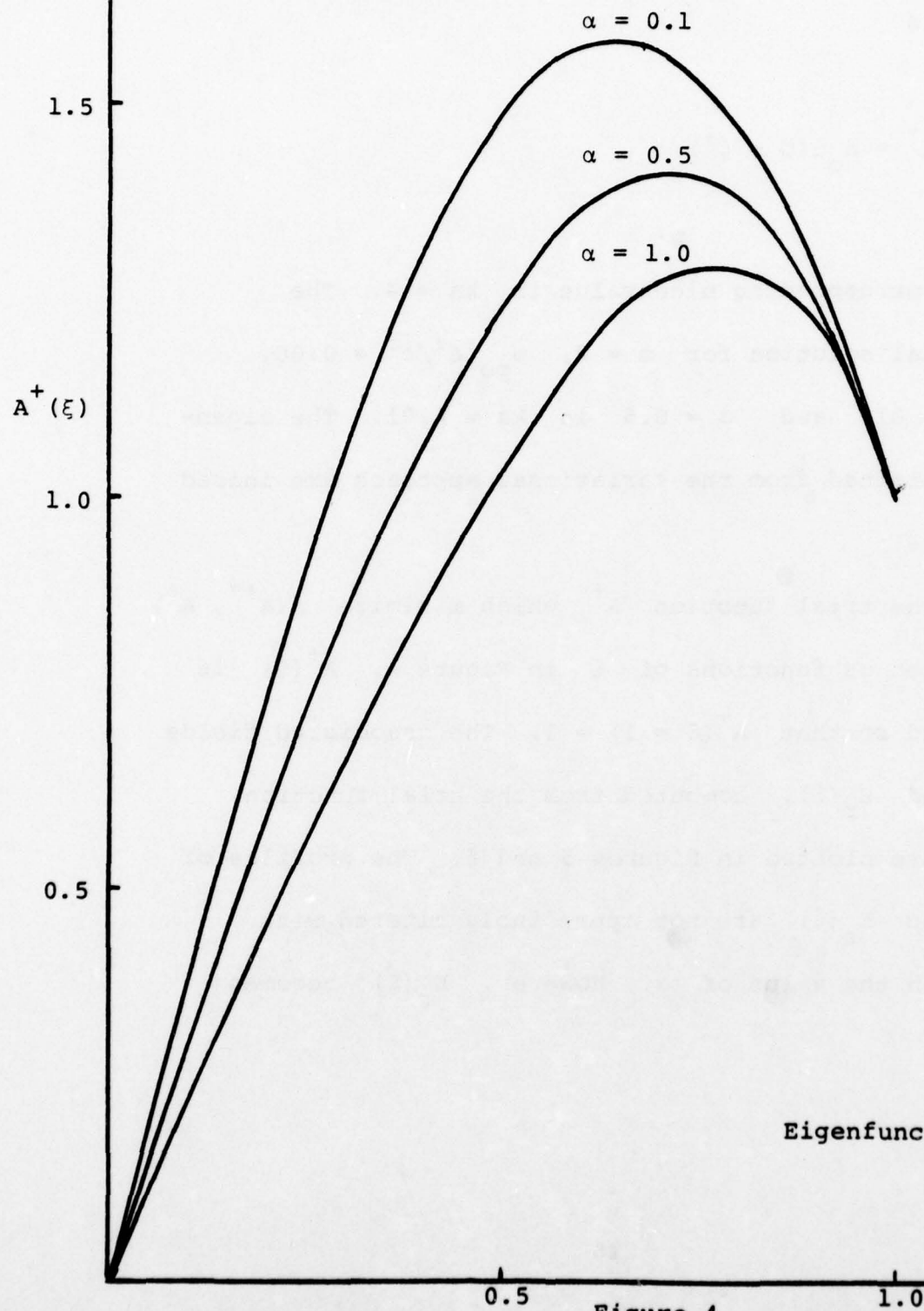
$m = 0$

$k_z a = 0.1,$ $\quad \dfrac{\omega_p^2 a^2}{c^2} = 0.6$

$E_z(\xi) \approx \dfrac{iA^+(1)}{2k_z a} \hat{E}_z(\xi)$

$E_z(\xi)$

10

$\alpha = 0.1$

$\alpha = 0.5$

$\alpha = 1.0$

5

Parallel Electric
Field: $E_z(\xi)$

0.5 1.0

20 Figure 5

$m = 0$

$k_z a = 0.1, \qquad \dfrac{\omega_p^2 a^2}{c^2} = 0.06$

$E_r(\xi) \approx \dfrac{A^+(1)}{2k_z^2 a^2} \hat{E}_r(\xi)$

$\hat{E}_r(\xi)$

$\alpha = 0$

$\alpha = 0.5$

$\alpha = 1.0$
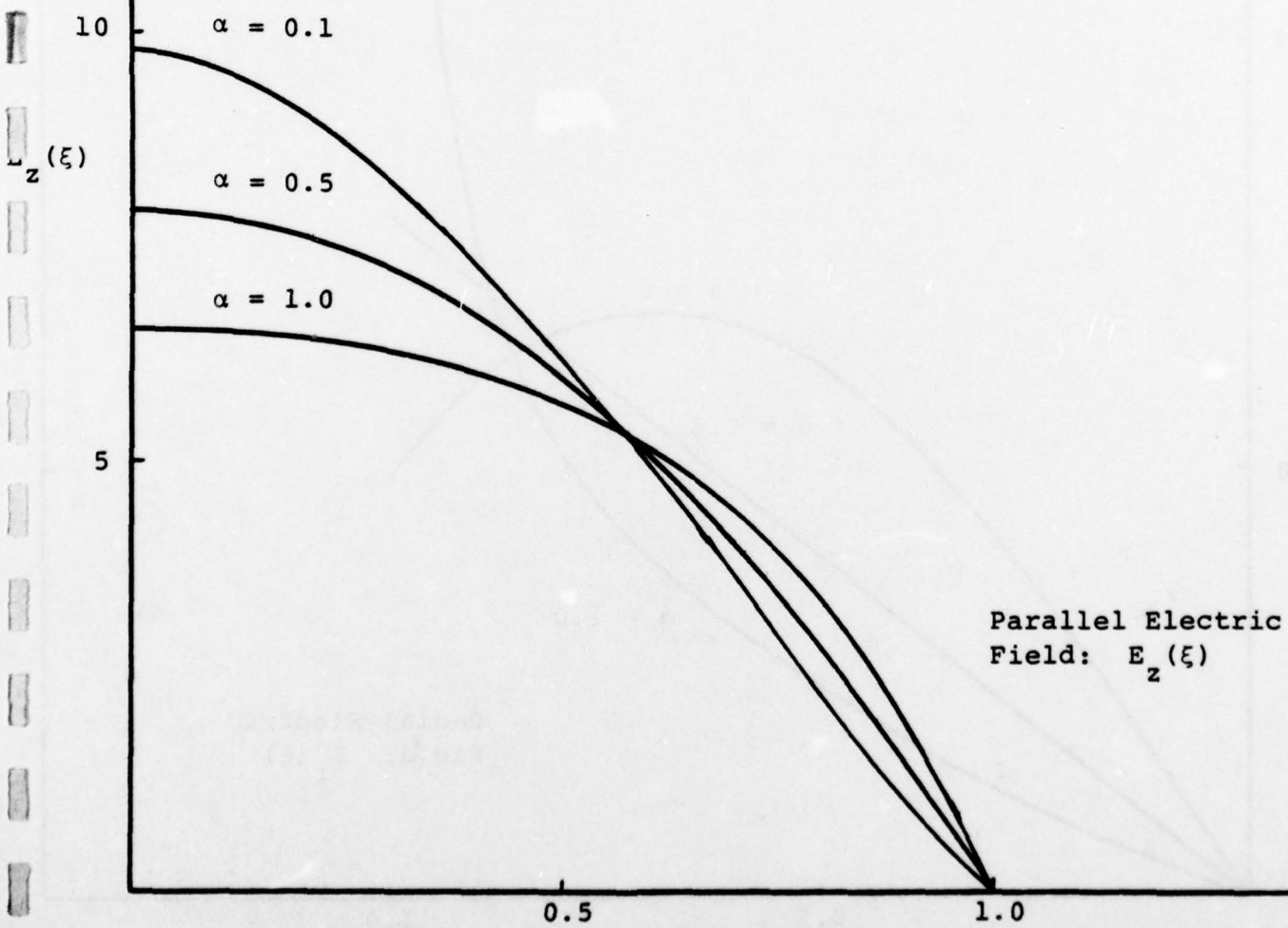
Radial Electric
Field: $E_r(\xi)$
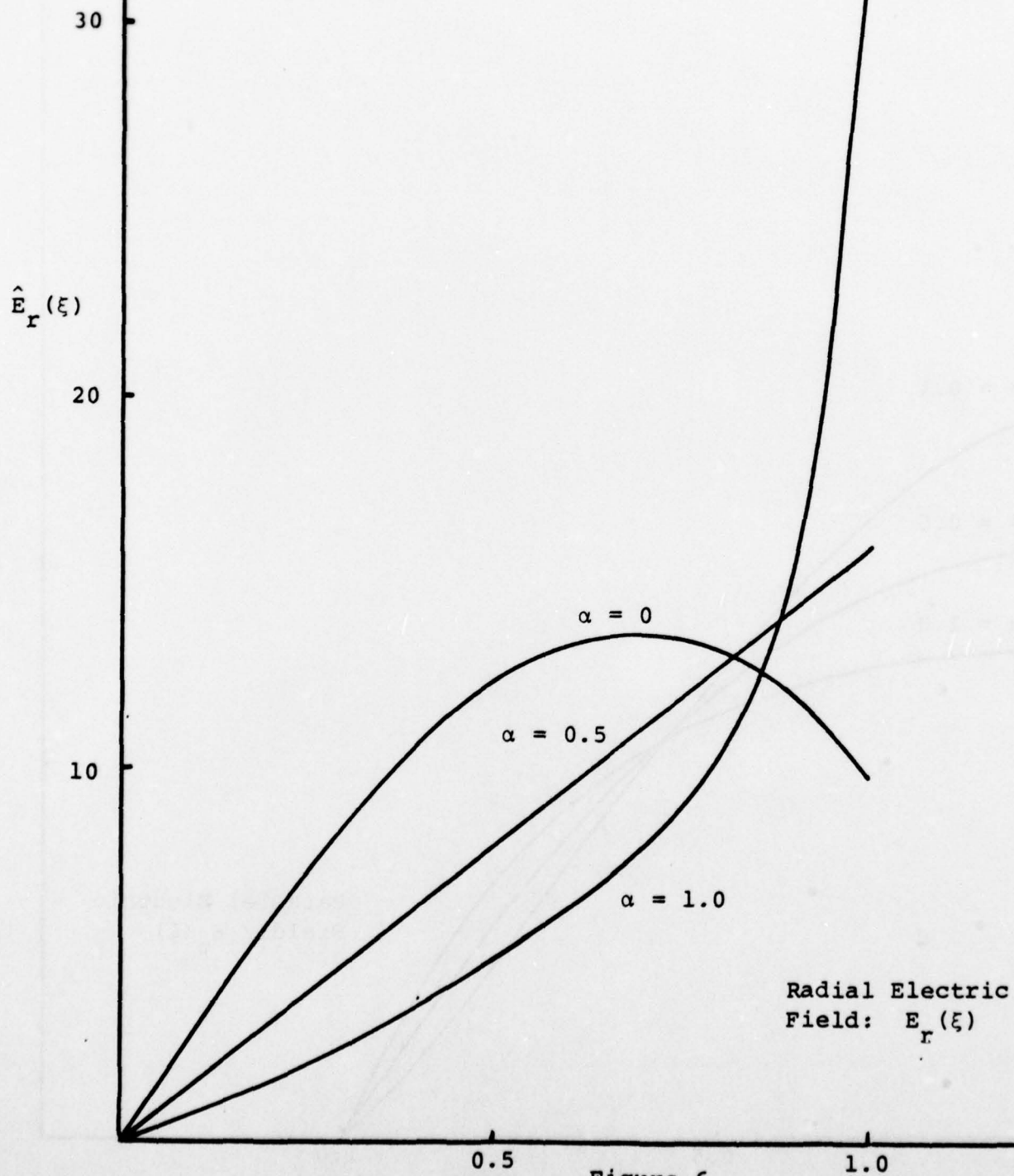
Figure 6

more sharply peaked at $\xi = 1$ when $\alpha > 0.5$, its magnitude at $\xi = 1$ being proportional to $k^2 a^2$ which increases with α.

IV. Discussion

The spatial variation in γ was expressed in terms of the parameter α:

$$\gamma = \gamma_o \left[1 + \frac{\alpha \omega_{po}^2}{4c^2} (r^2 - a^2) \right]$$

where α was assumed to be in the range

$$\left| \frac{4c^2}{a^2 \omega_{po}^2} \right| > \alpha \qquad .$$

A relativistic electron beam of constant γ_o entering a cylindrical waveguide bounded by conducting walls will produce a beam equilibrium having a spatial γ variation with $\alpha \sim 1$.

The magnitude of corresponding eigenvalues ka

increases with increasing α. For $m = 0$, the value of

$ka\left(\omega_{po}^2 a^2/c^2 < 1, \quad k_z a < 1\right)$ for the lowest eigenmode

(no nodes) increases from 2.95 to 5.77 as α

increases from zero to unity. The larger the magnitude

of ka the closer is the cyclotron motion of the electron

to resonance with the oscillating fields of the

corresponding eigenmode. Larger ka values impose some-

what more stringent restrictions on the temperature of the

electron beam in order to avoid significant "Landau"

damping, since Eq. (7) shows that the spatial location of

the cyclotron resonance then occurs much closer to the

beam surface. Hence, a finite energy spread would more

easily allow a few particles to be in resonance with the

wave.

Furthermore, $E_r(\xi)$ and, consequently, the

perturbed perpendicular electron velocities exhibit a

transition in profile to one which is sharply peaked at

$\xi = 1$ when $\alpha > \frac{1}{2}$ (m = 0). The surface perturbations are then larger than the interior perturbations. The effect of nonlinearities are, therefore, likely to be more significant on the surface than in the interior of the beam.

APPENDIX E

RELATIVISTIC E-BEAM PLASMA HEATING

by

W. E. Drummond and J. R. Thompson

Notes for a 1/2 hour presentation at the Fourth National School on
Plasma Physics, Novosibirsk

July 1974

(Appendix E contains 25 pages)

RELATIVISTIC ELECTRON BEAM PLASMA HEATING (20-30 min.)

A Synopsis

I. Introduction (5-7 min.)

wherein the problem of heating 10^{14}-10^{18} density plasmas
with beams is posed--and it is assumed that one gives a damn
about efficient (or rapid) heating--as for single pass, θ-pinch
geometry--and so optimization of the heating interactions is
desired

II. Return Current Heating (5-7 min.)

wherein it is argued that return current heating goes to pot
for $(n_p/n_B) \gtrsim 100$

III. Primary, hydrodynamical, beam-plasma interaction (10-15 min.)

wherein the scaling obtained from computer runs is discussed,
and it is argued that reasonable deposition efficiencies (>10%)
can be obtained even for $(n_p/n_B) \sim 10^5$ provided that the beam
quality assures a hydrodynamical interaction: $\theta_{rms} \lesssim 2(n_B/n_p)^{1/3}$.
This quality may be easier to achieve than the MA/cm^2 current
density required for return current heating.

RELATIVISTIC E-BEAM PLASMA HEATING

by

W. E. Drummond and J. R. Thompson

(Notes for a 1/2 hour presentation at the Fourth National
School on Plasma Physics, Novosibirsk, July 1974)

It is well known that advances in high energy, pulsed power
technology have made available extremely powerful electron beams,
capable of delivering .1-1 megajoules of directed beam energy within
.1 μsec. My remarks today will be confined to the prospects for
utilizing such beams for the heating of target plasmas of moderately
high density, 10^{14} -10^{18} cm^{-3}, in volumes of 10^3 -10^5 cm^3, to multi-
kilovolt temperatures. [I will not discuss pellet heating, and these
remarks will be less relevant for the heating of lower (<10^{14}cm^{-3})
density plasmas.]

I will further presume that it is either necessary or desirable
that the heating be accomplished rapidly and with a resonable efficiency
of energy deposition from the beam into the target plasma. For
example, this would be the case in any single pass heating, in which
the lifetime of interaction for a beam electron would be limited to
its transit time of a few nanoseconds. In this case it is important
to study the alternative mechanisms of beam-plasma interaction, so
that parameters might be selected to optimize one or another mechanism.

(There is another class of problems, which will not be further
discussed here, in which the primary concern is how to inject and
confine a powerful beam in a toroidal device for many thousands or

perhaps millions of plasma periods. For this problem, the extended time of interaction would permit almost any of the interaction mechanisms to couple much of the beam energy into the target, and the question of optimizing one or another interaction would be much less important.)

There exists an increasing body of experimental data, indicating the successful one pass heating of target plasmas with energy deposition efficiencies in the range of 10%-50%, for the case where the target plasmas were no more than a few hundred times denser than the electron beams. The experiments, in agreement with theory, have shown increasing energy deposition efficiencies as the beam to target density ratio is increased toward one. Therefore, in response to the demand for heating plasmas of higher and higher density, there has been a certain trend toward increasing the beam current (if necessary at the expense of particle energy) and reducing the beam size to further increase its density. This evolution becomes increasingly more difficult and technologically more demanding as one considers heating the higher density target plasmas which may be desired in future controlled fusion experiments. For example, to heat a $10^{16} cm^{-3}$ density target plasma with relativistic beam of density above 2% of the target density, one must be able to propagate current densities above a megampere/cm^2 for a distance of many cm. Such a beam would be much more intense than those commonly generated at particle densities of 10^{11}-10^{13} cm^{-3}, or current densities of some kA/cm^2.

It is an appreciation of the difficulty of this chore of propagating beams of such high current density, as one scales up to denser

-2-

fusion experiments, which has motivated us to examine the density scaling of the energy deposition efficiencies for various mechanisms of beam-plasma interaction, so as to determine the minimum required beam current density and any alternatives to very high beam density which may still allow adequate heating.

Let us suppose that the target plasma has been preionized, or else that the neutral gas pressure is sufficiently high (above ~30 mT or $10^{15} cm^{-3}$) that field induced cascade ionization produces a fully ionized target early in the beam pulse time. The induction fields of the electron beam will quickly drive a return current carried by the plasma electrons, provided that $\frac{\omega_p^2 a^2}{c^2} \simeq \frac{n_p a^2}{3 \times 10^{11}} \gg 1$. (Here ω_p is the target electron plasma frequency, a is the beam radius, and the condition has been shown by Sudan and others to be roughly appropriate with or without external magnetic fields.)

One mechanism for depositing beam energy into the target plasma is via the dissipation of this return current due to microturbulent interactions between the return current electrons and the target plasma ions. These interactions extract drift energy from the plasma electrons, which is replenished by the induction fields which transfer energy from the beam electrons to the plasma electrons. The scaling of these microturbulent interactions is illustrated on the first slide.

-3-

The first point to notice is that the return current drift velocit

scales with the beam to target plasma density ratio, and that heating

rate per target electron scales as the inverse square of the plasma

density. This is because the return current drift energy is what

directly feeds the turbulence. Consequently, the rate of return current

dissipation falls rather dramatically as one attempts to heat target

plasmas much denser than the beam.

The second point to notice is that there is evidence that the

"effective collision frequency," whose average value influences the

L/R current decay time, is <u>not</u> constant but in fact decreases as the

plasma heats up. For example, we and others (Morse, Biscamp) have

performed one-dimensional, particle computer calculations of electron-

ion interactions, in which the initial inductive coupling to the

beam electrons is mocked up by a constant current boundary condition

-4-

RETURN CURRENT HEATING

$$N_d = \frac{n_b}{n_p} \beta c$$

$$\frac{d T_e}{dt} \sim m N_d^2 \nu_{eff} \; ; \; \tau_{DECAY} \sim \frac{\omega_{pe}^2 a^2}{c^2 \langle \nu_{eff} \rangle}$$

CONSTANT CURRENT, 1-D COMPUTER RUN
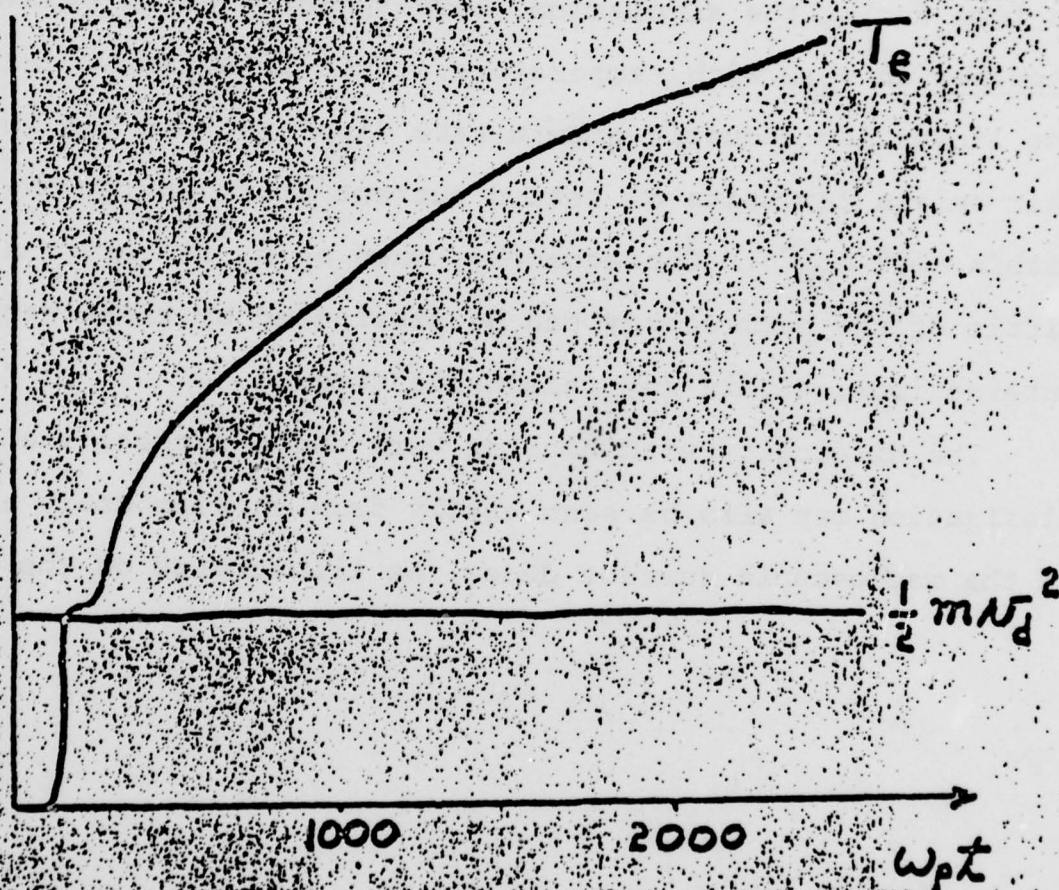
$$\frac{T_e}{m N_d^2} \sim \ln \left[1 + \frac{\omega_p t}{100} \right]$$

$$\nu_{eff} \sim \nu_0 \, e^{-T_e / m N_d^2}$$

$(\overset{\bullet}{E} + 4\pi J = 4\pi J_o)$. The resultant electron heating is as shown on the slide:

> (i) an initially rapid rise of T_e to $\epsilon_{drift} = \frac{1}{2} m v_d^2$ due to the two stream interaction, if $T_e < \epsilon_{drift}$ to start with, followed by

> (ii) a progressively slower increase in T_e above ϵ_{drift} due to ion-acoustic-like turbulence.

In this latter phase, the temperature only increases logarithmically in time during the simulation, corresponding to an exponential decrease in ν_{eff} with temperature. This is a faster decrease than the linear ion acoustic growth rate displays, and the implication is that only a few units of return current drift energy may be dissipated within $\sim 10^5 \omega_{pe}^{-1}$. Consequently, when n_B/n_p is very small, very little of the beam energy can be dissipated by these return current interactions, within any reasonable time.

The difficulty with heating very dense targets via return current dissipation may also be seen easily from an elementary examination of the macroscopic current decay, as illustrated on the next slide:
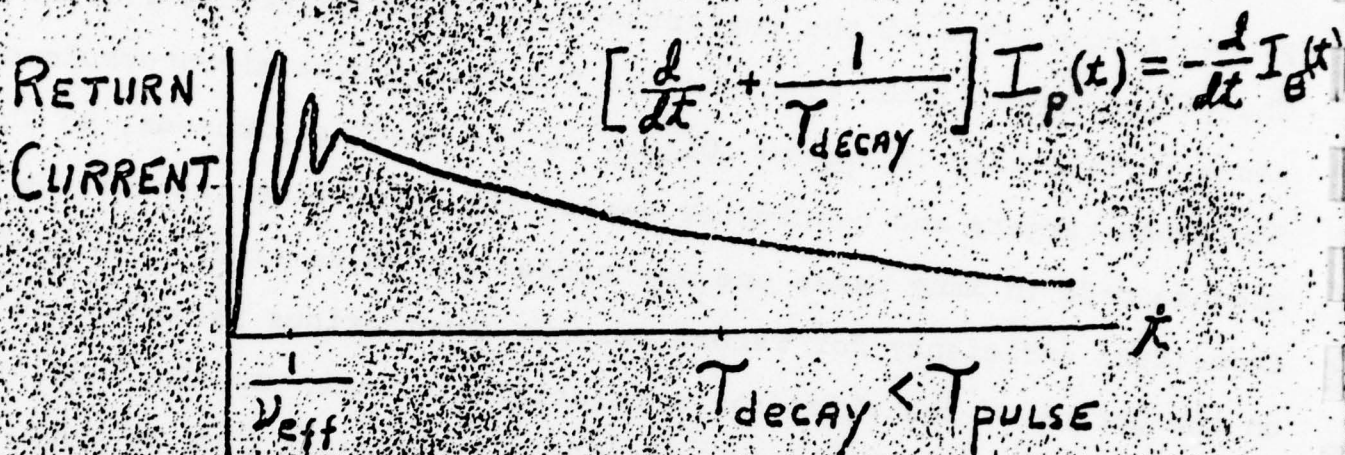
It is clear that if the return current decay time, which increases with the target plasma density, should become larger than the beam pulse time, then the return current will be inductively quenched prematurely when the tail of the beam passes by. This prevents completion of the resistive decay which heats the plasma. The effective collision frequency of the dissipative microturbulence tends to fall from .2 ω_{pi} to .01 ω_{pi} as the heating proceeds, so that for dense targets and centimeter beams, the decay time can well be microseconds in many cases and may exceed the pulse time. The energy deposition efficiency for return current interactions is indicated on the bottom of the slide for a relativistic beam, and the penalty for large decay times is evident. Since the transit time is only nanoseconds, the ratio of "times" will be small, and large ν/γ beam parameters are essential to increase the efficiency. (Here

$$\nu_B \equiv \frac{\omega_B^2 a^2}{4c^2} = \frac{I(kA)}{17\beta} \ ,$$ and G is a dimensionless geometrical factor

relating to flux linkage.)

In summary, dense target plasmas can only be heated effectively by return current interactions if the beam current and current density are increased to the point that ν_B/γ_B is large, $\tau_{decay}/\tau_{pulse}$ is not too large, and n_p/n_B is not too large. In short, one must confront the difficult problem of propagating ultra high beam current densities to heat dense target plasmas in this way.

$$\tau_{decay} \sim \underbrace{\frac{\omega_{pe}^2 a^2}{c^2}}_{\sim 10^6} \frac{1}{\nu_{eff}} \; ; \; \tau_{pulse} \sim 10^{-7} \text{ sec}$$

RETURN CURRENT

$$\left[\frac{d}{dt} + \frac{1}{\tau_{decay}} \right] I_p(t) = -\frac{d}{dt} I_\beta(t)$$

t

$\frac{1}{\nu_{eff}}$

$$\tau_{decay} < \tau_{pulse}$$

RETURN CURRENT

PREMATURE QUENCHING

t

$\frac{1}{\nu_{eff}}$

$$\tau_{pulse} < \tau_{decay}$$
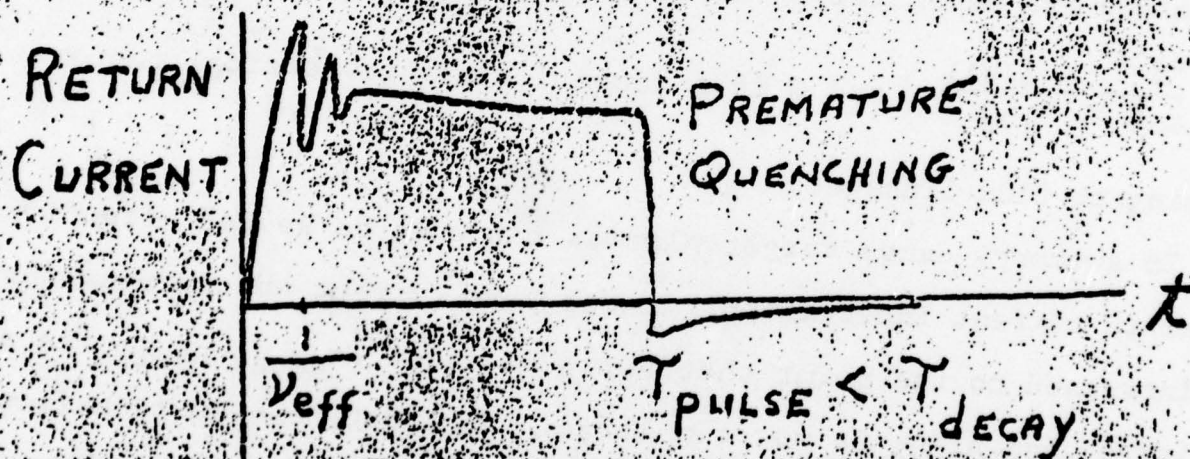
$$\left(\sim \frac{\nu_\beta}{\gamma_\beta} \frac{\tau_{transit}}{(\tau_{decay}, \tau_{pulse})_{max}} \ln G \right.$$

An alternative mechanism for depositing the beam energy in the target plasma is the _primary beam plasma_ interaction. This class of primary interactions is richly endowed with a large parameter space, which encompases a hydrodynamical and a kinetic regime, longitudinal and transverse waves, electrostatic and electromagnetic regimes, gyroeffects, relativistic effects, effects of finite geometry and inhomogeneity, and the various nonlinear effects which appear as the interaction evolves. Without attempting to survey all of this parameter space, I would only point out some of the interesting scalings of a well studied and important subclass of primary interactions, as indicated on the next slide.

This is the hydrodynamical interaction of a sufficiently mono-energetic relativistic beam, generating longitudinal electrostatic turbulence. We examine this interaction in one dimension for the

PRIMARY BEAM - PLASMA INTERACTION

COLD BEAM $\rightarrow$ HYDRODYNAMICAL

LONGITUDINAL (1-D) INTERACTION

WEAK : $\dfrac{\gamma_B n_B}{n_P} < 0.1$

$\rightarrow$ LINEAR, NON-REL. PLASMA RESPONSE

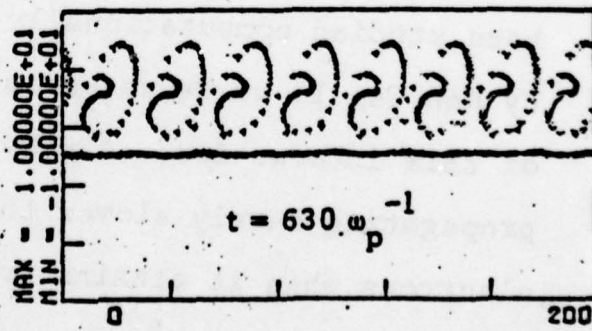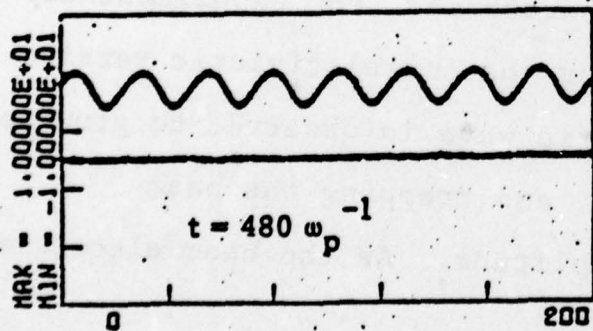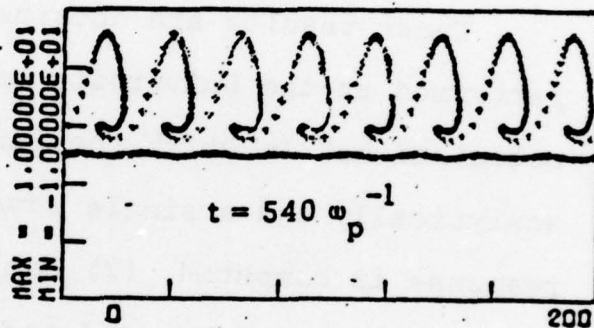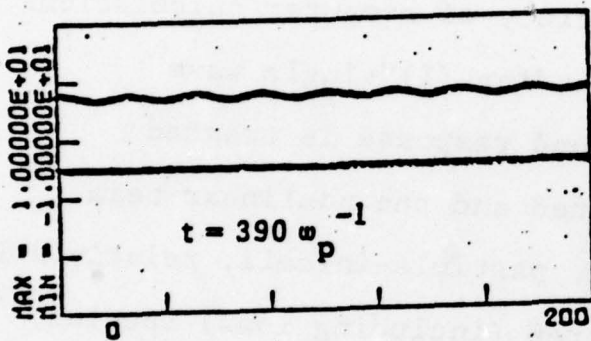INITIALLY SINGLE WAVE NONLINEAR
BEAM RESPONSE

$$\dfrac{\mathcal{E}}{(\gamma_B - 1)\, n_B\, mc^2}$$

$\mathcal{E}_{BEAM}$

$\epsilon \equiv \dfrac{\Delta \mathcal{E}_{BEAM}}{\mathcal{E}_{BEAM}(t=0)}$
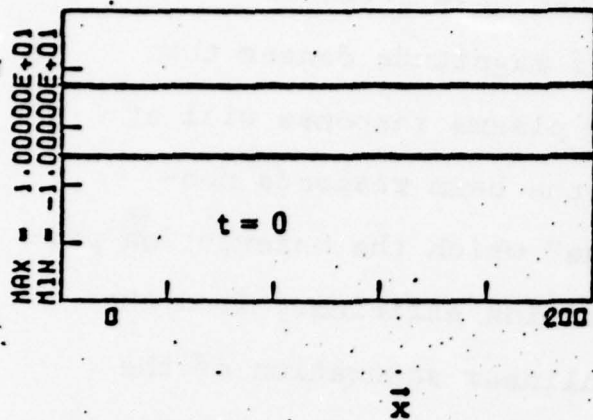
$\mathcal{E}_{FIELD}$

O t_s t
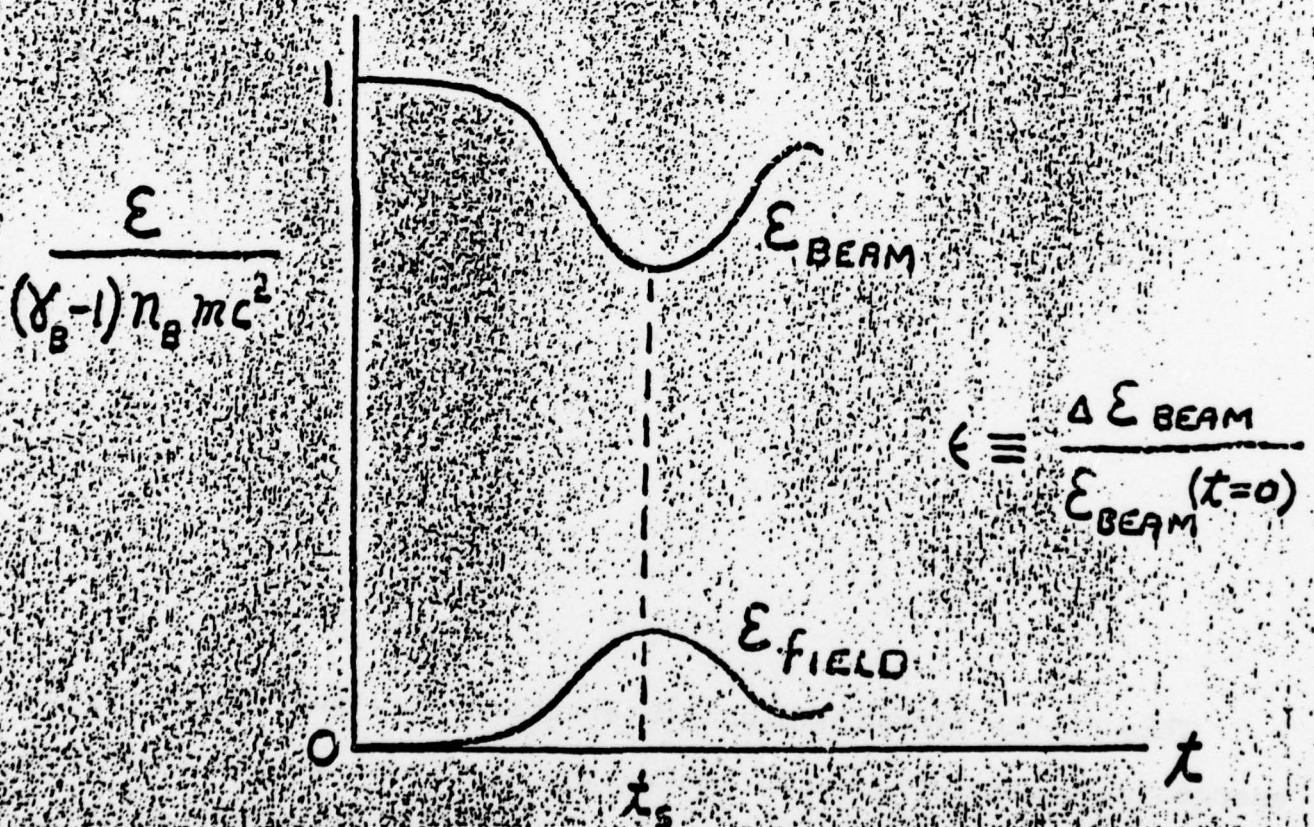
case where the beam is weak: $\gamma_B n_B/n_p < 0.1$ and where gyroeffects,
geometrical and inhomogeneity effects are negligible. The "weak
beam" regime is appropriate for the problem we have posed of
attempting to heat plasmas several orders of magnitude denser than
the electron beams, and it implies that the plasma response will at
first be linear and nonrelativistic, while the beam responds non-
linearly to the narrow spectrum "single wave" which the interaction pro-
duces. We are interested here in the deposition efficiency from the
beam, achieved by the time of the first nonlinear saturation of the
interaction--as defined on the slide--and in particular in how this
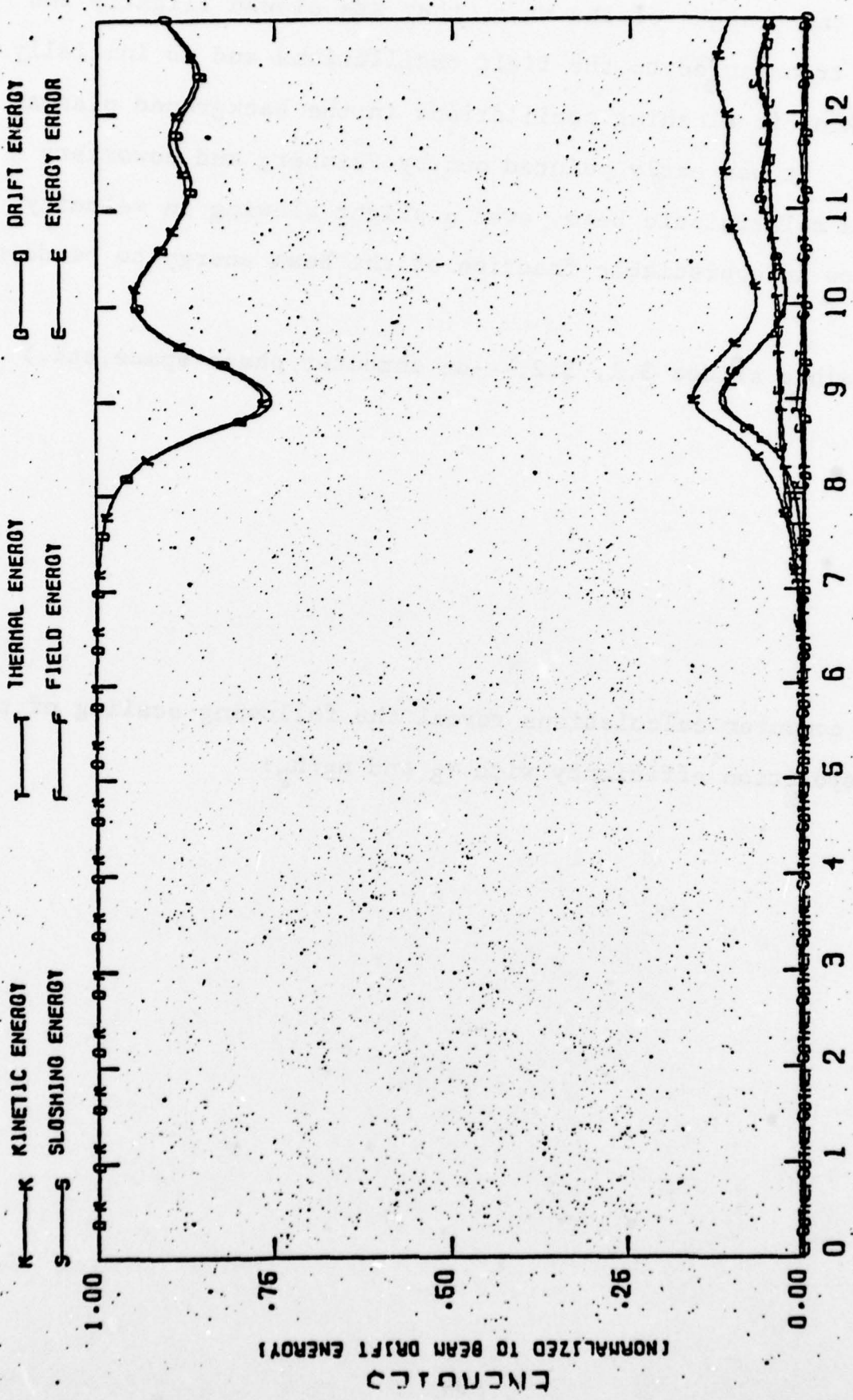efficiency depends on γ_B, n_B, and n_p.

These results are obtained from a variety of computer calculations
performed at the University of Texas, including (1)"single wave
calculations" in which the linear background response is treated
analytically and a single wave is legislated and the nonlinear beam
response is computed, (2) one dimensional, particle-in-cell, relativistic
calculations with two and occasionally three (including ions) species,
and (3)a very few, recent two-dimensional, relativistic, electro-
magnetic, particle calculations.

The physics of this interaction is by now very well known, having
been studied computationally in many laboratories, and experimentally
by Ken Gentle at Texas--among others--for the nonrelativistic version
of this interaction. A very pure electric wave is observed to grow up,
propagating barely slower than the beam, and trapping the beam
electrons when it attains sufficient amplitude. As the beam electrons

-8-

PHASE SPACE ($\gamma\beta$ vs. x)

for $\gamma_B = 5$, $n_p/n_B = 216$ INTERACTION
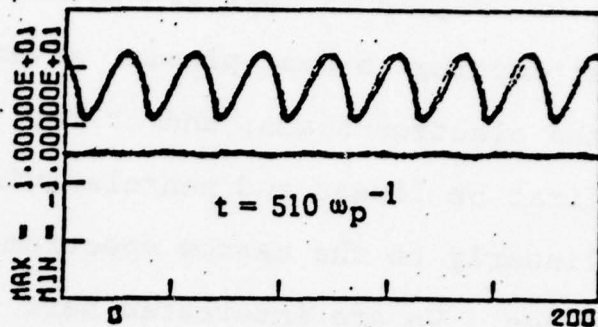
SUMMARY FOR RUN EER11 ENERGIES

K KINETIC ENERGY   D DRIFT ENERGY
S SLOSHING ENERGY   E ENERGY ERROR
T THERMAL ENERGY
F FIELD ENERGY

ENERGYS
(NORMALIZED TO BEAM DRIFT ENERGY)

1.00   .76   .50   .25   0.00

TIME IN 1000S OF STEPS

0 1 2 3 4 5 6 7 8 9 10 11 12

rotate in the troughs of the wave, they are slowed slightly and
energy is transferred to the field oscillations and to initially
coherent kinetic sloshing oscillations in the background plasma
electrons. It was early pointed out by Fainberg and coworkers
that for a relativistic beam, even a slight slowing in velocity
would allow an appreciable fraction of the beam energy to be deposited.

(Possible slides 3.1, 3.2,---on computer phase space,etc.)

The computer calculations reveal the following scaling of the
energy deposition efficiency with γ_B and n_B/n_p:
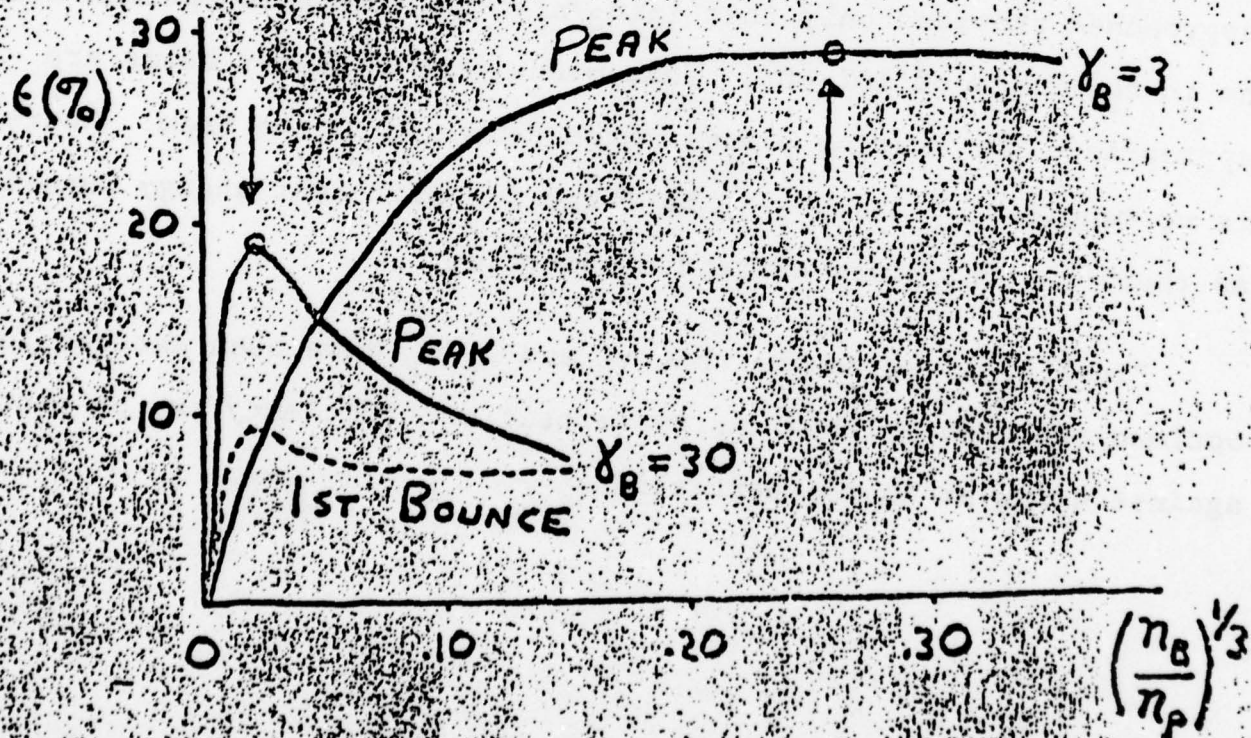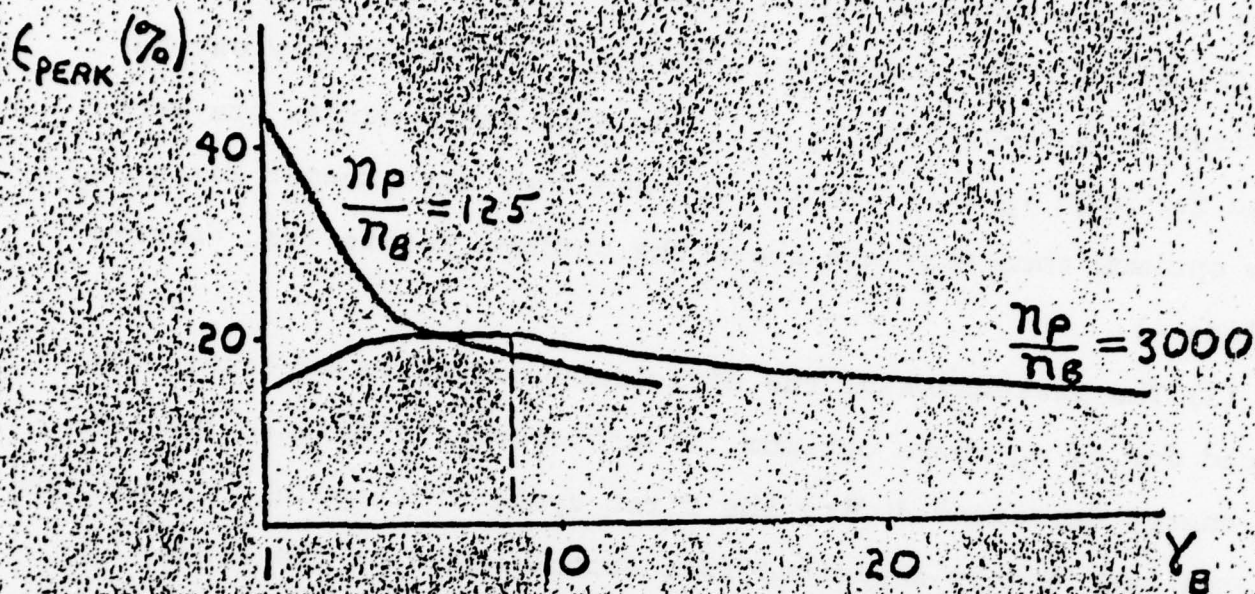
OPTIMUM $\gamma_B (n_B/n_P)^{1/3} \gtrsim 0.5$

(1) One conclusion is that for a fixed value of n_p/n_B below a few hundred, the efficiency declines with γ_B, while for larger values of n_p/n_B there is a weak peak in $\varepsilon(\gamma_B)$.

(2) Second, for fixed choices of γ_B, the efficiency may be optimized with respect to n_B/n_p. The efficiency curves are more peaked for high γ_B than for low γ_B, and they are steeper for n_B/n_p below optimum than they are above the optimum points (see "arrows" on slide 4).
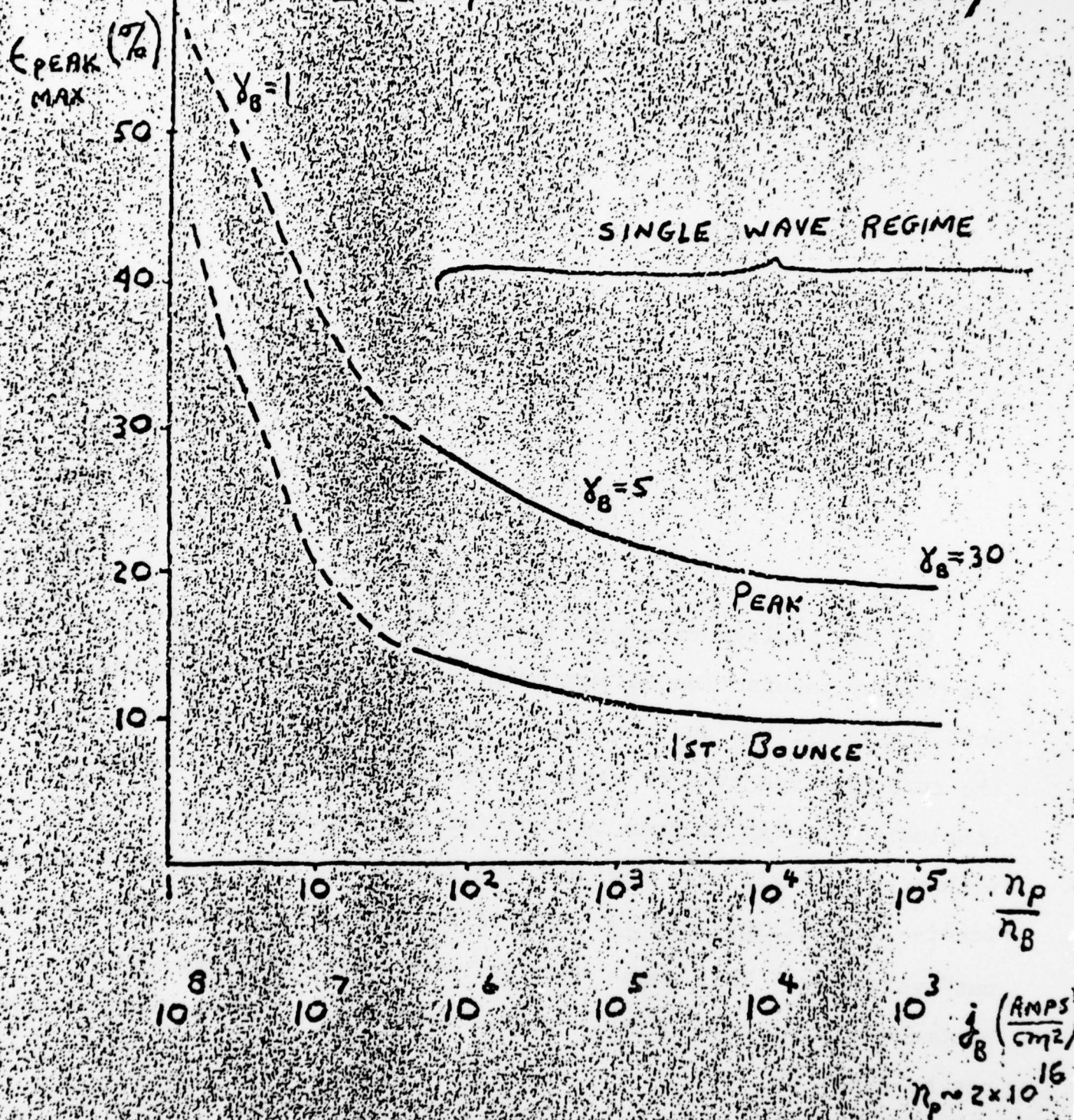
(3) The peakedness of the efficiency curves is substantially reduced for n_B/n_p above optimum, if efficiency is defined from the mean energy deposited during the first cycle of trapping, rather than from the peak energy deposited (see dotted curve on the slide).

(4) Consequently, the optimum deposition efficiency can be approached provided only that $\gamma_B(n_B/n_p)^{1/3} \gtrsim \frac{1}{2}$, and this optimum will be in the range of 10%-40%. This means that higher-γ beams are appropriate for heating plasmas much denser than the beam. There is no requirement that ν_B/γ_B be large for efficient energy deposition, as there is for return current dissipation.

Finally, if we assume that γ_B and n_B/n_p have been matched for optimum efficiency, this energy deposition efficiency may be plotted against n_p/n_B as in the next slide:

For the smaller values of n_p/n_B where the efficiency is highest, the primary interaction is supplemented by reverse current dissipation both the background and the beam response is highly nonlinear, and the turbulent spectrum is rather broad from the start. The chief conclusion we wish to draw is that for the larger values of n_p/n_B within the "single wave regime," the deposition efficiency--although lower--is still <u>appreciable</u>. The efficiency curves are "flattening-out" verses n_p. This means that extremely dense plasmas can be heated with much less dense, relativistic beams, if this interaction can be achieved.

ENERGY TRANSFER EFFICIENCY

$\epsilon_{PEAK \atop MAX} (\%)$

SINGLE WAVE REGIME

$\gamma_B = 1$

$\gamma_B = 5$

$\gamma_B = 30$

PEAK

1ST BOUNCE

$\frac{n_P}{n_B}$

$j_B \left(\frac{AMPS}{cm^2}\right)$

$n_P \sim 2 \times 10^{16}$

The primary difficulty is to assure that the beam is sufficiently monoenergetic that the interaction is at least marginally hydro-dynamical rather than kinetic in nature. This means that the angular scatter of momenta must not be too high--roughly that $\theta_{rms} \lesssim \frac{1}{\gamma_B} \approx 2(n_B/n_p)^{1/3}$. Achieving this beam quality is also relatively more difficult for dense target plasmas, but it might prove easier than propagating megamperes/cm^2. The point is that there is an _alternative_ way to go in trying to heat dense fusion plasmas with relativisitc electron beams. One can either improve the quality or else the current density of the beam. Although there has not been a large experimental effort to improve beam quality, steps such as introducing guide magnetic fields into the diode appear very promising.

Although this is the chief point of this talk, I should touch briefly on a few other points that have been neglected:

(1) Regarding gyroeffects--it will generally be technologically unfeasible to magnetize (i.e.; $\Omega_e > \omega_{pe}$) the target plasma at the densities we have been considering (10^{14} to 10^{18} cm^{-3}). However, it is entirely possible to magnetize the beam, such that $B^2/8\pi > n_B(\gamma_B-1)m$

(2) In the absence of a magnetic field, the beam plasma interaction with the fastest growth rate is the electrostatic _transverse_ beam instability, with $k_\perp > k_\parallel \simeq \omega_p/\beta c$. However, when $\gamma_B(n_B/n_p)^{1/3} < 1$, the transverse interaction saturates without creating so much momentum scatter that the longitudinal interaction is cast into the kinetic regim It is also possible to strengthen the guide magnetic field to the point $\left[(\Omega_e/\omega_p) \simeq (\gamma_B^2 n_B/n_p)^{1/3}\right]$ that the transverse interaction is

-12-

suppressed while the longitudinal interaction is unaffected. In any case, our preliminary two dimensional computer calculations, which allow both transverse and longitudinal interactions with B=0, show adequate energy deposition not much below the one dimensional predictions. (Similar results have been reported from NRL.)
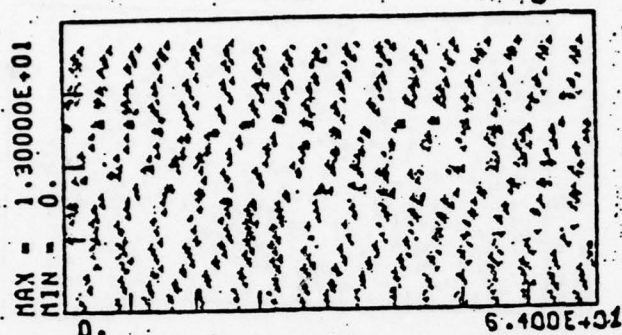
(3) The effect of collisions between the target plasma electrons and ions is rather weak on the hydrodynamical primary beam-plasma interaction, but it can lead to suppression of the kinetic beam plasma interaction (where the beam momentum scatter is too great.) This is why the beam quality must be assured for efficient heating. The target collisions will also lead to randomization of the coherent oscillations excited in the plasma electrons--generally on µsec time scales--and will lead to energy equilibration with the ions--generally on msec time scales.

(4) Finally we have not discussed the later time nonlinear effect such as parametric instabilities or trapped particle instabilities which can serve to further enhance the energy deposition efficiency, to randomize the turbulence (spread spectrum), and to heat the ions more quickly, provided that there is time for these interactions to occur. Since even the earliest interaction provides resonable deposition efficiencies when the necessary beam quality is achieved, the later interactions will be "icing on the cake."
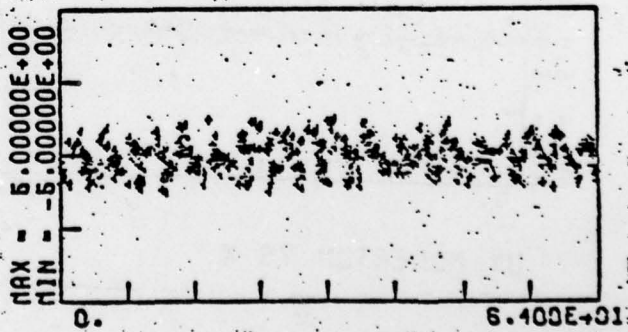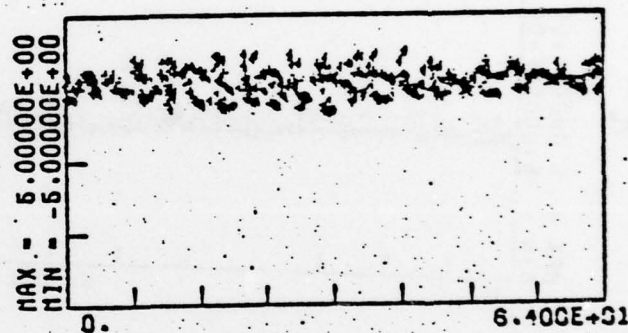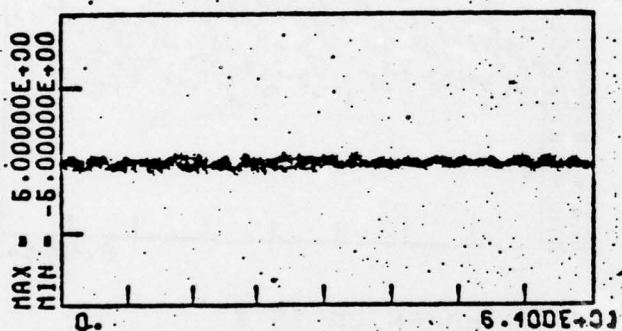
(Possible conclusion by showing some of the slides from a two dimensional, B=0, γ_B=3, n_p/n_B=8 beam plasma interaction with ϵ~25%)

-13-

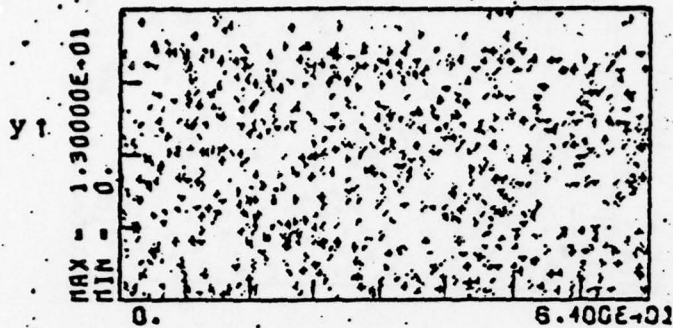# PHASE SPACE for 2-D, $\gamma_B = 3$, $n_p/n_B = 8$ INTERACTION

PLASMA

BEAM

MAX = 1.30000E+01
MIN = 0.

0.   6.400E+01

PARTICLE POSITIONS

$\vec{x}$

MAX = 1.30000E+01
MIN = 0.

0.   6.400E+01

PARTICLE POSITIONS

MAX = 5.00000E+00
MIN = -5.00000E+00

0.   6.400E+01

UX MOMENTUM VS X

$\vec{x}$

MAX = 5.00000E+00
MIN = -5.00000E+00

0.   6.400E+01

UX MOMENTUM VS X

MAX = 5.00000E+00
MIN = -5.00000E+00

0.   6.400E+01

UY MOMENTUM VS X

$\vec{x}$

MAX = 5.00000E+00
MIN = -5.00000E+00

0.   6.400E+01

UY MOMENTUM VS X

$$t = 50\,\omega_p^{-1}$$

PHASE SPACE for 2-D, $\gamma_B = 3$, $n_p/n_B = 8$ INTERACTION

PLASMA

y ↑

MAX = 1.30000E+01
MIN = 0.

0.   6.400E+01

PARTICLE POSITIONS
$\vec{x}$

BEAM

MAX = 1.30000E+01
MIN = 0.

0.   6.400E+01

PARTICLE POSITIONS

$\gamma\beta_x$ ↑

MAX = 5.00000E+00
MIN = -5.00000E+00

0.   6.400E+01

UX MOMENTUM VS X
$\vec{x}$

MAX = 5.00000E+00
MIN = -5.00000E+00

0.   6.400E+01

UX MOMENTUM VS X

$\gamma\beta_y$ ↑

MAX = 5.00000E+00.
MIN = -5.00000E+00

0.   6.400E+01

UY MOMENTUM VS X
$\vec{x}$

MAX = 5.00000E+00
MIN = -5.00000E+00

0.   6.400E+01

UY MOMENTUM VS X

$t = 80 \, \omega_p^{-1}$

FIELD AMPLITUDES vs. x,y at $t = 50\,\omega_p^{-1}$

E-X FIELD

-2.362E-02

1.980E-02

E-Y FIELD

-2.517E-02

2.305E-02

B-Z FIELD

1.601E-02

-1.573E-02
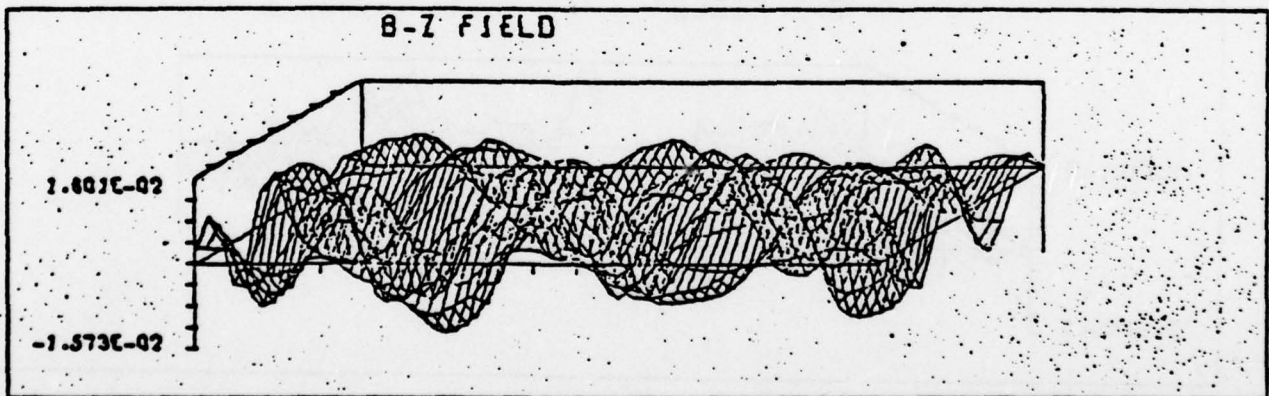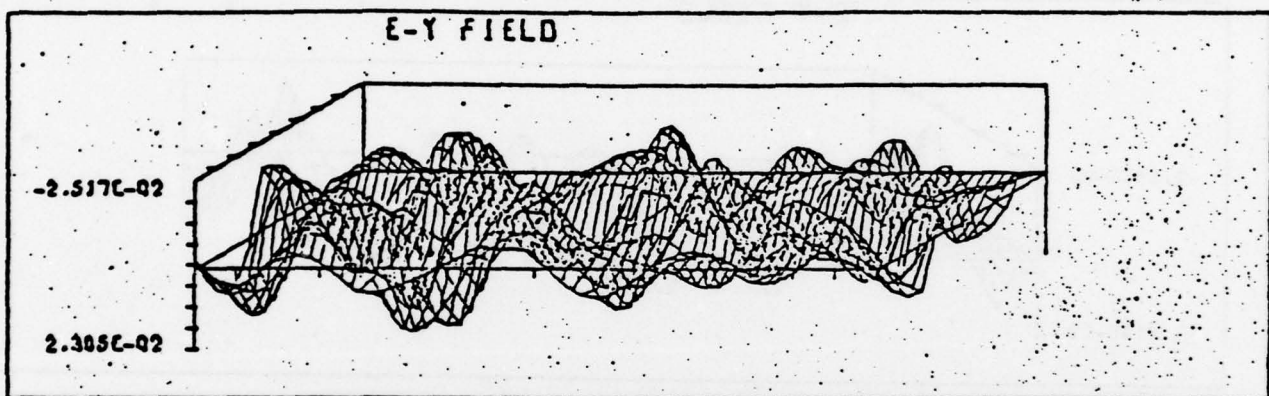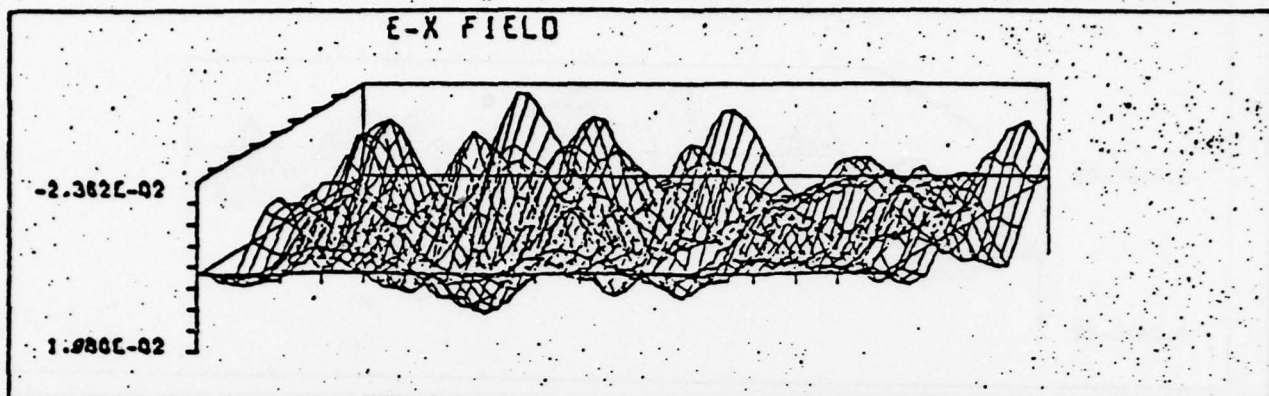
FIELD AMPLITUDES vs. x,y at $t = 80\,\omega_p^{-1}$
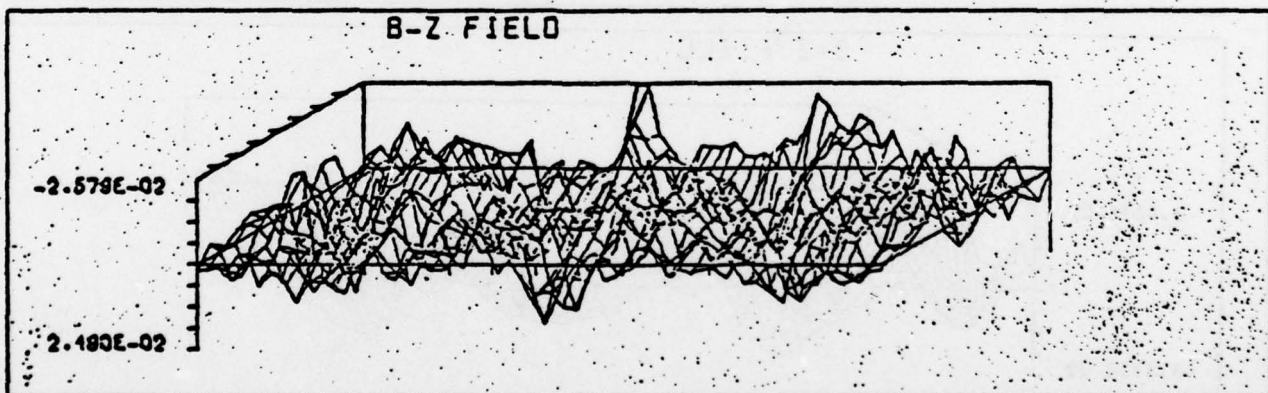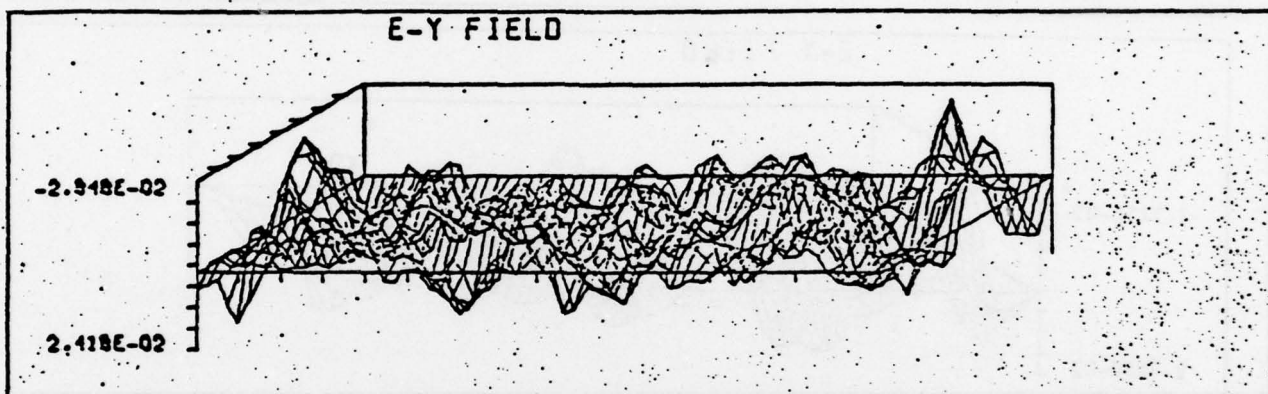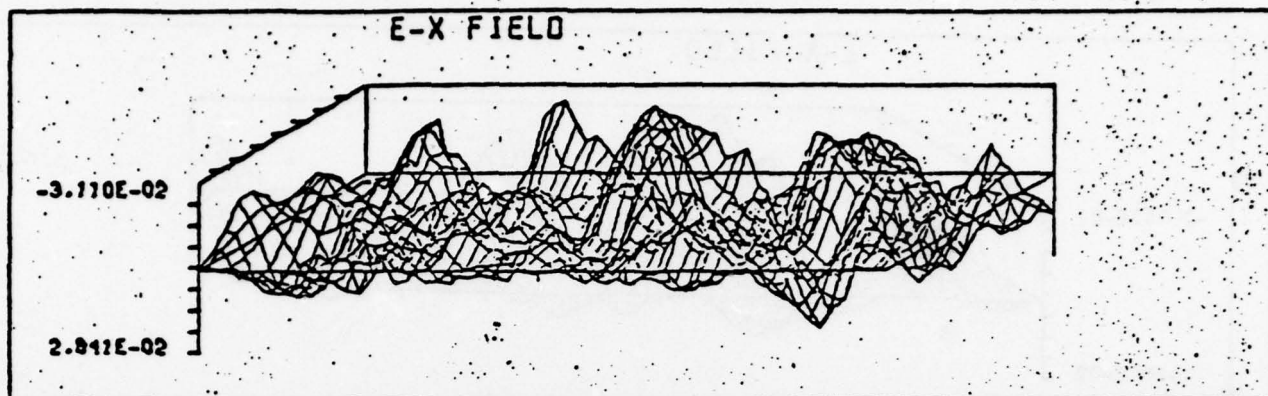
APPENDIX F

LETTER SUMMARY OF BEAM-PLASMA HEATING RESEARCH

AND COMPARISON OF RESULTS WITH THOSE OF

THODE, ET AL.

(1) Letter from Brendan B. Godfrey to James R. Thompson

(2) Letter from James R. Thompson to Richard L. Gullickson

(3) Letter from James R. Thompson to Brendan B. Godfrey

(Appendix F contains 14 pages)

40

UNIVERSITY OF CALIFORNIA
LOS ALAMOS SCIENTIFIC LABORATORY
(CONTRACT W-7405-ENG-36)
P.O. BOX 1663
LOS ALAMOS, NEW MEXICO 87545

IN REPLY
REFER TO: T-15(5-77)1   May 5, 1977
MAIL STOP: 531

Dr. J. R. Thompson
Austin Research Associates, Inc.
1901 Rutland Drive
Austin, Texas 78757

Dear Bob:

I have been reading over some of the work you and others at ARA
have done on relativistic electron beam-plasma interactions. The research
seems very interesting, but is not described in sufficient detail in the
reports I have, namely
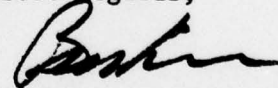
"Turbulent Heating of Plasmas by High Energy Particle Beams"

        I-ARA-76-U-80/ARA-236   (Aug. 76)
        I-ARA-75-U-139/ARA-195   (Aug. 75)
        I-ARA-74-U-139/ARA-160   (Aug. 74)
        I-ARA-73-U-88/ARA-106   (June 73) (Ch III only)

I would certainly appreciate any additional material you can send me.

    Enclosed are several reprints by Les Thode which you may find of
interest.

                              Best regards,

                              Brendan B. Godfrey

BBG: ncw
Encl: a/s
cc: B. B. Godfrey
    (2) ISD-5
    (2) T-15 File

Austin Research Associates, Inc.

August 22, 1977

Captain Richard L. Gullickson
Program Manager
Directorate of Physics
Air Force Office of Scientific Research
Bolling Air Force Base, D.C.   20332

Dear Dick:

A couple of months ago, while I was writing up some of the material
for the renewal proposal which we sent you on June 17, 1977, I received
from Brendan Godfrey a request for elaboration on some of the old beam-
plasma interaction research which we had performed and described in our
prior AFOSR reports. Apparently, a question had arisen during an AFWL
meeting on a proposed beam plasma heating experiment about how our
research compared with that of Les Thode, et al.

I was too busy to respond to this request for some time, but I
finally telephoned Brendan on August 1 and we discussed the research.
I understand that he had already submitted a preliminary comparison of
our research with Les Thode's research, and that any urgency associated
with the question had largely dissipated, inasmuch as AFWL made a
commitment to go ahead with their experiment. Nevertheless, I have
taken the time to make a few detailed comments on this research in a
letter to Brendan, and since the work was largely AFOSR-sponsored, I
have enclosed a copy of the letter herewith, for your information.

Despite some possible minor differences, which may be largely
semantic in nature, the main conclusion which struck me as I looked over
some 1975-76 publications by Thode, et al. (which Brendan had sent me)
was the near total agreement with my own conclusions in 1973-74, when I
was last active in this area. This is not to belittle the very valuable
research which has been accomplished in the meanwhile, including a
number of two-dimensional particle simulations to probe transverse
dynamical effects and magnetic field effects. Nevertheless, my early
conclusions that very high density plasmas might be heated with reasonable
efficiency by high quality (low angular scatter), high-γ (ultrarelativistic)
electron beams, via the primary beam-plasma longitudinal streaming
interaction, seem to be in agreement with Les Thode's conclusions. I
believe that our prescriptions for the optimum beam parameters are also
in quantitative agreement, although I have not seen any papers by Les on
the AFWL experiment in question. Assuming this to be the case, I am
wholeheartedly in favor of the experiment being performed.

I will be interested to hear how the Air Force Summer Study came out, and what conclusions were reached. Perhaps I'll give you a call in a week or so to discuss it.

Also, I presume that our AFOSR proposal is still on schedule in the reviewing process. Let me know if I can be of any more help there.

Finally, the typing is now about complete for submission of our publication on limiting currents. I should be sending you a copy in a week or so.

Best regards,

Bob Thompson

James Robert Thompson

JRT:sjb

Enclosure: I-ARA-74-U-114
           I-ARA-77-U-76 (ARA-281)

Austin Research Associates, Inc.

August 22, 1977

Dr. Brendan Godfrey
Group T-15, MS-531
University of California
Los Alamos Scientific Laboratory
P. O. Box 1663
Los Alamos, New Mexico 87545

Dear Brendan:

Following our telephone conversation of August 1 regarding beam-plasma heating, I have secured a copy of some lecture notes which were compiled for a July, 1974 presentation by Dr. Drummond at Novosibirsk, which summarize our understanding of the most important features of the problem as of that time. These notes are enclosed herewith (they are somewhat rough, as the presentation was only verbal.)

Inasmuch as I spent the better part of five years of my professional life (i.e., 1968 - 1973) working on this problem--mostly supported by AFOSR-- plus another year (i.e., 1973 - 1974) trying (unsuccessfully) to scare up support for an experiment to test some of our conclusions, I thought I would take the time to clarify our chief results somewhat.

The historical sequence of "our" own research is that we first applied a concentrated theoretical-computational-experimental attack on the nonrelativistic, one-dimensional (strong magnetic guide field), weak beam-plasma interaction, and we found a gratifying amount of agreement on the results.[1-5] We subsequently engaged in a period of protracted theoretical research designed to extend understanding to more and more effects: relativistic beams, electromagnetic effects, transverse waves, kinetic (or angular scattering) effects, gyroeffects, finite geometry effects, ion effects, trapped particle effects, parametric effects, etc. Simultaneously, our computer simulation capability (via Adam Drobot) was slowly improved to handle 1-D, relativistic, single wave calculations (a la Matsiborko, et al.[6]), then 1-D, relativistic particle simulations, and finally 2-D, relativistic, electromagnetic particle simulations. At the culmination of this research effort in 1973, the outstanding facts which struck me were:

(1) Technological developments in high voltage pulsed power seemed very promising, with relativistic electron beams already capable of delivering tens to hundreds of kJ. The future growth potential for engineering desirable beam properties, increasing the beam energy, etc. seemed very bright.

(2) Despite the large amount of attention then being given to return current interactions, partly because of their relevance to a number of existing experiments with $n_p/n_B < 100$, these interactions held little theoretical promise for heating plasmas at much larger density ratios.

(3) However, based only on the energy coupling obtainable from the primary, longitudinal, beam plasma interaction in the hydrodynamical regime, it already seemed possible to heat extremely dense target plasmas to fusion temperatures if the beam density, energy, and quality (i.e., angular scatter) could be properly controlled.

(4) Although the transverse waves and the beam cyclotron modes were not yet as well understood as the longitudinal plasma wave interaction, it seemed that they could only enhance the energy coupling and should not quench the longitudinal interaction. Even without this complete understanding of the transverse interactions, the preliminary evidence (discussed later) was already adequate to justify designing an experiment to heat with a high quality, highly relativistic beam, via the primary longitudinal interaction.

(5) Nevertheless, the thrust of the existing experimental effort seemed to be in the wrong direction, from the point of view of the application of single pass heating of very dense (i.e., $> 10^{15}$ electrons/cm^3) target plasmas, which I viewed as one of the most promising fusion goals to which the e-beam technology could be applied, as well as an area where it should have a distinct competitive advantage. That is, the existing effort seemed aimed at producing higher ν/γ beams—giving up γ for ν if necessary, and producing high current density beams. There was almost no effort to produce higher - γ beams, or to improve (or even measure) the beam quality. (In fairness, I should concede that a justifiable motivation for some of the emphasis on high current density—small cross section—beams was the pellet fusion problem.)

(6) This lack of interest in high - γ, high quality (low $\bar{\theta}$) beams existed despite the likelihood that the poor coupling efficiencies observed

occasionally for very dense target plasmas were probably due to interactions occurring in the kinetic regime where they were subject to collisional quenching. In short, there was not much appreciation for the dividends which would accrue from improved beam quality.

(7) Finally, again from the point of view of relevance to a high density heating experiment, it seemed to me that there was a bit too much theoretical attention devoted to the slower, late-time, nonlinear homogeneous theory--and perhaps not enough attention devoted to effects of inhomogeneities, finite pulse time, and finite target size.

It is the above points which I tried to make in my AFOSR reports covering the 1972 - 1974 research period, and particularly in my talk at the Working Group on the Interaction Between Plasmas and Intense Laser and Electron Beams, at the International Centre for Theoretical Physics, Trieste, Italy in August 1973, and in my paper[7] at the 1973 Philadelphia APS meeting. This paper in turn was the basis of the enclosed notes which were written up for Dr. Drummond's 1974 Novosibirsk lecture. If this material has left the impression that we were only concerned with one-dimensional effects, or that we had not done any work on transverse interactions or gyroeffects, that was unintentional. It is just that there were larger points which I was trying to make without getting bogged down with subtleties, and the computer evidence on transverse interactions was still too preliminary for any definitive statements to be made.

During 1973 - 1974, I tried to promote interest in a beam heating experiment of a dense target plasma with the high - γ beam at the Aurora facility, Harry Diamond Laboratories, with the payoff to be a plasma radiation source. I first had a long battle to convince them that collisional stabilization of the beam-plasma interaction could be avoided if the beam quality could be controlled. Then we performed a study for them which included a rough experimental design. We proposed to arrange $\gamma_B (n_B/n_p)^{1/3} \simeq 0.5$, with a strong magnetic guide field extended into the diode to give us a better chance of holding the angular scatter to $\theta_{rms} \leqslant \gamma_B^{-1} \simeq 2(n_B/n_p)^{1/3}$. This experimental proposal ultimately floundered, not because of skepticism regarding beam heating, but because the expected pulse duration of the emitted radiation was somewhat longer than desired.

Next, let me touch briefly on my 1973 understanding of some of the transverse effects. First of all, for an infinite magnetic guide field, the hydrodynamical, electromagnetic dispersion relation is

$$0 = 1 - \frac{\omega_p^2}{\omega^2} - \frac{\omega_B^2}{\gamma_B^3 (\omega - k_z \beta_B c)^2} + \frac{k_\perp^2 c^2}{k_z^2 c^2 - \omega^2}$$

and the most unstable wave occurs for $k_\perp = 0$ (when allowed by infinite transverse boundaries) and is electrostatic. However, in a waveguide, the minimum allowable $k_\perp \sim (2.4/a)$, and stability can result if the wall radius is small enough that this exceeds $\dfrac{\omega_p}{\gamma_B \beta_B c}$.

At the other extreme, when there is no magnetic field the hydrodynamical, electromagnetic dispersion relation is

$$0 = \left[1 - \frac{\omega_p^{\;2}}{\omega^2} - \frac{\omega_B^{\;2}}{\gamma_B^{\;3}(\omega - k_z \beta_B c)^2} \right] \left[\omega_p^{\;2} + \frac{\omega_B^{\;2}}{\gamma_B} + k^2 c^2 - \omega^2 \right] - \frac{k_\perp^{\;2} \beta_B^{\;2} c^2 \omega_B^{\;2} \omega_p^{\;2}}{\gamma_B \omega^2 (\omega - k_z \beta_B c)^2} .$$

This is always unstable, and includes a longitudinal and a transverse regime, defined according to whether $k_\perp$ is small or large. The longitudinal regime is electrostatic, while the transverse regime is electrostatic for large k_z and electromagnetic for small k_z. The case of $B_O = 0$, $k_\perp \to \infty$, $k_z \to 0$ is sometimes referred to as the Weibel instability. Simulations showed that rather than transferring much beam energy, it tended to cause the beam to filiment in the transverse plane. The fastest growth for $B_O = 0$ occurs for $k_z \simeq \omega_p/\beta_B c$, where the mode is electrostatic, and the growth rate of this streaming interaction is

$$\Gamma \simeq \frac{3^{1/2}}{2^{4/3}} \; \frac{\omega_p}{\gamma_B} \left(\frac{n_B}{n_p} \right)^{1/3} \left[\frac{\gamma_B^{\;2} k_\perp^{\;2} + k_z^{\;2}}{k_\perp^{\;2} + k_z^{\;2}} \right]^{1/3}$$

I usually define the longitudinal/transverse wave regimes via this expression. A transition region extends from $k_\perp = k_z/\gamma_B$ to $k_\perp = k_z$, with $k_\perp < k_z/\gamma_B$ being longitudinal and $k_\perp > k_z$ being transverse, and the middle region being a mixture.

Therefore, for an optimized interaction with $\gamma_B (n_B/n_p)^{1/3} \simeq 0.5$, I would expect the longitudinal wave regime to be characterized by $k_z \simeq \omega_p/c$ and $0 < k_\perp \lesssim k_z/\gamma_B \simeq 2(n_B/n_p)^{1/3} k_z$. Therefore, the "typical" case that you mentioned of $\leqslant 20°$ angles in k-space could be within what I term the longitudinal regime unless $\gamma_B \gg \cot 20° \simeq 2.75$, while the strongly transverse regime corresponds to angles $> 45°$. Clearly, the large grey area invites semantic debate. In fact, I now suspect that some of our apparent differences during our phone conversation were merely semantic, since I find the above mentioned range of $k_\perp$ cited in the very nice series of 1975-76 papers [8-13] which you sent me. Of course, in a

. waveguide it is theoretically possibly for the lowest allowable value of $k_\perp \sim (2.4/a)$ to fall outside of $\dfrac{k_z}{\gamma_B} \simeq \dfrac{\omega_p}{\gamma_B \beta_B c}$, thus eliminating the longitudinal regime, but for the problem of heating very dense plasmas this will not occur. In any case, it has always been clear that the eigenmode structure for a longitudinal interaction will necessarily have a non-zero $k_\perp$ component, so that two dimensional computer simulations are necessary for a good mock-up of the physics. Nevertheless, one expects that the basic processes observed in the 1-D simulations (i.e., longitudinal trapping, etc.) would continue to dominate the longitudinal regime of 2-D simulations, and we and others confirmed this to be the case.

A more crucial question is what happens to the strongly transverse waves with $k_\perp > k_\parallel$, whose growth rate exceeds that of the longitudinal waves by $\gamma_B^{2/3}$. One might expect these modes to saturate at relatively low amplitudes due to transverse velocity scatter since $k_\perp$ is large, and indeed, the Soviets (particularly Rudakov) made calculations of this. Then the question is whether the associated axial velocity spread due to this scattering would throw the coexisting longitudinal interaction into the kinetic regime. The answer was that for $\gamma_B (n_B/n_p)^{1/3} < 1$, it would not--the longitudinal interaction would remain hydrodynamical. My own calculations tended to confirm these results, although admittedly, when $\gamma_B (n_B/n_p)^{1/3} \simeq 0.5$ for an optimum interaction, one might expect the hydrodynamic criterion to remain only marginally obeyed. My experience suggested to me that this would probably be good enough, although the proof of the pudding is in the 2-D simulations. Our own 2-D, $B_O = 0$ simulations had just become available in 1973, and the preliminary results supported the above picture of the interaction, with continued longitudinal trapping, and with field amplitudes comparable to the 1-D prediction at the time of initial saturation of growth of the field amplitudes. Lampe, et al. reported similar preliminary results at the same 1973 APS meeting. This was essentially the state of affairs when I ceased active research on this problem. During our telephone conversation, I got the impression that perhaps subsequent 2-D simulations had led you to disavow the above described picture. However, in looking over the references[8-13] that you sent, I find general agreement and even affirmation of these arguments in several places. Perhaps you could point out whether and where any disagreement remains.

Next, consider the questions of gyroeffects. For this problem of heating a very dense plasma with $n_p \geqslant 10^4 n_B$, technological limitations will insure that $\Omega_e \ll \omega_p$ for the target plasma, so the magnetic corrections may be neglected for the streaming interactions with the target plasma modes. However, the magnetic field will allow transverse beam cyclotron modes as well as the longitudinal beam plasma modes. We found that the $k_\perp \to \infty$, $k_z \to 0$ Weibel instability may be stabilized if $\Omega_e > \beta_B \gamma_B^{1/2} (n_B/n_p)^{1/2} \omega_p$. The more interesting case is the streaming interaction, where peak growth occurs in the electrostatic regime, for $k_z \simeq \omega_p/\beta_B c$.

The electrostatic dispersion relation, for $|\omega| \gg \Omega_e$, is

$$0 = 1 - \frac{\omega_p^2}{\omega^2} - \frac{\omega_B^2 k_z^2 / k^2}{\gamma_B^3 (\omega - k_z \beta_B c)^2} - \frac{\gamma_B \omega_B^2 k_\perp^2 / k^2}{\gamma_B^2 (\omega - k_z \beta_B c)^2 - \Omega_e^2}$$

which yields the previously quoted growth rate when $B_o \to 0$. It may be seen that now beam-cyclotron modes coexist with the beam plasma modes, and each may interact with the background plasma mode. The beam-cyclotron interaction occupies the large-$k_\perp$, transverse region of phase space, where the beam gyroeffects modify the interaction from the above discussed case for $B_o = 0$). When $(\Omega_e/\omega_p) \ll 0.5 \gamma_B^{2/3} (n_B/n_p)^{1/3}$, the gyroeffects only cause a slight slowing of the usual transverse interaction, but when $0.5 \ \gamma_B^{2/3} (n_B/n_p)^{1/3} \ll \Omega_e/\omega_p \ll 1$, the transverse growth rate is slowed significantly to

$$\Gamma \simeq \frac{1}{2} \left(\frac{n_B}{n_p}\right)^{1/2} \frac{\omega_p^{3/2}}{\Omega_e^{1/2}}$$

for $k_\perp \gg k_z \simeq \omega_p/\beta_B c$. (Here I should apologize for my use of the word "suppressed" on page 13 of the Novosibirsk notes. This is misleading, since the transverse interaction is not stabilized, but is only slowed by the gyroeffects, and it will still be faster than the usual longitudinal interaction unless the magnetic field is raised by an additional factor of $\gamma_B^{4/3}$.) The more relevant question is again the nonlinear saturation level of the transverse beam-cyclotron interaction, and whether or not it throws the coexisting longitudinal interaction into the kinetic regime. Our estimation was that the transverse wave saturation would be at or below the level occuring for $B_o = 0$, since additional saturation mechanisms (e.g., finite $k\rho$ - effects) are now available. Therefore we expected the longitudinal interaction to remain hydrodynamical under the previous condition that $\gamma_B (n_B/n_p)^{1/3} \gtrless 1$. It was not clear to us in 1973 whether the modification in the interactions due to $B_o \neq 0$ would have a net effect of increasing or decreasing the energy coupling effeciency from the beam, although we expected the change in either direction to be modest-to-small. (Any loss in transverse interaction coupling might be made up in a more efficient longitudinal interaction.) In any case, we again deferred to the computer simulation evidence, which consisted for us of only two or three 2-D, $B_o \neq 0$ runs at that time. These indeed showed approximately the expected

amount of energy transfer by the initial nonlinear interaction, and continued
to show the trapping dynamics associated with the longitudinal interaction. My
own feeling was that the importance of the magnetic field was not likely to be
associated so much with the way the cyclotron modes directly influenced the energy
transfer, as with the way the field might improve the beam quality if it were
carefully designed in the diode and injection regions.

During our telephone conversation, I got the impression that your conclusions
regarding the magnetic field effects might differ from ours described above in
two respects. First, I thought that you were claiming that in a parameter range
recommended for a heating experiment, the transverse beam-cyclotron interaction
itself was observed to stablize via beam trapping. However, after looking over
your papers, I suspect that this was a misunderstanding and that you might agree
with us that it is the coexisting longitudinal beam-plasma interaction with the
background plasma mode which saturates by beam trapping. We have found that there
are almost always other avenues for nonlinear saturation of the beam-cyclotron
interaction which will enter prior to beam trapping.

The second possible difference is that I thought I understood you to say
that the magnetic field had a very strong influence on the energy coupled out of
the beam, and that there was an optimum magnetic field strength choice which would
allow significant gains in the energy coupling efficiency over a non-optimum choice.
However, in looking over one of your 1976 references[12], you seem to agree with our
own preliminary conclusion that the beam energy loss is only weakly dependent on
the magnitude of the magnetic field, if $\Omega_e < \omega_p$. Perhaps you could clarify whether
subsequent simulations led you to change the view expressed in this paper, or
whether there might again be semantic confusion over the adjective (strong, weak)
attached to your observations.

Before leaving the topic of streaming interactions which involve magnetic
field modes, let me mention two other areas not discussed above. First, when
$\Omega_e \ll \omega_p$, there will be Whistler and electron cyclotron modes in the background
plasma, in addition to the background plasma mode mentioned above, which are
candidates for interaction with the beam-plasma and beam-cyclotron modes. The
interaction between these and the beam-plasma mode will generally be stable for
a high velocity beam, since the beam mode will then pass above the knee of the
Whistler mode. However, the lower beam-cyclotron mode may be expected to intersect
the Whistler at low frequency and long wavelength, where ion effects and electro-
magnetic effects are important. However, we tended to dismiss this interaction
on the grounds of its being slower and probably less potent than the longitudinal
beam-plasma/target-plasma mode interaction. We never detected it in our simulations;
I wonder if you have?

The second area is the regime $\Omega_e \gg \omega_p$, which I have not discussed in detail on the grounds of technological infeasibility, for target plasma densities above 10^{15} cm^{-3}, or so. However, in looking over your reference on linear theory[8], I noticed that there appeared to be an error in the analytical expression presented for the frequency and growth rate of the interaction between beam-plasma modes and background cyclotron modes in this parameter regime. This is the portion of your table I which contains δ_+^{T3}, in your Region 3, and the growth rate expression appears to be illustrated by curves drawn on your Figures 13 and 14. The problem is that your expression for the growth rate is independent of the magnetic field strength, whereas the growth should clearly vanish as $\Omega_e \to \infty$. The relevant terms in the electrostatic dispersion relation are

$$0 = 1 - \frac{\omega_p^2 \sin^2\theta}{\omega^2 - \Omega^2} - \frac{\omega_B^2 \cos^2\theta}{\gamma_B^3 (\omega - k_z \beta_B c)^2}$$

where $\tan\theta = k_\perp / k_z$. In the regime $1 \ll \dfrac{\Omega_e}{\omega_p} \ll \dfrac{\gamma_B^{3/2}}{(n_B/n_p)^{1/2}} \dfrac{\sin^2\theta}{\cos\theta}$,

the peak growth rate is approximately given by

$$\Gamma \simeq \frac{3^{1/2}}{2^{4/3}} \frac{(n_B/n_p)^{1/3}}{\gamma_B} \frac{\omega_p^{4/3} \sin^{2/3}\theta \cos^{2/3}\theta}{(\Omega_e^2 + \omega_p^2 \sin^2\theta)^{1/6}}$$

where $k_z \beta_B c \simeq (\Omega_e^2 + \omega_p^2 \sin^2\theta)^{1/2}$. This growth rate is smaller than your expression, and is no longer symmetric about $\theta = 45°$ in qualitative agreement with your plotted computer results. Other small corrections and angular dependence may be harvested if the small neglected terms in the electrostatic dispersion relation are reintroduced, or if electromagnetic corrections are recovered. However, this formula shows the major effect.

If the magnetic field is strengthened further, to the point

$$\frac{\Omega_e}{\omega_p} > \frac{\gamma_B^{3/2}}{(n_B/n_p)^{1/2}} \frac{\sin^2\theta}{\cos\theta} \gg 1$$

. then (because of the increased relative significance of the splitting of the beam plasma modes) the interaction transits from the cubic regime to a slower quadratic regime, where

$$\Gamma \simeq \frac{1}{2} \cdot \frac{(n_B/n_p)^{1/4}}{\gamma_B^{3/4}} \; \frac{\omega_p^{3/2} \sin\theta \; \cos^{1/2}\theta}{\Omega_e^{1/2}}$$

and peak growth occurs for $k_z \beta_B c \simeq (\Omega_e^2 + \omega_p^2 \sin^2\theta)^{1/2} + \frac{\omega_B \cos\theta}{\gamma_B^{3/2}}$.

This growth rate falls off with increasing B_0 somewhat more rapidly than in the cubic regime. (Of course, there will still exist the interaction between the beam plasma mode and the background plasma mode, with peak growth for $\theta = 0$ but finite growth for large θ, which will compete with this cyclotron mode interaction.) Unfortunately, you did not run Ω_e/ω_p high enough in your calculations for the paper that this flaw in your formula would have caught your attention.

I only point this correction out for academic reasons, since I believe this strong - B_0 regime to be irrelevant for the beam-heating problem of interest. (While I am at it, I presume you have noticed the $1/2 \rightarrow 1/3$ typo in the next-to-last paragraph of page 346.)

I had thought of elaborating on kinetic effects somewhat, but I think I will pass over that since this letter is already so long and we seem to be pretty much in agreement there anyway. Let me just wholeheartedly endorse any experimental efforts to improve the beam quality.

One final area where we might have some small quantitative differences is in the energy coupling efficiency to be expected. Back in 1973-74, there was fairly general agreement that efficiencies in the range of 20% - 30% were reasonable expectations for a wide range of beam energy and density ratios above ~ 10, and allowing some late-time nonlinear interactions--but not carrying this to extremes. Some of our own predictions are depicted graphically in the Novosibirsk notes, but the graphs should be interpreted with some care. I am intrigued by your statement over the telephone that $\sim 60\%$ coupling efficiency may be expected in the optimum case for target plasma heating at very high density ratios, like $n_p/n_B \sim 10^4$. I did not notice any coupling efficiencies that high in your references, and I would have guessed that it could only be achieved by going to low density ratios of ~ 10 or so, or by allowing the beam to coexist with the target for an extraordinary length of time (or space). I would be curious to hear if perhaps there is some recent evidence which gives you this confidence, and if the evidence is simulations, whether any have shown this result at the very high density ratios of interest.

Before closing, let me say that in giving all this discussion of my under-
standing of some aspects of this problem, I certainly did not mean to imply that
I was telling you anything new, since I am well aware that you and many others
have been down this same path. Rather, I sought to fill some of the gap of
elaboration that you perceived in some of our earlier AFOSR reports. In fact,
I claim no originality for any but the earliest non-relativistic work that I did,
since the modus operandi for beam plasma work a few years ago was for ~ ten groups
around the country to co-discover things more or less independently.

Let me also say that in dwelling on some areas of possible small differences
in our work, I have probably misrepresented the dominant conclusion that struck me
in comparing our work--which is the extraordinary extent to which we are in agree-
ment. I certainly think that your careful exploration of two-dimensional effects
and the many two-dimensional simulations were well worthwhile and represented a
major advance in the field. I was particularly impressed with Les' paper surveying
the experimental results. It seems to me that the evidence supporting the type
of high - γ, high quality, beam heating experiment of very dense plasma targets
which I fought for in vain is now well nigh overwhelming, and if I can endorse
one of your proposals for such an experiment, I will be only too happy to do so.

If you do become actively involved in pursuing such an experiment, I would
be interested to receive any reports which might be issued on it. I presently have
no precise idea of the parameters which you have in mind, the experimental motiva-
tion (e.g., radiation source, fusion), and so forth.

                                        Best regards,

                                        Bob Thompson

                                        James R. Thompson

JRT:tb

Enclosure: Report I-ARA-74-U-114

cc: Capt. Richard Gullickson
     Dr. Adam Drobot

LETTER REFERENCES

1. W. E. Drummond, et al., Phys. Fluids $\underline{13}$, 2422 (1970).

2. J. R. Thompson, Phys. Fluids $\underline{14}$, 1532 (1971).

3. K. W. Gentle and C. W. Roberson, Phys. Fluids $\underline{14}$, 2780 (1971).

4. K. W. Gentle and J. Lohr, Phys. Rev. Lett. $\underline{30}$, 75 (1973).

5. K. W. Gentle and J. Lohr, Phys. Fluids $\underline{16}$, 1464 (1973).

6. N. G. Matsiborko, et al., Plasma Phys. $\underline{14}$, 591 (1972).

7. J. R. Thompson and A. T. Drobot, B.A.P.S. $\underline{18}$, 1350 (1973).

8. B. B. Godfrey, et al., Phys. Fluids $\underline{18}$, 346 (1975).

9. L. E. Thode and R. N. Sudan, Phys. Fluids $\underline{18}$, 1552 (1975).

10. L. E. Thode and R. N. Sudan, Phys. Fluids $\underline{18}$, 1564 (1975).

11. L. E. Thode, Phys. Fluids $\underline{19}$, 305 (1976).

12. L. E. Thode and B. B. Godfrey, Phys. Fluids $\underline{19}$, 316 (1976).

13. L. E. Thode, Phys. Fluids $\underline{19}$, 831 (1976).

A P P E N D I X   G

SELF CONSISTENT EQUILIBRIA OF UNNEUTRALIZED
RELATIVISTIC ELECTRON BEAMS

(Appendix G Contains 26 Pages)

41

In order to be able to exploit the powerful electron beams which technology has made available for a number of interesting applications, such as collective ion acceleration, it is first necessary to understand the equilibrium properties of the electron beam itself. The most fundamental question is to determine the conditions under which an equilibrium of forces can be arranged such that the electron beam may propagate in vacuum away from the diode into a drift tube in a grossly stable configuration. If such a force equilibrium is not achieved, the unneutralized electron beam will rapidly blow itself apart by the powerful self electromagnetic fields generated by its own space charge. A second objective of such an equilibrium analysis is to determine the self consistent radial profiles of all equilibrium quantities, including the electromagnetic fields and the number density and flow velocity of the electron beam. These equilibrium properties will in turn be needed to determine the linearized eigenmodes (or waves) which may be supported upon the electron beam.

Although one important application for this analysis is collective ion acceleration, the contribution of the

1

subject ions (to be accelerated) to this equilibrium is neglected in this calculation. The first reason for this is that for many accelerator configurations, the electron beam must propagate stably for some distance in vacuum prior to the introduction of ions, so that an analysis of pure electron beam equilibria is required. Second, the accelerator can operate in principal in the "test ion" regime, where the ion contributions to the equilibria and waves are truly negligible. Finally, it is anticipated that the highest density of ions which may be accelerated will still be much less dense than the electrons, so that the ion effects may be treated as a perturbation on the fields supported by the electron beam.

The electron equilibrium may be examined by considering the single particle equations of motion together with the Maxwell equations for the self-consistent electromagnetic fields.

$$\frac{d}{dt} \gamma \underline{\beta} = - \frac{e}{mc} (\underline{E} + \underline{\beta} \times \underline{B}) \; ; \qquad \frac{d}{dt} \underline{x} = \underline{\beta} c \qquad (1)$$

$$\nabla \cdot \underline{B} = 0 = \nabla \times \underline{E} + \frac{1}{c} \frac{\partial}{\partial t} \underline{B} \qquad (2)$$

$$\nabla \cdot \underline{E} = - 4\pi en \qquad (3)$$

$$\nabla \times \underline{B} = \frac{1}{c} \frac{\partial}{\partial t} \underline{E} - 4\pi en \, \underline{\beta} \qquad (4)$$

Here $e = - |e|$, m are the electron charge and mass, and $\underline{\beta}c$, $(\gamma - 1)mc^2$ are its velocity and kinetic energy. Since the single particle equations of motion (1) are the characteristics of the collisionless Vlasov equation, the equilibrium distribution function $f_o(\underline{x}, \underline{\beta})$ may be constructed from any constants of the single particle motion. We shall adopt a cold fluid model of the electron beam, in which the beam pressure is neglected, and n, $\underline{\beta}$ are the electron number density and flow velocity, which may in general be functions of $\underline{x}$, t.

The existence of steady state beam equilibrium solutions is by no means guaranteed. The crucial condition is the balance of radial forces, which may be expressed as

3

$$\frac{d}{dt} \gamma\beta_r = \frac{e}{mc} \left\{ - E_r + \beta_z B_\phi - \beta_\phi B_z + \frac{mc^2}{e} \frac{\gamma\beta_\phi^2}{r} \right\} = 0$$

(5)

in the cylindrical coordinates r, ϕ, z. The basic assumptions are that the equilibrium is steady state $(\partial/\partial t = 0)$ and cylindrically symmetric $(\partial/\partial\phi = 0)$ throughout the vacuum waveguide. It is further assumed that there is a downstream region away from the beam diode, for which the equilibrium is approximately independent of axial position $(\partial/\partial z = 0)$. Practically speaking, this will be true even throughout an ion acceleration section of the waveguide, wherein the waves and ions are accelerated, if the z-variation in equilibrium quantities is small compared to the r-variation, and if the z-variation in equilibrium quantities is small (or adiabatic) compared to the z-variation in wave quantities, characterized by the axial wavelength.

The fields E_r and B_ϕ are the self-fields of the electron beam, determined in the downstream equilibrium region from the equations

4

$$\frac{1}{r} \frac{\partial}{\partial r} r \, E_r = - 4\pi e \, n \tag{6}$$

$$\frac{1}{r} \frac{\partial}{\partial r} r \, B_\phi = - 4\pi e \, n \, \beta_z \quad . \tag{7}$$

It may be seen that both E_r and B_ϕ are negative, and that E_r is larger than B_ϕ in magnitude. Consequently there can be no equilibrium (in vacuum) for which $\beta_\phi = 0$, since the sum of the first two terms of equation (5) are always positive, evidencing a net outward force on the electrons. This net outward force must be overcome by the $- \beta_\phi B_z$ pinch force, without the final centrifugal force destroying the balance. Here B_z is presumed to be an externally generated magnetic guide field, which is slightly reduced by the beam's diamagnetic precession in ϕ according to

$$\frac{\partial B_z}{\partial r} = 4\pi e \, n \, \beta_\phi \quad . \tag{8}$$

5

If the fields E_r, B_ϕ, B_z are presumed to be known, equation (5) may be examined for the conditions which these fields must obey in order that equilibria exist for which $\beta_r = 0 = \frac{d}{dt} \beta_r$. This analysis is most easily accomplished in an inertial frame of reference for which β_z locally vanishes (notice that in general β_z will vary with r). In such a "beam" frame, the equilibrium condition (5) may be written as

$$\beta_\phi^2 (1 - \beta_\phi^2)^{-1/2} = \frac{e}{mc^2} r E_r + \frac{e}{mc^2} r B_z \beta_\phi \ . \qquad (9)$$

As a function of β_ϕ, the left-hand side of equation (9) increases monotonically from zero and diverges as β_ϕ approaches one, while the right-hand side is a linear function of β_ϕ (if the diamagnetic β_ϕ-dependence of B_z is ignored) with a positive slope and negative intercept at $\beta_\phi = 0$. There will obviously be two solutions if the functions intersect (i.e., two distinct equilibria) and no solutions if they do not.

6

A detailed algebraic analysis of equation (9) reveals
the following necessary and sufficient condition for the
existence of equilibria:

$$2 \; \frac{\overline{\omega_{PB}^2(r)}}{\Omega_B^2(r)} \; Q\left[\frac{-E_{rB}(r)}{B_z(r)} \right] \leq 1 \tag{10}$$

where

$$\overline{\omega_{PB}^2(r)} \equiv - \frac{2\,eE_{rB}(r)}{mr} = \frac{4\pi e^2}{m} \; \frac{1}{r^2} \int_0^{r^2} dr'^2 \; n_B(r'^2)$$

$$\Omega_B(r) \equiv \frac{e}{mc} \, B_z(r)$$

$$Q(x) \equiv \frac{\frac{1}{2}\left[1 - (1 + 8x^2)^{1/2}\right] + 2x^2}{4x\left[\frac{1}{2}(1 + 8x^2)^{1/2} - \frac{1}{2} - x^2\right]^{3/2}} \geq 1$$

and the function $Q(x)$ is sketched in Figure (1) below.
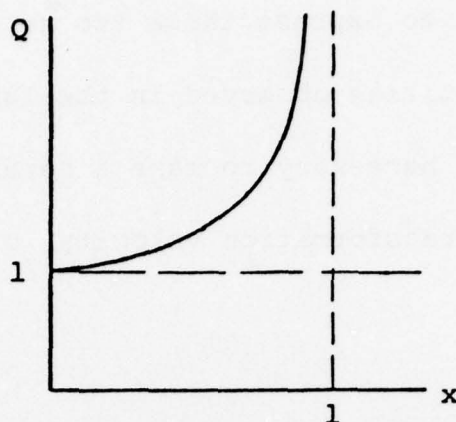
Figure 1.   Function Q(x)

Here E_{rB} and n_B are the radial electric field and the electron density as seen from the local beam frame, and $B_z(r)$ is the total axial magnetic field--including diamagnetic corrections.

Equation (10) immediately implies two necessary conditions for equilibrium. First is that the argument of Q, $-E_{rB}/B_z$ must be less than one, which is obvious from equations (9) or (5) since otherwise the net forces are manifestly positive. Second, since $Q \geq 1$, the coefficient of Q in equation (10) must be less than one. This second condition ensures that the centrifugal forces do not destroy the equilibrium.

8

In order to express these two necessary criteria in terms of quantities observed in the laboratory frame of reference, it is necessary to make a Lorentz transformation, with the transformation velocity $c \beta_z(r)$. The results are

$$1 > \frac{-E_r(r)}{\gamma_T(r) \, B_z(r)} = \frac{\frac{1}{2} \frac{4\pi e^2}{mc} \frac{1}{r} \int\limits_{o}^{r^2} dr'^2 \, n(r'^2)}{\gamma_T(r) \, \Omega_B(r)} \tag{11}$$

$$1 > \frac{2 \frac{4\pi e^2}{m} \frac{1}{r^2} \int\limits_{o}^{r^2} dr'^2 \, n(r'^2)}{\gamma_T(r) \, \Omega_B^2(r)} \tag{12}$$

where $\gamma_T(r) = [1 - \beta_z^2(r)]^{-1/2}$. Both conditions (11) and (12) must be obeyed for all r. Since the numerator of condition (11) increases roughly as r, while the denominator of (11) increases only weakly with r, condition (11) will be most stringent near the beam edge $r = a$. The numerator of condition (12) is roughly constant, while the

9

denominator increases weakly with r, so that condition (12) will be most stringent near the beam axis $r = 0$.

For virtually all cases of interest, both conditions (11) and (12) will be well satisfied and the equilibria may be readily analyzed in terms of the corresponding small parameters. In this case, the two equilibrium solutions for β_ϕ will be well separated; the "slow" equilibrium (for which β_ϕ is lowest) is the one desired for the accelerator applications.

In order to self-consistently compute the various equilibrium quantities, assumptions about the nature of the beam equilibrium are required, since many different equilibria are possible in general. It is most accurate to make these assumptions about the conditions of creation of the beam at the cathode, with conservation equations then utilized to complete determination of the equilibrium quantities in the downstream, z-independent region of the waveguide. In this way, the accessibility of the equilibrium is included in the calculation, which would not be the case if ad hoc assumptions were instead made about the downstream equilibrium.

10

Therefore, we shall assume that the electron beam is born at the cathode with $\beta_{\phi C} = 0$, $\gamma_C = 1$, and uniform current density $j_C = -ecn_o\beta_{oz}$ throughout the initial beam radius a_o. The cathode is assumed to be at a uniform, negative electric potential $\Phi_C < 0$. The beam is assumed to flow from the cathode through a diode acceleration region where it is raised to ground potential $\Phi = 0$ and then injected into a cylindrical waveguide whose conducting walls are also at ground potential.

The initial beam properties which are assumed above may be related to the corresponding beam properties in the downstream, z-independent equilibrium through the use of three conservation equations. In this way, the chore of computing the actual beam trajectories all the way from the cathode to the downstream equilibrium region may be avoided.

The first equation is the conservation of canonical angular momentum, which follows from the assumption of azimuthal symmetry. It may be written as

$$\int_0^{r_o} dr'^2\, B_{zo} = \int_0^{r^2} dr'^2\, B_z - \frac{2\,mc^2}{e}\, r\, \gamma\beta_\phi \tag{13}$$

11

where r_o is the initial radius of an electron at radius r in the downstream equilibrium, and B_{zo} is the external guide magnetic field in the cathode region, which is assumed to be known.

From the assumption that the equilibrium is steady-state in time, the continuity equation implies conservation of particles within annular rings:

$$n_o \, \beta_{oz} = n\beta_z \, \frac{dr^2}{dr_o^2} \tag{14}$$

while the force equations imply an energy constant:

$$\gamma - \frac{e}{mc^2} \, \phi = 1 - \frac{e}{mc^2} \, \phi_C \equiv \gamma_o \tag{15}$$

where $(\gamma_o - 1)mc^2$ is the final energy given to the electrons during acceleration within the diode region. For the case in which a foil anode is used, it may be considered to be held at ground potential $\phi = 0$, so that γ_o may be interpreted as the γ-factor of electrons

12

at the instant that they penetrate the anode foil. However, the application of equation (15) is not restricted solely to the case of foil anode configurations.

Now the solution for the equilibrium may be obtained by iteration. Let us assume that

$$n = n_c + \delta n \qquad (16)$$

$$\beta_z = \beta_c + \delta\beta_z \qquad (17)$$

where n_c, β_c are the values of n, β_z at the center of the beam, and the ansatz is made that $|\delta n| \ll n_c$, $|\delta\beta_z| \ll \beta_c$. Next one may define

$$\Omega_c \equiv \frac{e \ B_{zc}}{\gamma_c \ mc} \qquad (18)$$

$$\omega_{pc}^2 \equiv \frac{4\pi e^2 \ n_c}{m \ \gamma_c} \qquad (19)$$

13

$$\varepsilon_1 \equiv \left(\frac{\omega_{pc}^2 \, a}{2 \, \gamma_c \, \Omega_c \, c} \right)^2 \tag{20}$$

$$\varepsilon_2 \equiv \frac{2 \, \omega_{pc}^2}{\gamma_c^2 \, \Omega_c^2} \tag{21}$$

where $\gamma_c = (1 - \beta_c^2)^{-1/2}$ and it is assumed that $\varepsilon_1 \ll 1$, $\varepsilon_2 \ll 1$.

From equations (6) - (8) the electromagnetic field profiles are determined

$$B_\phi \simeq \beta_c E_r \simeq - 2\pi e \, n_c \, \beta_c \, r \tag{22}$$

$$B_z \simeq B_{zc} \left(1 + \varepsilon_1 \frac{r^2}{a^2} \right) . \tag{23}$$

and from equation (5) the equilibrium precessional velocity is determined

$$\beta_\phi \simeq \frac{\varepsilon_1^{1/2}}{\gamma_c} \frac{r}{a} \left[\frac{1 + \frac{1}{4} \varepsilon_2}{1 + \varepsilon_1 \frac{r^2}{a^2}} \right] \tag{24}$$

14

It is heuristically worthwhile to evaluate the necessary equilibrium conditions (11) and (12) at this point. To lowest order, condition (11) becomes

$$1 > \frac{-E_{rB}(a)}{B_z} \approx \frac{\omega_{pc}^2 a}{2 \gamma_c \Omega_c c} = \varepsilon_1^{1/2} \approx \frac{I_e(kA)}{5 B_z(kG) a(cm) \gamma \beta_z}$$

(25)

and condition (12) becomes

$$1 > \frac{2 \omega_{pB}^2}{\Omega_B^2} \approx \frac{2 \omega_{pc}^2}{\gamma_c^2 \Omega_c^2} = \varepsilon_2 \approx \frac{I_e(kA)}{0.7 B_z^2(kG) a^2(cm) \gamma \beta_z} \quad (26)$$

where γ and β_z have not been subscripted in the final expressions since we have not yet taken account of their radial variations. It may later be seen that $\gamma \beta_z$ @ $r = a$ is appropriate for condition (25) while $\gamma \beta_z$ @ $r = 0$ is appropriate for condition (26).

It is now apparent that $\varepsilon_1^{1/2}$, which reflects the first necessary condition for equilibrium, also

15

characterizes the strength of the axial diamagnetism (which varies as ϵ_1) and of the beam-frame precessional velocity $[\beta_{\phi B}(r = a) \approx \epsilon_1^{1/2}]$. Likewise ϵ_2, which reflects the second necessary condition for equilibrium, also characterizes the strength of centrifugal effects. Therefore, for the majority of cases where ϵ_1 and ϵ_2 are quite small, these complicating effects of diamagnetism, relativistic precession, and centrifugal effects may be treated as small corrections.

If the diamagnetic corrections are neglected in equation (24), then $\beta_\phi \propto r$ and the electron beam precesses as a rigid body. Given the precessional velocity from equation (24), then r^2/r_o^2 may be determined from equation (13). One finds

$$\frac{dr^2}{dr_o^2} \approx \frac{B_{zo}}{B_{zc}} \left(1 + \frac{1}{2}\epsilon_2 - \epsilon_1 \frac{r^2}{a^2} \right) \tag{27}$$

$$\frac{a^2}{a_o^2} \approx \frac{B_{zo}}{B_{zc}} \left(1 + \frac{1}{2}\epsilon_2 - \frac{1}{2}\epsilon_1 \right) \tag{28}$$

16

where B_{zo} is assumed to be uniform across the cathode surface. To lowest order, equation (13) implies that the electron beam propagates on magnetic flux surfaces; the small corrections due to the mechanical angular momentum acquired by the electrons are the $\frac{1}{2} \varepsilon_2$ terms in equations (27) and (28).

From equation (14), the downstream equilibrium particle density may now be expressed as

$$n \simeq \frac{n_o \, \beta_{oz} \, a_o^2}{a^2} \; \frac{\left[1 - \varepsilon_1\left(\frac{1}{2} - \frac{r^2}{a^2}\right)\right]}{\beta_z} \quad . \tag{29}$$

Finally, the radial dependence of γ may be determined from solving Poisson's equation in the downstream equilibrium region where the z-variation is negligible compared to the r-variation. The beam extends from $r = 0$ to $r = a$, with a vacuum gap from $r = a$ to the conducting waveguide walls at $r = b$. The third conservation equation (15) may be used to define γ in terms of the electric potential Φ for all r in the range $0 \leq r \leq b$. Hence the boundary condition $\Phi(r = b) = 0$

17

is equivalent to $\gamma(r = b) = \gamma_o$. One thereby arrives at the following differential equation and boundary condition for $\gamma(r)$:

$$\frac{1}{r} \frac{d}{dr} r \frac{d\gamma}{dr} = \frac{4\pi e^2}{mc^2} n \tag{30}$$

$$\left(\gamma + \ell n \, \frac{b}{a} \, r \, \frac{d\gamma}{dr}\right)_{r=a} = \gamma_o \tag{31}$$

where the Poisson equation has already been integrated through the vacuum gap to yield the modified boundary condition (31) at the beam edge. Equations (30) and (31) now determine the amount of γ-reduction (i.e., slowing) which the electron beam undergoes because of the space charge in the drift tube.

Equations (29) - (31) may be recognized as specifying the limiting current phenomena which we previously investigated in the limit of an infinite magnetic guide field (i.e., see Appendix C). In that limit however, $\varepsilon_1 \rightarrow 0$,

18

$\varepsilon_2 \to 0$, $B_{zo} \to B_{zc}$, $a \to a_o$ and equation (29) is simplified considerably. In this previous limiting current calculation, the parameter space of γ_o and b/a was explored exhaustively for expressions which would accurately predict the limiting current threshold. However, for the present calculation we will assume that the application is such that operation of the electron beam diode near the limiting current threshold is not required. Then extreme precision as to the determination of the limiting current should not be necessary, and the first order iteration which we have begun should be of sufficient accuracy.

Inserting equation (29) into equation (30), with $\beta_z \simeq \beta_c$, one then obtains the results

$$\gamma(r) \simeq \gamma_c + \Delta\gamma \, \frac{r^2}{a^2} \left[1 - \frac{1}{4} \varepsilon_1 \left(1 - \frac{r^2}{a^2} \right) \right]$$

$$\simeq \gamma_c + \Delta\gamma \, \frac{r^2}{a^2} \tag{32}$$

where

19

$$\gamma_c = \gamma_o - \frac{\nu}{\beta_c} \left(2 \ln \frac{b}{a} + 1 - \frac{1}{4} \epsilon_1 \right) \tag{33}$$

$$\Delta\gamma = \frac{\nu}{\beta_c} \left(1 - \frac{1}{4} \epsilon_1 \right)$$

$$\nu \equiv \frac{\pi n_o e^2 a_o^2 \beta_{oz}}{mc^2} = \frac{I_e}{mc^3/e} = \frac{I_e}{17 \text{ kA}} \tag{34}$$

and we shall assume that

$$1 \gg \frac{\Delta\gamma}{\gamma_c} = \frac{\nu \left(1 - \frac{1}{4} \epsilon_1 \right)}{\gamma_c \beta_c} = \frac{\omega_{pc}^2 a^2}{4c^2} \left(1 + \frac{1}{4} \epsilon_1 \right)$$

$$= \frac{2 \epsilon_1 \left(1 + \frac{1}{4} \epsilon_1 \right)}{\epsilon_2} . \tag{35}$$

Here condition (35) is imposed purely for theoretical

simplicity, since a wide range of interesting practical

applications are still possible which obey this restriction

20

to moderate electron currents. Other cases could also be examined, but we shall not do so herein. If one is within the pencil beam regime, for which $\gamma_o^{2/3} \ll 1 + 2 \ln b/a$, then condition (35) is valid up to the limiting current threshold--as discussed below. Otherwise, condition (35) may still be valid if the beam current is sufficiently below the limiting current.

If equation (33) is solved for $\nu(\gamma_c)$, ν is found to have a maximum value when

$$\gamma_c \simeq \gamma_o^{1/3} - \frac{\varepsilon_{1L}\,(\gamma_o - \gamma_o^{1/3})}{6\left(2\,\ln\dfrac{b}{a} + 1\right)} \equiv \gamma_{cL} \tag{36}$$

where ε_{1L} is ε_1 evaluated for $\gamma_c = \gamma_{cL} \simeq \gamma_o^{1/3}$. The ε_{1L} correction in equation (36) reflects the γ_c dependence of ε_1 in equation (33). We shall assume that

$$1 \gg \frac{\varepsilon_{1L}}{2}\,\frac{\gamma_o^{2/3}}{2\,\ln\dfrac{b}{a} + 1} \tag{37}$$

21

so that this correction is small. When $\gamma_c = \gamma_{cL}$, then $\nu = \nu_L = \nu_{max}$, and the corresponding maximum value of I_e is called I_L, the limiting current. It is the largest electron current which may be propagated within the drift tube, and is given by

$$I_L \simeq \frac{(\gamma_o^{2/3} - 1)^{3/2} \, mc^3/e}{2 \, \ell n \, \frac{b}{a} + 1 - \frac{1}{4} \, \varepsilon_{1L}} \, . \qquad (38)$$

Equations (36) and (38) are expressions of first order accuracy within the pencil beam regime for the limiting current parameters γ_{cL} and I_L, which reflect the finite magnetic field influence through the parameter ε_{1L}. In the infinite magnetic field limit, $\varepsilon_{1L} \to 0$ and these expressions reduce to the usual pencil beam interpolation results. It may be noted that as the magnetic guide field is reduced, ε_{1L} increases, γ_{cL} decreases, and I_L increases--in qualitative agreement with some reported numerical simulations of this problem.

22

Using the expressions for β_ϕ and γ in equations (24) and (32), one may solve for β_z from $\beta_z = (1 - \gamma^{-2} - \beta_\phi^2)^{1/2}$. The result is

$$\beta_z \simeq \beta_c \left[1 + \left(\frac{\Delta\gamma}{\gamma_c^3 \beta_c^2} - \frac{\epsilon_1}{2 \gamma_c^2 \beta_c^2} \right) \frac{r^2}{a^2} \right] , \qquad (39)$$

which exhibits the corrections to β_c. From condition (35) one may observe that the $\epsilon_1/2 \gamma_c^2 \beta_c^2$ correction is smaller than the $\Delta\gamma/\gamma_c^3 \beta_c^2$ correction by a factor of $\frac{1}{4} \epsilon_2$. Hence the dominant radial dependence of β_z derives from the space charge slowing, which affects the center electrons relatively more than those on the edge of the beam. The ansatz $1 \gg |\delta\beta_z|/\beta_c \simeq \Delta\gamma/\gamma_c^3 \beta_c^2$ follows from the assumption $I_e \ll I_L$, but the ansatz may also be obeyed fairly well even when $I_e \lesssim I_L$.

If equation (39) is inserted in equation (29), an improved expression for the radial dependence of the beam density is obtained:

23

$$n \simeq n_c \left[1 - \left(\frac{\Delta\gamma}{\gamma_c^3 \beta_c^2} - \epsilon_1 - \frac{\epsilon_1}{2 \gamma_c^2 \beta_c^2} \right) \frac{r^2}{a^2} \right] \tag{40}$$

Again, our previous assumptions imply that the $\epsilon_1/2 \gamma_c^2 \beta_c^2$ correction is smaller than the $\Delta\gamma/\gamma_c^3 \beta_c^2$ correction, and that the ansatz $1 >> |\delta n|/n_c$ is obeyed. However the relative size of the ϵ_1 diamagnetic correction and the $\Delta\gamma/\gamma_c^3 \beta_c^2$ space charge correction is not determined from the preceeding assumptions.

If the results from equations (39) and (40) are inserted into equations (6) and (7), improved expressions for the self-fields E_r and B_ϕ are obtained:

$$E_r \simeq - 2\pi e\, n_c\, r \left[1 - \frac{1}{2} \left(\frac{\Delta\gamma}{\gamma_c^3 \beta_c^2} - \epsilon_1 - \frac{\epsilon_1}{2 \gamma_c^2 \beta_c^2} \right) \frac{r^2}{a^2} \right]$$

$$\tag{41}$$

$$B_\phi \simeq - 2\pi e\, n_c\, \beta_c\, r \left[1 + \frac{1}{2} \epsilon_1 \frac{r^2}{a^2} \right] \tag{42}$$

24

Equation (23) for B_z is still correct to lowest order in the small parameters.

At this point, one could continue with a second major iterative cycle through the equations to obtain still higher order corrections. However, since we expect our various assumptions of smallness to be fairly well obeyed for most applications of interest, we will stop after listing one further updated expression for the equilibrium precessional velocity:

$$\beta_\phi \simeq \frac{\epsilon_1^{1/2}}{\gamma_c} \frac{r}{a} \left[\frac{1 + \frac{1}{4} \epsilon_2}{1 + \left(\frac{\Delta\gamma}{2 \gamma_c \beta_c^2} + \frac{\Delta\gamma}{\gamma_c} \right) \frac{r^2}{a^2}} \right] \quad . \tag{43}$$

If the radial dependences herein derived are inserted into the necessary condition (11) for the existence of equilibria, there results

$$1 > \epsilon_1^{1/2} \frac{r}{a} \left[1 - \frac{r^2}{a^2} \left(\frac{\Delta\gamma}{\gamma_c} + \frac{\Delta\gamma}{2 \gamma_c^3 \beta_c^2} - \frac{\epsilon_1}{4 \gamma_c^2 \beta_c^2} \right) \right] \tag{44}$$

25

Since our previous assumptions insure that $[(\Delta\gamma/\gamma_c) +$ $(\Delta\gamma/2 \; \gamma_c^3 \; \beta_c^2) - (\epsilon_1/4 \; \gamma_c^2 \; \beta_c^2)] < \frac{1}{3}$, the right-hand side of equation (44) is largest at $r = a$ as we previously hypothesized. The small correction terms to the zero order result $1 > \epsilon_1^{1/2}$ are only present because we chose to define ϵ_1 in terms of on-axis quantities in equation (20).

Likewise, condition (12) is found to be most restrictive at the center of the beam, and it reduces simply to $1 > \epsilon_2$ since ϵ_2 was originally defined in terms of on-axis quantities.

A P P E N D I X   H

LINEAR THEORY OF COLLECTIVE WAVES SUPPORTED BY
AN UNNEUTRALIZED RELATIVISTIC
ELECTRON BEAM

(Appendix H Contains 34 Pages)

42

Among the important applications which have been suggested in recent years for high energy relativistic electron beams are the use of such beams as a medium for the collective acceleration of ions. An important subclass of these collective acceleration schemes are based upon the utilization of self-consistent collective eigenmodes, or waves, supported by the electron beam--within which waves, the subject ions are to be confined during the process of ion-wave acceleration. For example, the Auto-Resonant acceleration concept seeks to utilize the negative energy electron cyclotron wave, while the Converging Guide acceleration concept seeks to utilize the negative energy longitudinal plasma wave. We will examine herein the derivation of the dispersion relation for these waves, paying attention to certain effects of centrifugal forces, Coriolis forces, and longitudinal compression which are negligible when the electrons are ultrarelativistic (i.e., $\gamma_o^{-2} \ll 1$), but which must be retained for the case of lower energy electrons. Likewise, the effects due to an axial magnetic guide field of finite strength are retained in general, although these effects become negligible in the infinite magnetic field

1

limit which is often adopted when plasma waves are examined. The more general analysis which is presented here will permit an appraisal of the validity of the "ultrarelativistic" and the "infinite magnetic field" limits which are frequently taken, and will display the coupling effects between the plasma waves and the electron cyclotron waves.

The mathematical complications which arise within linear theory may be traced to the complications inherent in the equilibrium of such unneutralized relativistic electron beams. The self-fields E_r and B_ϕ of the electron beam combine to produce a net outward force $- e(E_r - \beta_z B_\phi) \simeq - e \gamma_o^{-2} E_r$ acting upon the electrons, which can only be counterbalanced if the electrons have a precessional velocity $\beta_\phi c$ in an axial magnetic guide field, so that the magnetic pinch force $- e \beta_\phi B_z$, reduced somewhat by the outward centrifugal force $\gamma_o mc^2 \beta_\phi^2/r$, restores the radial force equilibrium. This precession of the electrons in turn produces a diamagnetic reduction in the axial magnetic field within the beam, and slightly alters the radial distribution of the electrons relative to that at the cathode

2

before the precession is established. Finally, the injection

of the electron beam into an evacuated waveguide is accom-

panied by some r-dependent slowing of the beam due to space

charge forces. This produces a slight outward radial

gradient to the axial beam velocity, and corresponding

r-dependence for the beam density and relativistic γ-factor.

All of the above mentioned effects produce complicated radial

dependence in the beam density and velocity parameters, which

in turn cause the self-fields E_r and B_ϕ and the diamag-

netic correction to the axial magnetic field B_z to have

complicated r-dependence.

These complicating features in the self-consistent

equilibrium quantities produce a corresponding complication

in the radial eigenvalue problem which must be solved to

yield the linear wave dispersion relation. The extent of

the complication is apparent from examining the linearized

version of the relativistic force equation:

$$\frac{d}{dt} \gamma \underline{\beta} = - \frac{e}{mc} (\underline{E} + \underline{\beta} \times \underline{B}) \tag{1}$$

3

where $e = -|e|$, m are the electron charge and mass,
$\gamma_o = (1 - \underline{\beta}_o^2)^{-1/2}$, $\underline{\beta}_o = \beta_z \hat{z} + \beta_\phi \hat{\phi}$ is the normalized,
zero-order velocity vector of the electrons, and $\underline{E}_o = E_r \hat{r}$,
$\underline{B}_o = B_z \hat{z} + B_\phi \hat{\phi}$ are the zero-order electromagnetic fields.
In zero-order (i.e., equilibrium), the radial component of
the force equation (1) is

$$- \gamma_o \frac{c \beta_\phi^2}{r} = - \frac{e}{mc} (E_r - \beta_z B_\phi + \beta_\phi B_z) \qquad (2)$$

while in first-order, the force equation may be written as

$$\tilde{\underline{\beta}} \underbrace{\left(\frac{d}{dt} \gamma\right)_o}_{0} + \underline{\beta}_o \left(\widetilde{\frac{d}{dt} \gamma}\right) + \tilde{\gamma} \left(\frac{d}{dt} \underline{\beta}\right)_o + \gamma_o \left(\widetilde{\frac{d}{dt} \underline{\beta}}\right) =$$

$$- \frac{e}{mc} (\tilde{\underline{E}} + \tilde{\underline{\beta}} \times \underline{B}_o + \underline{\beta}_o \times \tilde{\underline{B}}) \qquad (3)$$

where a tilde denotes first-order (i.e., wave) quantities.
The $\hat{r}$, $\hat{\phi}$, and $\hat{z}$ components of equation (3) are as
follows:

4

$$\tilde{\gamma}\left(\frac{-e}{mc\gamma_o}\right)[E_r - \beta_z B_\phi + \beta_\phi B_z] + \gamma_o\left[\frac{\partial}{\partial t} + \frac{c\beta_\phi}{r}\frac{\partial}{\partial \phi} + c\beta_z\frac{\partial}{\partial z}\right]\tilde{\beta}_r$$

$$- 2\gamma_o c \frac{\beta_\phi \tilde{\beta}_\phi}{r} = \frac{-e}{mc}[\tilde{E}_r - \beta_z\tilde{B}_\phi + \tilde{\beta}_\phi B_z + \beta_\phi\tilde{B}_z - \tilde{\beta}_z B_\phi]$$

$$(4)$$

$$\beta_\phi\left(\frac{-e}{mc}\right)[\tilde{\beta}_r E_r + \beta_\phi\tilde{E}_\phi + \beta_z\tilde{E}_z] + \gamma_o\left[\frac{\partial}{\partial t} + \frac{c\beta_\phi}{r}\frac{\partial}{\partial \phi} + c\beta_z\frac{\partial}{\partial z}\right]\tilde{\beta}_\phi$$

$$+ \gamma_o\frac{c\beta_\phi}{r}\tilde{\beta}_r + \gamma_o c\,\tilde{\beta}_r\frac{\partial}{\partial r}\beta_\phi = \frac{-e}{mc}[\tilde{E}_\phi - \tilde{\beta}_r B_z + \beta_z\tilde{B}_r]$$

$$(5)$$

$$\beta_z\left(\frac{-e}{mc}\right)[\tilde{\beta}_r E_r + \beta_\phi\tilde{E}_\phi + \beta_z\tilde{E}_z] + \gamma_o\left[\frac{\partial}{\partial t} + \frac{c\beta_\phi}{r}\frac{\partial}{\partial \phi} + c\beta_z\frac{\partial}{\partial z}\right]\tilde{\beta}_z$$

$$+ \gamma_o c\,\tilde{\beta}_r\frac{\partial}{\partial r}\beta_z = \frac{-e}{mc}[\tilde{E}_z + \tilde{\beta}_r B_\phi - \beta_\phi\tilde{B}_r] \qquad (6)$$

5

Here, the downward pointing arrows indicate terms which are present because of the equilibrium precession of the beam, while the upward pointing arrows indicate terms which are present because of the self-fields of the beam equilibrium. There are seventeen such terms in these equations, all of which have complicated r-dependence and all of which are missing for the case of a charge- and current-neutralized beam, for an ultrarelativistic beam, or for a beam in an infinite magnetic guide field.

It is clear that the arrowed terms vanish individually for a neutralized beam. The ultrarelativistic limit may be taken formally by tending γ_o, B_z, n (hence E_r, B_ϕ) to infinity in such a way that the ratio of any two such quantities remains finite. In this way, the relativistic plasma and cyclotron frequencies remain finite, but longitudinal mass terms and precessional terms, which vary as γ_o^{-3}, tend to zero. Thus the β_ϕ terms of equations (4) - (6) tend to zero and the remaining self-field terms cancel to with $O(\gamma_o^{-2})$ and may be omitted. One also finds that $\tilde{\beta}_z \propto \gamma_o^{-3} \to 0$, so that there is no longitudinal beam compression in the ultrarelativistic limit.

6

For the infinite magnetic field limit, β_ϕ, $\tilde{\beta}_r$, and $\tilde{\beta}_\phi$ tend to zero as B_z^{-1}, and only the $\hat{z}$-equation (6) is required to relate $\tilde{\beta}_z$ to the perturbed wave fields. Hence the perturbed electron motion is strictly axial in this case, and longitudinal plasma waves are allowed. By comparison, in the ultrarelativistic limit, the perturbed electron motion is purely transverse, and electron cyclotron waves are allowed.

Although neither of these limits is appropriate in general, one can still define parameters ϵ_1, ϵ_2, and $\beta_\phi(a) \simeq \epsilon_1^{1/2}/\gamma_o$ as in Appendix G, which are small for most cases of interest and thus simplify the theory. (Notice that each of these parameters would vanish within the ultra-relativistic limit, or within the infinite magnetic field limit.) Of the above three small parameters, the largest for many cases of interest is ϵ_2, reflecting the centrifugal and Coriolis force effects. The parameters ϵ_1 and $\beta_\phi(a)$ represent effects of axial diamagnetism, $\beta_\phi \times \underline{\tilde{B}}$ forces, $\beta_\phi \tilde{n}$ current density sources, and relativistic beam-frame precession which have a relative magnitude of only a few percent or less for many cases of interest. We shall neglect

7

these latter effects, but retain the large ε_2 centrifugal effects within the linear theory. In addition, it is necessary to retain effects such as longitudinal compression which have a relative magnitude of γ_o^{-2}, and are not at all small for electron beams which are not ultrarelativistic.

Finally, there are the small parameters $\Delta\gamma/\gamma_c$ and $\Delta\gamma/\gamma_c^3\beta_c^2$, also discussed in Appendix G. These parameters reflect the radial variation in beam energy due to effects of space-charge slowing. They are small only if the electron beam current is well below the Alfvén-Lawson limits, which--fortunately--is often the case. Nevertheless, these corrections can sometimes be as large as ten percent or more, in which case they should be included in the analysis. In addition, these parameters do not formally vanish in either the ultrarelativistic or the infinite magnetic field limits, and they consequently have relevance for many accelerator applications. (In fact, for the converging guide accelerator these parameters may have to be appreciable in order for the plasma wave phase velocity to be somewhat low at the front of the accelerator.) However, because these effects produce

8

radial dependence which greatly complicates the mathematical
eigenvalue problem within linear theory, we shall neglect
them for the present calculation. This will allow the linear
theory to be solved in terms of relatively simple eigenfunc-
tions (i.e., Bessel functions), and will allow us to examine
the modifications which arise due to the retention of the
ε_2 and γ_o^{-2} terms which are omitted for ultrarelativistic
beams. Also, the coupling between the plasma and cyclotron
waves may be examined within such a calculation.

Elsewhere, the effects of the radial variation in
γ on the electron cyclotron wave are considered within the
ultrarelativistic limit in Appendix D, and the effects on
the longitudinal plasma wave are considered within the
infinite magnetic field limit in Appendix I.

The approximations discussed above for this linear
theory calculation imply that the electron density n, the
axial velocity $\beta_z c$, and the kinetic energy $(\gamma - 1)mc^2$ may
be treated as constants with respect to r, as may be seen
from the expressions derived in Appendix G. Hence we shall
denote them as $n = n_o$, $\beta_z = \beta_o$, $\gamma = \gamma_o$. In addition we
may let $\gamma_o = (1 - \beta_o^2)^{-1/2}$ since the β_ϕ corrections

9

to γ_o will be negligible under these approximations. Furthermore, the axial magnetic field B_z may be treated as uniform in r, and we may define the usual characteristic frequencies

$$\Omega \equiv \frac{e\,B_z}{\gamma_o\,mc} \tag{7}$$

$$\omega_p^2 \equiv \frac{4\pi\,n_o\,e^2}{\gamma_o\,m} \quad, \tag{8}$$

and the small parameters

$$\epsilon_1 \equiv \left(\frac{\omega_p^2\,a}{2\,\gamma_o\,\Omega c} \right)^2 \ll 1 \tag{9}$$

$$\epsilon_2 \equiv \left(\frac{2\,\omega_p^2}{\gamma_o^2\,\Omega^2} \right)^2 \ll 1 \quad . \tag{10}$$

The equilibrium self-fields of the beam are then given by

10

$$B_\phi \simeq \beta_o E_r \simeq - 2\pi e\, n_o\, \beta_o\, r \qquad (11)$$

and the equilibrium velocity of precession/c is

$$\beta_\phi \simeq \frac{\omega_p^2\, r}{2\, \gamma_o^2\, \Omega c} = \frac{\epsilon_1^{1/2}}{\gamma_o}\, \frac{r}{a} \qquad . \qquad (12)$$

Among the approximations invoked for this calculation are the orderings

$$\epsilon_1 \ll \epsilon_2 \ll 1 \qquad (13)$$

and

$$\epsilon_1 \ll \beta_\phi(a) \ll \gamma_o^{-2},\, 1 \qquad . \qquad (14a)$$

No assumption is invoked about the size of γ_o^{-2}, so that the calculation may be relevant even for a nonrelativistic beam. Assumption (14a) may also be written as

$$1 \gg \gamma_o\, \epsilon_1^{1/2} \simeq \gamma_o^2\, \beta_\phi(a) \simeq \left| \frac{E_r(a)}{B_z} \right| \qquad . \qquad (14b)$$

11

There will exist some cases of interest for which condition (13) is fairly well obeyed, but condition (14) is not. However, for these cases, $\gamma_o^{-2} \ll 1$ and the violation of condition (14) merely means that the γ_o^{-2} effects are no larger than the neglected β_ϕ and ϵ_1 effects, and so the γ_o^{-2} effects should be neglected as well.

Returning again to the linear theory of waves supported by such an equilibrium, the force equations, continuity equation, and Maxwell's field equations are linearized and transformed with respect to the basis functions $\exp i(\ell\phi + k_z z - \omega t)$. It is convenient to define the following wave field variables

$$A^+ \equiv \tilde{E}_r + i\,\tilde{E}_\phi + i\,\beta_o\tilde{B}_r - \beta_o\tilde{B}_\phi \tag{15}$$

$$A^- \equiv \tilde{E}_r - i\,\tilde{E}_\phi - i\,\beta_o\tilde{B}_r - \beta_o\tilde{B}_\phi \quad . \tag{16}$$

For this case in which β_o is constant, Maxwell's equations imply the following pair of equations for $A^\pm$

12

$$\left(\frac{1}{r} \frac{\partial}{\partial r} r \frac{\partial}{\partial r} - \frac{(\ell \pm 1)^2}{r^2} - k_z^2 + \frac{\omega^2}{c^2} \right) A^{\pm} =$$

$$- \frac{4 \pi i \Delta \omega}{c^2} (\tilde{J}_r \pm i \tilde{J}_\phi)$$

$$+ 4\pi \left(\frac{\partial}{\partial r} \mp \frac{\ell}{r} \right) \left(\tilde{\rho} - \frac{\beta_o}{c} \tilde{J}_z \right) \tag{17}$$

where $\Delta\omega \equiv \omega - k_z \beta_o c$ and $\tilde{\rho}, \tilde{\underline{J}}$ are the beam charge and current density. In general, there will be boundary conditions at the conducting wall at $r = b$ to ensure that $\tilde{E}_z$, $\tilde{E}_\phi$, $\tilde{B}_r$ vanish there, and in addition there must be jump conditions at the beam edge $r = a$ to properly patch the beam interior field solutions to the vacuum gap field solutions. However, a great deal of this complexity may be avoided when the vacuum gap is narrow (i.e., $b - a \ll a$), since then only the beam interior solutions are required and the boundary conditions may be applied at the beam edge. We shall make this assumption, in which case the boundary conditions reduce to

13

$$(A^+ - A^-)_{r=a} = 0 \tag{18}$$

$$\left[\frac{1}{r}\frac{\partial}{\partial r} r (A^+ + A^-)\right]_{r=a} = 8\pi \left(\tilde{\rho} - \frac{\beta_o}{c} \tilde{J}_z\right)_{r=a} . \tag{19}$$

From the variables $A^{\pm}$, the perturbed electric and
magnetic fields are found as follows

$$\tilde{E}_z = \frac{i}{2\left(k_z - \beta_o \frac{\omega}{c}\right)}\left[\frac{1}{r}\frac{\partial}{\partial r} r (A^+ + A^-) + \frac{\ell}{r} (A^+ - A^-) - 8\pi\left(\tilde{\rho} - \frac{\beta_o}{c}\tilde{J}_z\right)\right]$$
$$\tag{20}$$

$$\tilde{E}_r = \frac{-1}{2\left(k_z\beta_o - \frac{\omega}{c}\right)}\left[2 \beta_o i \frac{\partial \tilde{E}_z}{\partial r} + \frac{\omega}{c} (A^+ + A^-)\right] \tag{21}$$

$$\tilde{E}_\phi = \frac{i}{2\left(k_z\beta_o - \frac{\omega}{c}\right)}\left[\frac{\omega}{c} (A^+ - A^-) - \frac{2i\ell \beta_o}{r} \tilde{E}_z\right] \tag{22}$$

14

$$\tilde{B}_z = \frac{1}{2\left(k_z \beta_o - \frac{\omega}{c}\right)} \left[\frac{1}{r} \frac{\partial}{\partial r} r (A^+ - A^-) + \frac{\ell}{r} (A^+ + A^-) \right] \qquad (23)$$

$$\tilde{B}_r = \frac{-1}{2\left(k_z \beta_o - \frac{\omega}{c}\right)} \left[i k_z (A^+ - A^-) + \frac{2\ell}{r} \tilde{E}_z \right] \qquad (24)$$

$$\tilde{B}_\phi = \frac{-1}{2\left(k_z \beta_o - \frac{\omega}{c}\right)} \left[2i \frac{\partial \tilde{E}_z}{\partial r} + k_z (A^+ - A^-) \right] \qquad (25)$$

The perturbed beam charge and current densities are related to the perturbed velocities and number density as follows

$$\tilde{\rho} = - e \tilde{n} \qquad (26)$$

$$\tilde{J}_z = - ec (\beta_o \tilde{n} + n_o \tilde{\beta}_z) \qquad (27)$$

$$\tilde{J}_r = - ec \, n_o \, \tilde{\beta}_r \qquad (28)$$

15

$$\tilde{J}_\phi = - ec \, (n_o \tilde{\beta}_\phi + \tilde{n} \, \beta_\phi) \simeq - ec \, n_o \, \tilde{\beta}_\phi \qquad (29)$$

where the β_ϕ term in equation (29) is neglected according to the previously discussed approximation (14).

The force equations (4) - (6) simplify under our approximations to the form

$$i \, \frac{\delta\omega}{\Omega} \tilde{\beta}_r - \left(1 - \frac{2 \, c\beta_\phi}{r\Omega}\right) \tilde{\beta}_\phi = \frac{1}{B_z} (\tilde{E}_r - \beta_o \tilde{B}_\phi) = \frac{A^+ + A^-}{2 \, B_z}$$

$$\qquad (30)$$

$$\left(1 - \frac{2 \, c\beta_\phi}{r\Omega}\right) \tilde{\beta}_r + \frac{i\delta\omega}{\Omega} \tilde{\beta}_\phi = \frac{1}{B_z} (\tilde{E}_\phi + \beta_o \tilde{B}_r) = \frac{A^+ - A^-}{2i \, B_z}$$

$$\qquad (31)$$

$$i\delta\omega \, \tilde{\beta}_z = \frac{e}{\gamma_o \, mc} [\gamma_o^{-2} \, \tilde{E}_z - \beta_\phi (\tilde{B}_r + \beta_o \tilde{E}_\phi)] \simeq \frac{e}{\gamma_o^3 \, mc} \tilde{E}_z$$

$$\qquad (32)$$

16

where approximation (14) is invoked to simplify equation (32), and $\delta\omega \equiv \omega - k_z\beta_o c - \dfrac{\ell\beta_\phi c}{r} = \Delta\omega - \ell\omega_\phi$. Here $\omega_\phi = \beta_\phi c/r = \dfrac{1}{4}\,\varepsilon_2\,\Omega$ is the precessional frequency of the beam equilibrium.

Finally, the continuity equation is employed to relate $\tilde{n}$ to $\underset{\sim}{\tilde{\beta}}$ as follows

$$\tilde{n} = n_o\left(\frac{k_z c}{\delta\omega}\,\tilde{\beta}_z + \frac{c}{i\delta\omega}\,\frac{1}{r}\,\frac{\partial}{\partial r}\,r\,\tilde{\beta}_r + \frac{\ell c}{\delta\omega r}\,\tilde{\beta}_\phi\right)\ . \tag{33}$$

It may be observed that the ε_2 effects are represented through the ϕ-portion of the convective derivative terms (i.e., $\ell\omega_\phi = \dfrac{1}{4}\,\ell\varepsilon_2\Omega$) and through the centrigugal and Coriolis force terms in equations (30) and (31), which are the terms with coefficients $\dfrac{2\,c\beta_\phi}{r\Omega} = \dfrac{1}{2}\,\varepsilon_2$. These latter effects may be conveniently retained by introducing the modified variables

$$\bar{B}_z \equiv B_z\left(1 - \frac{1}{2}\,\varepsilon_2\right);\ \bar{\Omega} \equiv \Omega\left(1 - \frac{1}{2}\,\varepsilon_2\right) \tag{34}$$

17

in terms of which equations (30) and (31) become

$$i \frac{\delta\omega}{\bar{\Omega}} \tilde{\beta}_r - \tilde{\beta}_\phi = \frac{A^+ + A^-}{2 \bar{B}_z} \qquad (35)$$

$$\tilde{\beta}_r + \frac{i\delta\omega}{\bar{\Omega}} \tilde{\beta}_\phi = \frac{A^+ - A^-}{2i \bar{B}_z} \qquad (36)$$

The source terms $\tilde{J}_r + i \tilde{J}_\phi$ in equation (17) require only $\tilde{\beta}_r$, $\tilde{\beta}_\phi$ which may be readily related to $A^\pm$ via the $\hat{r}$, $\hat{\phi}$ force equations (35) and (36). However, the source terms $\tilde{\rho} - \frac{\beta_o}{c} \tilde{J}_z$ require $\gamma_o^{-2} \tilde{n} - n_o\beta_o \tilde{\beta}_z$, which couples the continuity equation and the $\hat{z}$ force equation to Maxwell's equations.

From equations (28), (29), (35), and (36), one finds

$$-\frac{4\pi i \, \Delta\omega}{c^2} (\tilde{J}_r \pm i \tilde{J}_\phi) = \frac{\omega_p^2}{c^2} \frac{\Delta\omega}{\delta\omega \pm \bar{\Omega}} A^\pm \quad . \qquad (37)$$

18

while from equations (20), (26), (27), (32), (33), (35), and (36), one finds that

$$8\pi\left(\tilde{\rho} - \frac{\beta_o}{c}\tilde{J}_z\right) = -2\,T_\ell\left\{\frac{1}{r}\frac{\partial}{\partial r}\,r\left[\frac{A^+}{1+\delta_\ell} + \frac{A^-}{1-\delta_\ell}\right]\right.$$

$$+ \frac{\ell}{r}\left[\frac{A^+}{1+\delta_\ell} - \frac{A^-}{1-\delta_\ell}\right]$$

$$\left.+ \frac{\beta_o\ell\omega_\phi}{k_z c - \beta_o\omega}\left[\frac{1}{r}\frac{\partial}{\partial r}\,r\,(A^+ + A^-) + \frac{\ell}{r}\,(A^+ - A^-)\right]\right\}$$

$$(38)$$

where

$$T_\ell \equiv \frac{\dfrac{\omega_p^2}{2\,\gamma_o^2\,\delta\omega^2}}{1 - \dfrac{\omega_p^2}{\gamma_o^2\,\delta\omega^2}\left(1 + \dfrac{\beta_o\ell\omega_\phi}{k_z c - \beta_o\omega}\right)} \qquad (39)$$

19

$$\delta_\ell \equiv \frac{\delta\omega}{\Omega} \quad . \tag{40}$$

One may now insert equations (37) and (38) for the self-consistent beam source terms into the pair of equations (17) to obtain a pair of coupled, second-order differential equations for the wave field variables $A^\pm$. First however, it may be noted that the complicating effects associated with the $\ell\omega_\phi$ terms, which are present also in $\delta\omega$, δ_ℓ, and T_ℓ, will be removed for the important cases of $\ell = 0$ (i.e., ϕ-symmetric sausage modes or compressional modes) or $\omega_\phi = \frac{1}{4}\varepsilon_2\Omega \rightarrow 0$ (e.g., the infinite magnetic field limit). When $\varepsilon_2 \ll 1$, these ω_ϕ effects will tend to influence the plasma and cyclotron waves significantly only at large values of ℓ—where some fluting perturbations might be anticipated for the electron beam.

Let us briefly consider the infinite magnetic field limit, for which $\omega_\phi \rightarrow 0$, $\delta\omega \rightarrow \Delta\omega$, $\delta_\ell \rightarrow 0$, $\tilde{J}_r \rightarrow 0$, $\tilde{J}_\phi \rightarrow 0$. In this limit, the pair of equations (17) may be expressed as

20

$$\left[\frac{1}{r}\frac{\partial}{\partial r} r \frac{\partial}{\partial r} - \frac{(\ell \pm 1)^2}{r^2} - k_z^2 + \frac{\omega^2}{c^2}\right] A^\pm =$$

$$- T\left(\frac{\partial}{\partial r} \mp \frac{\ell}{r}\right)\left[\frac{1}{r}\frac{\partial}{\partial r} r (A^+ + A^-) + \frac{\ell}{r} (A^+ - A^-)\right]$$

(41)

where

$$T \equiv T_\ell(\omega_\phi \to 0) = T_{\ell=0} = \frac{\dfrac{\omega_p^2}{2 \gamma_o^2 \Delta\omega^2}}{1 - \dfrac{\omega_p^2}{\gamma_o^2 \Delta\omega^2}} .$$

(42)

The boundary conditions (18) and (19) then become

$$(A^+ - A^-)_{r=a} = 0 = \left[\frac{1}{r}\frac{\partial}{\partial r} r (A^+ + A^-)\right]_{r=a} .$$

(43)

The pair of equations (41) may be put in the form

$$\left[(1+2T)\frac{\partial}{\partial r}\frac{1}{r}\frac{\partial}{\partial r} r - \frac{\ell^2}{r^2} - k_z^2 + \frac{\omega^2}{c^2}\right](A^+ + A^-) = \frac{2\ell}{r}\left[-T\frac{\partial}{\partial r} + \frac{1+T}{r}\right](A^+ - A^-)$$

(44a)

21

$$\left[\frac{\partial}{\partial r} \frac{1}{r} \frac{\partial}{\partial r} r - (1+2T) \frac{\ell^2}{r^2} - k_z^2 + \frac{\omega^2}{c^2}\right] (A^+ - A^-) = \frac{2\ell}{r} \left[T \frac{\partial}{\partial r} + \frac{1+T}{r}\right] (A^+ + A^-)$$

(44b)

from which it is apparent that the modes decouple for
$\ell = 0$, since then there is one equation and one outer
boundary condition (in addition to regularity at $r = 0$)
for each of the variables $A^+ + A^-$ and $A^+ - A^-$. Equation
(44a) is seen to yield the longitudinal plasma wave disper-
sion in this case, while equation (44b) describes electro-
magnetic waves. To discover the decoupling which might
occur for $\ell \neq 0$, one is led to define the variable

$$R \equiv \frac{1}{r} \frac{\partial}{\partial r} r (A^+ + A^-) + \frac{\ell}{r} (A^+ - A^-) \qquad (45)$$

since this combination appears on the right hand side of
equation (41) and one also finds that $\tilde{E}_z \propto R$. Sure enough,
the equations (44a) and (44b) imply that

$$\left[\frac{1}{r} \frac{\partial}{\partial r} r \frac{\partial}{\partial r} - \frac{\ell^2}{r^2} - \frac{k_z^2 - \frac{\omega^2}{c^2}}{1 + 2T}\right] R = 0 \qquad (46)$$

22

while the boundary conditions (43) imply that $R(r = a) = 0$.
It follows that $R(r) = J_\ell (k_\perp r)$, where the dispersion
relation is given by

$$k_\perp^2 = \left(\frac{\lambda_{\ell n}}{a} \right)^2 = - \left(k_z^2 - \frac{\omega^2}{c^2} \right) \left(1 - \frac{\omega_p^2}{\gamma_o^2 \, \Delta\omega^2} \right) \tag{47}$$

and the $\lambda_{\ell n}$ are the zeroes of $J_\ell (\lambda) = 0$ (e.g., $\lambda_{01} = 2.4$).
Equation (47) is the desired dispersion relation for longi-
tudinal plasma waves in the infinite magnetic field limit.
One may also define a variable conjugate to R which may
be shown from equations (44) to obey an equation which
describes electromagnetic waves. However, we shall not
explore these waves here.

The second case which we wish to examine in some
detail is that of $\ell = 0$, ϕ-symmetric sausage modes or
compressional modes of oscillation. This case is important
for the applications of collective ion-wave acceleration
since it is the $\ell = 0$ waves within which the ions are to
be trapped and accelerated. For $\ell = 0$, it is again true
that $\delta\omega \rightarrow \Delta\omega$, and we shall employ the variables T and

23

$$\delta \equiv \delta_{\ell=0} = \frac{\Delta\omega}{\Omega} \tag{48}$$

$$p_{\pm}^2 = k_z^2 - \frac{\omega^2}{c^2} + \frac{\omega_p^2}{c^2} \frac{\Delta\omega}{\Delta\omega \pm \overline{\Omega}} \tag{49}$$

If the sources of equations (37) and (38) are then inserted into equations (17) - (19), there results

$$\left(\frac{\partial}{\partial r} \frac{1}{r} \frac{\partial}{\partial r} r - p_{\pm}^2 \right) A^{\pm} = - T \frac{\partial}{\partial r} \frac{1}{r} \frac{\partial}{\partial r} r \left(\frac{A^+}{1+\delta} + \frac{A^-}{1-\delta} \right)$$

$$\tag{50}$$

$$(A^+ - A^-)_{r=a} = 0 \tag{51}$$

$$\left[\frac{1}{r} \frac{\partial}{\partial r} r \ (A^+ + A^-) \right]_{r=a} = - 2T \left[\frac{1}{r} \frac{\partial}{\partial r} r \left(\frac{A^+}{1+\delta} + \frac{A^-}{1-\delta} \right) \right]_{r=a}$$

$$\tag{52}$$

24

The pair of equations (50) would be uncoupled in the ultrarelativistic limit where T vanishes, but otherwise they are coupled due to the γ_0^{-2} compressional effects. This coupled set of second order equations is equivalent to the following uncoupled pair of fourth order equations

$$\left[\frac{\partial}{\partial r}\frac{1}{r}\frac{\partial}{\partial r}r - \frac{p_+(1+\delta)(1-\delta+T)}{1-\delta^2+2T}\right]\left[\frac{\partial}{\partial r}\frac{1}{r}\frac{\partial}{\partial r}r\right.$$

$$\left.- \frac{p_-^2(1-\delta)(1+\delta+T)}{1-\delta^2+2T}\right]A^\pm = \frac{T^2p_+^2p_-^2(1-\delta^2)}{(1-\delta^2+2T)^2}A^\pm$$

(53)

which may be solved in terms of Bessel functions since the coefficients are independent of r. If one makes the ansatz

$$A^+ = \alpha_1^+ J_1(k_{\perp 1}r) + \alpha_2^+ J_1(k_{\perp 2}r)$$

(54)

25

$$A^- = \alpha_1^- J_1(k_{\perp 1}r) + \alpha_2^- J_1(k_{\perp 2}r) \tag{55}$$

then equation (53) reduces to a quadratic equation for $k_\perp^2$ which must be obeyed by both $k_{\perp 1}^2$ and $k_{\perp 2}^2$, which are therefore the two roots of the quadratic:

$$\left[k_\perp^2 + \frac{p_+^2(1+\delta)(1-\delta+T)}{1-\delta^2+2T} \right]\left[k_\perp^2 + \frac{p_-^2(1-\delta)(1+\delta+T)}{1-\delta^2+2T} \right]$$

$$- \frac{T^2 p_+^2 p_-^2(1-\delta^2)}{(1-\delta^2+2T)^2} = 0 \quad . \tag{56}$$

If equations (54) and (55) are inserted into equations (50) and the boundary conditions (51) and (52), one finally arrives at the dispersion relation, which may be cast in the form

$$G_1 \frac{k_{\perp 1}a\, J_o(k_{\perp 1}a)}{J_1(k_{\perp 1}a)} + G_2 \frac{k_{\perp 2}a\, J_o(k_{\perp 2}a)}{J_1(k_{\perp 2}a)} = 0 \tag{57}$$

26

where

$$G_1 = \cfrac{\left(1 + \cfrac{2T}{1+\delta}\right) + \left(1 + \cfrac{2T}{1-\delta}\right)\left\{\cfrac{\cfrac{T\,p_+^2(1-\delta)}{1-\delta^2+2T}}{\left[k_{\perp1}^2 + \cfrac{p_-^2(1-\delta)(1+\delta+T)}{1-\delta^2+2T}\right]}\right\}}{1 - \left\{\cfrac{\cfrac{T\,p_+^2(1-\delta)}{1-\delta^2+2T}}{\left[k_{\perp1}^2 + \cfrac{p_-^2(1-\delta)(1+\delta+T)}{1-\delta^2+2T}\right]}\right\}}$$

$$(58)$$

and

$$G_2 = -\,G_1(k_{\perp1}^2 \rightarrow k_{\perp2}^2) \quad . \tag{59}$$

The familiar infinite magnetic field and ultrarelativistic limits correspond in this notation to $\delta \rightarrow 0$ and $T \rightarrow 0$, respectively. For an improved analysis which retains the effects of coupling between the cyclotron and plasma waves and yet exploits the smallness of the ε_2 parameter which characterizes the frequency separation of these two modes, one merely treats either δ or T as a small (but nonzero)

27

parameter--depending upon which mode is being examined.
We conclude this calculation by considering the case of
the negative energy cyclotron mode, for which we may
anticipate that $\Delta\omega \simeq -\Omega$, hence $\delta \simeq -1$ and
$T \simeq \frac{1}{4} \epsilon_2 \ll 1$. Now let $k_{\perp 1}^2$ be that solution of equation
(56) which is near the zero of the first square bracket

$$k_{\perp 1}^2 \simeq - \frac{p_+^2(1 + \delta)(1 - \delta + T)}{1 - \delta^2 + 2T} + \ldots \qquad (60)$$

and likewise $k_{\perp 2}^2$ will be the remaining solution which is
near the zero of the second square bracket

$$k_{\perp 2}^2 \simeq - \frac{p_-^2(1 - \delta)(1 + \delta + T)}{1 - \delta^2 + 2T} + \ldots \qquad . \qquad (61)$$

Referring to equation (49), one notes that $p_+^2 < 0$ is
associated with the negative energy cyclotron mode, and
therefore $k_{\perp 1}^2 > 0$ and $k_{\perp 1}$ will be the corresponding
perpendicular wave number for that mode. Likewise, when

28

$\Delta\omega \simeq -\Omega$, $p_-^2 > 0$ and thus $k_{\perp 2}^2 < 0$. Consequently, the Bessel functions in equation (57) of argument $k_{\perp 2}a$ actually behave like the corresponding modified Bessel functions I_0 and I_1 of real arguments. Furthermore, for $|k_{\perp 2}a|^2 \simeq p_-^2 a^2 \lesssim 1$, these Bessel functions may be expanded as

$$\frac{k_{\perp 2}a\, J_0(k_{\perp 2}a)}{J_1(k_{\perp 2}a)} \simeq 2 - \frac{1}{4}k_{\perp 2}^2 a^2 \simeq 2 + \frac{1}{4}p_-^2 a^2 \quad . \qquad (62)$$

The functions G_1 and G_2 may also be expanded for $\delta \simeq -1$, $|p_-^2/p_+^2| \ll 1$, $T \ll 1$ to yield

$$G_1 \simeq 1 \qquad\qquad (63)$$

$$G_2 \simeq 1 + T\left[1 + \frac{p_-^2}{p_+^2}\left(1 + \frac{T}{1+\delta}\right)\right]$$

so that the dispersion relation (57) becomes

29

$$\frac{k_{\perp 1} a \, J_O(k_{\perp 1} a)}{J_1(k_{\perp 1} a)} \simeq -2\left\{1 + \frac{p_-^2 a^2}{8} + T\left[1 + \frac{p_-^2}{p_+^2}\left(1 + \frac{T}{1+\delta}\right)\right]\right\} \simeq -2$$

$$(64)$$

Since the right hand side is approximately constant,
equation (64) approximately determines the numerical value
of $k_{\perp 1} a$, and then equation (56) becomes the dispersion
relation relating ω and k_z. The smallest solution of
equation (64) is given by

$$k_{\perp 1} a \simeq 2.95 + \frac{1}{5.66}\left\{\frac{p_-^2 a^2}{4} + 2T\left[1 + \frac{p_-^2}{p_+^2}\left(1 + \frac{T}{1+\delta}\right)\right]\right\} \simeq 2.95$$

$$(65)$$

Finally, if equations (34), (42), (48), and (49) are
inserted into equation (56), the dispersion relation for
linear waves becomes

30

$$O = \left(\Omega^2 - \frac{2\omega_p^2}{\gamma_o^2}\right)(k^2c^2 - \omega^2)\left[\Delta\omega^2(k^2c^2 - \omega^2)\right.$$

$$\left. - \frac{\omega_p^2}{\gamma_o^2}(k_z^2c^2 - \omega^2)\right]$$

$$- \Delta\omega^2\left(\Delta\omega^2 - \frac{\omega_p^2}{\gamma_o^2}\right)(k^2c^2 + \omega_p^2 - \omega^2)^2 \qquad (66)$$

where $k^2 = k_{\perp 1}^2 + k_z^2$ and $\Delta\omega = \omega - k_z\beta_o c$. This disper-
sion relation contains eight waves: four light waves, two
longitudinal plasma waves, and two cyclotron waves. If
equation (66) is examined for the case of $\omega^2 << k_z^2c^2 < k^2c^2$
for which the four light waves are decoupled, it is quadradic
in $\Delta\omega^2$, and the solution which represents the two cyclotron
waves may be written as

31

$$\Delta\omega^2 = \frac{1}{2}\left[\frac{k^4 c^4 \left(\Omega^2 - \frac{2\omega_p^2}{\gamma_o^2}\right)}{(k^2 c^2 + \omega_p^2)^2} + \frac{\omega_p^2}{\gamma_o^2}\right]$$

$$+ \frac{1}{2}\left\{\left[\frac{k^4 c^4 \left(\Omega^2 - \frac{2\omega_p^2}{\gamma_o^2}\right)}{(k^2 c^2 + \omega_p^2)^2} + \frac{\omega_p^2}{\gamma_o^2}\right]^2\right.$$

$$\left. - \frac{4\omega_p^2 \left(\Omega^2 - \frac{2\omega_p^2}{\gamma_o^2}\right) k^2 k_z^2 c^4}{\gamma_o^2 (k^2 c^2 + \omega_p^2)^2}\right\}^{1/2} \tag{67}$$

If equation (67) is further expanded for

$$2\frac{\omega_p}{\gamma_o}\frac{\left(\Omega^2 - \frac{2\omega_p^2}{\gamma_o^2}\right)^{1/2} kk_z c^2}{(k^2 c^2 + \omega_p^2)} << \frac{k^4 c^4 \left(\Omega^2 - \frac{2\omega_p^2}{\gamma_o^2}\right)}{(k^2 c^2 + \omega_p^2)^2} + \frac{\omega_p^2}{\gamma_o^2}$$

$$\tag{68}$$

one obtains

$$\Delta\omega^2 \simeq \frac{k^4 c^4 \left(\Omega^2 - \frac{2\omega_p^2}{\gamma_o^2}\right)}{(k^2 c^2 + \omega_p^2)^2} + \frac{\omega_p^2}{\gamma_o^2} \frac{k_{\perp 1}^2}{k^2} \quad . \tag{69}$$

Finally, for $\omega_p^2 \ll k^2 c^2$, $\gamma_o^2 \Omega^2$ one obtains

$$\Delta\omega = \omega - k_z \beta_o c \simeq - \Omega\left[1 - \frac{\omega_p^2}{k^2 c^2} - \frac{\omega_p^2}{\gamma_o^2 \Omega^2}\left(1 - \frac{k_{\perp 1}^2}{2k^2}\right)\right]$$

$$\tag{70}$$

as the dispersion relation for the negative energy cyclotron mode. Here the correction term $- \omega_p^2/\gamma_o^2 \Omega^2$ is due to the centrifugal and Coriolis forces on the electrons, while the correction $+ \omega_p^2 k_{\perp 1}^2/2k^2 \gamma_o^2 \Omega^2$ is due to the longitudinal compression of the electrons which couples longitudinal plasma modes to the cyclotron modes through the T terms.

The dispersion relation (70) is the starting point for all subsequent linear analysis which must be performed to examine the nature of the negative energy cyclotron waves.

Having developed a framework within which the linear mode analysis of cyclotron and plasma waves may proceed inclusive of coupling effects, we will conclude by reiterating that it is the smallness of the ε_1 and ε_2 parameters of equations (9) and (10) which validates the frequently adopted limits of "infinite magnetic fields" [wherein $\delta = O(\varepsilon_2^{1/2}) \ll 1$ for plasma waves] or of "ultrarelativistic beams" [wherein $T = O(\varepsilon_2) \ll 1$ for cyclotron waves]. In addition, it is the orderings of conditions (13) and (14) and the neglect of $\Delta\gamma/\gamma_c$ effects which allow solution for the beam eigenfunctions in terms of Bessel functions.

34

A P P E N D I X   I

LINEAR THEORY OF PLASMA WAVES SUPPORTED BY A
RADIALLY VARYING ELECTRON BEAM IN A
MAGNETIZED WAVEGUIDE

(Appendix I Contains 27 Pages)

43

The possibility of utilizing the negative energy, longitudinal plasma wave supported by an electron beam for collective ion acceleration (i.e., the converging guide accelerator) has been previously studied in some detail, but mainly in the limit of an infinite magnetic guide field and in the limit of pencil beam geometry, for which $\gamma_0^{2/3} \ll 1 + 2 \ln b/a$ [where $(\gamma_0 - 1)mc^2$ is the injection energy of the beam electrons and b/a is the ratio of the radius of the conducting waveguide to that of the beam]. One of the difficulties encountered in these prior calculations [e.g., R. J. Briggs, Phys. Fluids 19, 1257 (1976)] is that the phase velocity of the plasma waves can only be made small (for loading the ions into the wave) by increasing the electron current extremely close to the limiting current which can be propagated without virtual cathode formation. It is of interest to explore whether these unfortunate results still hold for more realistic nonpencil beam geometries where the radial variation in the equilibrium quantities γ, β_z, n is significant.

For this analysis, we shall adopt the infinite magnetic field limit. Then the beam equilibrium calculation

1

will be just as described in the limiting current publication
of Appendix C, to which the equilibrium analysis of Appendix
G reduces in the limit $\varepsilon_1 \to 0$, $\varepsilon_2 \to 0$. To this equilibrium
analysis we shall couple a linear theory calculation of the
plasma waves, which differs from that in Appendix H in that
we shall here focus on the $\Delta\gamma/\gamma_c$ effects and ignore the
finite magnetic field effects.

We begin by reviewing the equations for the equi-
librium quantities. For a steady state electron beam diode,
two constants of the motion for electrons are

$$\gamma - \frac{e}{mc^2} \phi = \gamma_A = 1 - \frac{e}{mc^2} \phi_c \tag{1}$$

$$n \beta_z = n_A(r) \beta_A \tag{2}$$

where $-e$, m are the charge and mass of the electrons,
$(\gamma_A - 1)mc^2$ is the electron energy at the anode, $\beta_A c$ is
the axial electron velocity at the anode, n_A is the
electron number density at the anode, and $\phi_c < 0$ is the
electrostatic potential at the cathode. It is assumed that

2

the anode is grounded electrically to the waveguide walls (i.e., $\Phi_A = 0$) and that the electrons are born at the cathode with zero energy (i.e., $\gamma_C = 1$). since Φ_C is an equipotential, γ_A must be independent of r, and to conform to prior notation we will let $\gamma_A = \gamma_o$, $\beta_A = \beta_o = (1 - \gamma_o^{-2})^{1/2}$. In principle, n_A may vary with r if a way is devised for the cathode to emit nonuniformly. Therefore we shall let $n_A = n_o g(r)$, where n_o is the mean density of the beam, such that

$$\nu \equiv \frac{\pi n_o e^2 a^2 \beta_o}{mc^2} = \frac{I_e}{mc^3/e} \quad . \tag{3}$$

Here a is the beam radius (constant for a uniform, infinite magnetic field), I_e is the electron current, and $mc^3/e = 17$ kA. Consequently, $g(r)$ must have the normalization

$$1 = \frac{2}{a^2} \int_0^a dr \, r \, g(r) \tag{4}$$

Finally, the radial profile for the equilibrium quantity $\gamma(r)$ is determined from the radial Poisson equation

3

$$\frac{1}{r} \frac{d}{dr} r \frac{d\gamma}{dr} = \begin{cases} \dfrac{4\nu g(r)}{a^2 \beta_z} & , & r \leq a \qquad \text{(5a)} \\ \\ 0 & , & a < r \leq b \qquad \text{(5b)} \end{cases}$$

subject to $\gamma(r \rightarrow 0)$ being regular, and

$$\gamma(r = b) = \gamma_0 \qquad , \qquad\qquad\qquad (6)$$

and where $\beta_z = (1 - \gamma^{-2})^{1/2}$. Equations (5b) and (6) may be combined to yield the alternative boundary condition

$$\left(\gamma + \ln \frac{b}{a} r \frac{d\gamma}{dr}\right)_{r=a} = \gamma_0 \qquad . \qquad\qquad (7)$$

Techniques for the solution of these equations are discussed in Appendix C. In principle, equation (5a) determines $\gamma(\gamma_c, \nu, r/a)$, where $\gamma_c \equiv \gamma(r = 0)$. Then the boundary condition (7) determines $\gamma_0(\gamma_c, \nu, b/a)$, or equivalently $\nu(\gamma_c, \gamma_0, b/a)$. As a function of γ_c, ν has a peak value

4

$\nu_L(\gamma_o, b/a)$ when $\gamma_c = \gamma_{cL}(\gamma_o, b/a)$. Several numerical solutions for $\nu(\gamma_c, \gamma_o, b/a)$ are illustrated in Figure 1, which may be compared with Figure 1 of Appendix C.

The condition of limiting current is $\partial\nu/\partial\gamma_c = 0$, which may be seen to correspond to the condition $\partial\gamma_o/\partial\gamma_c = 0$, since $0 = \partial\gamma_o/\partial\gamma_c + (\partial\gamma_o/\partial\nu)(\partial\nu/\partial\gamma_c)$. From equation (7), this limiting current condition becomes

$$\frac{\partial\gamma_o}{\partial\gamma_c} = \left(T + \ln\frac{b}{a}\ r\ \frac{\partial T}{\partial r}\right)_{r=a} = 0 \tag{8}$$

where the function $T = \dfrac{\partial\gamma(\gamma_c,\ \nu,\ r/a)}{\partial\gamma_c} = T(\gamma_c,\ \nu,\ r/a)$ is determined by differentiating equation (5a) to obtain

$$\frac{1}{r}\frac{d}{dr}\ r\ \frac{dT}{dr} = -\ \frac{4\nu g(r)}{\gamma^3\beta_z^3}\ T \tag{9}$$

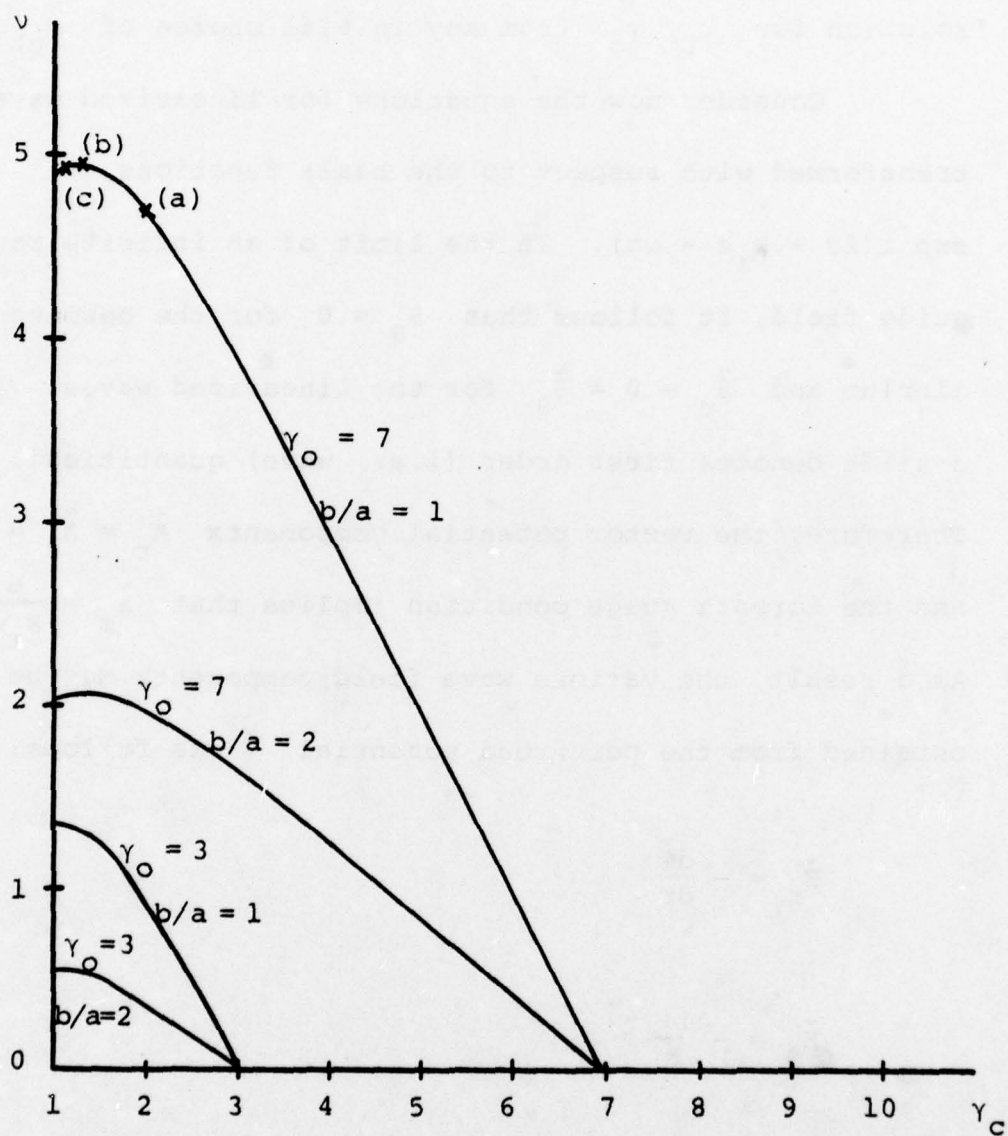subject to the interior boundary conditon

$$T(r = 0) = 1\quad . \tag{10}$$

5

Figure 1. Dimensionless current ν as a function of the relativistic factor γ_c of center electrons, for fixed values of γ_0, b/a.

6

Appendix C describes how a scaled version of equations (5a), (7), (8), (9), and (10), using the dimensionless variable $y = \nu r^2/a^2$, may be used to achieve an efficient numerical solution for ν_L, γ_0 from any initial choice of γ_{cL}, b/a.

Consider now the equations for linearized waves, transformed with respect to the basis functions $\exp i(\ell\theta + k_z z - \omega t)$. In the limit of an infinite magnetic guide field, it follows that $\beta_\theta = 0$ for the beam equilibrium and $\tilde{\beta}_r = 0 = \tilde{\beta}_\theta$ for the linearized waves. [Here a tilde denotes first order (i.e., wave) quantities]. Therefore, the vector potential components $\tilde{A}_r = \tilde{A}_\theta = 0$, and the Lorentz guage condition implies that $\tilde{A}_z = \dfrac{\omega}{k_z c} \tilde{\phi}$. As a result, the various wave field components may be obtained from the perturbed potential $\tilde{\phi}$ as follows:

$$\tilde{E}_r = -\frac{d\tilde{\phi}}{dr} \tag{11}$$

$$\tilde{E}_\theta = -\frac{i\ell}{r} \tilde{\phi} \tag{12}$$

$$\tilde{E}_z = i\left(\frac{\omega^2 - k_z^2 c^2}{k_z c^2}\right) \tilde{\phi} \tag{13}$$

7

$$\tilde{B}_r = -\frac{\omega}{k_z c}\,\tilde{E}_\theta = \frac{\omega}{k_z c}\,\frac{i\ell}{r}\,\tilde{\phi} \tag{14}$$

$$\tilde{B}_\theta = \frac{\omega}{k_z c}\,\tilde{E}_r = -\frac{\omega}{k_z c}\,\frac{d\tilde{\phi}}{dr} \tag{15}$$

$$\tilde{B}_z = 0 \tag{16}$$

The perturbed axial equation of motion is

$$i\,\Delta\omega\,\tilde{\beta}_z = \frac{e}{mc}\,\frac{\tilde{E}_z}{\gamma^3} \tag{17}$$

where $\Delta\omega \equiv \omega - k_z c\,\beta_z(r)$. The perturbed continuity equation is

$$\Delta\omega\,\tilde{n} - k_z c\,n\tilde{\beta}_z = 0 \quad . \tag{18}$$

Using equations (13), (17), and (18) to relate the perturbed charge density $\tilde{\rho} = -e\,\tilde{n}$ to $\tilde{\phi}$, the perturbed Poisson

8

equation may be cast in the form

$$\left\{ \frac{1}{r} \frac{d}{dr} r \frac{d}{dr} - \frac{\ell^2}{r^2} + \left(k_z^2 - \frac{\omega^2}{c^2} \right) \left[- 1 + \frac{4\nu g(r) c^2}{\gamma^3 \beta_z \, \Delta\omega^2 a^2} \right] \right\} \tilde{\phi} = 0 \ .$$

(19)

It is understood that $g(r) = 0$ by definition in the vacuum gap region $a < r \leq b$. Equation (19) for $\tilde{\phi}$ is subject to the boundary conditions that $\tilde{\phi}(r \to 0)$ be regular, and that

$$\tilde{\phi}(r = b) = 0 \qquad\qquad\qquad (20)$$

so that $\tilde{E}_\theta$, $\tilde{E}_z$, and $\tilde{B}_r$ vanish at the conducting wall. In the same fashion that the alternative boundary condition (7) was derived for the equilibrium differential equation, we may combine an analytical solution to equation (19) for $\tilde{\phi}$ in the vacuum gap with equation (20) to obtain the alternative boundary condition

9

$$\left\{ \tilde{\phi} + \frac{1}{a\sqrt{k_z^2 - \frac{\omega^2}{c^2}}} \left[\frac{K_\ell\left(a\sqrt{k_z^2 - \frac{\omega^2}{c^2}}\right) - \frac{K_\ell\left(b\sqrt{k_z^2 - \frac{\omega^2}{c^2}}\right)}{I_\ell\left(b\sqrt{k_z^2 - \frac{\omega^2}{c^2}}\right)} I_\ell\left(a\sqrt{k_z^2 - \frac{\omega^2}{c^2}}\right)}{K_\ell'\left(a\sqrt{k_z^2 - \frac{\omega^2}{c^2}}\right) - \frac{K_\ell\left(b\sqrt{k_z^2 - \frac{\omega^2}{c^2}}\right)}{I_\ell\left(b\sqrt{k_z^2 - \frac{\omega^2}{c^2}}\right)} I_\ell'\left(a\sqrt{k_z^2 - \frac{\omega^2}{c^2}}\right)} \right] \times r \frac{d\tilde{\phi}}{dr} \right\}_{r=a} = 0 \qquad (21)$$

where I_ℓ, K_ℓ are the usual modified Bessel functions of the first and second kind, and I_ℓ', K_ℓ' are the derivatives of these functions with respect to their arguments.

It may also be shown that the solution to equation (19) for $\tilde{\phi}$ which is regular near $r = 0$ must vary as $\tilde{\phi} \propto r^\ell$. We will henceforth restrict attention to the case of $\ell = 0$, θ-symmetric plasma waves, since these eigenmodes are the ones that would be utilized for the collective

10

acceleration applications. For $\ell = 0$, without loss of generality we may assert the interior boundary condition

$$\tilde{\Phi}(r = 0) = 1 \tag{22}$$

since only the shape of $\tilde{\Phi}(r)$ is determined from equations (19) and (21).

The r-dependence of the coefficients of equation (19) is generally quite complex, since the γ and β_z r-dependence generated by equations (5) - (7) appears not only through $1/\gamma^3\beta_z$, but also through $\Delta\omega$. In addition, g may have r-dependence. However, we shall first consider the special case in which all of this r-dependence is weak, since analytical expressions may then be developed for the eigenfunction $\tilde{\Phi}$ and for the plasma wave dispersion relation. Let us also consider the case for which $b = a$ and $\gamma_o \gg 1$, within the "fat beam limit," which is opposite to the "pencil beam limit" within which the previous analytical expressions were derived (e.g., by R. J. Briggs, <u>ibid</u>.). Let $g(r) = 1$ and $\nu \ll \nu_L$ so that the r-dependence of the

11

equilibrium is weak. From equations (5a) and (7), one finds

$$\gamma(r) \simeq \gamma_0 - \frac{\nu}{\beta_k}\left(1 - \frac{r^2}{a^2}\right) \tag{23a}$$

where

$$\beta_z(r) \simeq \beta_k \tag{23b}$$

to lowest order, and the value β_k about which we expand may be selected later for convenience. (For greatest accuracy, β_k should be the value of β_z at some intermediate value of r between 0 and a.)

Equation (19) may be put in the dimensionless form

$$\left[\frac{1}{R}\frac{d}{dR}R\frac{d}{dR} + k_\perp^2(R)a^2\right]\tilde{\Phi}(R) = 0 \tag{24}$$

where

$$k_\perp^2(R)a^2 \equiv (1 - \beta_\phi^2)\left[-k_z^2a^2 + \frac{4\nu}{\gamma^3\beta_z(\beta_z - \beta_\phi)^2}\right] \tag{25}$$

12

$$R \equiv r/a$$

$$\beta_\phi \equiv \omega/k_z c$$

and the boundary conditions (21) and (22) become

$$\tilde{\phi}(R = 0) = 1 \qquad ;$$

(26a)

$$\tilde{\phi}(R = 1) = 0 \qquad .$$

(26b)

Let $k_\perp^2(R) = k_{\perp 0}^2 + \delta k_\perp^2(R)$ and $\tilde{\phi}(R) = \tilde{\phi}^{(0)}(R) + \tilde{\phi}^{(1)}(R)$. Then the zero-order eigenfunction obeys

$$\left[\frac{1}{R} \frac{d}{dR} R \frac{d}{dR} + k_{\perp 0}^2 a^2 \right] \tilde{\phi}^{(0)}(R) = 0$$

(27a)

$$\tilde{\phi}^{(0)}(R = 0) = 1$$

(27b)

$$\tilde{\phi}^{(0)}(R = 1) = 0$$

(27c)

13

whose solution is

$$\tilde{\phi}^{(0)}(R) = J_o(k_{\perp 0}a R) = J_o(k_{\perp 0} r) \qquad (28)$$

where

$$k_{\perp 0}a = \lambda_{on} = 2.4, \quad \ldots \qquad . \qquad (29)$$

The first order eigenfunction must then obey

$$\left[\frac{1}{R}\frac{d}{dR} R \frac{d}{dR} + k_{\perp 0}^2 a^2\right] \tilde{\phi}^{(1)}(R) = - \delta k_{\perp}^2(R)a^2 \; \tilde{\phi}^{(0)}(R)$$

$$(30a)$$

$$\tilde{\phi}^{(1)}(R = 0) = 0 \qquad (30b)$$

$$\tilde{\phi}^{(1)}(R = 1) = 0 \qquad (30c)$$

The Rayleigh-Ritz procedure may be used to generate the dispersion relation for plasma waves, correct to first order, from equations (30):

14

$$0 = \int_0^1 dR \; R \; \tilde{\phi}^{(0)2}(R) \; \delta k_\perp^2(R)$$

$$= \int_0^1 dR \; R \; J_0^2(k_{\perp 0}a \; R) \left\{ (1 - \beta_\phi^2) \left[\frac{4\nu}{\gamma^3 \beta_z (\beta_z - \beta_\phi)^2} - \kappa_z^2 a^2 \right] \right.$$

$$\left. - k_{\perp 0}^2 \; a^2 \right\} \tag{31}$$

Consequently, with $\beta_z \simeq \beta_k$ = constant, the plasma wave dispersion relation may be written as

$$k_{\perp 0}^2 a^2 = \lambda_{on}^2 = (1 - \beta_\phi^2) \left[\frac{4\nu}{\beta_k (\beta_k - \beta_\phi)^2} \left\langle \gamma^{-3} \right\rangle - k_z^2 a^2 \right]$$

$$\tag{32}$$

where

$$\left\langle \gamma^{-3} \right\rangle \equiv \frac{\int_0^1 dR \; R \; J_0^2(k_{\perp 0}a \; R) \gamma^{-3}(R)}{\int_0^1 dR \; R \; J_0^2(k_{\perp 0}a \; R)} \; . \tag{33}$$

15

Therefore, the weak r-dependence in the coefficient of equation (24) should be averaged over the zero-order eigen-functions of the equation, to determine the dispersion relation. Let β_k now be chosen such that

$$\left\langle \gamma^{-3} \right\rangle = \gamma_k^{-3} = (1 - \beta_k^2)^{3/2} \quad . \tag{34}$$

The dispersion relation (32) may be seen to agree with the result obtained in Appendix H, equation (47) if one identifies γ_k, β_k with the constant values γ_o, β_o of Appendix H. It is a quartic equation for β_ϕ as a function of k_z. If one expands for $\beta_\phi = \beta_k + \delta\beta_\phi$, $|\delta\beta_\phi| << \beta_k$, $(2\beta_k\gamma_k^2)^{-1}$, one obtains

$$\beta_\phi = \frac{\omega}{k_z c} \simeq \beta_k - \frac{2 \, \nu^{1/2}}{\gamma_k^{5/2} \, \beta_k^{1/2} a\sqrt{k_{\perp 0}^2 + \gamma_k^{-2} k_z^2}} + \dots$$

$$\tag{35}$$

where $\gamma_k = \gamma_o - O(\nu)$, $\beta_k = \beta_o - O(\nu)$, as determined from

16

equations (23), (33), and (34). The following features may be observed about the scaling of the plasma wave phase velocity in equation (35):

(i)   the phase velocity increases weakly as a function of k_z, although this increase will not be noticeable until k_z is larger than $\gamma_k k_{\perp 0}$;

(ii) the phase velocity is lowest for the lowest $k_\perp$ modes;

(iii) as $\nu \to 0$, $\beta_\phi \to \beta_k \to \beta_o$ so that the plasma wave phase velocity approaches the electron beam velocity;

(iv) as the electron current is increased from zero, the phase velocity decreases below the beam velocity, although throughout the regime $\nu/\nu_L \ll 1$ of this approximation, the decrease is only a small correction to β_k. Thus $\beta_\phi(\nu)$ will appear fairly flat near $\beta_\phi \simeq \beta_k$ for $\nu \ll \nu_L$.

Since the lowest phase velocities are realized in the long wavelength limit, let's consider the case of $\ell = 0$ and $k_z \to 0$. We shall make the ansatz that β_ϕ remains bounded in this case, or that $\omega \to 0$ as well. Then for $g(r)$ and b/a arbitrary, equation (19) reduces to

$$\left[\frac{1}{r}\frac{d}{dr} r \frac{d}{dr} + \frac{4\nu g(r)(1 - \beta_\phi^2)}{\gamma^3 \beta_z (\beta_z - \beta_\phi)^2}\right] \tilde{\Phi} = 0 \tag{36}$$

while the boundary condition (21) reduces to

$$\left(\tilde{\Phi} + \ell n \frac{b}{a} r \frac{d\tilde{\Phi}}{dr}\right)_{r=a} = 0 \tag{37}$$

and

$$\tilde{\Phi}(r = 0) = 1 \tag{38}$$

It is now apparent that as $\beta_\phi \to 0$, equations (36) - (38) for $\tilde{\Phi}$ approach the limiting current conditions (8) - (10)

18

for the variable T. Consequently, as $\nu \to \nu_L$, the phase velocity must vanish for arbitrary choices of the density profile and b/a.

Finally, numerical solutions have been determined to equations (19) - (22), and typical results are illustrated in Figures 1 - 7 for cases with $g(r) = 1$ and $\ell = 0$. The equilibrium quantities $\gamma(r)$, $\beta_z(r)$ which appear in the coefficient of equation (19) are determined from a numerical solution to the equilibrium equations (5) - (7).

In Figure 2, the dispersion relation $\omega(k_z)$ is plotted for the lowest $k_\perp$ mode, for the case $\gamma_o = 7$ and b/a = 1, but for three different choices of γ_c: (a) $\gamma_c > \gamma_{cL}$, (b) $\gamma_c = \gamma_{cL}$, (c) $\gamma_c < \gamma_{cL}$. These three curves in Figure 2 may be correlated with the three points marked (a), (b), (c) on the corresponding $\nu(\gamma_c)$ curve in Figure 1. The predicted scaling of β_ϕ vs. k_z, ν may be observed. Equation (35) was also found to be quantitatively correct when $\nu \ll \nu_L$. The possibility of negative phase velocities for $\gamma_c < \gamma_{cL}$ is possibly associated with the transition to virtual cathode formation which is experimentally observed
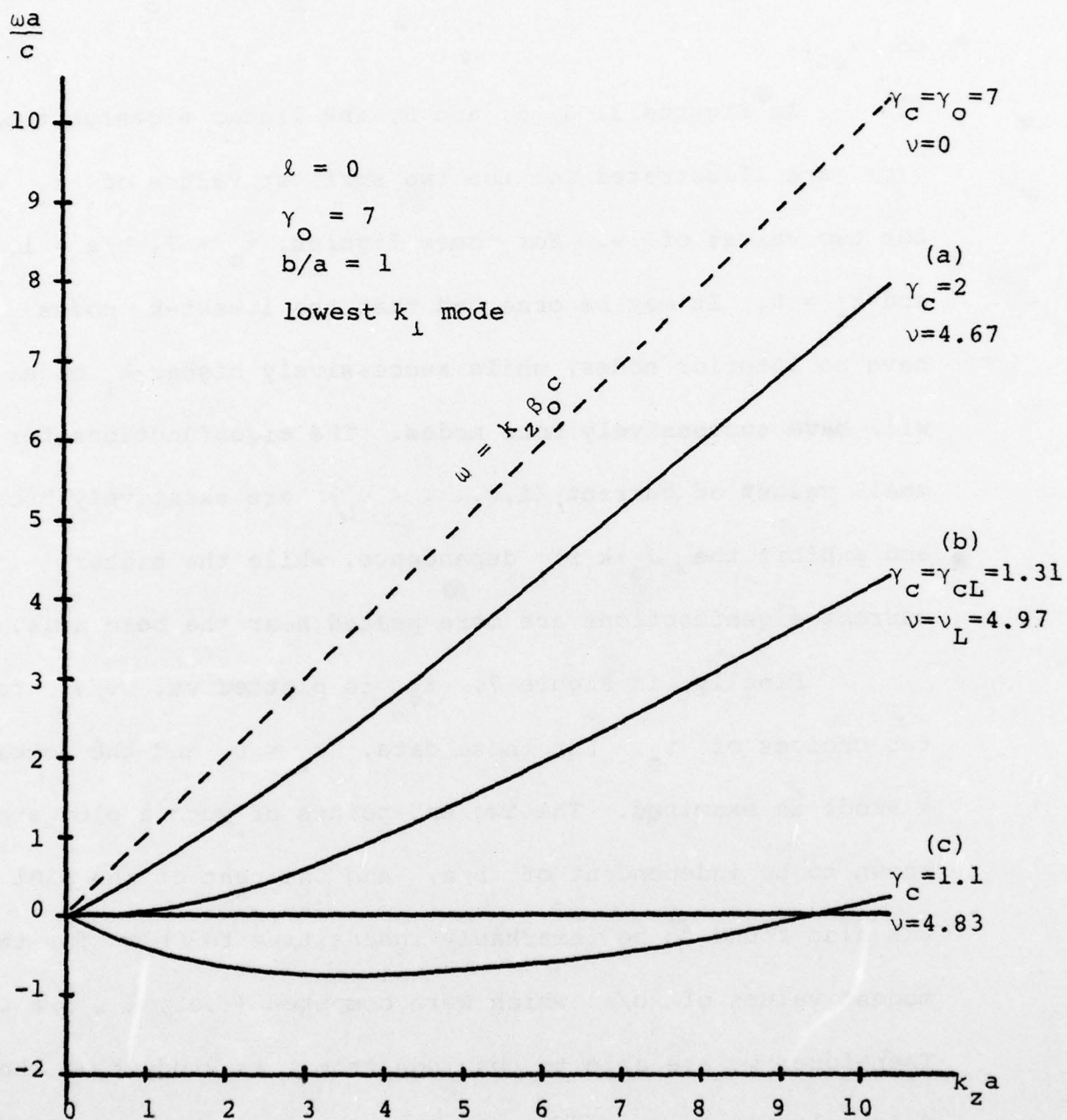
19

Figure 2. Dispersion relation $\omega(k_z)$ for θ-symmetric plasma waves with γ_o, b/a fixed, for various γ_c, ν.

to occur after ν has been raised to ν_L and γ_c reduced to γ_{cL}.

In Figures 3, 4, 5, and 6, the linear eigenfunctions $\tilde{\phi}(r)$ are illustrated for the two smallest values of $k_\perp$ and for two values of ν. For these figures, $\gamma_o = 7$, $b/a = 1$, and $k_z = 0$. It may be observed that the lowest-$k_\perp$ modes have no interior nodes, while successively higher-$k_\perp$ modes will have successively more nodes. The eigenfunctions for small values of current (i.e., $\nu < \nu_L$) are relatively broad, and exhibit the $J_o(k_\perp r)$ dependence, while the higher current eigenfunctions are more peaked near the beam axis.

Finally, in Figure 7, β_ϕ is plotted vs. ν/ν_L for two choices of γ_o. For these data, $k_z = 0$ and the lowest $k_\perp$-mode is examined. The two end-points of such a plot are known to be independent of b/a, and the rest of the plot was also found to be remarkably insensitive to b/a for the modest values of b/a which were computed (i.e., $1 \le b/a \le 2$). Therefore, we are able to conclude from this study that the difficulty in lowering the plasma wave velocity seems to persist even in the fat beam regime where the radial variation in the equilibrium quantities γ, β_z, n is significant. It
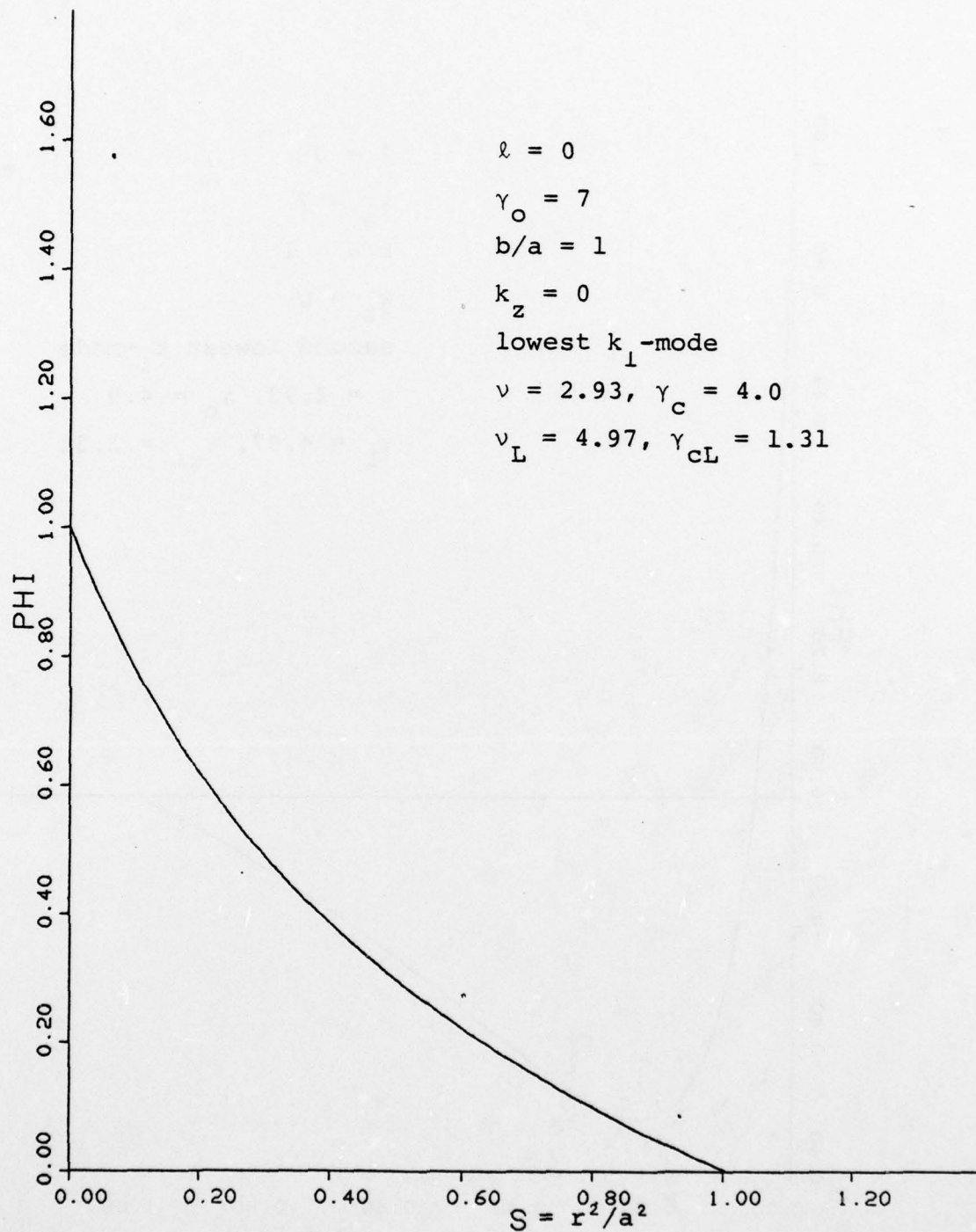
21

Figure 3. Perturbed potential eigenfunction for lowest
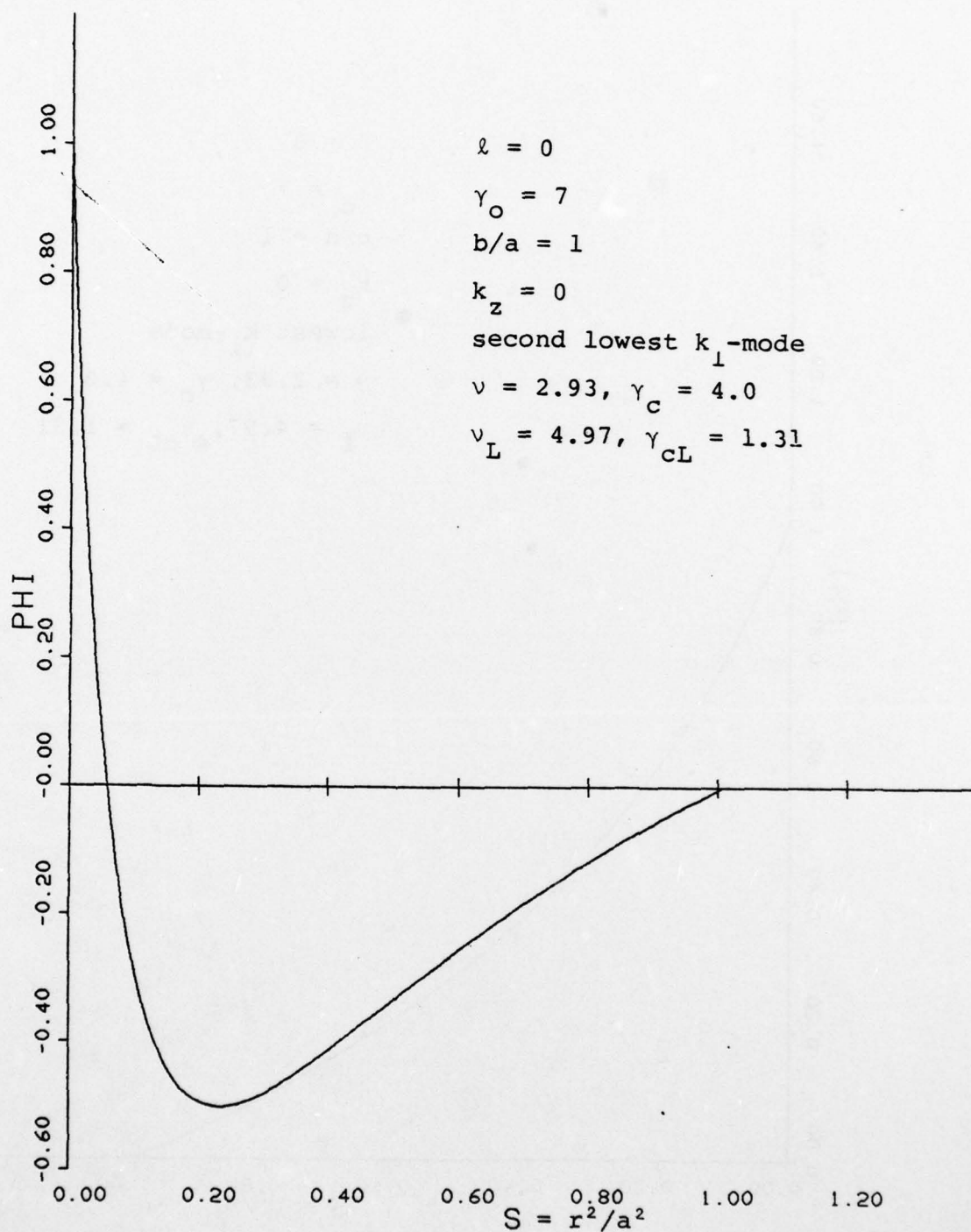k⊥ plasma wave with $\nu < \nu_L$.

22

$\ell = 0$

$\gamma_o = 7$

$b/a = 1$

$k_z = 0$

second lowest $k_\perp$-mode

$\nu = 2.93$, $\gamma_c = 4.0$

$\nu_L = 4.97$, $\gamma_{cL} = 1.31$

Figure 4. Perturbed potential eigenfunction for second lowest $k_\perp$ plasma wave with $\nu < \nu_L$.

23

$\ell = 0$

$\gamma_o = 7$

$b/a = 1$

$k_z = 0$

lowest $k_\perp$-mode

$\nu \simeq \nu_L \simeq 4.97$

$\gamma_c \simeq \gamma_{cL} \simeq 1.31$

PHI

1.60 1.40 1.20 1.00 0.80 0.60 0.40 0.20 0.00

0.00   0.20   0.40   0.60   0.80   1.00   1.20

$S = r^2/a^2$
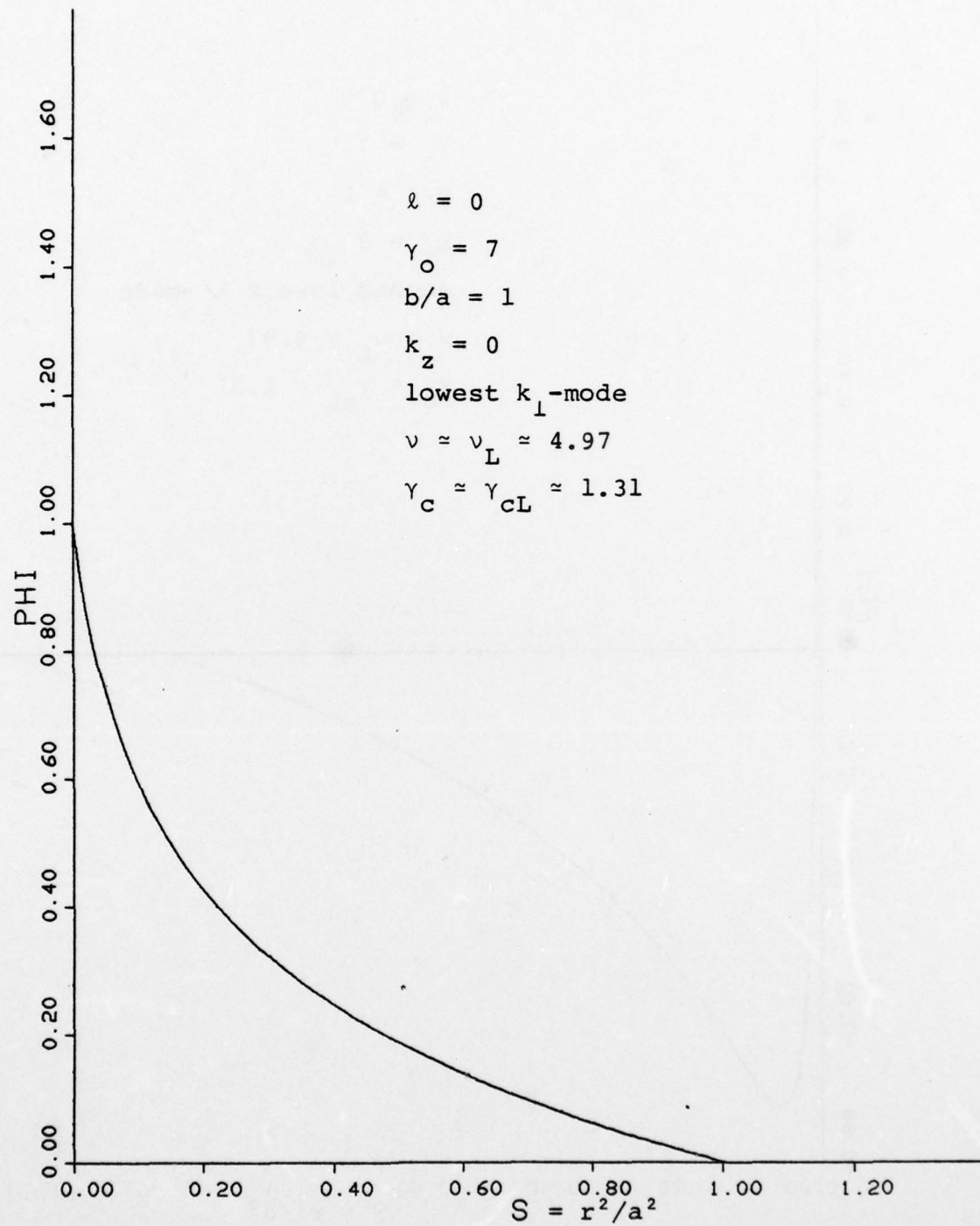
Figure 5. Perturbed potential eigenfunction for lowest
$k_\perp$ plasma wave with $\nu = \nu_L$.

24
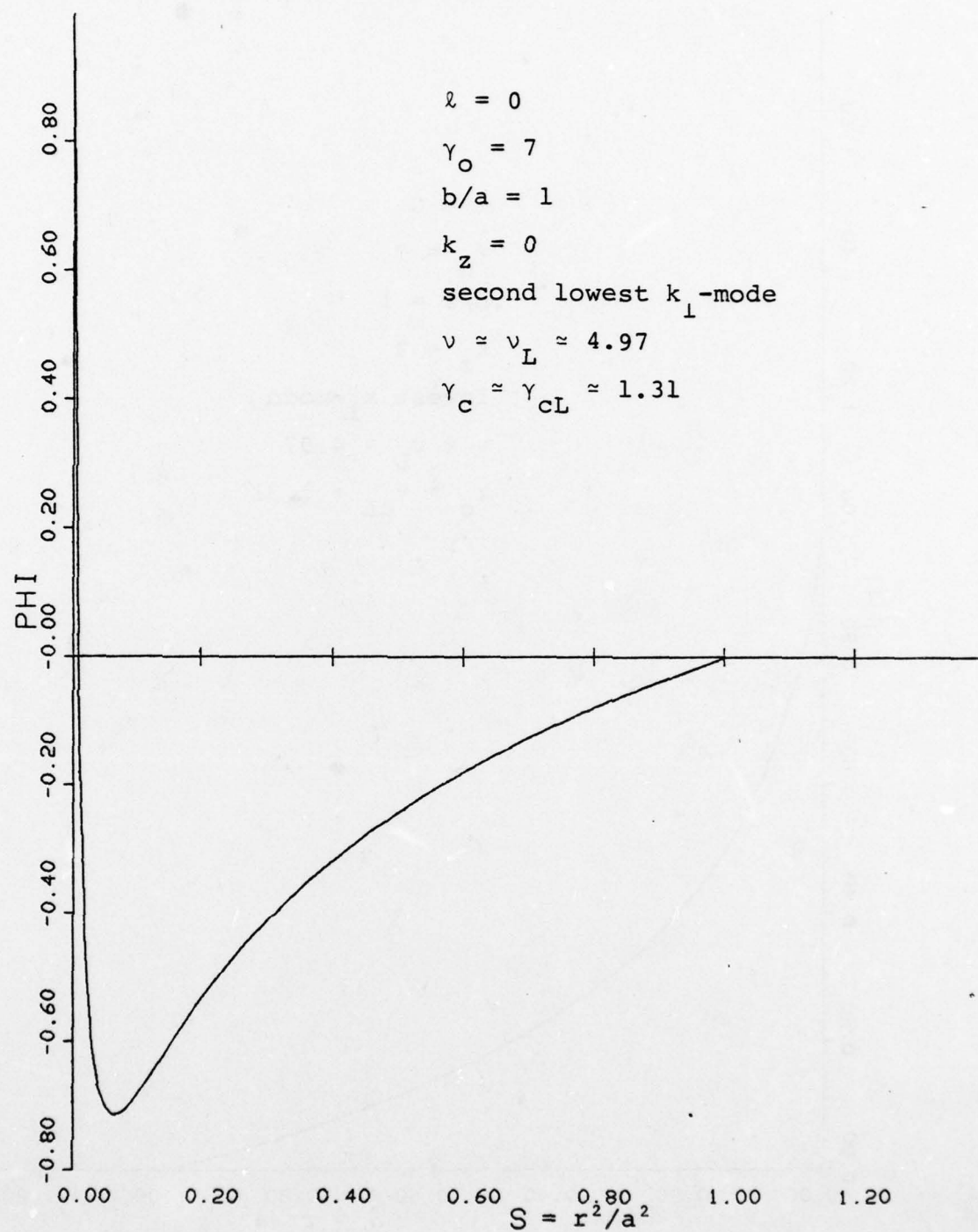
Figure 6. Perturbed potential eigenfunction for second lowest $k_\perp$ plasma wave with $\nu \simeq \nu_L$.
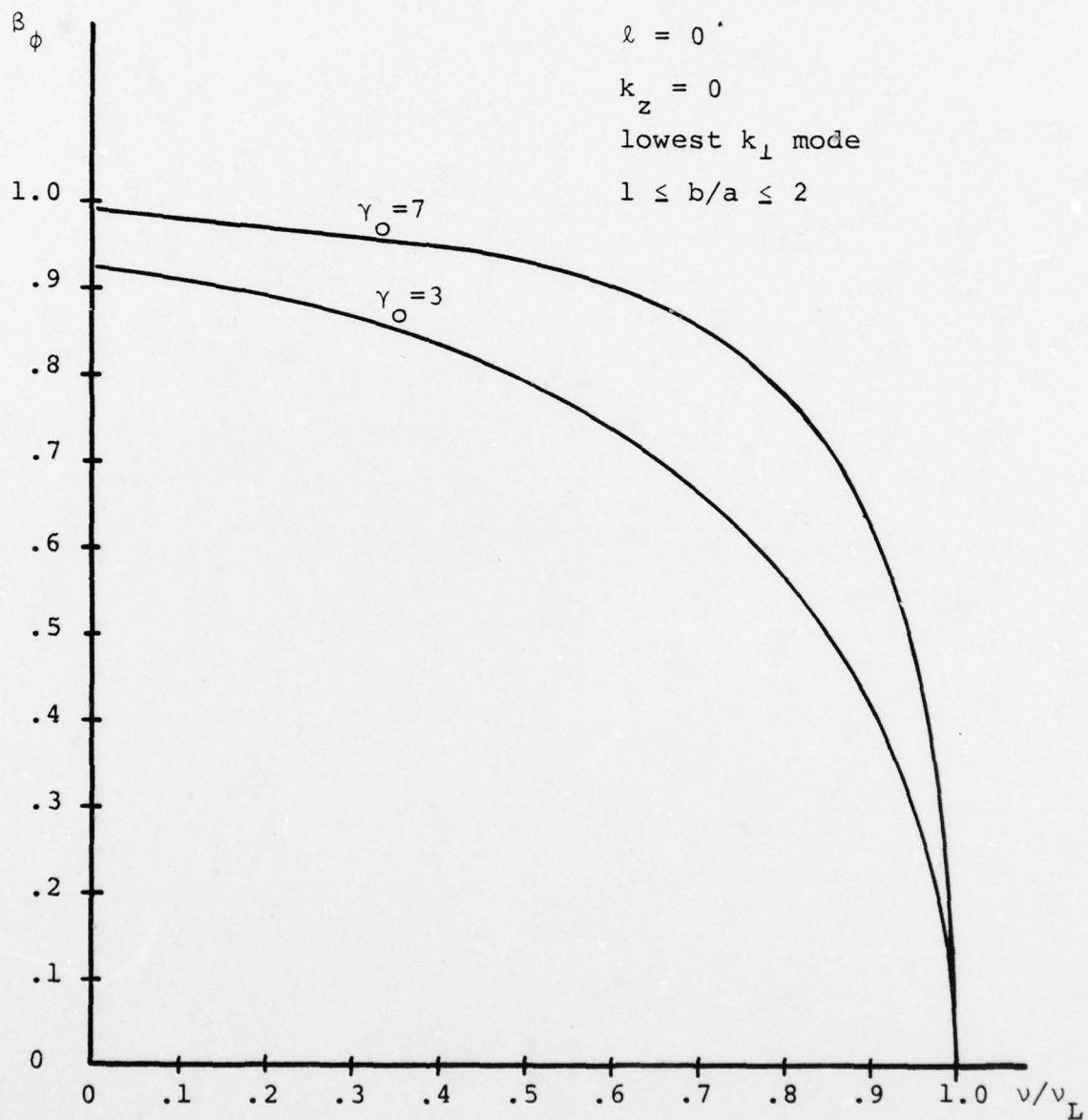
25

Figure 7. Plasma wave phase velocity vs. ν/ν_L for long wavelength, θ-symmetric, low $k_\perp$ modes

26

1.0

2.8 2.5

3.2 2.2

3.6

1.1 4.0 2.0

1.8
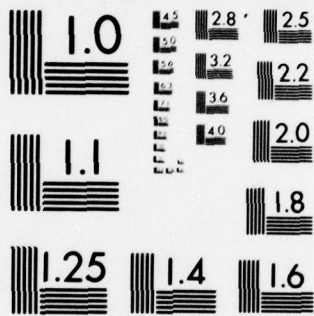
1.25 1.4 1.6

MICROCOPY RESOLUTION TEST CHART
NATIONAL BUREAU OF STANDARDS-1963-A

remains necessary to increase the electron current very near

to the limiting current to achieve $\beta_\phi \ll \beta_o$.

A P P E N D I X   J

THE EFFECTS OF FINITE THERMAL SPREAD ON THE
ELECTRON CYCLOTRON BEAM MODES

(Appendix J Contains 16 Pages)

For a cold relativistic electron beam propagating with velocity $u \rightarrow c$ along a magnetic guide field in the z-direction, the frequency ω of the electron cyclotron beam mode with wave number k_z is

$$\omega \approx k_z u - \Omega + \frac{\omega_p^2 \, \Omega}{k^2 c^2}$$

where

$$k^2 = k_z^2 + k_\perp^2 \gg \frac{\omega^2}{c^2}$$

$$\frac{\omega_p^2}{k^2 c^2} \ll 1$$

Ω and ω_p are the relativistic electron cyclotron and plasma frequencies respectively. The perturbed electron perpendicular velocity $v_\perp$ associated with the cyclotron beam mode is

$$v_\perp \propto \frac{1}{\omega - k_z v_z + \Omega}$$

1

Thus a thermal spread in v_z of magnitude Δv_z:

$$v_z \rightarrow u + \Delta v_z$$

such that

$$k_z \ \Delta v_z \sim \frac{\omega_p^2 \ \Omega}{k^2 c^2}$$

will modify the perturbed perpendicular velocities and hence the linear dispersion relation of the electron cyclotron beam mode for a cold beam.

A relativistic electron beam will acquire a thermal spread in v_z after passage through an anode foil. If the foil is thin enough, the scattering of the electron beam by the foil results in a negligibly small spread in energy but rotates the electron velocity vector in velocity space. A finite spread in propagation velocities occurs.

In this appendix, we investigate the effects of a finite thermal spread in v_z on the dispersion relation for the electron cyclotron beam mode.

Equilibrium

We consider a slab equilibrium of the electron beam, infinite in extent in the z- and y-directions and bounded by conducting walls at $x = \pm a$. The beam propagates along a magnetic guide field B_{oz} in the z-direction.

The electron beam equilibrium is described by the equilibrium distribution function

$$f_o(\mathcal{E}, P_z) = \begin{cases} D_o \delta(\mathcal{E} - \mathcal{E}_o) \, g_o[p_\perp^2(\mathcal{E}, P_z)], & P_z > 0 \\ \\ 0, & P_z < 0 \end{cases}$$

(1)

where $\mathcal{E}$ and P_z are the energy and z-component of the canonical momentum respectively:

$$\mathcal{E} = m\gamma c^2 - e\phi_o(x)$$

$$P_z = p_z - \frac{e}{c} A_{oz}(x)$$

3

$$\gamma = \left[1 + \frac{p^2}{m^2c^2}\right]^{1/2}$$

and

$$g_o(p_\perp^2) = \exp\left(-\frac{p_\perp^2}{\hat{p}^2}\right)$$

$$p_\perp^2(\mathcal{E}, P_z) = \frac{\mathcal{E}^2}{c^2} - m^2c^2 - P_z^2 \quad .$$

$\hat{p}^2 \ll m^2\gamma^2c^2$ is a measure of the thermal spread.

The equilibrium beam density is

$$N_o = \int d^3p \, f_o$$

$$= 2\pi \int_{-\infty}^{+\infty} dP_z \int_{\mathcal{E}_b(P_z)}^{\infty} d\mathcal{E} \, \frac{(\mathcal{E} + e\Phi_o)}{c^2} \, f_o$$

where

$$\mathcal{E}_b(P_z) = \left[\left(P_z + \frac{e}{c} A_{oz}\right)^2 c^2 + m^2c^4\right]^{1/2} - e\Phi_o$$

4

We restrict the discussion to the case of a low density ultrarelativistic electron beam where $\mathcal{E}_o \gg e\Phi_o$, eA_{oz}. In this limit

$$N_o = \frac{2\pi\, D_o\, \gamma_o}{c} \int_0^{p_o} dP_z \exp\left[-\frac{(p_o^2 - P_z^2)}{\hat{p}^2}\right]$$

$$\approx \frac{\pi\, D_o\, m\gamma_o}{p_o} \hat{p}^2 \tag{2}$$

where

$$p_o^2 = \frac{\mathcal{E}_o^2}{c^2} - m^2c^2 \gg \hat{p}^2$$

Equation (2) relates the normalization constant D_o to the beam density N_o.

Similarly, the equilibrium current is

$$J_{oz} = - e \int d^3p \, \frac{p_z}{m\gamma} f_o \approx - e \, \frac{N_o\, p_o}{m\gamma_o}$$

5

From Maxwell's equations, the equilibrium electric
potential Φ_o and magnetic potential A_{oz} can be
determined.

The equilibrium electron trajectories may be
approximated by

$$p_z' \approx p_z$$

$$p_x' \approx p_\perp \cos \{\Omega(t' - t) + \psi\}$$

$$p_y' \approx p_\perp \sin \{\Omega(t' - t) + \psi\}$$

$$z' \approx z + \frac{p_z}{m\gamma} (t' - t)$$

$$x' - x \approx \frac{p_\perp}{m\gamma\Omega} [\sin \{\Omega(t' - t) + \psi\} - \sin \psi]$$

where

$$\Omega = \frac{e B_{oz}}{m\gamma c}$$

Dispersion Relation

Let the perturbed electromagnetic fields have the form

$$\underline{E}(\underline{r}, t) \rightarrow \underline{E}(x) \exp [- i\omega t + i k_z z], \quad \text{etc.}$$

The linearized perturbed distribution function is given by

$$f_1(\underline{p}, x) = e \int_{-\infty}^{t} dt' \left[\underline{E}(x') + \frac{p_x' \, \underline{B}(x')}{m\gamma c} \right] \cdot \frac{\partial f_o}{\partial p'} \qquad (3)$$

where the time integral is taken over the equilibrium trajectories.

Neglecting finite Larmor radius terms of order $(k_\perp^2 \, p_\perp^2)/(m^2 \gamma^2 \Omega^2) \ll 1$,

7

$$f_1(\underline{p},x) \approx \frac{e}{m\gamma} \frac{\partial f_0}{\partial \mathcal{E}} \int^t dt' \exp\left\{-i\omega(t'-t) + i\frac{k_z P_z}{m\gamma}(t'-t)\right\}$$

$$\times \left[E_x(x)\, p_\perp \cos\{\Omega(t'-t)+\psi\} \right.$$

$$+ E_y(x)\, p_\perp \sin\{\Omega(t'-t)+\psi\} + \dots$$

$$\left. + p_z\left\{E_z(x) + (x'-x)\frac{\partial E_z}{\partial x} + \dots\right\}\right]$$

$$+ e\frac{\partial f_0}{\partial P_z} \int^t dt' \exp\left\{-i\omega(t'-t) + i\frac{k_z P_z}{m\gamma}(t'-t)\right\}$$

$$\times \left[E_z(x) + (x'-x)\frac{\partial E_z}{\partial x} + \dots \right.$$

$$+ \frac{p_\perp}{m\gamma c} B_y(x) \cos\{\Omega(t'-t)+\psi\}$$

$$\left. - \frac{p_\perp}{m\gamma c} B_x(x) \sin\{\Omega(t'-t)+\psi\} + \dots \right]$$

$$\tag{4}$$

8

The perpendicular perturbed currents are

$$J^{\pm}(x) = - e \int d^3p \; f_1 \; \frac{(p_x \pm i \; p_y)}{m\gamma}$$

$$= - e \int_0^{2\pi} d\psi \int_{-\infty}^{+\infty} dP_z \int_{\mathcal{E}_b(P_z)}^{\infty} d\mathcal{E} \; p_1 \; e^{\pm i\psi} \; f_1 \quad (5)$$

The electron cyclotron beam modes have frequency $\omega \sim (k_z P_z)/(m\gamma) - \Omega$ so that

$$\left| \frac{1}{\omega - \dfrac{k_z P_z}{m\gamma} + \Omega} \right| >> \left| \frac{1}{\omega - \dfrac{k_z P_z}{m\gamma}} \right| \; .$$

Substituting equation (4) for f_1 in equation (5),

$$J^+ \simeq 2\pi\, i\, e^2 \int\limits_{-\infty}^{+\infty} dP_z \int\limits_{\mathcal{E}_b}^{\infty} d\mathcal{E}\; \frac{f_0(\mathcal{E},P_z)}{\left(\omega - \dfrac{k_z P_z}{m\gamma} + \Omega\right)}$$

$$\cdot \left[E^+\left\{ 1 - \frac{p_\perp^2(\mathcal{E},P_z)}{2\,m^2\gamma^2 c^2}\; \frac{k_z^2 c^2 - \omega\,\dfrac{k_z P_z}{m\,\gamma} + \omega\Omega}{\Omega\left(\omega - \dfrac{k_z P_z}{m\gamma} + \Omega\right)} \right\} \right.$$

$$\left. + i\,B^+\left\{ \frac{P_z}{m\gamma c} - \frac{p_\perp^2(\mathcal{E},P_z)}{2\,m^2\gamma^2 c^2}\; \frac{\left(k_z c\,\Omega + \omega\,k_z c - \dfrac{\omega^2 P_z}{m\gamma c}\right)}{\Omega\left(\omega - \dfrac{k_z P_z}{m\gamma} + \Omega\right)} \right\} \right]$$

$$\simeq \frac{i\,\omega_p^2}{2\pi}\,\frac{p_0^2}{\hat{p}^2 k_z c} \left[E^+\left\{ \left(1 + \frac{\omega}{k_z c} - \frac{\Delta}{\Omega}\right)[1 - e^Q\, Q\, E_1(Q)] \right.\right.$$

$$\left. - \left(\frac{\omega}{k_z c} - \frac{\Delta}{\Omega}\right) e^Q\, E_1(Q) \right\}$$

$$+ i\,B^+\left\{ \left(1 + \frac{\omega}{k_z c}\,\frac{(k_z c - \omega)}{\Omega}\right)[1 - e^Q\, Q\, E_1(Q)] \right.$$

$$\left.\left. - \frac{\omega}{k_z c}\,\frac{(k_z c - \omega)}{\Omega}\, e^Q\, E_1(Q) \right\} \right]$$

10

$$\approx i \frac{\omega_p^2}{2\pi} \frac{p_o^2}{\hat{p}^2 k_z c} (E^+ + i B^+)[1 - e^Q Q E_1(Q)] \tag{6}$$

$$J^- \approx i \frac{\omega_p^2 (E^- - i B^-)}{4\pi(\omega - k_z c - \Omega)} \tag{7}$$

where

$$E^\pm = E_x \pm i E_y$$

$$B^\pm = B_x \pm i B_y$$

$$\frac{\partial E_z}{\partial x} = i k_z E^+ - \frac{\omega}{c} B^+$$

$$\Delta = \omega + \Omega - k_z c$$

$$Q = \frac{2 p_o^2}{\hat{p}^2} \frac{\Delta}{k_z c}$$

and we have assumed that $\left|\frac{\omega}{k_z c}\right|$, $\left|\frac{\Delta}{\Omega}\right| \ll 1$. $E_1(Q)$ is the

11

exponential integral

$$E_1(Q) = \int\limits_{Q}^{\infty} \frac{d\phi \; e^{-\phi}}{\phi}$$ (8)

From Maxwell's equations

$$\frac{\partial^2 A^+}{\partial x^2} - \left(k_z^2 - \frac{\omega^2}{c^2}\right) A^+ \approx i(k_z c - \omega) \frac{4\pi}{c^2} J^+$$

$$\approx - \frac{2 \, p_o^2}{\hat{p}^2} \frac{\omega_p^2}{c^2} \frac{(k_z c - \omega)}{k_z c} \{1 - e^Q \, Q \, E_1(Q)\} A^+$$ (9)

$$\frac{\partial^2 A^-}{\partial x^2} - \left(k_z^2 - \frac{\omega^2}{c^2}\right) A^- \approx i(k_z c - \omega) \frac{4\pi}{c^2} J^-$$

$$\approx + \frac{\omega_p^2}{c^2} \frac{(k_z c - \omega)}{(k_z c - \omega + \Omega)} A^-$$ (10)

where

12

$$A^{\pm} = E^{\pm} \pm i \, B^{\pm}$$

The solutions of these equations are

$$A^{+} = \alpha_1 \sin \kappa^{+} x + \alpha_2 \cos \kappa^{+} x$$

$$A^{-} = \beta_1 \sin \kappa^{-} x + \beta_2 \cos \kappa^{-} x$$

where

$$\kappa^{+2} = -k_z^2 + \frac{\omega^2}{c^2} + 2 \frac{\omega_p^2}{c^2} \frac{p_o^2}{\hat{p}^2} \frac{(k_z c - \omega)}{k_z c} \{1 - e^Q Q E_1(Q)\}$$

(11)

$$\kappa^{-2} = -k_z^2 + \frac{\omega^2}{c^2} - \frac{\omega_p^2}{c^2} \frac{(k_z u - \omega)}{(k_z c - \omega + \Omega)}$$
(12)

The boundary conditions on $A^{\pm}$ at $x = \pm a$ where

the beam is bounded by conducting walls are

13

$$A^+ = A^-$$

$$\frac{\partial A^+}{\partial x} + \frac{\partial A^-}{\partial x} = 0 \tag{13}$$

For solutions antisymmetric in $A^\pm$, the dispersion relation is

$$\kappa^+ \cot \kappa^+ a + \kappa^- \cot \kappa^- a = 0 \tag{14}$$

If $\kappa^- a \ll 1$, $\kappa^+ a \cot \kappa^+ a \approx -1$, and $\kappa^+ a \approx 2.03, 4.91, \ldots$. The frequency ω is then given by equation (11). In terms of Q, the frequency ω is

$$\omega = k_z c - \Omega + \frac{Q}{2} \frac{\hat{p}^2}{p_o^2} k_z c$$

$$\equiv k_z c - \Omega + \frac{Q}{2} \frac{\hat{v}^2}{c^2} k_z c \tag{15}$$

In the limit of $Q \gg 1$,

$$E_1(Q) \rightarrow \frac{e^{-Q}}{Q} \left[1 - \frac{1}{Q} + \frac{2}{Q^2} + \ldots \right]$$

14

and from equation (11),

$$Q \approx \frac{2 \, p_o^2}{\hat{p}^2} \frac{\omega_p^2}{(k^2 c^2 + \omega_p^2)} \frac{\Omega}{k_z c} - 2$$

The frequency ω is

$$\omega \approx k_z c - \Omega + \frac{\omega_p^2}{k^2 c^2} \Omega - \frac{\hat{v}^2}{c^2} k_z c$$

where $k^2 = k_z^2 + \kappa^{+2} \gg \frac{\omega^2}{c^2}$ and we have assumed that $\frac{\omega_p^2}{k^2 c^2} \ll 1$. We also require that $\frac{2 \, \omega_p^2}{k^2 \hat{v}^2} \frac{\Omega}{k_z c} \gg 1$ for validity of the asymptotic representation of $E_1(Q)$.

A finite thermal spread introduces a correction $\Delta \omega \approx - \frac{\hat{v}^2}{c^2} k_z c$ to the frequency of the electron cyclotron beam mode.

As $\frac{\hat{v}^2}{c^2}$ increases, the magnitude of Q which solves equation (11) decreases. Q remains real and consequently ω is real. In the limit of $\frac{k^2 \hat{v}^2}{\omega_p^2} \to 2 \frac{\Omega}{k_z c}$, $Q \to 0$ and the frequency $\omega \to k_z c - \Omega$. The neglect of finite Larmor

15

radius effects in this discussion imposes the condition
$\omega_p^2 \ll \Omega^2$.

In conclusion, if the thermal spread is low enough so that $\dfrac{k^2 \hat{v}^2}{\omega_p^2} < \dfrac{2\Omega}{k_z c}$ and finite Larmor radius effects can be neglected $(k_\perp^2 \hat{v}^2)/(\Omega^2) \ll 1$, the solutions of equation (11) for ω are real, and the electron cyclotron beam modes propagate undamped by thermal effects.